EUB/AGS Earth Sciences Report 2006-05

Subsurface Characterization of Acid-Gas Injection Operations in Northeastern British Columbia

Ministry of
Energy, Mines and
Petroleum Resources

Alberta Energy and Utilities Board

Alberta Geological Survey

AGS

EUB/AGS Earth Sciences Report 2006-05

Subsurface Characterization of Acid-Gas Injection Operations in Northeastern British Columbia

Alberta Energy and Utilities Board
Alberta Geological Survey

B.E. Buschkuehle and K. Michael

December 2006

ISBN 0-7785-3824-9

Buschkuehle, B.E. and Michael, K. (2006): Subsurface characterization of acid-gas injection operations in northeastern British Columbia; Alberta Energy and Utilities Board, EUB/AGS Earth Sciences Report 2006-05, 142 p.

Published December 2006 by:
Alberta Energy and Utilities Board
Alberta Geological Survey
4th Floor, Twin Atria Building
4999 – 98th Avenue
Edmonton, Alberta
T6B 2X3
Canada

Tel: (780) 422-3767 (Information Sales)
Fax: (780) 422-1918
E-mail: EUB.AGS-Infosales@eub.ca
Website: www.ags.gov.ab.ca

Contents

Tables

Figures

Acknowledgments

The authors acknowledge the technical and financial support provided by the British Columbia Ministry of Energy and Mines, especially close working relationships with Mark Hayes and Sachie Morii. Furthermore, financial support to conduct this study was received from Environment Canada, Alberta Environment, Climate Change Central, Alberta Energy Research Institute, Saskatchewan Industry and Resources, Keyspan, Western Economic Development, and Total. In addition, the authors gratefully appreciate the tremendous support in database management, graphics and report preparation provided by their colleagues Nancy Crann and Chris Crocq.

Abstract

Injection of acid gas in northeastern British Columbia takes place at six sites into four different stratigraphic intervals. Acid gas mixed with water is injected into the Permo–Carboniferous aquifer at Ring. At Boundary Lake–South and West Stoddart, dry acid gas is injected into aquifers of the Permian Belloy Formation and the Triassic Halfway Formation, respectively. At Caribou, the only injection site within the deformed part of the Rocky Mountain Fold and Thrust Belt, acid gas is injected into the Triassic Halfway aquifer and the Carboniferous Debolt aquifer. Injection into depleted gas reservoirs takes place at Bubbles and Jedney, where the injection horizon is the Triassic Baldonnel Formation. The oldest acid-gas injection sites in the study area are Boundary Lake–South and Jedney, where injection commenced in 1996. By the end of 2004, more than 890 kt of acid gas had been injected into deep geological formations in the northeastern British Columbia region.

If only the natural setting is considered, including geology and flow of formation waters, the basin and local-scale hydrogeological analyses indicate that injecting acid gas into these deep geological units in northeastern British Columbia is basically a safe operation with no potential for acid gas migration to shallower strata, potable groundwater and the surface. In the unlikely event of migration, it would take in the order of several thousand years before acid gas could be detected in the Bullhead aquifer at Boundary Lake–South. Once in the Bullhead aquifer, the acid gas theoretically would have to move for approximately another 15 000 years before reaching the ground surface in the outcrop area of the Bullhead aquifer. At West–Stoddart, updip-migrating acid gas will be captured in neighbouring production wells. However, once production ceases, it will take hypothetically in the order of 90 000 years before acid gas reaches the ground surface. At Ring, acid gas will initially form a gas cap at the top of the aquifer. If the acid gas were to reach the Cretaceous Bullhead aquifer, further migration will be impeded by overlying thick and tight shales. At Caribou–Halfway, vertical migration will be prevented by the effective aquitard characteristics of the Charlie Lake Formation. In addition, low-permeability sediments of the Fernie Group and Fort St. John Group provide additional vertical barriers to flow to shallow aquifers. At Caribou–Debolt, the Montney Formation forms a thick, confining aquitard at the top of the Permo–Carboniferous aquifer, and there are no indications for the possibility of leakage to overlying aquifers. Additional barriers preventing vertical leakage to shallow aquifers or the ground surface are formed by the succession of the Lower Charlie Lake, the Fernie and the Wilrich–Fort St. John aquitards. At Bubbles and Jedney, where acid gas is injected into depleted reservoirs, density and viscosity values show that if the acid gas is injected at the bottom of the reservoir, it will stay there and gradually fill up the reservoir. If the acid gas is injected at a level higher than the bottom of the reservoir, the acid gas will flow to the bottom of the reservoir with a similar effect.

The entire stratigraphic interval from the Debolt Formation to the Baldonnel Formation is overlain by thick shales within the Fernie, Bullhead and Fort St. John groups. There are many barriers to acid gas migration from an injection zone into other strata, and the flow process, if it will ever happen, would take an extremely long time on a geological time scale. Any acid gas plume would disperse and dissolve in formation water during flow on such large time and spatial scales.

Based on available data, it seems there is no potential for acid gas leakage through fractures. However, the possibility for upward leakage of acid gas exists along wells that were improperly completed and/or abandoned, or along wells whose cement and/or tubing have degraded or may degrade in the future as a result of chemical reactions with formation brine and/or acid gas. A review of the status and age of wells that penetrate the respective injection unit at each site shows that most wells were drilled in the 1990s, and that less than 25% of the wells are abandoned. No leakage has been detected and reported; however, the potential for this occurring in the future should be considered by both operators and regulatory agencies.

1 Introduction

During the past decade, oil and gas producers in Western Canada (Alberta and British Columbia) have been faced with a growing challenge to reduce atmospheric emissions of hydrogen sulphide (H_2S), which is produced from 'sour' hydrocarbon pools. Sour oil and gas are hydrocarbons containing H_2S and carbon dioxide (CO_2), which have to be removed before the produced oil or gas is sent to market. Since surface desulphurization through the Claus process is uneconomic, and the surface storage of the produced sulphur constitutes a liability, increasingly more operators are turning to acid gas disposal by injection into deep geological formations. Acid gas is a mixture of H_2S and CO_2, with minor traces of hydrocarbons, which is the byproduct of 'sweetening' sour hydrocarbons. In addition to providing a cost-effective alternative to sulphur recovery, the deep injection of acid gas reduces emissions of noxious substances into the atmosphere and alleviates the public concern resulting from sour gas production and flaring.

The first acid-gas injection operation was approved in 1989 and started in 1990 in Alberta. To date, 45 injection operations have been approved in Alberta and British Columbia; their locations are shown in Figure 1. In Alberta, the Oil and Gas Conservation Act requires operators to apply for and obtain approval from the Alberta Energy and Utilities Board (EUB), the provincial regulatory agency, to dispose of acid gas. The provincial regulatory agency in British Columbia is the Oil and Gas Commission (OGC), which requires similar application and approval procedures. Before approving any operation, the EUB and OGC review the application to maximize conservation of hydrocarbon resources, minimize environmental impact and ensure public safety. To adequately address these matters, the EUB or OGC requires the applicants submit information regarding surface facilities, injection well configurations, operations and geological characteristics of the injection reservoir or aquifer. After approval for acid gas injection is granted, the operators must submit biannual progress reports on the operations to the regulatory agencies.

Although the purpose of the acid-gas injection operations is to dispose of H_2S, significant quantities of CO_2 are being injected at the same time because it is costly to separate the two gases. To date, more CO_2 than H_2S has been injected into deep geological formations in Western Canada. In the context of current efforts to reduce anthropogenic emissions of CO_2, these acid-gas injection operations represent an analogue to geological storage of CO_2. The latter is an immediately available and technologically feasible way of reducing CO_2 emissions into the atmosphere that is particularly suited for land-locked regions located on sedimentary basins, such as the Alberta Basin in Western Canada. Large-scale injection of CO_2 into depleted oil and gas reservoirs and into deep saline aquifers is one of the most promising methods of geological storage of CO_2, and in this respect, it is no different from acid-gas injection operations. However, before implementation of greenhouse gas geological storage, a series of questions needs addressing, the most important ones relate to the short and long-term fate of the injected CO_2. Thus, the study of the acid-gas injection operations in Western Canada provides the opportunity to learn about the safety of these operations and the fate of the injected gases, and represents a unique opportunity to investigate the feasibility of CO_2 geological storage.

Geographically, most of the acid-gas injection operations in Western Canada can be grouped in several clusters (Figure 1). The six operations (seven sites) that are the subject of this report (Ring–Debolt, Boundary Lake South–Belloy, West Stoddart–Halfway, Bubbles–Baldonnel, Jedney–Baldonnel and Caribou–Debolt) form the cluster in the northeastern British Columbia region and inject acid gas into Carboniferous to Triassic strata. An acid-gas injection operation usually is associated with a single gas plant that is the source of the acid gas stream. However, if the acid gas from one plant is injected into different stratigraphic units, or has different compositions (i.e., dry gas, acid gas mixed with water),

separate applications have to be submitted for each case. Hence, an acid gas operation may have more than one injection site. For example, the Norcen–Caribou operation in northeastern British Columbia has two injection sites, at one well the acid gas is being injected into the Triassic Halfway Formation and at the other into the Carboniferous Debolt Formation. At West Stoddart, acid gas is injected through two wells 4.5 km apart into the Halfway Formation, dry acid gas being injected through one and wet acid gas (mixed with produced water) through the other. As a result, this report covers the characterization of eight injection sites at five acid-gas operations in northeastern British Columbia and one in northwestern Alberta.

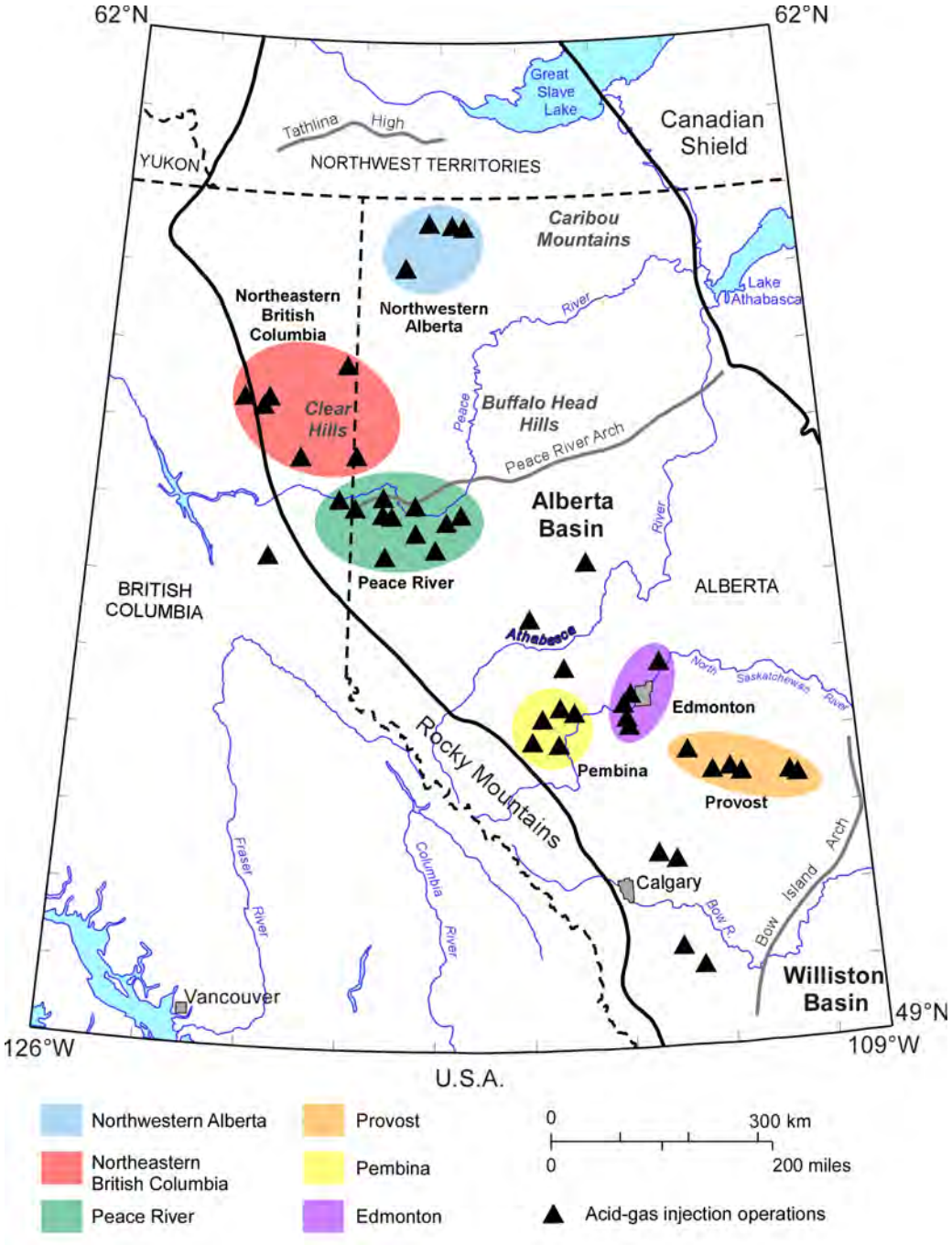

Figure 1. Location of acid-gas injection operation clusters and isolated acid-gas injection operations in Western Canada at the end of 2004.

Previous work characterized the subsurface at the injection sites in the Pembina area of west-central Alberta and the Edmonton area of central Alberta (Characteristics of acid-gas injection operations in Western Canada, final report, S. Bachu et al., prepared for the Acid Gas Management Committee, 2004; Subsurface characterization of the Brazeau Nisku Q Pool reservoir for acid gas injection, S. Bachu et al., prepared for the Acid Gas Management Committee, 2003; Subsurface characterization of the Pembina–Wabamun acid-gas injection area, S. Bachu et al., prepared for the Acid Gas Management Committee, 2003). Future reports are planned for the Provost, Peace River and northwestern Alberta areas (Figure 1). The subsurface characterization of the acid-gas injection operations in northeastern British Columbia will address issues of the disposal and/or sequestration of acid and greenhouse gases, specifically in Carboniferous to Triassic strata. In addition, the southeastern part of the injection area in British Columbia is close to the Peace River Graben/Embayment and therefore might be affected by faulting. The characterization is based on reservoir-scale data and information submitted by the operators to the EUB or OGC, on basin-scale work performed at the Alberta Geological Survey (AGS) during the last 15 years, and on local and reservoir-scale work performed by the AGS specifically for this report.

2 Selection of an Acid-Gas Injection Site

In Alberta, applications for acid gas disposal must conform to the specific requirements listed in Chapter 4.2 of Guide 65 that deals with applications for conventional oil and gas reservoirs (Alberta Energy and Utilities Board, 2000). In British Columbia, organizations have to prepare their applications following the guidelines under section 100 of the *Petroleum and Natural Gas Act*. The selection of an acid-gas injection site needs to address various considerations:

- proximity to sour oil and gas production that is the source of acid gas;
- confinement of the injected gas;
- effect of acid gas on the rock matrix;
- protection of energy, mineral and groundwater resources;
- equity interests;
- wellbore integrity; and
- public safety (Keushnig, 1995; Longworth et al., 1996).

The surface operations and subsurface aspects of acid gas injection depend on the properties of the H_2S and CO_2 mixture, which include, but are not limited to, nonaqueous phase behaviour, water content, hydrate formation and the density and viscosity of the acid gas (Carroll and Lui, 1997; Ng et al., 1999).

2.1 Acid Gas Properties

The acid gas obtained after the removal of H_2S and CO_2 from the sour gas may also contain 1% to 3% hydrocarbon gases and is saturated with water vapour in the range of 2% to 6%. In their pure state, CO_2 and H_2S have similar phase equilibria, but at different pressures and temperatures (Carroll, 1998a). They exhibit the normal vapour/liquid behaviour with pressure and temperature (Figure 2), with CO_2 condensing at lower temperatures than H_2S. Methane (CH_4) also exhibits this behaviour, but at much lower temperatures. The phase behaviour of the acid-gas binary system is represented by a continuous series of two-phase envelopes (separating the liquid and gas phases) located between the unary bounding systems in the pressure–temperature space (Figure 2).

If water is present, both CO_2 and H_2S form hydrates at temperatures up to 10°C for CO_2 and more than 30°C for H_2S (Carroll and Lui, 1997). If there is too little water, the water is dissolved in the acid gas and hydrates will generally not form. However, phase diagrams show that hydrates can form without

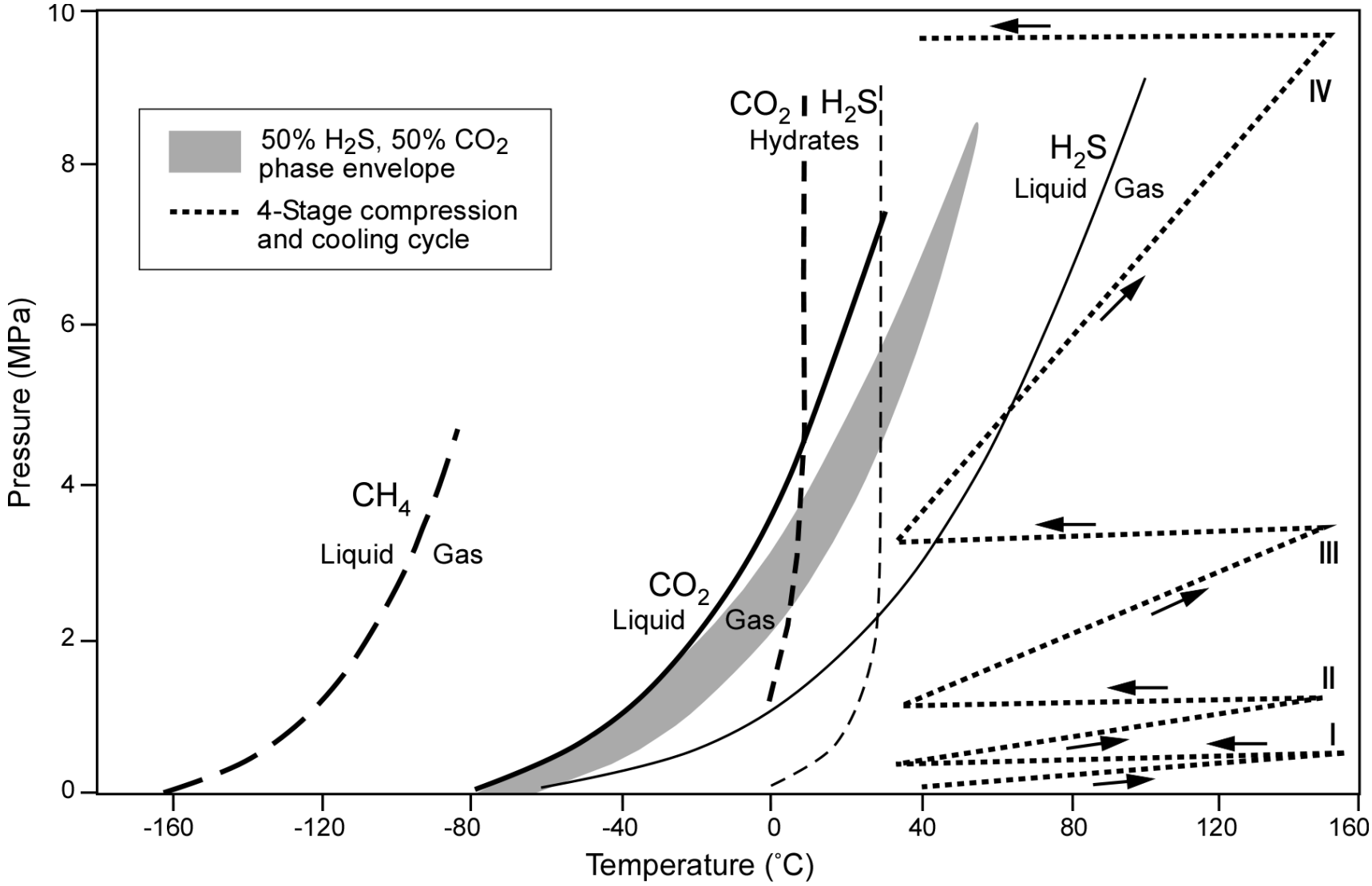

Figure 2. Phase diagrams for methane (CH_4), carbon dioxide (CO_2), hydrogen sulphide (H_2S) and a 50% to 50% acid gas mixture; hydrate conditions for CO_2 and H_2S (after Wichert and Royan, 1996, 1997). A four-stage compression and cooling cycle is also shown.

free water being present (Carroll, 1998a, b); thus, operating above the hydrate-forming temperature is desirable. Unlike the case of hydrocarbon gases, the solubility of water in both H_2S and CO_2, hence in acid gas, decreases as pressure increases up to 3 to 8 MPa, depending on temperature, after which it dramatically increases (Figure 3). The solubility minimum reflects the pressure at which the acid gas mixture passes into the dense liquid phase, where the solubility of water can increase substantially with increasing pressure due to the molecular attraction between these polar compounds (Wichert and Royan, 1996, 1997).

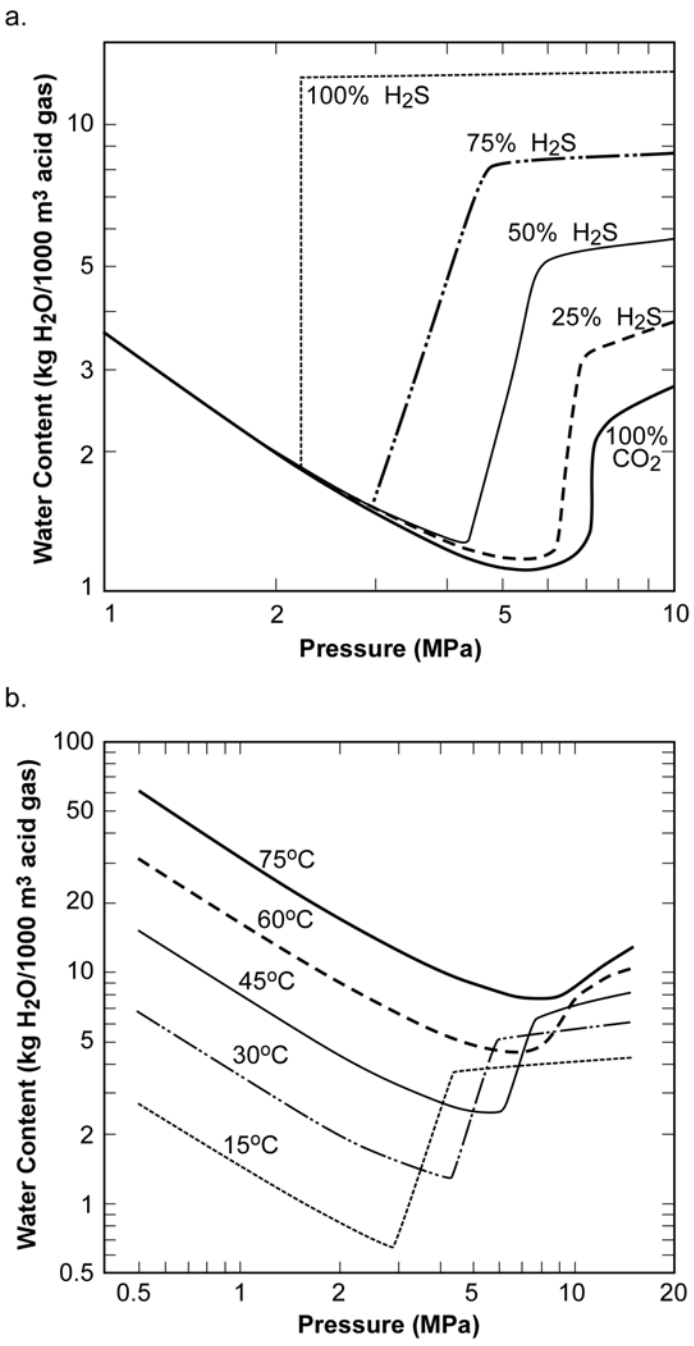

Figure 3. Solubility of water in acid gas as a function of pressure for: a) different acid gas compositions (CO_2 and H_2S) at 30°C, and b) different temperatures for an acid gas with a composition of 49% CO_2, 49% H_2S and 2% CH_4.

To optimize storage and minimize risk, the properties of the acid gas mixture are important in facility design and operation because the acid gas needs to be injected:

(1) in a dense-fluid phase, to increase storage capacity and decrease buoyancy;

(2) at bottomhole pressures greater than the formation pressure for injectivity;

(3) at temperatures generally greater than 35°C to avoid hydrate formation, which could plug the pipelines and injection wells; and

(4) with water content lower than the saturation limit to avoid corrosion.

After separation, the water-saturated acid-gas stream leaves the regeneration unit at 35 to 70 kPa and must be cooled and then compressed for injection to pressures in excess of the subsurface storage formation pressure. Typically, four stages of compression are required to provide the required discharge pressure. By the fourth stage in a cycle, compression will tend to dewater the acid gas up to a maximum pressure between 3 and 5 MPa (Figure 3), if there are no hydrocarbon impurities present. Further compressing the acid gas to higher pressures increases the solubility of water in the acid gas, such that any residual excess water dissolves into the acid gas and more than counteracts the decrease in solubility due to inter-stage cooling. To avoid pump cavitation, the acid gas must not enter the two-phase region during compression. Once the acid gas is compressed, it is transported through a pipeline to the injection wellhead usually a short distance from the gas plant. The high pressures after the fourth compression stage stabilize, upon cooling, the high-density liquid phase of the acid gas.

Although a number of safety valves are always installed, both in the well and in the surface facilities, to isolate the containment lines for the acid-gas injection system into small volumes, the release of even small volumes of acid gas can be harmful. Consequently, the operators are required to have a detailed emergency response plan (ERP) in case of leakage that may affect humans. An emergency planning zone (EPZ) (i.e., area of land that may be affected by the release of H_2S) is defined around the sour gas facility.

2.2 Criteria for Site Selection

The general location of an acid-gas injection well is often influenced by the proximity to sour oil or gas production facilities that are the source of acid gas. The specific location is based on a general assessment of the regional geology and hydrogeology to evaluate the potential for containment and avoidance of leakage (Longworth et al., 1996) and includes:

1) Size of the injection zone to confirm it is large enough to volumetrically hold all of the injected acid gas over the lifetime of the project;
2) Thickness and extent of the overlying confining layer (cap rock) and any stratigraphic traps or fractures that may affect its ability to contain the acid gas;
3) Location and extent of the underlying or lateral bounding formations;
4) Folding or faulting in the area and an assessment of seismic (neotectonic) risk;
5) Rate and direction of the natural flow system to assess the potential for migration of the injected acid gas;
6) Permeability and heterogeneity of the injection zone;
7) Chemical composition of the formation fluids (water for aquifers, oil or gas for reservoirs);
8) Formation temperature and pressure;
9) Analyses of formation and cap rock drillcore (if available); and

10) A complete and accurate drilling history of offsetting wells within several kilometres of the injection well to identify any wells or zones that may be impacted by the injected acid gas.

Knowledge of the geological setting and characteristics is critical to assess the integrity of the host formation or reservoir and the short and long-term fate of the injected acid gas. Of particular importance are potential migration pathways from the injection zone to other formations, shallow groundwater and/or the surface. These potential pathways are of three types: the cap rock pore space ('membrane' type), natural and/or induced fractures ('cracks') through the confining strata, and improperly completed and/or abandoned wells ('punctures'). To avoid diffuse gas migration through the cap rock pore space, the difference between the pressure at the top of the injection aquifer or reservoir and the pressure in the confining layer must be less than the cap rock threshold displacement pressure, which is the pressure needed for the acid gas to overcome the capillarity barrier and displace the water that saturates the cap rock pore space. To avoid acid gas migration through fractures, the injection zone must be free of natural fractures, and the injection pressure must be below a certain threshold to ensure fracturing is not induced. The maximum bottomhole injection pressure is set by regulatory agencies at less than 90% of the fracturing pressure of the reservoir rock. If injection takes place into a depleted oil or gas reservoir, the maximum bottomhole injection pressure is usually set at no more than the initial reservoir pressure. From this point of view, injection into a depleted oil or gas reservoir has the advantages of injection pressures being low and wells and pipelines already in place (Keushnig, 1995). Without site-specific tests, the pressures are limited by pressure-depth correlations, based on basin-wide statistical data for the Alberta Basin. An evaluation of the stress regime at the acid-gas injection sites in Western Canada was performed to assess the relationship between the maximum allowed wellhead injection pressures and the rock fracturing threshold pressures (Characteristics of acid-gas injection operations in Western Canada, Final Report, S. Bachu et al., prepared for the Acid Gas Management Committee, 2004). This study showed that maximum bottomhole injection pressures are well below the minimum horizontal stress, hence lower than the fracture pressure. Thus, there is no danger of opening existing fractures or of inducing new ones.

2.3 Issues

For the most part, critical issues are environmental and safety-related, and they directly affect the economics of acid gas injection. Acid gas leaks can result in loss of life or contamination of the biosphere and atmosphere. Surface safety is addressed through engineering, installation of safety valves and monitoring systems, and emergency procedures for the case of H_2S leaks. Subsurface issues are of two interrelated categories: the effect of the acid gas on the rock matrix and well cements, and plume containment.

When the acid gas contacts the subsurface formation, it will readily dissolve in the formation water in an aquifer, or connate water in a reservoir, and create weak carbonic and sulphuric acids. This leads to a significant reduction in pH that accelerates water-rock reactions. Depending on mineralogy, mineral dissolution or precipitation may occur, affecting the porosity and permeability of the hostrock. The fact that both CO_2 and H_2S are dissolving in the formation water leads to some complex reaction paths where carbonates precipitate and dissolve, and pyrite/pyrrhotite precipitates (Gunter et al., 2000; Hitchon et al., 2001). Dissolution of some of the rock matrix in carbonate strata, or of the carbonates surrounding the sand grains in sandstone units results in lower injection pressures in the short term as a result of increased permeability. A major concern with the injection process is the potential for formation damage and reduced injectivity near the acid gas scheme. The reduction in injectivity could possibly be the result of fines migration, precipitation and scale potential, oil or condensate banking and plugging, asphaltene and elemental sulphur deposition, and hydrate plugging (Bennion et al., 1996).

Cement compatibility with the acid gas, primarily in the injection well, but also in neighbouring wells, is crucial for safety and containment. For example, a noncarbonate and calcium cement blend shattered when tested in an acid gas or CO_2 stream for several weeks (Whatley, 2000; Scherer et al., 2004). Thus, the compatibility of the acid gas with the cement that bonds the casing to the formation must be tested at a minimum. While the cement for the newly implemented acid-gas operation can be tested and properly selected prior to drilling, the cements in nearby wells are already in place and their condition is largely unknown. Some of these wells could be quite old (several decades), with the cement already in some stage of degradation as a result of brine composition. The acid gas, when reaching these wells, may enhance and hasten the cement degradation, leading to possible leaks through the well annulus and/or along casing.

If the acid gas is injected into the originating or other oil or gas pool, the main concern is the impact on further hydrocarbon recovery from the pool and acid gas production at the wellhead, although the injection operation and enhanced oil recovery may prove successful, like in the case of the Zama X2X pool (Davison et al., 1999). In fact, this operation has been proven so successful that Apache Canada Ltd. applied in 2004 for acid-gas miscible flooding of the Zama Z3Z pool for enhanced oil recovery and intends to use acid-gas enhanced oil recovery at several other pools over the coming years. If the gas mixture is injected into an aquifer, the degree to which it forms a plume and migrates from the injection well depends on various factors, including pressure and temperature, solubility, interplay between driving forces like buoyancy and aquifer hydrodynamics, and aquifer heterogeneity, which controls gravity override and viscous fingering.

The fate of the injected acid gas in the subsurface is not known, because subsurface monitoring is not currently required and is difficult and expensive. Only the wellhead gas composition, pressure, temperature and rate must be reported to the regulatory agencies EUB and OGC, respectively. Thus, a proper understanding of the geology and hydrogeology of the acid-gas injection unit (reservoir or aquifer) is critical in assessing the fate of the injected acid gas and the potential for migration and/or leakage into other units.

3 Basin-Scale Setting of Acid-Gas Injection Sites in Northeastern British Columbia

The six acid-gas injection operations that are the subject of this report are located in the northwestern part of the Alberta Basin (Figure 1) in northeastern British Columbia and northwestern Alberta, and will be referred to as the northeastern British Columbia study area in this report. The Phanerozoic rock record has a southwestward-thickening sedimentary wedge reaching a thickness of over 6 km close to the limit of the disturbed belt (LDB) of the Rocky Mountains (Wright et al., 1994). Toward the northeast, the sedimentary wedge laps onto the Canadian Shield, where it is terminated by erosion or nondeposition. The geology, stratigraphy and hydrostratigraphy of the sedimentary succession in the northern part of the Alberta Basin (north of the Peace River Arch, Figure 4) are different from those south of the Peace River Arch (Figure 5) because of differences in the tectonostratigraphic evolution, with corresponding effects on the flow of formation waters (Bachu, 1999). This report presents the geology and hydrostratigraphy of the Alberta Basin with emphasis on the area north of the Peace River Arch. The geology is based on Porter et al., (1982), Ricketts (1989) and Mossop and Shetsen (1994) (and references cited therein), and the hydrogeology follows work by Bachu (1997, 1999).

Of the six acid-gas injection operations in the northeastern British Columbia area, two inject into the Mississippian Rundle Group (Debolt Formation), one into the Permian Belloy Formation, two into the Triassic Halfway Formation, and two into the Triassic Baldonnel Formation (Figure 4). Therefore, the Mississippian to Jurassic succession will be discussed in more detail within the basin-scale framework.

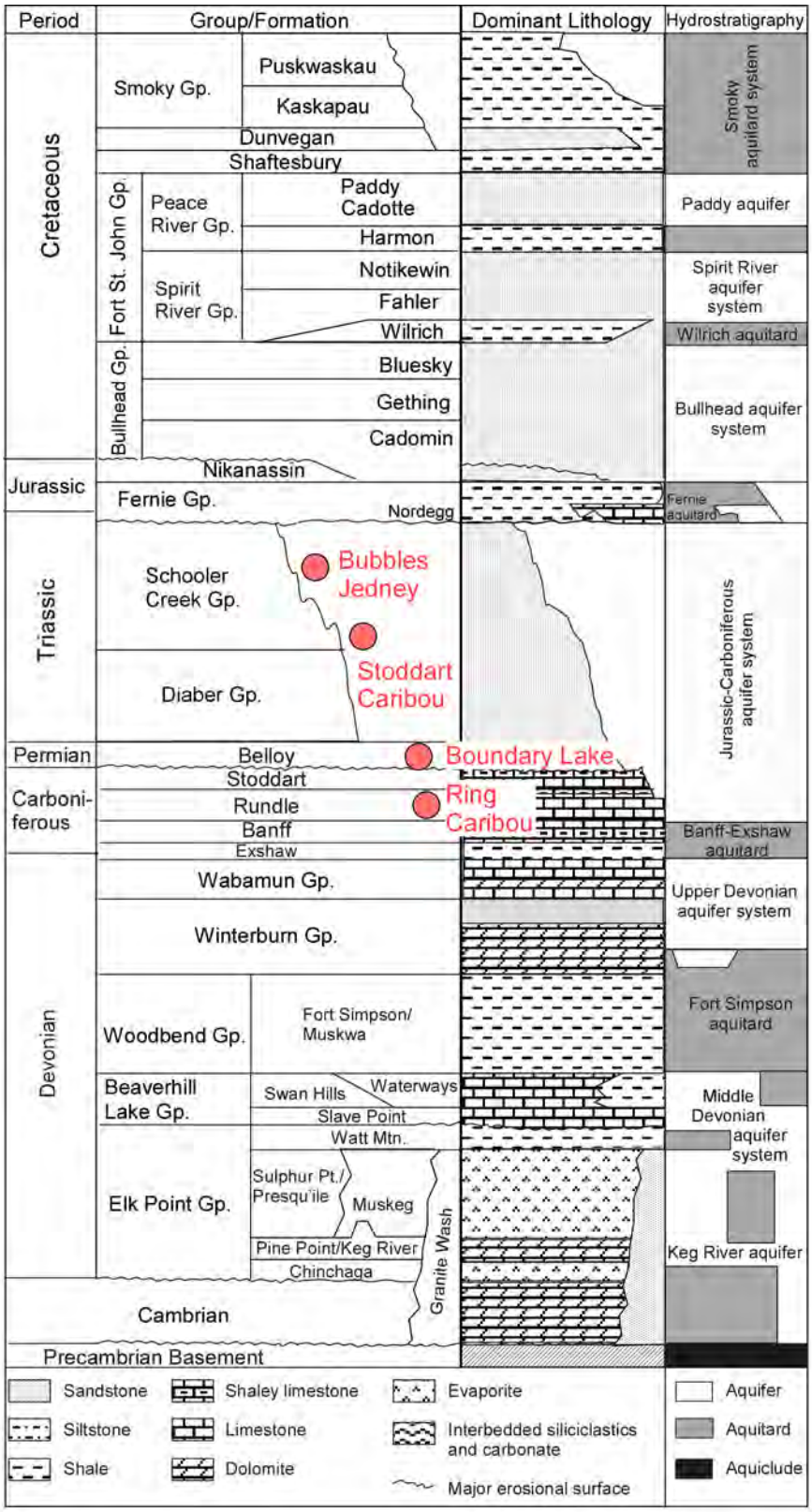

Figure 4. Basin-scale stratigraphic and hydrostratigraphic delineation and nomenclature, as well as general lithology for the northern part of the Alberta Basin. Acid-gas injection horizons are indicated by red circles.

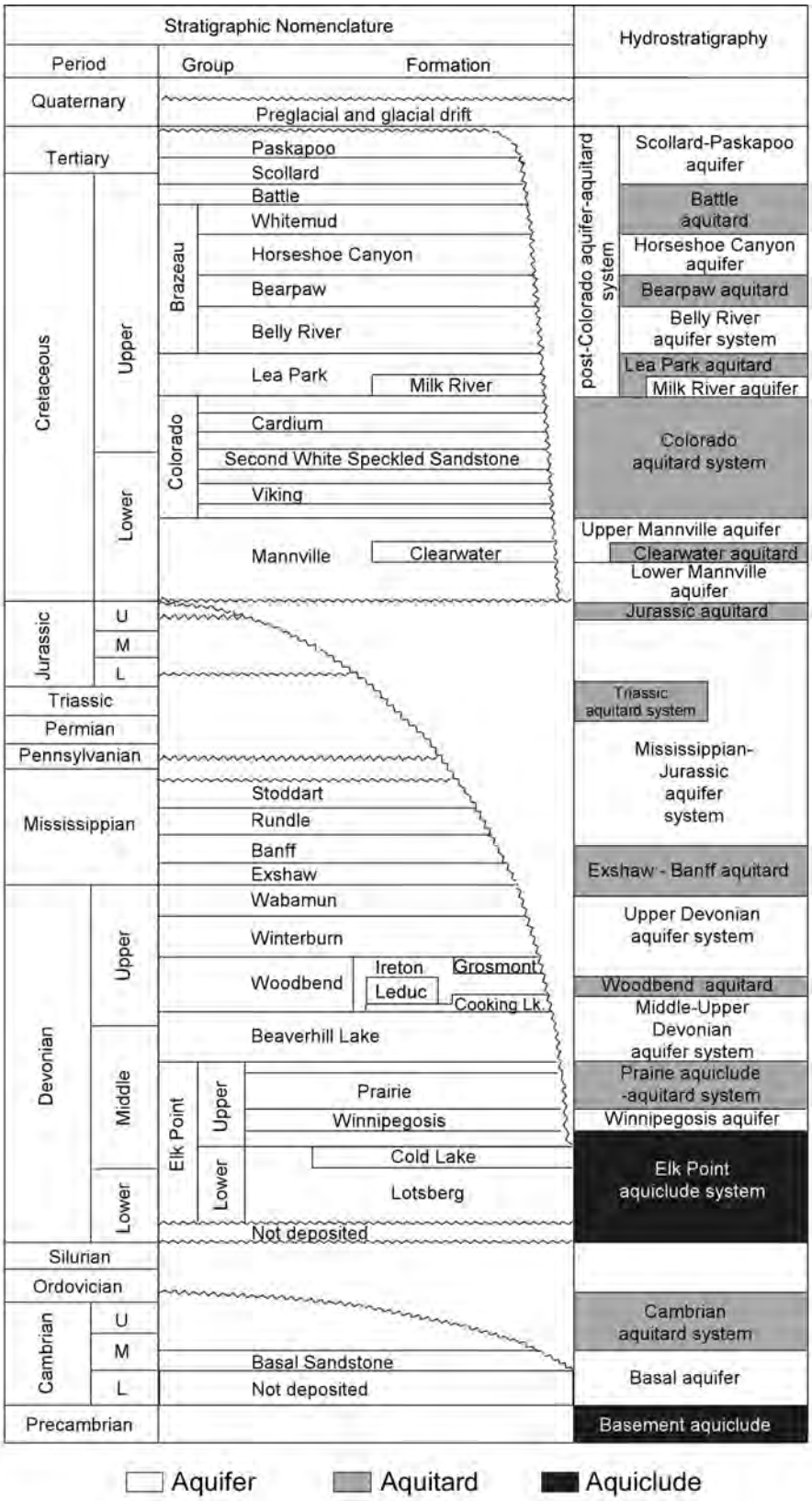

Figure 5. Basin-scale stratigraphic and hydrostratigraphic delineation and nomenclature for the southern and central parts of the Alberta Basin (after Bachu, 1999).

Different stratigraphic and hydrostratigraphic nomenclature is used in the various parts of the Alberta Basin (Figures 4 and 5). In the following section, common stratigraphic names used in the northeastern part of British Columbia will be shown in parentheses following the general stratigraphic classification used, for example, in the Atlas of the Western Canada Sedimentary Basin (Mossop and Shetsen, 1994).

3.1 Basin Geology and Hydrostratigraphy

The Alberta Basin sits on a stable Precambrian Platform and is bound by the Rocky Mountain Trench to the west and southwest, the Tathlina High to the north and the Canadian Precambrian Shield to the northeast (Figure 1). The Bow Island Arch separates the Alberta Basin from the Williston Basin to the southeast. The basin was initiated during the late Proterozoic by rifting of the North American craton. It consists at the base of a Middle Cambrian to Middle Jurassic passive-margin succession dominated by shallow-water carbonates and evaporites with some intervening shales (Porter et al., 1982). From the Late Jurassic to Early Tertiary, accretion of allochthonous terranes to the western margin of the proto North American continent during the Columbian and Laramide orogenies pushed sedimentary strata eastward, resulting in the Rocky Mountains thrust and fold belt, and creating conditions for foreland-basin development east of the deformation front. Because of lithospheric loading and isostatic flexure, the Precambrian basement tilted westward, with a gentle slope of <4 m/km in the east near the Canadian Shield, becoming steeper westward, to >20 m/km near the deformation front. Because of this tilting and significant pre-Cretaceous erosion, progressively older Jurassic to Middle Devonian strata subcrop from west to east at the sub-Cretaceous unconformity. Deposition during the foreland stage of basin development was dominated by synorogenic clastics, mainly muds and silts, derived from the evolving Cordillera. The basin fill attained maximum thickness and burial during the Laramide Orogeny in the Paleocene. Tertiary to Recent erosion since then has removed an estimated 2000 to 3800 m of sediments in the southwest (Nurkowski, 1984; Bustin, 1991). As a result of these depositional and erosional processes, the undeformed part of the Alberta Basin comprises a wedge of sedimentary rocks increasing in thickness from zero, at the Canadian Shield in the northeast, to close to 6000 m in the southwest at the thrust and fold belt. The present topography of the undeformed part of the basin has a basin-scale trend of decreasing elevations from highs in the 1200 m range in the southwest to lows around 200 m in the north-northeast at Great Slave Lake, which is the lowest topographic point in the basin.

Hydrostratigraphically, the Precambrian crystalline basement constitutes an aquiclude, except possibly for fault and shear zones that may have served as conduits for fluid flow and may still be active today. Thin, diachronous basal sandstone units (Basal Sandstone in the south and Granite Wash in the area of the Peace River Arch) cover the Precambrian basement. As a result of pre-Middle Ordovician erosional bevelling and of major pre-Middle Devonian erosion, Cambrian strata are eroded near the Peace River Arch. Ordovician strata are present only in the southeast along a narrow band of the basin edge, and Silurian strata are completely absent. The Cambrian Basal Sandstone unit forms the Basal Cambrian aquifer, whereas the shale–dominated Cambrian and Ordovician strata form the Cambrian aquitard system.

A Middle Devonian interbedded succession of low-permeability anhydritic red beds and carbonates, halite and argillaceous carbonates of the Lower Elk Point Group overlies the Cambrian units or Granite Wash detritus, and forms the Elk Point aquitard system. The overlying platformal and reefal carbonates of the Upper Elk Point Group Keg River Formation form the Keg River aquifer. This unit is overlain over most of the basin by the thick evaporites of the Prairie Formation (Muskeg Formation), followed by shales of the Watt Mountain Formation, which together form the Prairie aquitard system. In the northern part of the Alberta Basin, the time-equivalent Sulphur Point/Presqui'ile Barrier reef complex forms a carbonate aquifer on top of the Keg River aquifer. Because of variable lithology (mixed siliciclastics and evaporites) of the Prairie Formation in the western part of the basin, and salt dissolution along the eastern basin

edge, this hydrostratigraphic system has aquiclude characteristics where the salt is present and aquitard characteristics where the salt is absent, or present only in minor quantities.

The Elk Point Group is unconformably overlain by the Middle Devonian Beaverhill Lake Group. It has been subdivided into the Slave Point, Swan Hills and Waterways formations. Reef growth occurred along the margins of the Slave Point platforms (e.g., fringing the Peace River landmass). The platformal and reefal carbonates of the Slave Point and Swan Hills formations together form the main aquifer unit within the Beaverhill Lake Group. The basinal deposits of the overlying Waterways Formation have, depending on location and dominant lithology, either aquifer or aquitard characteristics.

The Upper Devonian Woodbend Group conformably overlies the Beaverhill Lake Group. Extensive platform carbonates and associated reefs of the Cooking Lake and Leduc formations were deposited contemporaneously with thick, organic-rich shales of the Majeau Lake Member and Duvernay Formation. Calcareous shales and argillaceous limestones of the Ireton (Fort Simpson/Muskwa) Formation cover the Leduc reefs and associated shale units. In northeastern Alberta, a large carbonate shelf platform, the Grosmont Formation, developed over the prograding Ireton Formation. Hydrostratigraphically, the Cooking Lake and Leduc carbonates form the Cooking Lake aquifer, which together with the aquifers of the underlying Beaverhill Lake Group, form the Middle–Upper Devonian aquifer system (Figure 5). The Ireton, Duvernay and Majeau Lake (Fort Simpson/Muskwa) formations form the Ireton aquitard in south and central Alberta. The Grosmont Formation is an aquifer included in the overlying Upper Devonian aquifer system because of its hydraulic continuity with and influence on the Winterburn and Wabamun aquifers in the area of subcrop in the northeast (Anfort et al., 2001). The Woodbend Group in the northwestern part of the Alberta Basin is formed dominantly by the Fort Simpson/Muskwa Formation shales, which form the Fort Simpson aquitard – equivalent to the Ireton aquitard in the rest of the basin. The Woodbend Group is conformably overlain by the Winterburn Group, which has been subdivided into the Nisku, Calmar and Graminia formations (Jean–Marie, Kakisa–Redknife and Trout River). The Nisku Formation at the base of the Winterburn Group comprises fossiliferous shelf and reef carbonates in southern and northeastern Alberta with a transition to more open-marine, deeper-water carbonates and shales in west-central Alberta. It is followed by widespread dolomitic silts and shales of the Calmar Formation. The overlying Graminia Formation consists of transgressive shallow shelf carbonates of the Blue Ridge Member and a northwestward thickening wedge of the "Graminia Silt" (Burrowes and Krause, 1987).

The Winterburn Group is conformably overlain by carbonates and evaporites of the Wabamun Group. Wabamun carbonates consist of dolomitic limestones and calcareous dolomites, with dolomites predominating in the lower and middle parts of the group and limestones in the upper part. In southeastern Alberta, these carbonates interfinger with peritidal evaporites (mainly anhydrite) of the Stettler Formation. Close to the end of Wabamun time, open marine limestones of the Big Valley Formation were deposited over most of Alberta.

The widespread platform carbonates, interspersed with minor shales of the Winterburn and Wabamun groups at the basin scale, form the Upper Devonian aquifer system (Figures 4 and 5). In the northeastern corner of the Alberta Basin, the lithology of both the Wabamun and Winterburn groups is dominated by shales, locally forming the Besa River aquitard. Reefs of the underlying Leduc Formation breach the Ireton aquitard in places, thus establishing local hydraulic communication between the Middle–Upper Devonian aquifer system and the overlying Upper Devonian aquifer system, including the Grosmont aquifer (Bachu and Underschultz, 1993; Rostron and Tóth, 1996, 1997; Hearn and Rostron, 1997; Anfort et al., 2001).

The thin, organic-rich, competent shales of the Exshaw Formation were unconformably deposited on top of the Wabamun Group during the Late Devonian to Early Mississippian and form the base of the Carboniferous succession. The Carboniferous comprises three main lithofacies associations (Richards et al., 1994) (Figure 6). The lower association is represented by interbedded shales and carbonates of the Banff Formation, which was deposited in a basin to slope environment, generally thickening to the southwest (basinward). Upward and northwestward, these basin and slope deposits develop into a second assemblage of platform and ramp carbonates of the Rundle Group. The upper lithofacies association consists of mixed siliciclastics and carbonates of the Stoddart Group, which were deposited in a slope to continental setting.

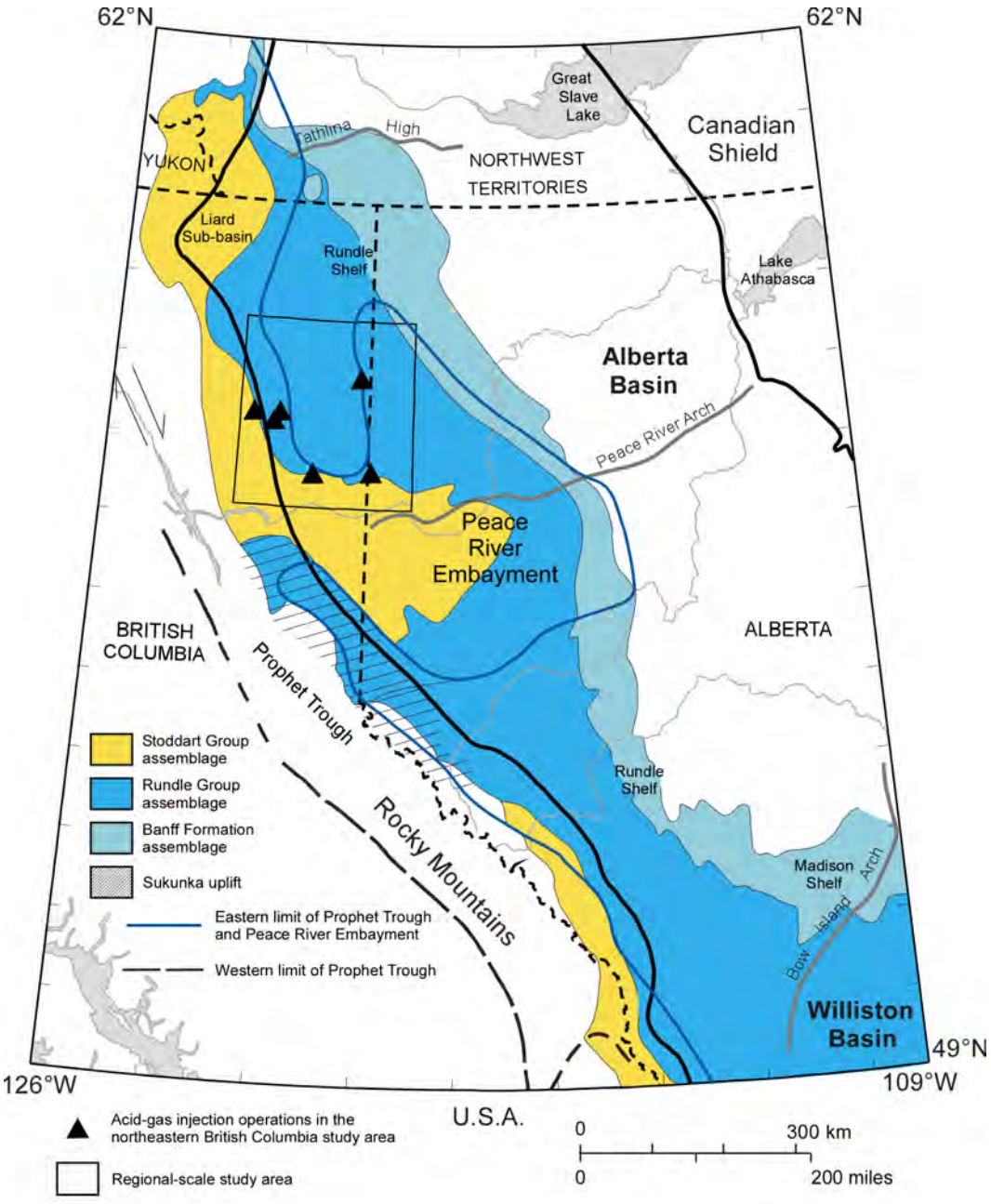

Figure 6. Tectonic elements and Carboniferous lithofacies assemblages in the Alberta Basin (modified from Richards et al., 1994).

The Permian succession unconformably overlies in most places the Carboniferous strata and consists generally of marine carbonaceous, phosphatic and dolomitic sandstones. Permian sediments were deposited in a shallow-marine shelf setting within the Ishbel Trough, the Liard Sub-Basin (Ishbel Group), and in the Peace River Embayment (Belloy Formation) (Figure 7). The depositional extent of Permian sediments is similar, yet slightly larger, to the underlying Carboniferous Stoddart Group (Figure 6). This is the result of the tectonic setting during the Permian, where the Stoddart Group sediments filled the Peace River embayment and the Belloy Formation was draped over it. Generally, the Permian is unconformably overlain by Lower Triassic strata; however, enhanced sub-Mesozoic erosion locally resulted in an unconformable contact between Permian and Cretaceous strata.

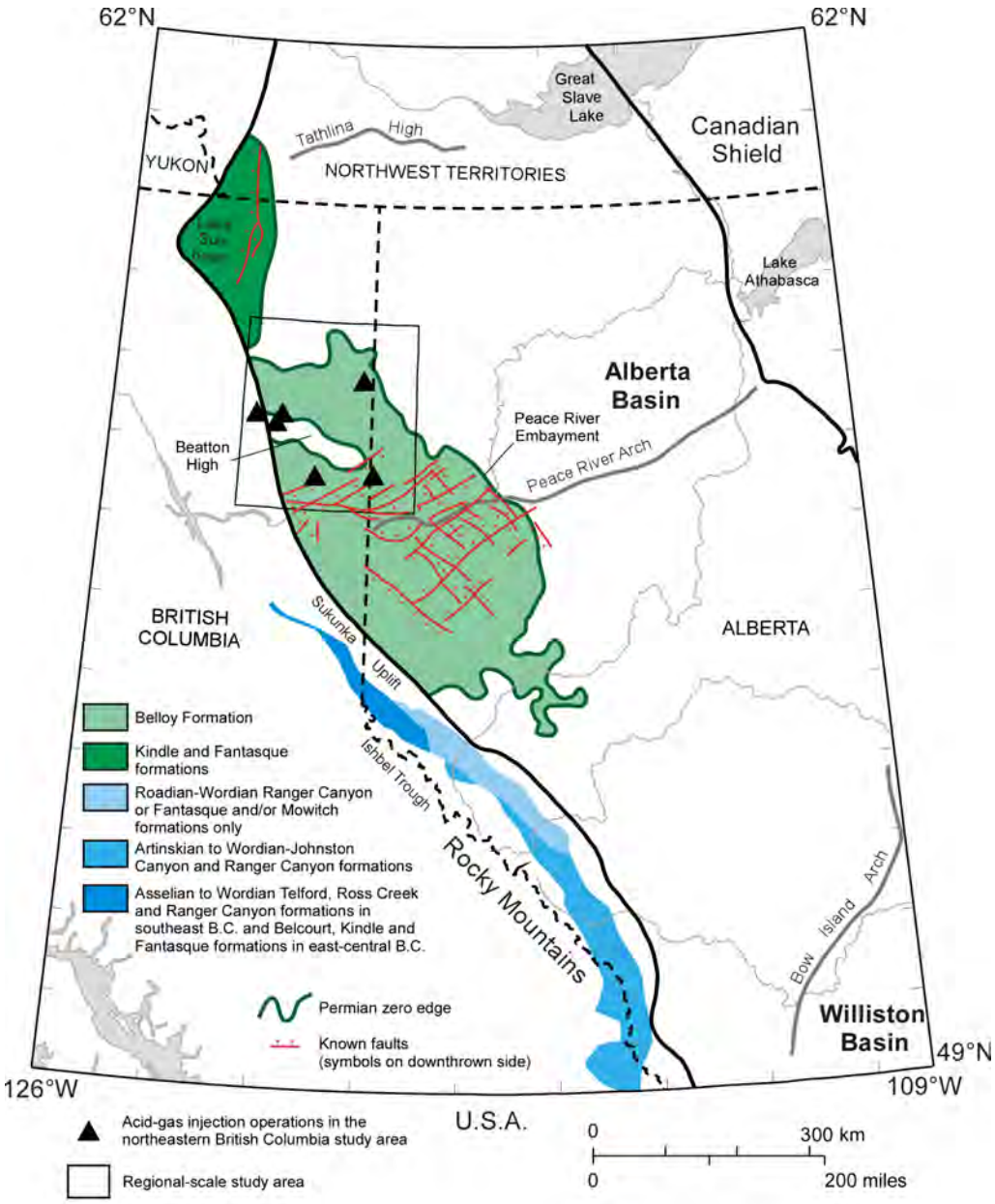

Figure 7. Tectonic elements and lithofacies distribution of Permian strata in the Alberta Basin. Note the difference between the clastic-dominated Belloy and Kindle formations in the Peace River and Liard sub-basin areas, versus the carbonate-dominated deposition in the Ishbel Trough. Injection occurs in the clastic-dominated Belloy Formation (modified after Henderson et al., 1994).

In the Alberta Basin, Triassic strata were deposited mainly in one large central sub-basin, the Peace River Embayment, which extended eastward from the western ocean onto the North American craton (Figure 8). The embayment was connected to the Liard Sub-Basin in the north and to deposits in the Rocky Mountains in the south. The Triassic can be subdivided into the Diaber Group and the Schooler Creek Group. Triassic sediments in the Alberta Basin were deposited as a series of three major transgressive-regressive third or fourth-order cycles (Gibson et al., 1989; Edwards et al., 1994). The first (lowermost) cycle involves sediments deposited along a tidally influenced, deltaic coastline with corresponding deep-marine and distal shelf deposits. The depositional environments of the second cycle show similarities to barrier-island/tidal coastlines, such as those along the modern Texas Gulf coast or the Persian Gulf. The third major cycle is dominated by shallow-water carbonates.

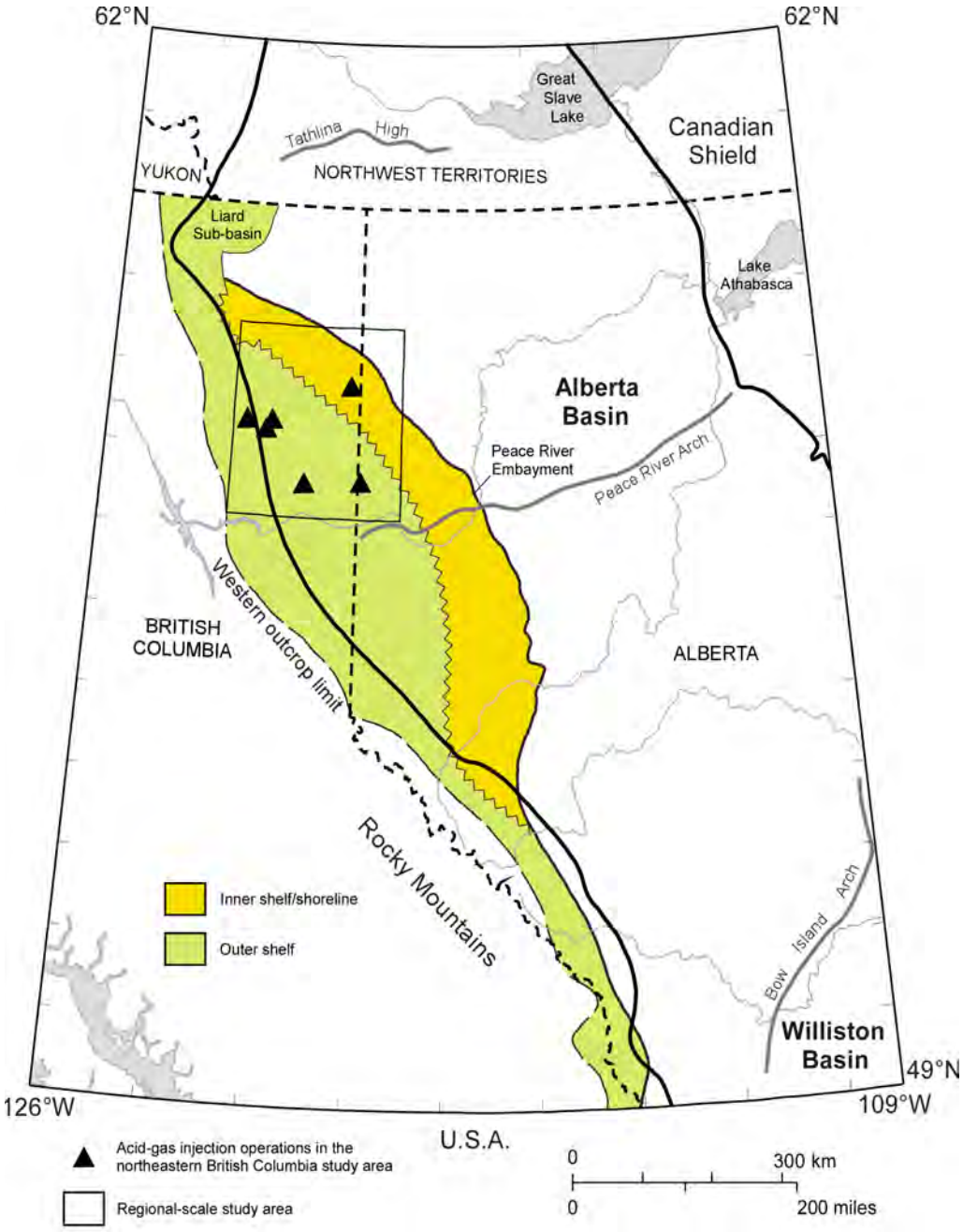

Figure 8. Depositional setting of Triassic sediments in the Alberta Basin (modified from Edwards et al., 1994).

The Lower to lower Upper Jurassic Fernie Group unconformably overlies the Triassic. Pre-orogenic, Lower Jurassic strata are characterized by thin platform limestones and phosphates and organic-rich shales with many disconformities (Smith, 1994). Upper Jurassic strata of Alberta and northeastern British Columbia record the early stages of the Columbian Orogeny (Smith, 1994). The first clear evidence of orogenic activity is found in lower Upper Jurassic strata, marked by westerly derived fine sediments. The Fernie Group is overlain by the Late Jurassic/Early Cretaceous sandstones and minor shales of the Minnes Group and Nikanassin Formation.

Hydrostratigraphically, the shales of the Exshaw Formation and the shale-dominated lower part of the Banff Formation form the Banff–Exshaw aquitard (Figure 4). At the basin scale, the entire Upper Banff to Lower Jurassic succession forms the Jurassic–Carboniferous aquifer system. Regionally important aquitards occur within the Triassic. The Jurassic shales form the Fernie aquitard, whereas the uppermost Jurassic sandstone units are part of the overlying Cretaceous Bullhead aquifer.

Uplift, exposure and erosion of older strata during the Late Jurassic to Early Cretaceous (Columbian Orogeny) resulted in a major erosional unconformity. Along this pre-Cretaceous unconformity, southwestward-dipping strata of Jurassic to Cambrian age subcrop below the Cretaceous Mannville Group, becoming progressively older to the northeast (Figure 9).

The Cretaceous strata represent a major period of subsidence and sedimentation and are divided into several depositional successions. The Mannville Group and age-equivalent strata (Bullhead and Fort St. John groups) are the oldest Cretaceous rocks in the Alberta Basin. The Mannville Group strata, the depositional response to the Columbian Orogeny (Porter et al., 1982), consist of fluvial and estuarine valley-fill sediments, as well as sheet sands and shales deposited by repeated marine transgressive-regressive events. The Lower Mannville Group was deposited over a broad unconformity surface cut by big valley systems. In the southern part of the basin, the Mannville Group forms at the basin-scale a single sandstone-dominated aquifer, while in the central-to-northern part, the Lower and Upper Mannville aquifers are separated by the intervening shale-dominated Clearwater (Wilrich) aquitard. In the northern part of the Alberta Basin, the entire Mannville Group consists of marine shales (Buckinghorse Formation) and forms the lower portion of the Fort St. John aquitard. At a local scale, the lithology and, therefore, the hydrostratigraphy of the Mannville Group are much more complex, with lateral and vertical discontinuities caused by siliciclastic deposition in a fluvio-deltaic environment.

The overlying Colorado Group (Upper Fort St. John Group, Smoky Group) was deposited during a lull in tectonic plate convergence when the basin had a widespread marine transgression. Colorado strata consist predominantly of thick shales that form aquitards, within which there are isolated, thin, sandy units that form aquifers. Some of the sandstones, like the Viking (Paddy–Cadotte), Dunvegan and Cardium formations, are laterally extensive. Others are more restricted areally, like the Second White Speckled Sandstone, which is present only in the southern part of the Alberta Basin.

Post-Colorado Cretaceous and Tertiary strata were deposited during the Laramide Orogeny and the subsequent period of tectonic relaxation, and consist of eastward-thinning, nonmarine clastic wedges intercalated with argillaceous sediments. This cyclicity is best developed in the southern and southwestern parts of the basin, where the Milk River, Belly River, Horseshoe Canyon and Scollard–Paskapoo formations form the clastic wedges, and the Lea Park, Bearpaw, Whitemud and Battle formations comprise the intervening shales. In the central and northern parts of the basin, most of these cycles are absent due to either nondeposition or erosion. The clastic wedges form aquifers, while the intervening shales form aquitards. Varieties of pre-glacial, glacial and post-glacial surficial deposits of Quaternary age overlie the bedrock over the entire basin.

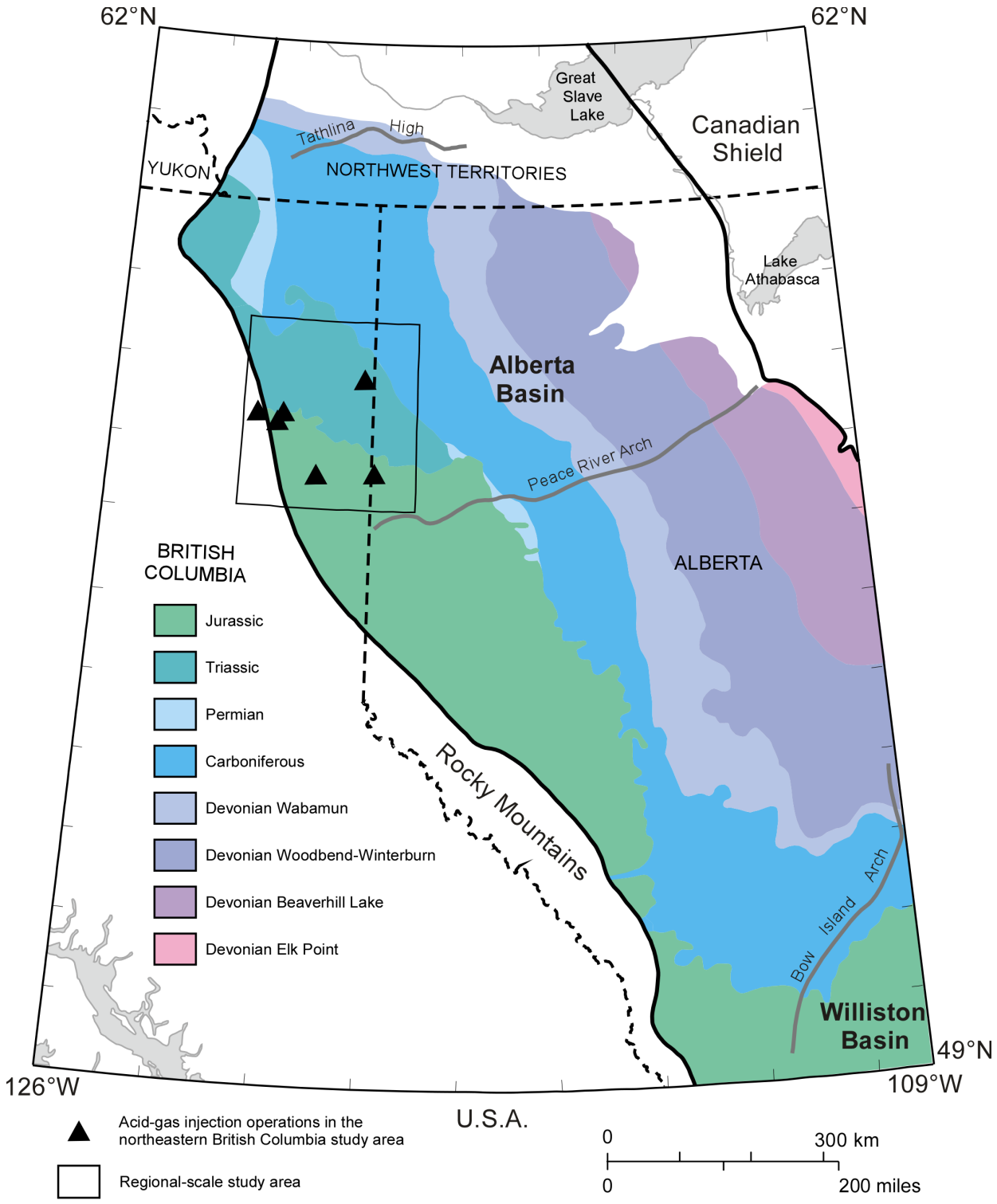

Figure 9. Structure map of the sub-Cretaceous unconformity surface. Colour coding indicates the age and lithology of strata underlying the unconformity. The strata become progressively older to the north and east (from Hayes et al., 1994).

3.2 Basin-Scale Flow of Formation Water

The flow of formation water in the Alberta Basin is well understood at the basin scale because of work performed over the last three decades by various researchers, starting with the pioneering work of Hitchon (1969a, b) and ending with a comprehensive summary and synthesis of previous work by Bachu (1999). The flow in the deformed part of the basin (the Rocky Mountains and the thrust and fold belt) seems to be driven by topography in local-scale systems. Recharge takes place at the surface throughout the entire system, with discharge as springs, in lakes and along river valleys. In most cases, fresh groundwater of meteoric origin discharges along various faults and thrust sheets, such as the Brazeau, Burnt Timber and McConnell, that separate the flow systems in the Rocky Mountain thrust and fold belt from the flow systems in the undisturbed part of the basin (Wilkinson, 1995; Grasby and Hutcheon, 2001). In the undeformed part of the Alberta Basin (from the eastern edge of the deformation front in the southwest to the edge of the exposed Precambrian Shield in the northeast), the flow regime is relatively complex due to basin evolution, geology, lithology and hydrostratigraphy, resulting in the interaction of various flow-driving mechanisms. The flow of formation water at the basin-scale is discussed separately for the south-central and northern parts of the Alberta Basin because of distinct differences in hydrogeology between areas south and north of the Peace River Arch.

3.2.1 Flow of Formation Water in the South-Central Part of the Alberta Basin

Various flow-driving mechanisms are active in the south-central part of the Alberta Basin, resulting in complex flow patterns in the different hydrostratigraphic units.

3.2.1.1 Topography-Driven Flow

The flow of formation water is driven by topography in local, intermediate, regional and basin-scale systems, from regions of recharge at high elevations to regions of discharge at low elevations. A basin-scale flow system is recharged with fresh meteoric water in the south where Devonian, Carboniferous and Cretaceous aquifers crop out at high elevation in Montana. Water flows northward and discharges at outcrop of the Grosmont aquifer along the Peace River (Figure 10). The aquifers in this flow system are the Upper Devonian and Carboniferous–Jurassic in the region of respective subcrop at the sub-Cretaceous unconformity, the Grosmont and the Lower Mannville. They are all in hydraulic contact in southeastern and central Alberta due to the absence of intervening aquitards because of pre-Cretaceous erosion (Figures 5 and 10). In this basin-scale flow system, low hydraulic heads corresponding to discharge areas propagate far upstream, inducing widespread, subhydrostatic pressures as a result of high aquifer permeability downstream (Anfort et al., 2001).

3.2.1.2 Flow Driven by Erosional and/or Post-Glacial Rebound

During sediment loading, water flows vertically in compacting sand-shale successions out of overpressured shaly aquitards into the adjacent sandstone aquifers (expulsion), then laterally in the sandstones outward to the basin edges. Directions of water movement are reversed during erosional unloading, and transient effects last for long periods in rocks characterized by very low hydraulic diffusivity. Significant underpressuring in shales drives the flow of formation waters in the intervening aquifers laterally inward from the permeable basin edges, and vertically into the rebounding shaly aquitards (‘suction’). This type of flow is present at both local and large scales in the southern and southwestern part of the Alberta Basin in the siliciclastic Mannville, Viking, Second White Speckled Sandstone, Belly River and Horseshoe Canyon aquifers in the Cretaceous succession (Figures 5 and 10) (Tóth and Corbet, 1986; Parks and Tóth, 1993; Bachu and Underschultz, 1995; Anfort et al., 2001; Michael and Bachu, 2001). The flow is driven by erosional and post-glacial rebound in the thick intervening shales of the Colorado Group, and Lea Park, Bearpaw and Battle formations, as a result of up to 3800 m of sediments having been eroded in the area since the peak of the Laramide Orogeny some

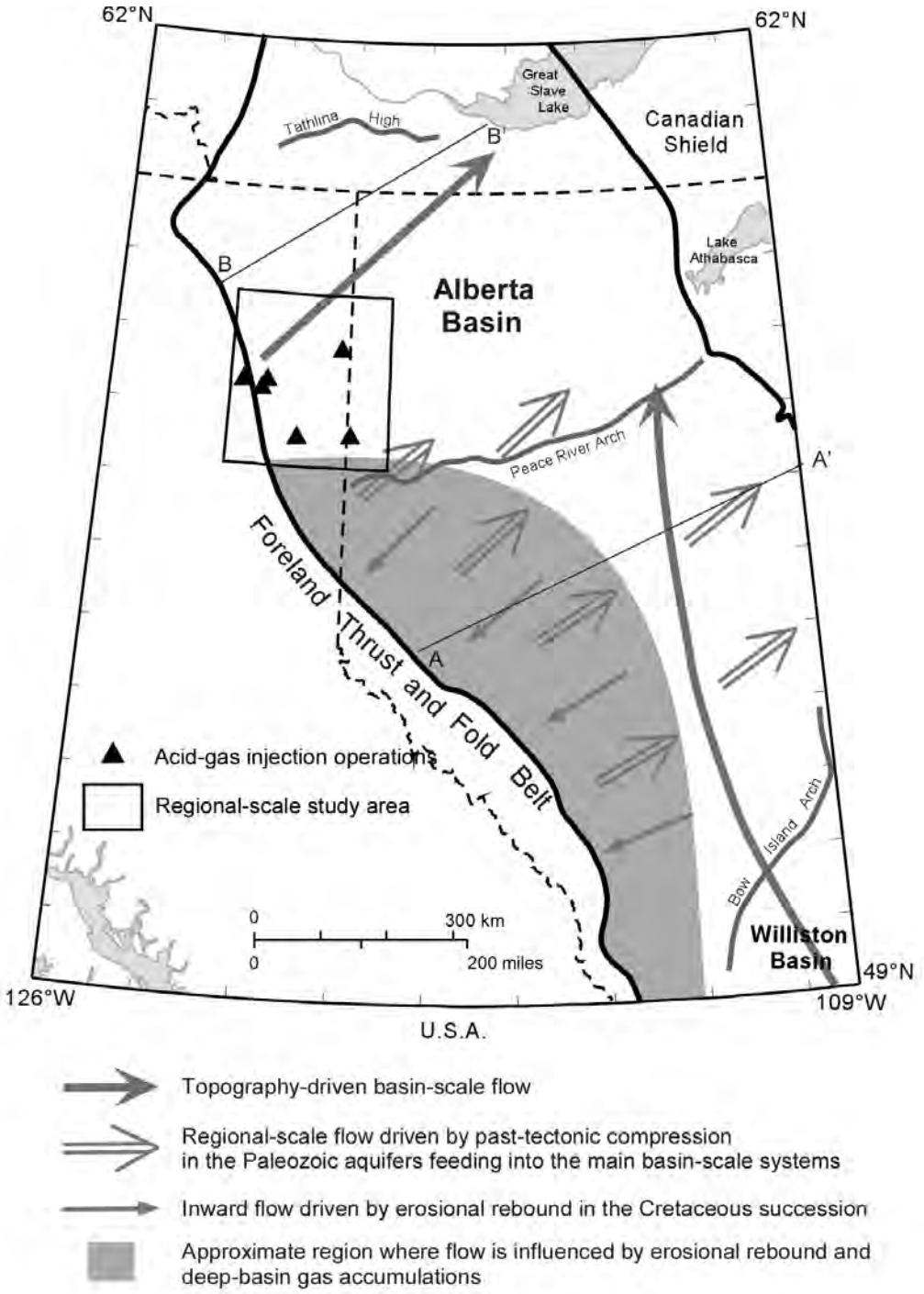

Figure 10. Diagrammatic representation of flow systems in the Alberta Basin (after Bachu, 1999). Cross-sections A-A' and B-B' area shown in Figure 11.

60 My ago (Nurkowski, 1984; Bustin, 1991), and following the retreat of 2 km thick Laurentide ice sheets since the Pleistocene. The flow in these Cretaceous aquifers is in a transient state, driven inward from the aquifers' eastern boundary to the west-southwest, downdip toward the thrust and fold belt. The aquifers are severely underpressured in places, with corresponding hydraulic heads being less than 200 m close to the thrust and fold belt (Bachu et al., 2002; Bachu and Michael, 2003). These hydraulic heads are lower

than the lowest topographic elevation in the basin at Great Slave Lake, more than 1500 km away in the northeast.

3.2.1.3 Hydrocarbon-Saturated 'Deep Basin'

During the process of hydrocarbon generation, solid kerogen in the pore space undergoes a phase change into fluid hydrocarbons. This process leads to volumetric expansion and generation of internal stresses that create overpressures capable of displacing formation water from the pore space and driving flow (Hedberg, 1974; Spencer, 1987; Osborne and Swarbrick, 1997). However, the overpressures caused by active hydrocarbon generation can be maintained only if the respective reservoirs are well sealed by very low permeability rocks. Burial of the basin strata and subsequent hydrocarbon generation during the Laramide Orogeny created dominantly hydrocarbon-saturated zones in the deeper parts of the Cretaceous to Triassic strata, the hydrocarbons being downdip of the water-saturated zones (Masters, 1984; Michael and Bachu, 2001). The water-saturated zone directly updip of the hydrocarbon-saturated zones is generally underpressured, suggesting that the rate of hydrocarbon leakage from the reservoir rocks is presently higher than the rate of hydrocarbon generation, and that formation water can re-imbibe these zones. Therefore, the hydrocarbon–water interface may be characterized as a transient, relative-permeability barrier that moves downdip toward the deformation front with the uplift of the basin. Overpressures are maintained in the deep parts of those hydrocarbon-saturated zones in which the rate of active thermogenic hydrocarbon generation is sufficiently high. Formation water flow in the Lower Cretaceous aquifers is mostly toward the receding hydrocarbon-saturated regions and the sinks created by erosional and post-glacial rebound of the intervening shales. In general, the hydrocarbon-saturated region represents a relative-permeability and pressure barrier with respect to lateral hydraulic communication within each aquifer, and to vertical cross-formational flow from underlying Paleozoic strata.

3.2.1.4 Tectonic Compression

Unlike compaction and erosion, which create vertical stresses in the fluid-saturated sedimentary succession, tectonic compression during orogenic events creates lateral stresses and pressure pulses that lead to water expulsion from the overridden and thrusted rocks into the foreland basin. These pressure pulses dissipate over several million years, depending on the hydraulic diffusivity of the sedimentary succession (Deming and Nunn, 1991). In the deep part of the Alberta Basin in the southwest, the flow of formation waters in the Devonian and Mississippian–Jurassic aquifer systems is northeastward updip until it reaches the sub-Cretaceous unconformity; where it joins the northward basin-scale, gravity-driven flow system (Figures 10 and 11a) (Hitchon et al., 1990; Bachu and Underschultz, 1993, 1995; Rostron and Tóth, 1997; Anfort et al., 2001). In the deeper Basal Cambrian and Winnipegosis aquifers, the flow of formation waters is also northeastward updip to their respective northeastern boundary (Hitchon et al., 1990; Bachu and Underschultz, 1993). The salinity of formation waters in these aquifers generally increases southwestward downdip (Hitchon et al., 1990; Bachu and Underschultz, 1993, 1995; Rostron and Tóth, 1997; Anfort et al., 2001; Michael and Bachu, 2001, 2002; Michael et al., 2003). Up to their respective eastern erosional or depositional boundary, all of these aquifers are separated by intervening strong aquitards. Direct freshwater meteoric recharge from the surface of these aquifers in either the deformed or the undeformed parts of the basin in the southwest is not possible, or is very unlikely for a variety of reasons (Bachu, 1999; Michael and Bachu, 2001, 2002; Bachu et al., 2002; Michael et al., 2003). Based on the high salinity of formation waters in the deep Paleozoic aquifers in the southwestern part of the basin, and because of the lack of an identified recharge source and mechanism, Bachu (1995) postulated the flow in these aquifers is driven by past tectonic compression. This hypothesis is supported by isotopic analyses of formation waters and late-stage cements in both the deformed and undeformed parts of the basin (Nesbitt and Muehlenbachs, 1993; Machel et al., 1996; Buschkuehle and Machel, 2002).

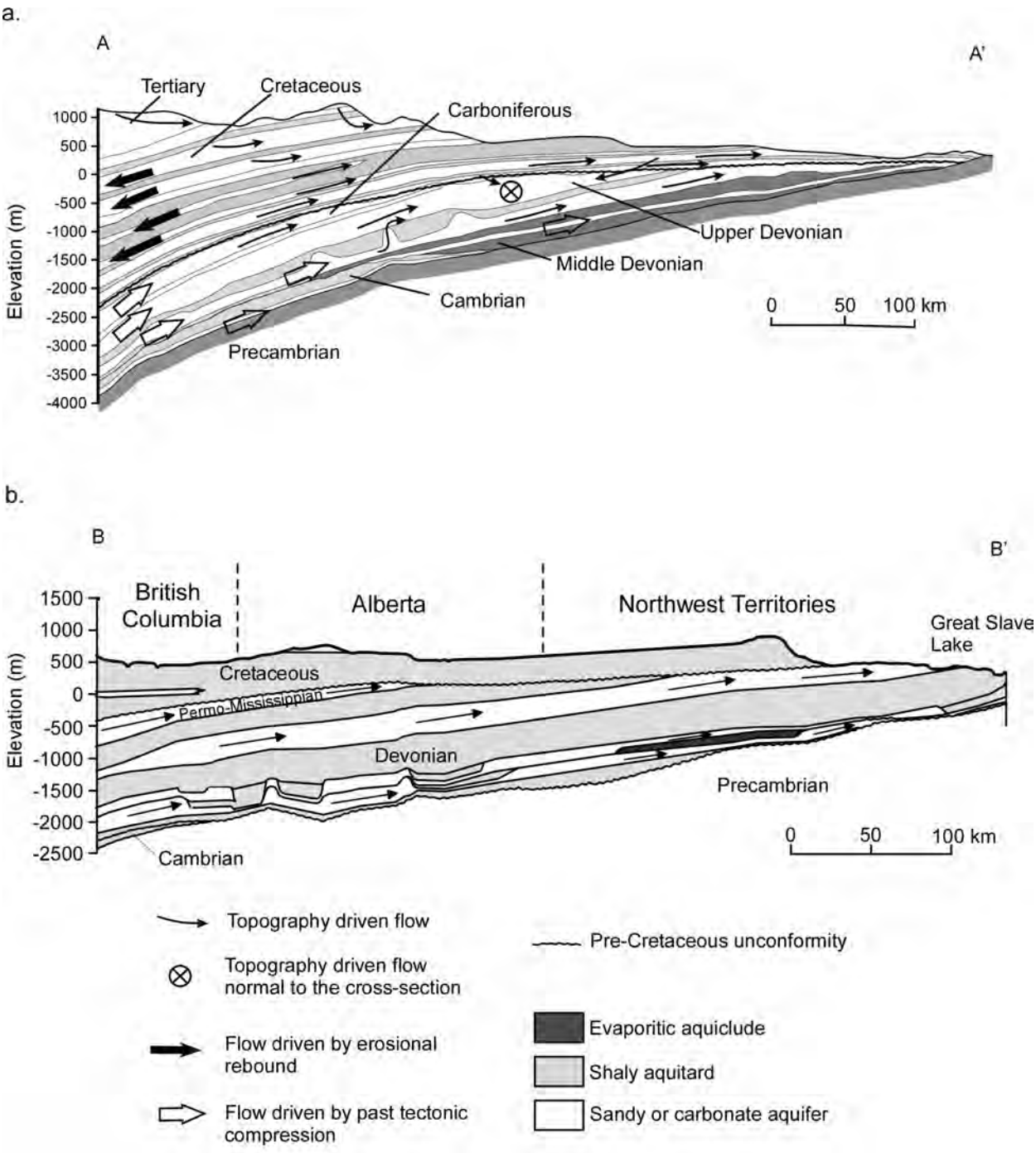

Figure 11. Diagrammatic representation of flow systems and hydrostratigraphy in the Alberta Basin: a) in the central part, and b) in the northern part (after Bachu, 1999). The location of the cross-sections is shown in Figure 10.

3.2.1.5 Buoyancy

The flow of formation water is driven in the gravitational field by hydraulic gradients and by density differences (buoyancy). Generally, Paleozoic waters are more saline than Mesozoic waters (Hitchon, 1969a, b; Bachu, 1999; Anfort et al., 2001; Michael and Bachu, 2001, 2002; Michael et al., 2003). The increase in salinity is mild in Cretaceous strata, rather abrupt at the sub-Cretaceous unconformity, and steep in Paleozoic strata, particularly near evaporitic beds (Bachu, 1999). In southern Alberta, water

salinity in Upper Devonian and Carboniferous aquifers is lower than in the central and northern parts of the basin and comparable with water salinity in Mesozoic aquifers, as a result of meteoric water recharge at outcrop in Montana (Anfort et al., 2001). The existence of high-salinity connate waters in the Paleozoic and Triassic strata shows that the basin has not yet been flushed of the original waters existing in the basin at the time of deposition. Thus, buoyancy, rather than generating or enhancing the flow of formation waters in the Alberta Basin, retards it, to the point of stagnation or sluggishness in some places. A zone of mixing between high-salinity Paleozoic waters and fresher water is present in the Lower Mannville aquifer in the south-central part of the basin, in the region where Devonian aquifers subcrop at the sub-Cretaceous unconformity (Bachu, 1995; Rostron and Tóth, 1997; Anfort et al., 2001).

3.2.1.6 Cross-Formational Flow

Generally, there is little cross-formational flow in the Alberta Basin because of its 'layer-cake' structure, where strong aquitards separate the major aquifers and aquifer systems in the sedimentary succession. Cross-formational flow takes place over large areas only where aquitards are weak. Such cases are the Clearwater and Watt Mountain aquitards in the northeast in the Athabasca area (Bachu and Underschultz, 1993) and the Calmar aquitard in the Upper Devonian aquifer system (Rostron and Tóth, 1997; Anfort et al., 2001). Localized, direct cross-formational 'pipe' flow between aquifers takes place across Devonian aquitards and aquicludes only in places where Winnipegosis and Leduc reefs breach through the intervening shaly aquitards. Such 'pipes' were identified between the carbonate platforms of the Woodbend Group and the Winterburn Group in the Cheddarville and Bashaw areas, and along the Rimbey–Meadowbrook reef trend (Bachu and Underschultz, 1993; Wilkinson, 1995; Rostron and Tóth, 1996, 1997; Anfort et al., 2001). Reefs of the Leduc Formation create a path for direct hydraulic communication across the Ireton aquitard between the underlying and overlying Cooking Lake–Leduc and Upper Devonian aquifer systems. Otherwise, mixing of formation waters from different aquifers, and consequently of fresh meteoric and connate waters, takes place at the sub-Cretaceous unconformity in the area where various Devonian strata subcrop (Figure 9 and 11a) (Hitchon et al., 1990; Bachu and Underschultz, 1993, 1995; Rostron and Tóth, 1997; Anfort et al., 2001).

3.2.2 Flow of Formation Water in the Northern Part of the Alberta Basin

The hydrogeology of the northern part of the Alberta Basin, which is the focus of this study, is generally less complex than the hydrogeology of the central and southern parts, partly because of the less complex hydrostratigraphy, as well as events and processes controlling flow. The major aquifers or aquifer systems are, in ascending order, the Middle and Upper Devonian aquifer system, the Jurassic–Mississippian aquifer system, the Bullhead aquifer, the Paddy–Cadotte aquifer and the Dunvegan aquifer (Figure 4). The main intervening aquitards are formed by the shales of the Devonian Besa River Formation (Horn River and Fort Simpson), the Jurassic Fernie Group and the Cretaceous Buckinghorse Formation. Toward the north, the basin lithology becomes increasingly shale-dominated, and a large portion of the sedimentary succession has aquitard characteristics. As a result, the boundary between terrestrial and marine sedimentation represents the northern limit of the Cretaceous Bullhead aquifer, and the Devonian aquifer systems terminate along the northern limit of the Presqu'ile Barrier. North of the Peace River Arch, flow in the entire sedimentary succession is driven mainly by basin topography from recharge areas along the thrust and fold belt and Bovie Lake Fault to discharge in the northeast at Great Slave Lake (Figure 10 and 11b). The Devonian Presqu'ile Barrier reef complex at the northern basin edge forms a high-permeable conduit in the Middle Devonian aquifer system that focuses flow, affecting the geothermal regime at discharge around Great Slave Lake (Bachu, 1997). Intermediate flow systems exist in areas of regional topographic highs, like the Caribou Mountains, Clear Hills and Buffalo Head Hills (Figure 1), mainly affecting flow in the Mesozoic to Mississippian succession (Tóth, 1978; Hitchon et al., 1990; Bachu, 1997). Mixing of formation waters from different aquifers, and consequently of fresh meteoric and high-salinity connate waters, takes place at the sub-Cretaceous unconformity where

the intervening Fernie aquitard is thin or absent and where Triassic to Mississippian strata subcrop. In this area, the density contrast between high-salinity brine and fresher formation water causes a negative buoyancy effect, that is opposite to the generally updip flow direction of formation waters, therefore impeding flow in the Lower Cretaceous–Mississippian succession. The detailed regional hydrostratigraphy and flow of formation waters in the Mississippian to Bullhead Group succession will be characterized in the following sections.

4 Regional-Scale Setting of Acid-Gas Injection Sites in Northeastern British Columbia

To better understand the geology, hydrogeology and flow of formation water at the acid-gas injection sites in the northeastern British Columbia study area, and the containment of the injected acid gas, a regional-scale study area was defined between 56.16°N to 58.5°N and 119.00°W to 123.00°W (Figure 12). Acid gas injection occurs in the Triassic–Carboniferous interval (Figure 13), which is the focus of this chapter. The overlying units, the Jurassic Fernie Group and the Cretaceous Bullhead Group, will also be discussed because of their significance to regional flow. Various erosional events during Carboniferous to Jurassic times resulted in several unconformities within the related strata, the most prominent being the pre-Cretaceous unconformity along which Jurassic to Carboniferous formations subcrop below the Cretaceous Bullhead Group (Figure 14). The stratigraphic and structural relationships between the various formations and injection units are shown along an updip cross-section in Figure 15.

4.1 Geology of the Carboniferous to Cretaceous Bullhead Group Succession

4.1.1 Carboniferous

In the regional-scale study area, a thick Carboniferous succession was deposited in the Peace River Embayment, which was a major zone of subsidence in northwestern Alberta and northeastern British Columbia during the Carboniferous to Triassic time. Due to a series of erosional and nondepositional events from the Carboniferous to early Cretaceous, Carboniferous formations successively subcrop from southwest to northeast underneath Permian, Triassic or Cretaceous strata (Figure 14). The total thickness of the Carboniferous strata increases from 400 m in the northeast to 1000 m in the southwest. The major stratigraphic subdivisions in the Carboniferous are the Banff Formation, Rundle Group and Stoddart Group. The Rundle and Stoddart groups can be further subdivided into the Pekisko, Shunda and Debolt formations, and the Golata, Kiskatinaw and Taylor Flat formations, respectively (Figure 13).

The Banff Formation and the Rundle Group form overall shallowing-upward successions. Calcareous shales of the Lower Banff and Pekisko formations were deposited in a basin to slope setting, passing upward into shallow and restricted shelf carbonates in the upper Banff, as well as in the Shunda and Debolt formations (O'Connell, 1990). In the study area, the Debolt Formation can be further subdivided into upper, middle and lower members that correspond to three main regional transgressions (Richards et al., 1994). The lower unit comprises cherty, skeletal limestone with minor amounts of calcareous shale and finely crystalline dolomite. The middle member consists of argillaceous and silty carbonates with minor evaporites. Acid gas is injected into the upper Debolt Formation, which consists of clean limestone and dolostone. The top of the Debolt Formation dips southwestward from approximately 0 m to -1500 metres above sea level (Figure 16a), and its depth ranges from 500 to 2500 m below the ground surface (Figure 16b). The thickness of the Debolt Formation in the regional-scale study area ranges from 0 m at its erosional edge in the northeast to 350 m in the southwest.

The Debolt Formation is overlain by the Golata Formation, which exhibits a distinct change from carbonate to siliciclastics depositional settings. The Golata Formation consists of siltstones and shales

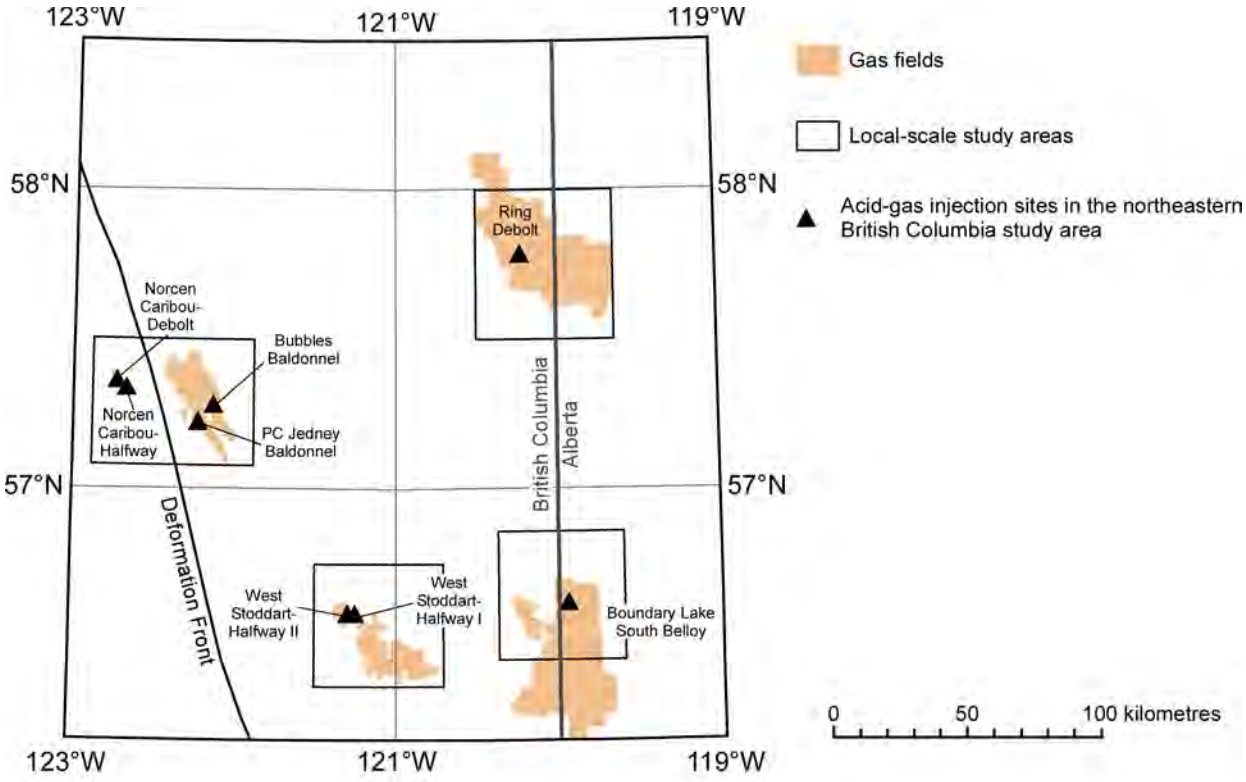

Figure 12. Location of acid-gas injection sites, related major gas fields and local-scale study areas in the northeastern British Columbia regional-scale study area.

deposited in tidal or estuarine, delta-like complexes (Barclay et al., 1990). The overlying sandstone-dominated Kiskatinaw Formation was deposited in a coastal plain environment sourced from the east, and changing westward into more open marine limestones and shales (Barclay et al., 1990). The Taylor Flat Formation, the uppermost formation in the Stoddart Group, was deposited in an open marine, outer shelf environment and consists of sandy carbonates that grade into calcareous sandstones and shale (Barclay et al., 1990, Richards et al., 1994).

Most of the boundaries between the various Carboniferous formations are conformable, at least in the centre of the Peace River Embayment. Toward the basin margins, however, formation contacts, especially in the Upper Cretaceous succession, become increasingly unconformable due to nondeposition and erosion in more terrestrial environments. Ultimately, the entire Stoddart Group is absent in the northern part of the study area, and the Lower Carboniferous Debolt Formation is overlain by the Permian Belloy Formation.

4.1.2 Permian (Belloy Formation)

Sediments of the Permian Belloy Formation were deposited in a shallow-marine shelf setting (Naqvi, 1972) and consist of interbedded siliciclastics and carbonates. Dolomitic sandstones were deposited preferentially along the margins of the Peace River Embayment, in tidally influenced shoreline environments (Figure 17). The Permian strata mainly occur in a narrow belt on the interior platform in the Peace River and Liard River areas, owing to localization of deposition and truncation beneath several sub-Mesozoic unconformities. For the purpose of this study, reference is being made to the geological framework of the Permian Belloy Formation deposited within the Peace River Embayment, more

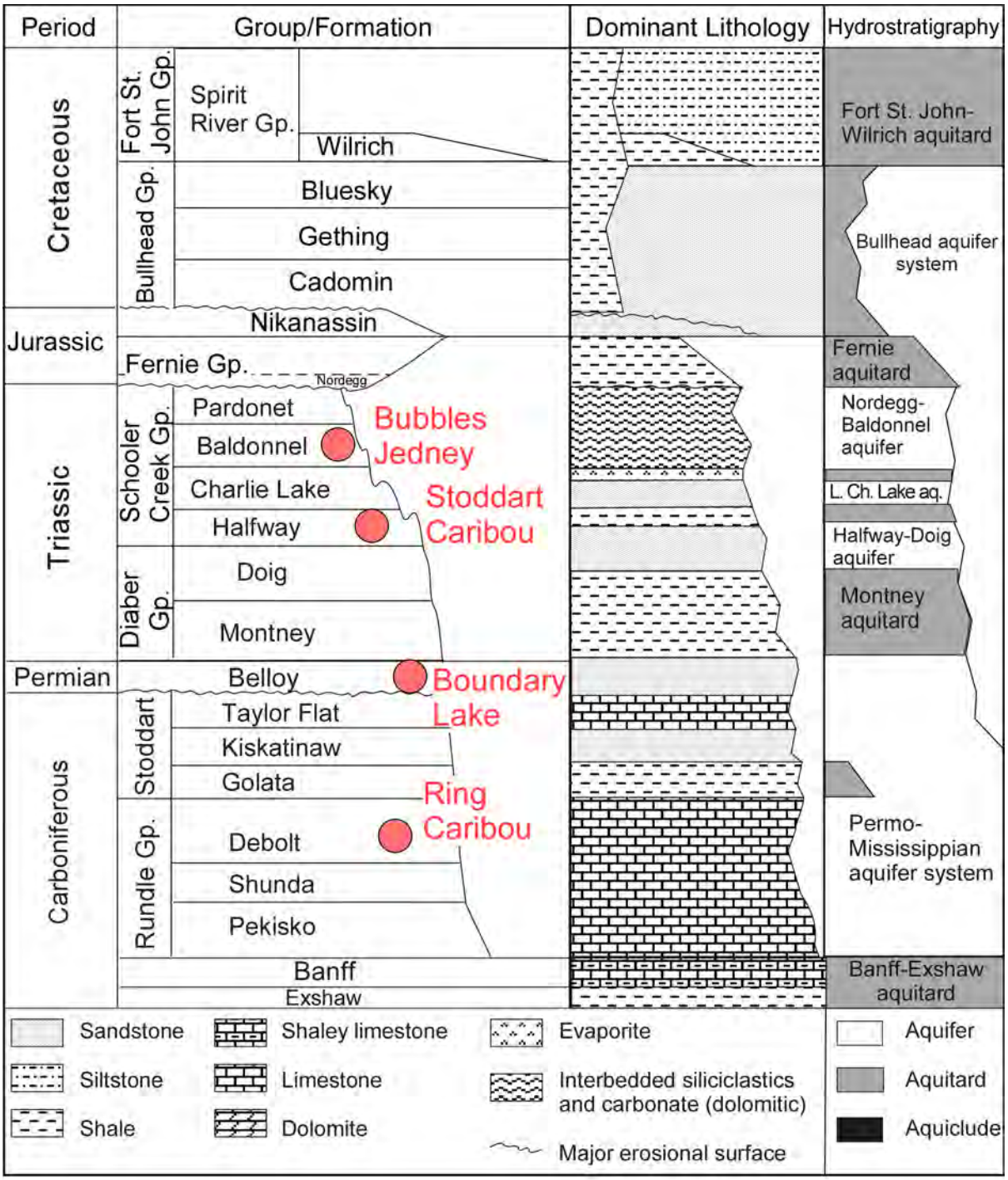

Figure 13. Stratigraphy, general lithology and hydrostratigraphy of the Mississippian to Lower Cretaceous (Spirit River Group) succession in the study area. Acid-gas injection horizons are indicated by red circles.

specifically the northern flank of this embayment, as seen in Figure 7. The Belloy Formation sandstones pass westwards and toward the basin centre into less porous dolostones and deeper marine limestones and siltstones (Henderson et al., 1994). In the eastern part of the study area, the Belloy Formation can be subdivided locally into three units:

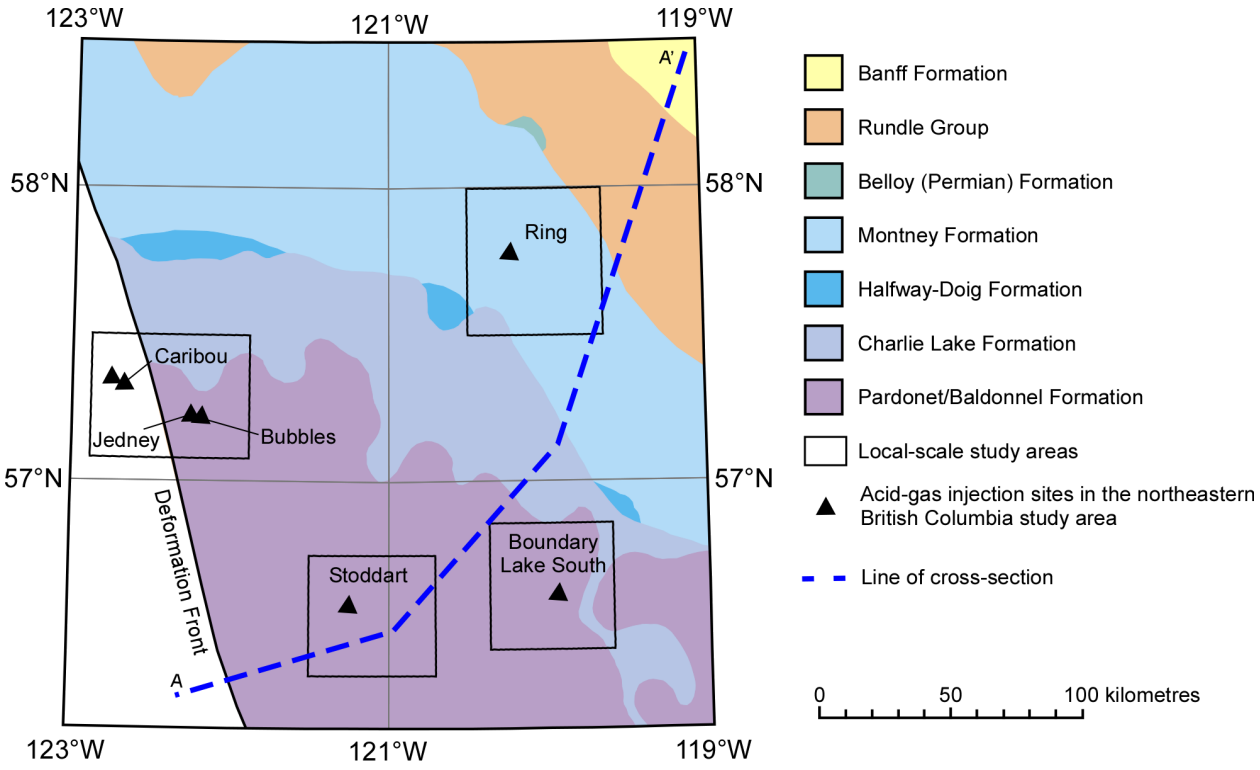

Figure 14. Structure map of the sub-Cretaceous unconformity surface in the regional-scale study area. Colour coding indicates age and lithology of strata underlying the unconformity. The strata become progressively older to the north and east (from Hayes et al., 1994). Cross-section A-A' is shown in Figure 15.

1) a lower carbonate member, consisting of fine-grained, glauconitic quartz arenites, siltstone and cherty, dolomitic limestone;
2) a middle sandstone member, consisting of medium-grained, glauconitic and phosphatic quartz arenites; and
3) an upper carbonate member, consisting of dolomitic limestone, dolostone, glauconitic sandstones and bedded chert (Halbertsma, 1959; Henderson et al., 1994).

Both the top and the bottom of the Permian form unconformable boundaries with overlying Triassic to Lower Cretaceous strata and underlying Carboniferous strata, respectively. The thickness of the Permian increases southward from 0 m at its erosional edge to approximately 100 m (Figure 17). The top of the Permian dips southwestward from -100 m to -1600 metres above sea level (Figure 18a) and the depth ranges from 600 m to 2300 m below the ground surface (Figure 18b).

4.1.3 Triassic

Triassic sediments were deposited as a series of three major transgressive–regressive (T–R) third or fourth- order cycles (Gibson et al., 1989; Edwards et al., 1994). The first (lowermost) T–R cycle is represented by the Montney Formation (Lower Daiber Group) and comprises sediments deposited along a tidally influenced, deltaic coastline with corresponding deep-marine and distal shelf deposits. Along its eastern subcrop edge, the Montney Formation consists of thin shoreface sandstones mixed with finer siliciclastics (Figure 19). The Montney Formation thickens southwestwards to more than 250 m, passing into calcareous and dolomitic siltstones and shales that were deposited in a shelf to shelf-slope environment. The top of the Montney Formation dips southwestward from -100 m to -1200 metres above

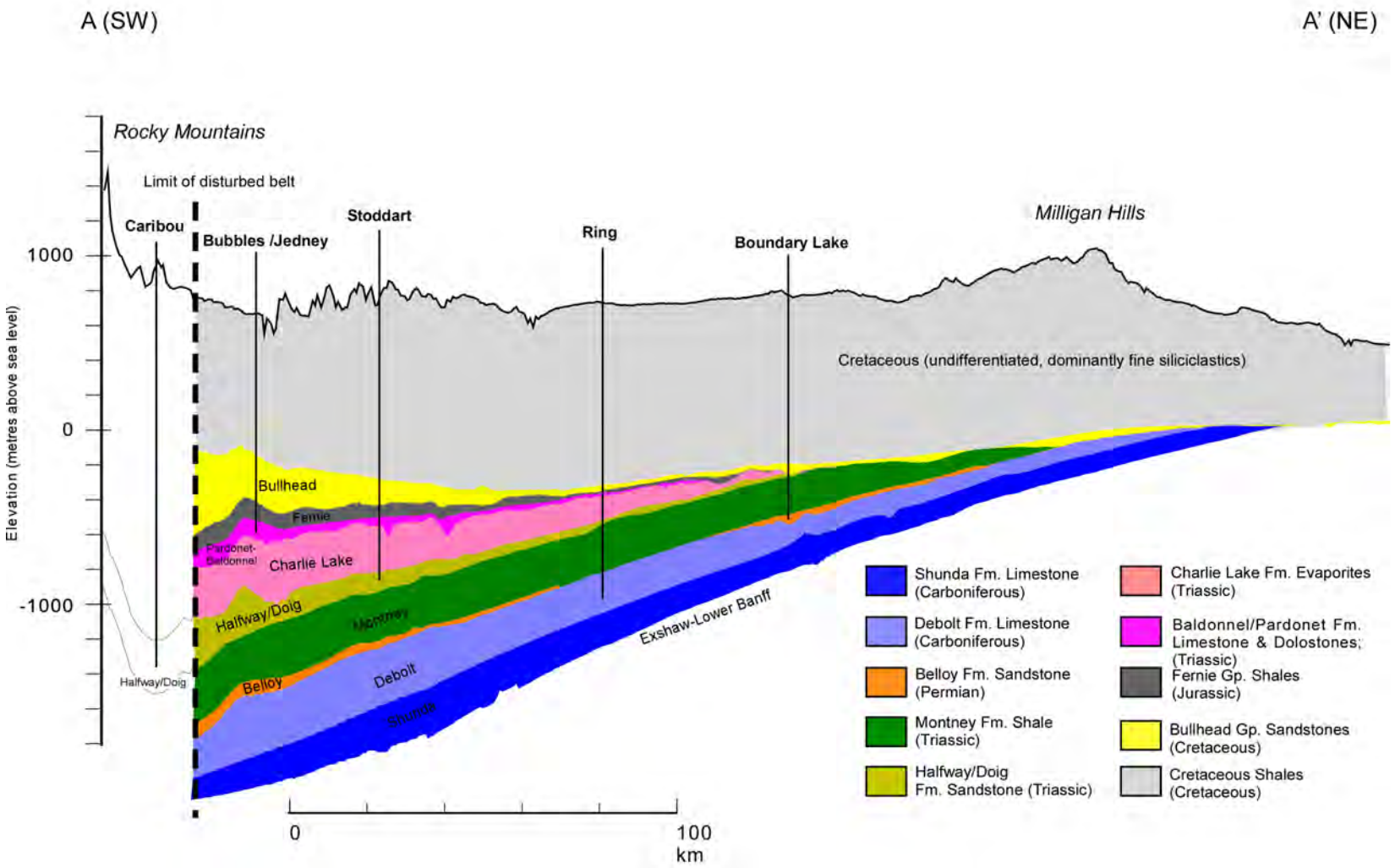

Figure 15. Stratigraphic updip cross-section through the regional-scale study area showing the relative position of the various target horizons in the Carboniferous–Triassic succession for acid-gas injection in northeastern British Columbia. The deformation in the Rocky Mountains is schematically indicated by the syncline in the Halfway/Doig aquifer. The location of the cross-section is shown in Figure 14.

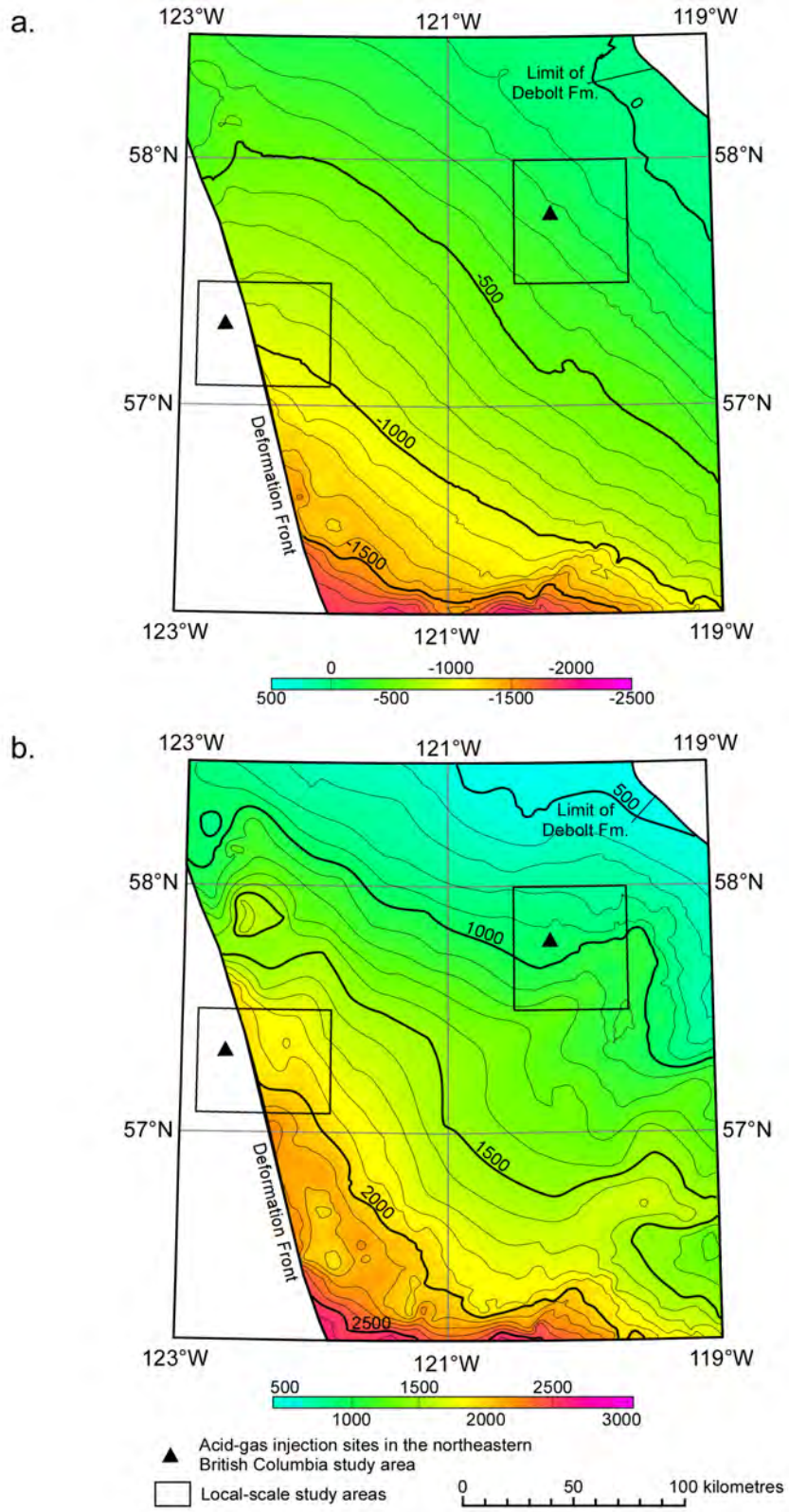

Figure 16. Main geological features of the Debolt Formation carbonates in the regional-scale study area: a) top structure elevation, and b) depth to top. The location of the injection sites (Caribou, Ring) and the local-scale study areas are also shown. Contours in metres. Contour interval = 100 m.

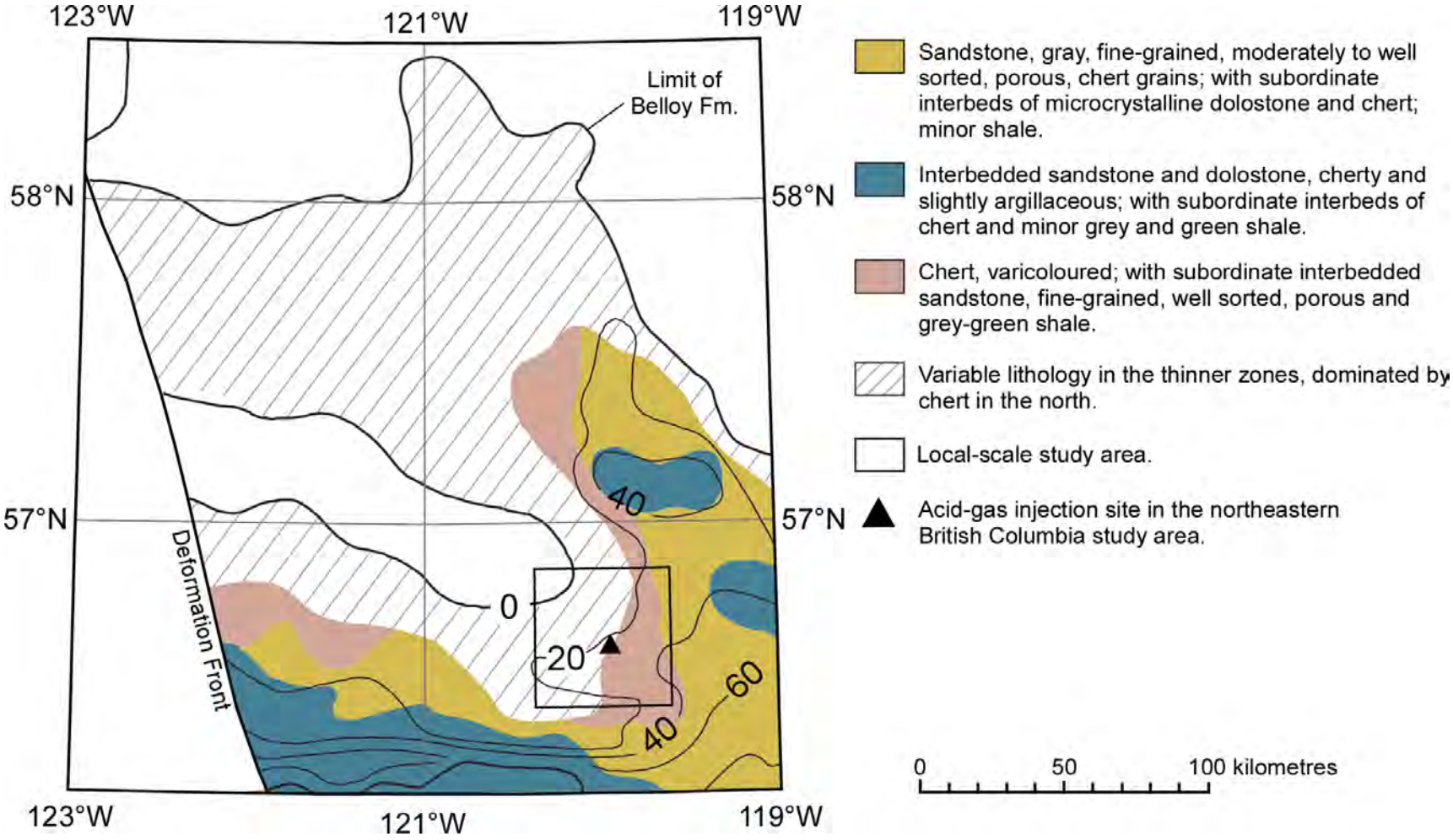

Figure 17. Generalized lithofacies and isopach of the Permian succession in the regional-scale study area. Injection takes place predominately in the sandstones of the Belloy Formation, as indicated by the position of the injection site. The local-scale study area is also shown (modified after Henderson et al., 1994). Contours in metres. Contour interval = 20 m.

sea level (Figure 20a), and its depth ranges from 650 m to 2000 m below the ground surface (Figure 20b). Strata of the overlying Doig Formation (upper Daiber Group), Halfway and Charlie Lake formations (Lower Schooler Creek Group) represent the second T–R cycle. Due to similar lithologies, it is often difficult to assign a distinct contact between the Doig and Halfway formations, and the combined thickness increases from 0 m along the subcrop edge to 450 m along the deformed belt in the southwest (Figure 21). The Doig Formation has a succession of fine sandstones, siltstones and shales deposited in a marine shelf environment. Sandstone/coquina-filled estuarine channels occur locally in the upper part of the Doig Formation. Sandstones of the Halfway Formation are deposited in a beach/barrier island setting (Gibson and Edwards, 1990) and are generally coarser than the sandstones in the overlying Doig Formation. Discontinuous accumulations of quartzose sandstone and dolomitic coquina along the subcrop edge of the Halfway Formation grade westward into thick, continuous shoreface sandstones (Edwards et al., 1994). The top of the Halfway–Doig dips southwestward from -200 m to -1000 metres above sea level (Figure 22a), and the depth ranges from 1000 m to 1800 m below the ground surface (Figure 22b). The overlying Charlie Lake Formation represents the peak of the second T–R cycle and comprises a succession of intercalated siliciclastics (shale, siltstone very fine to medium-grained sandstone), carbonates (micro to cryptocrystalline, silty dolostone and skeletal limestone) and evaporites (anhydrite, gypsum and minor halite) up to 500 m thick (Figure 23). Sediments of the Charlie Lake Formation were deposited in a near-shore marine to sabkha/aeolian environment. The abrupt lateral and vertical facies changes observed in the Charlie Lake Formation can be attributed to the sensitivity of sedimentation on an evaporitic, shallow-water shelf with low slope to subtle changes in sea level (Gibson and Barclay, 1989). The top of the Charlie Lake Formation dips southwestward from -150 m to -800 metres above sea level (Figure 24a), and its depth ranges from 1000 m to 1500 m below the ground surface (Figure 24b).

The third major T–R cycle is formed by the Baldonnel and Pardonet formations (upper Schooler Creek Group) and is dominated by shallow-water carbonates. The combined thickness ranges between 0 m along the erosional subcrop edge and 90 m along the deformation front of the Rocky Mountains (Figure 25). The Baldonnel Formation conformably overlies the Charlie Lake Formation and consists predominantly of dolostones with minor limestone, shale and carbonate breccia (Gibson and Edwards, 1990). The Baldonnel Formation is characterized by several shallowing-upward sequences, each cycle typically represented by a succession of mudstone and/or wackestone at the base, overlain by bioclastic pack and grainstone, followed by evaporitic, silty dolostone and capped by dolomitic mudstone. Conformably overlying parts of the Baldonnel Formation are sediments of the Pardonet Formation. Due to pre-Jurassic erosion, the Pardonet Formation is present only near the Rocky Mountain Foothills, in the southwestern corner of the study area. Deep-water carbonaceous limestone and siltstone pass eastward into dominantly clean dolostone that was deposited in shallower water. The top of the Pardonet–Baldonnel interval dips southwestward from -300 m to -700 metres above sea level (Figure 26a) and depth ranges from 1000 m to 1400 m below the ground surface (Figure 26b). The Pardonet–Baldonnel interval is unconformably overlain by Jurassic strata.

The Triassic strata of the Alberta Basin were deposited within the tectonically active, subsiding Peace River Embayment (Figure 8). This embayment is interpreted by Davies (1997) to be a right-lateral, strike-slip, pull-apart basin with subsequent thermal subsidence that resulted in deposition of progressively more widely distributed post-rift Mississippian, Pennsylvanian, Permian and Triassic sediments. Structural highs or elements that influenced Triassic sedimentation included the en-echelon (parallel structural features) Sukunka and Beatton Highs (Figure 7), the southwestern extension of the Fort St. John ‘Graben,’ and Late Cretaceous–Early Tertiary thrust faulting and folding. Although the latter formed most of the current traps, there is strong evidence that north-northwest trending folds north of the Peace River block (for example, Jedney, Bubbles trends) were formed or were forming during the

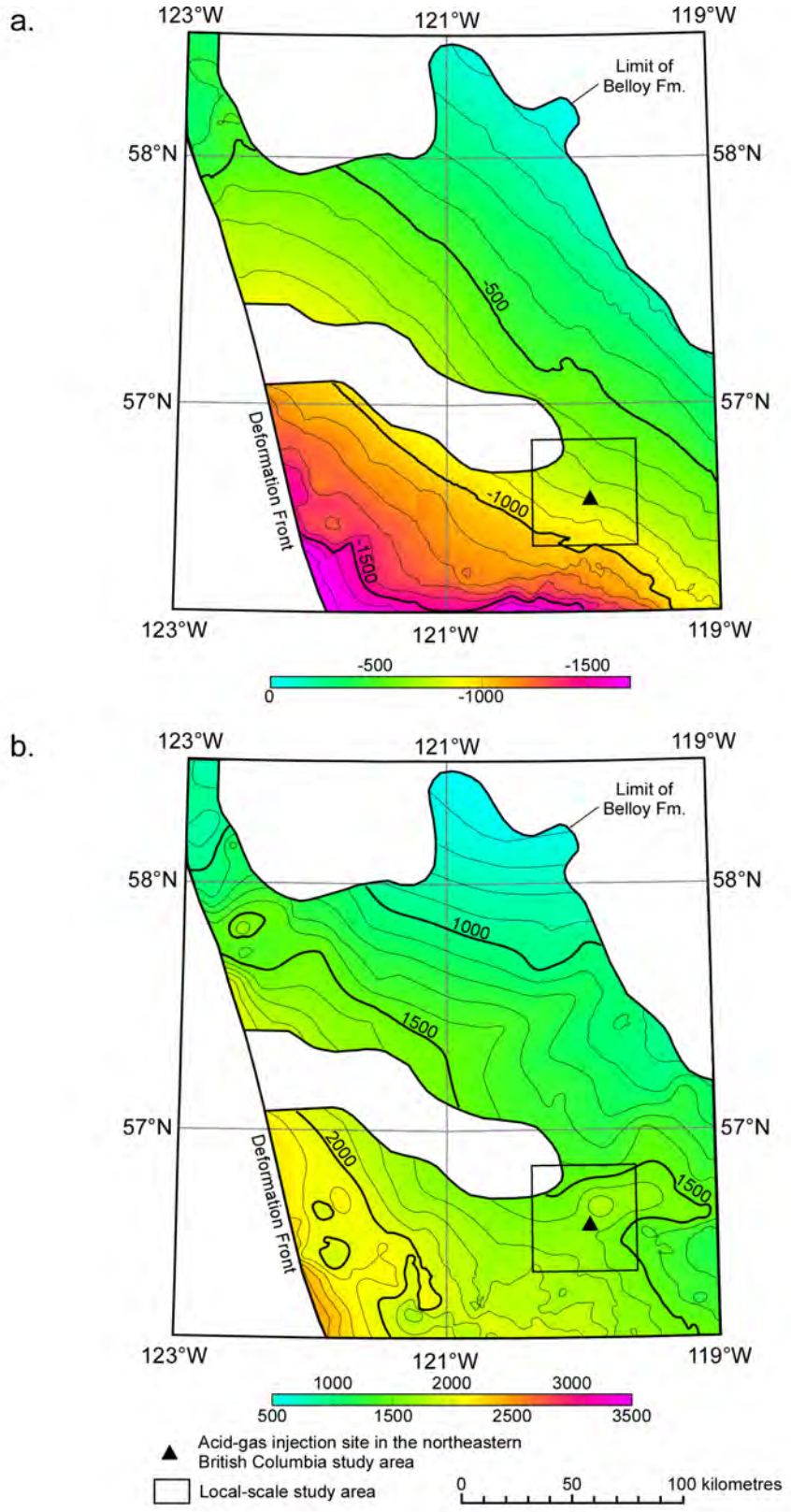

Figure 18. Main geological features of the Permian Belloy Formation sandstones in the regional-scale study area: a) top structure elevation, and b) depth to top. The location of the Boundary Lake–South injection site and the local-scale study area is also shown. Contours in metres. Contour interval = 100 m.

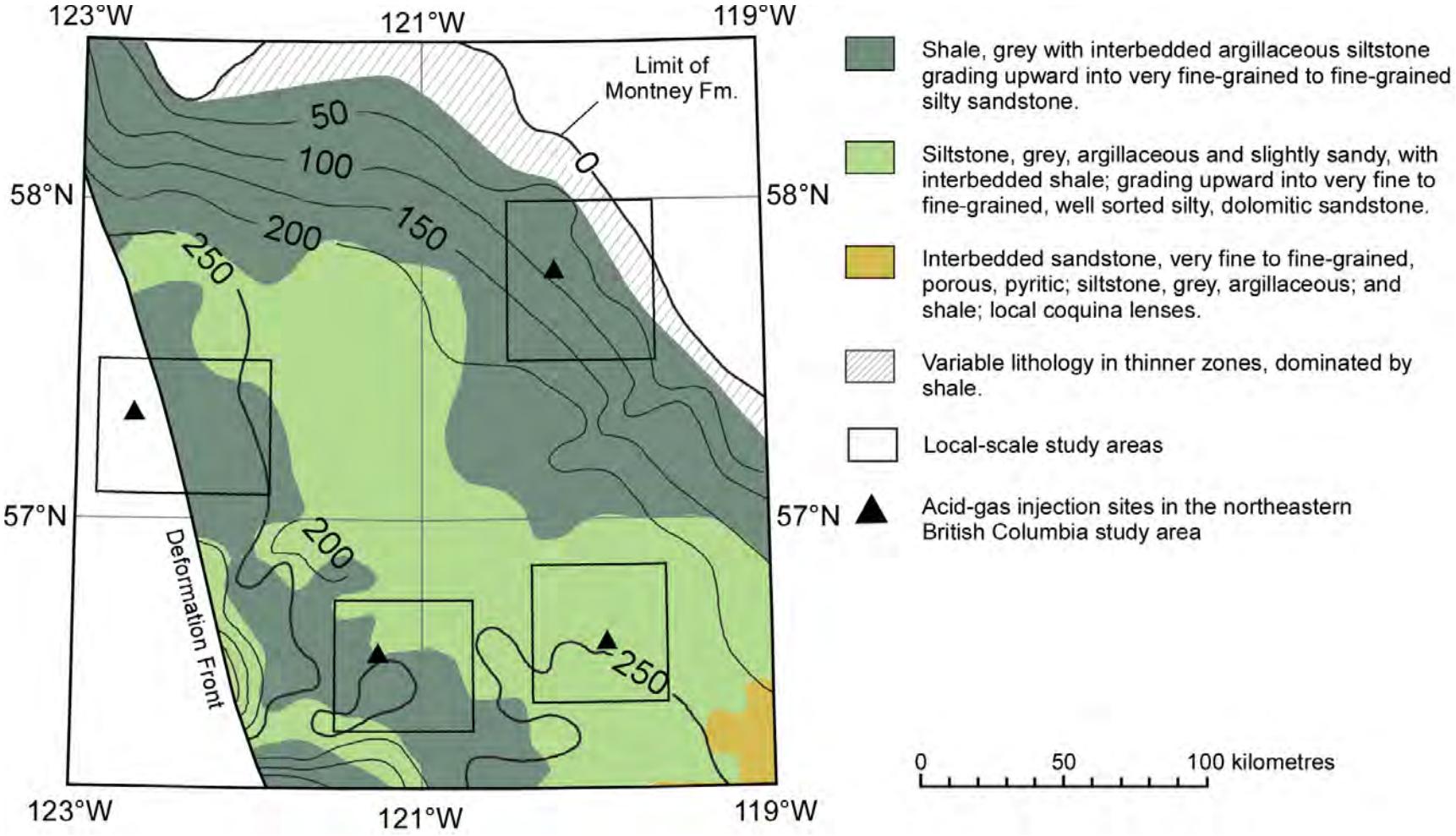

Figure 19. Generalized lithofacies and isopach of the Triassic Montney Formation in the regional-scale study area. The Montney shales are the cap rock or underlying seal for several injection sites, which are also shown with their respective local-scale study areas (modified from Edwards et al., 1994). Contours in metres. Contour interval = 50 m.

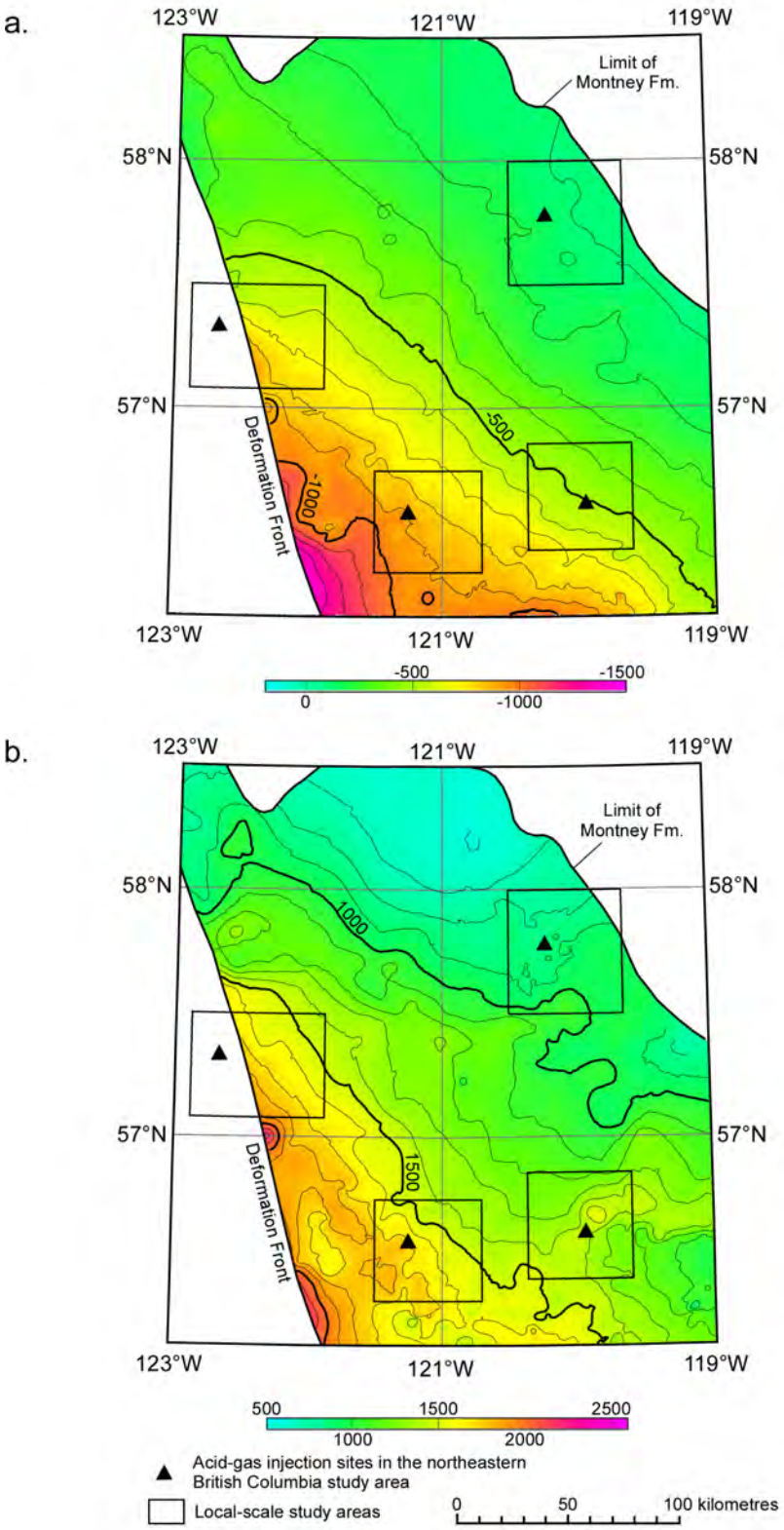

Figure 20. Main geological features of the Triassic Montney Formation shales in the regional-scale study area: a) top structure elevation, and b) depth to top. The location of the injection sites (Ring, Caribou, Stoddart, Boundary Lake–South) and the local-scale study area are also shown. Contours in metres. Contour interval = 100 m.

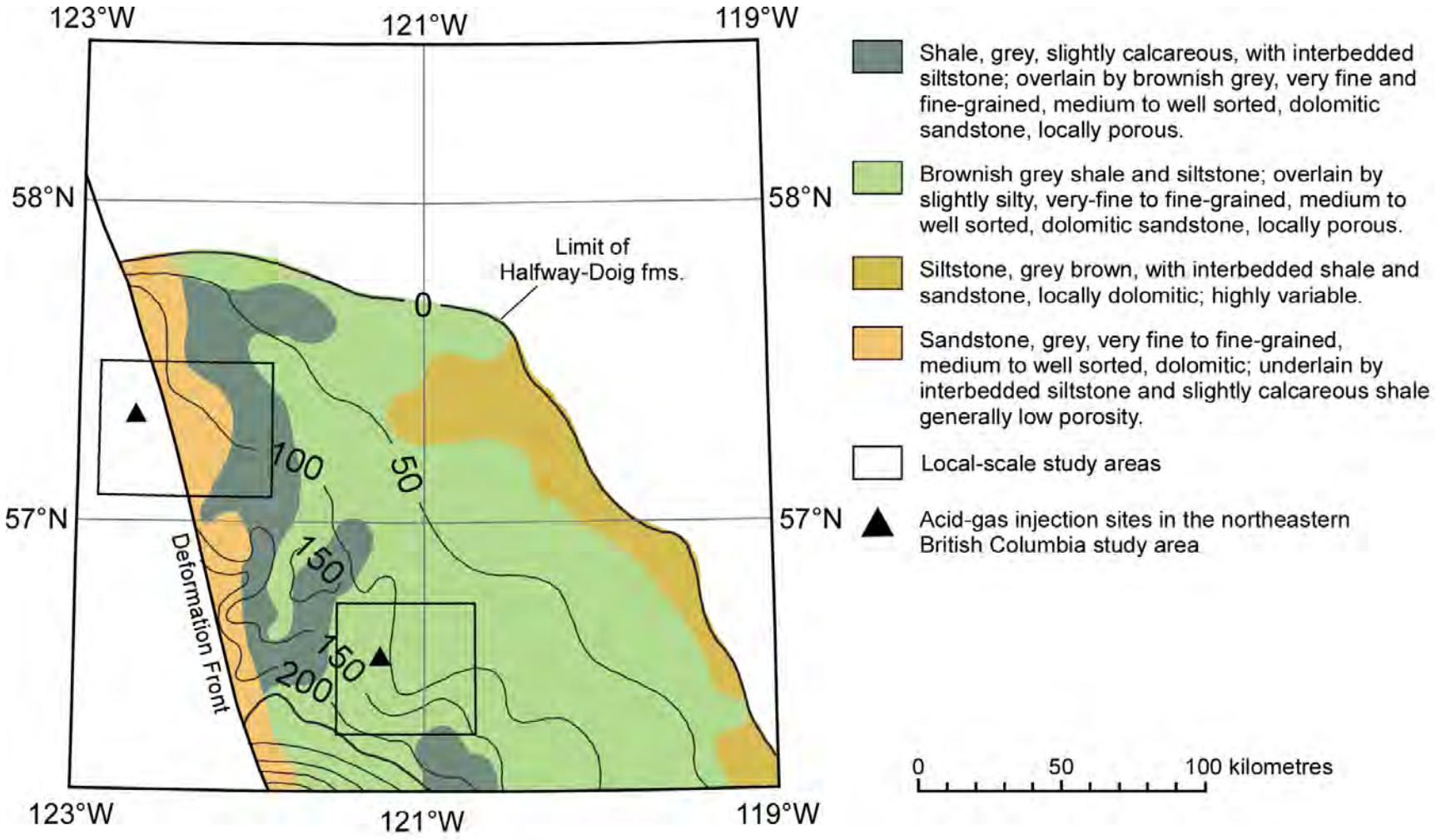

Figure 21. Generalized lithofacies and isopach of the Triassic Halfway/Doig interval in the regional-scale study area. Injection into the Halfway sandstones takes place at Stoddart in the south and Caribou in the north of the two shown injection sites. Their respective local-scale study areas are also shown (modified from Edwards et al., 1994). Contours in metres. Contour interval = 50 m.

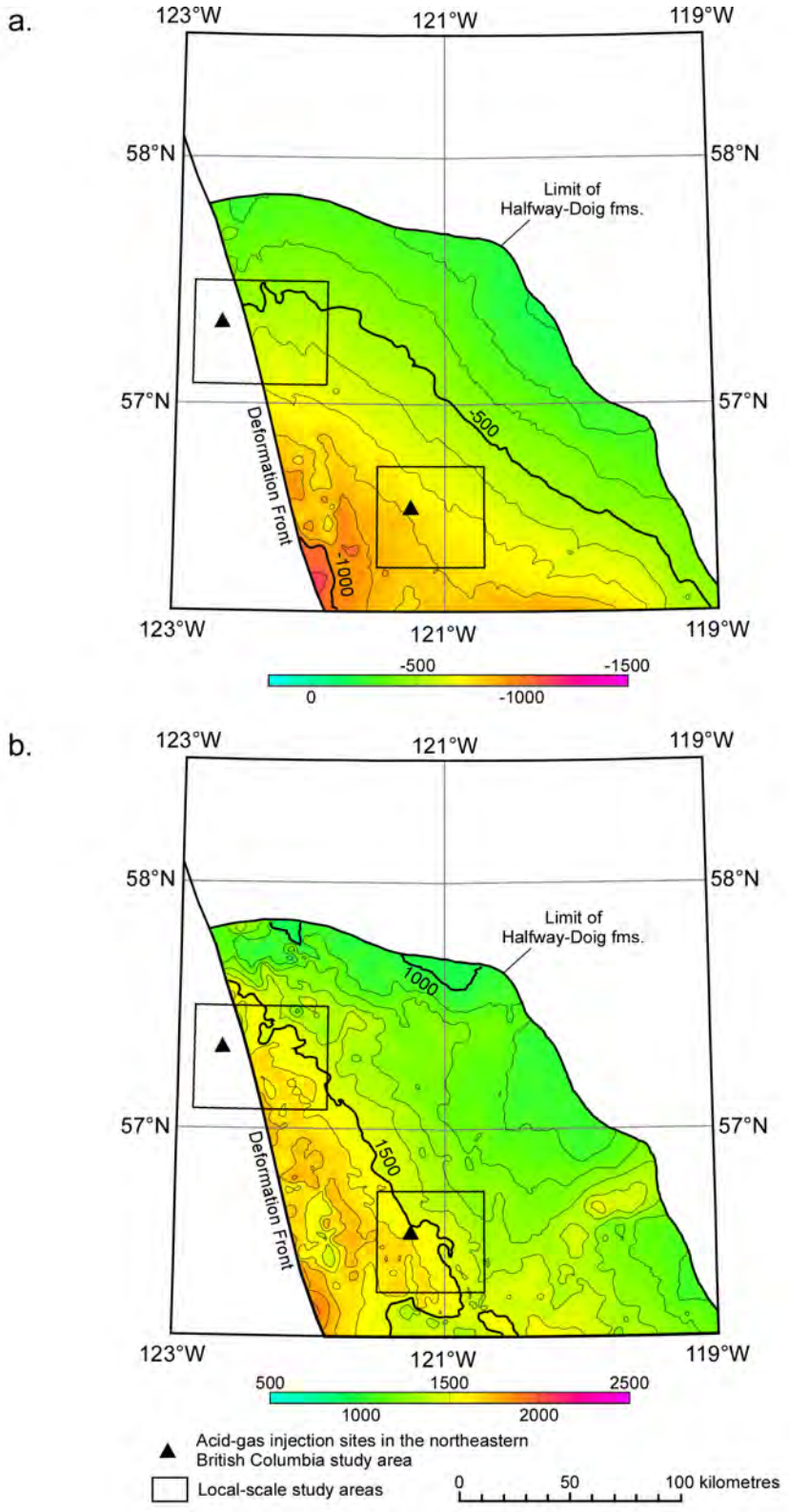

Figure 22. Main geological features of the Triassic Halfway/Doig interval in the regional-scale study area: a) top structure elevation, and b) depth to top. The location of the injection sites (Caribou, Stoddart) and the local-scale study area are also shown. Contours in metres. Contour interval = 100 m.

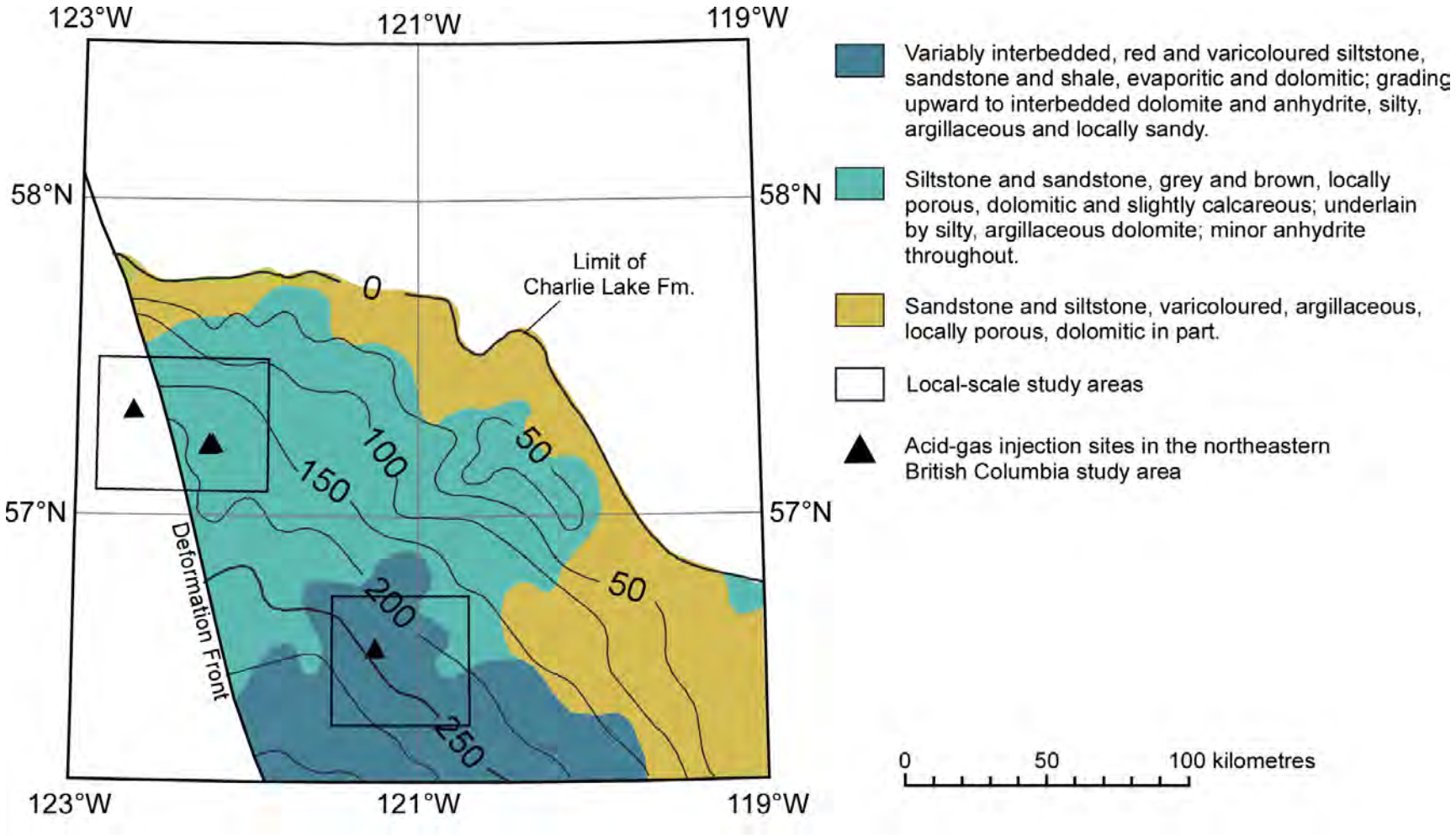

Figure 23. Generalized lithofacies and isopach of the Triassic Charlie Lake Formation in the regional-scale study area. The Charlie Lake Formation evaporites are the cap rock for the Caribou and Stoddart–Halfway operations, which are shown with their respective local-scale study areas (modified from Edwards et al., 1994). Contours in metres. Contour interval = 50 m.

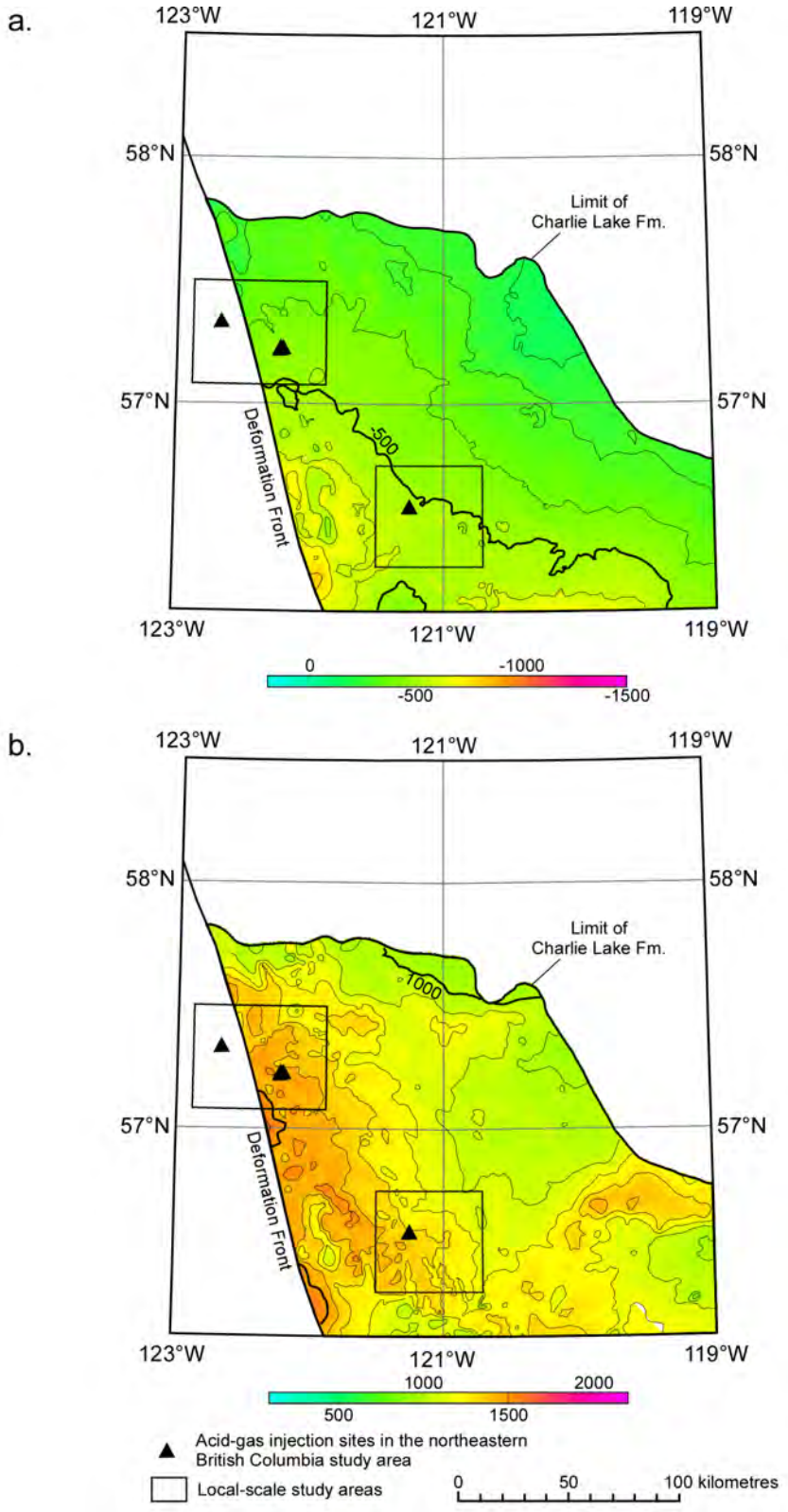

Figure 24. Main geological features of the Triassic Charlie Lake Formation in the regional-scale study area: a) top structure elevation, and b) depth to top. The location of the injection sites (Caribou, Bubbles, Jedney, Stoddart) and the local-scale study areas are also shown. Contours in metres. Contour interval = 100 m.

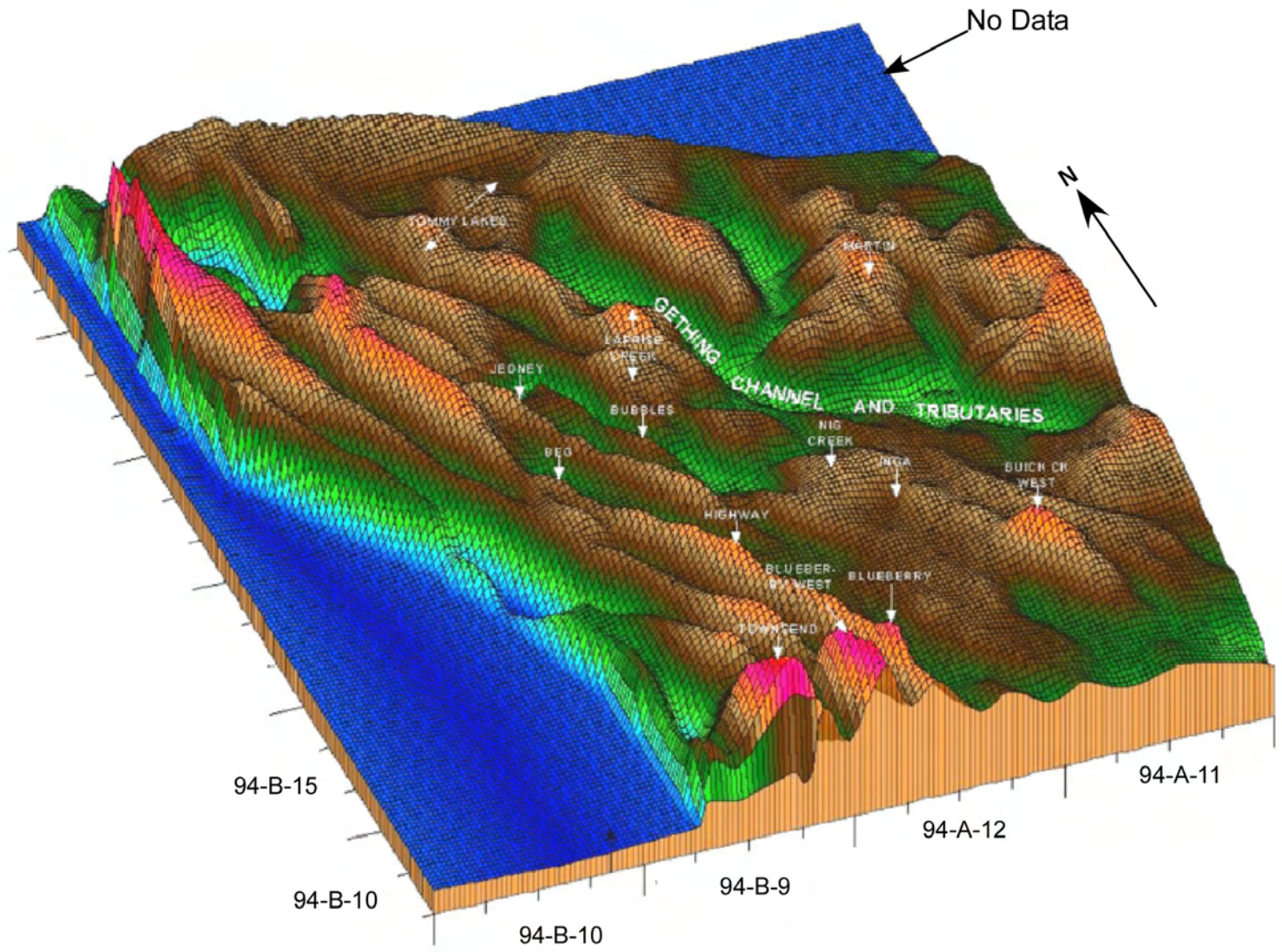

Figure 25. Generalized lithofacies and isopach of the Baldonnel–Pardonet interval in the regional-scale study area. Injection into the Baldonnel takes place at Bubbles and Jedney, which are shown with their respective local-scale study area (modified from Edwards et al., 1994). Contours in metres. Contour interval = 10 m.

Jurassic time. This is consistent with evidence for the latest Triassic to Early Jurassic uplift or tilting of the Grassy High, and in various fault blocks where Triassic units were eroded or truncated prior to Jurassic deposition. Figure 27 is a third-order residual structure map of the top of the Triassic north of the Peace River block in northeastern British Columbia, showing north-northwest–trending folds and faults that define most of the Baldonnel traps in that area, including the Bubbles and Jedney fields (Davies et al., 2004). As previously noted, these folds may have been initiated in Jurassic time.

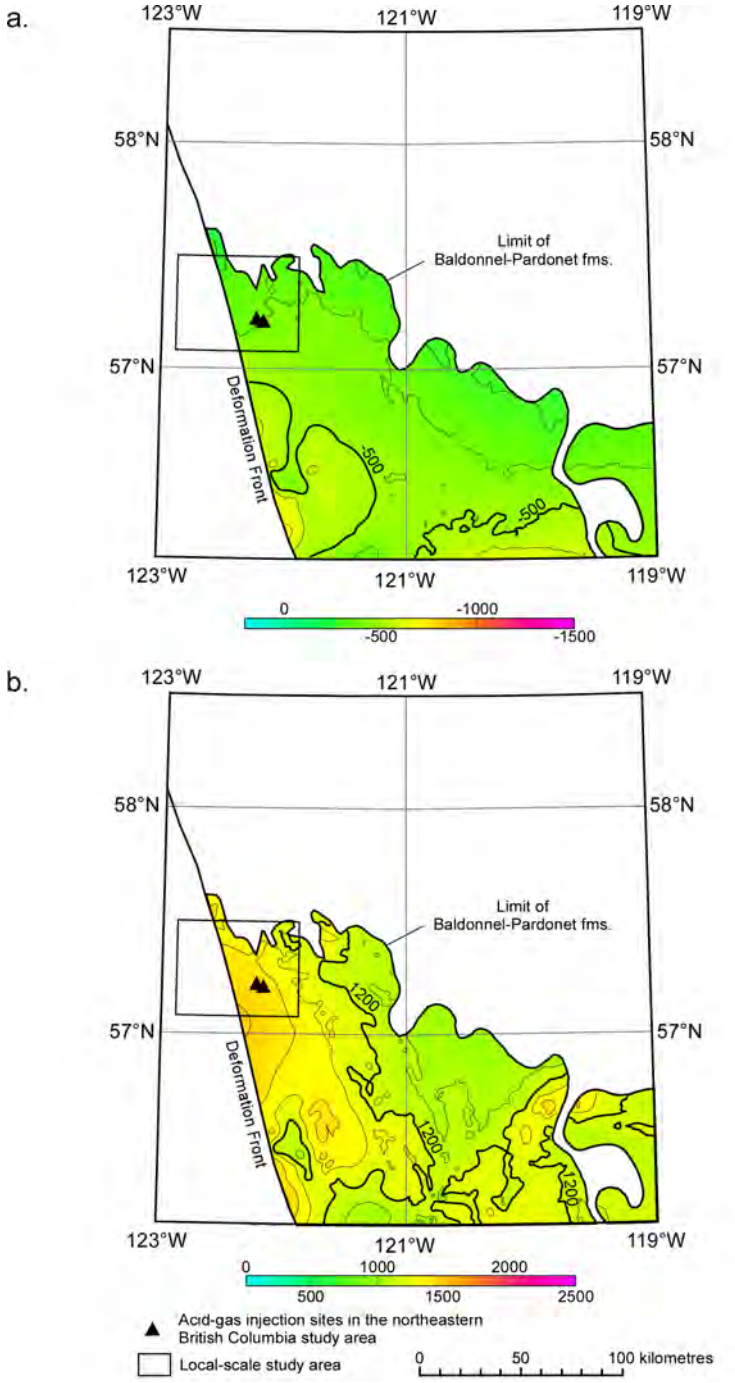

Figure 26. Main geological features of the Triassic Baldonnel–Pardonet interval in the regional-scale study area: a) top structure elevation, and b) depth to top. The location of the injection sites (Bubbles, Jedney) and the local-scale study area are also shown. Contour in metres. Contour interval = 100 m.

4.1.4 Jurassic

The shale-dominated Jurassic succession in the regional-scale study area can be subdivided into two main sequences that are separated by a regional unconformity. The lower sequence is formed by a thin platform succession consisting of shelf limestones, banded chert (Nordegg Member) and shales of the Lower Jurassic Lower Fernie Group. The upper sequence comprises Upper Fernie Group shales and sandstones of the Nikanassin Formation and Minnes Group. These Upper Jurassic strata represent an easterly tapering orogenic clastic wedge that filled the Columbian foredeep to the west and gradually changed into thin shelf equivalent strata to the east. Middle Jurassic strata are absent due to pre-Late Jurassic uplift and erosion (Poulton et al., 1990). The Jurassic is present only in the southwestern half of the study area due to pre-Cretaceous erosion, and its thickness ranges from 0 m to more than 100 m along the deformation front (Figure 28). This isopach does not contain the sandstones of the Nikanassin Formation at the top of the Jurassic, which are included in the Lower Cretaceous Bullhead Group succession instead, because of comparable lithology and hydrostratigraphic characteristics. The top of the Jurassic Fernie Group dips southwestward from -300 m to -500 metres above sea level (Figure 29a), and its depth ranges from 1000 m to 1300 m below the ground surface (Figure 29b).

4.1.5 Lowermost Cretaceous (Bullhead Group)

Although not a target for acid gas injection in northeastern British Columbia, the sandstones of the lowermost Cretaceous Bullhead Group form an important aquifer that is in hydraulic communication with the underlying Carboniferous to Triassic aquifers along the pre-Cretaceous unconformity. The Lower Cretaceous Bullhead Group is subdivided into the Cadomin and Gething formations. The Cadomin Formation at the base of the Bullhead Group comprises deltaic conglomerates and coarse sandstones that were shed eastward from the Cordillera into the foredeep basin. The overlying Gething Formation consists of a thick wedge of fluvial sandstone and siltstone that were deposited eastward over the Cadomin Formation up to the foredeep hinge line. Farther east, the sediments of the Gething Formation fill a broad northwest-trending valley system, the Spirit River Channel (Figure 30), that is incised more than 100 m into the Jurassic (Jackson, 1984). The northern part of the study area represents a paleo-high (Keg River Highlands), where no Bullhead Group sediments were deposited. Here, onlapping marine shales of the middle to upper Lower Cretaceous Buckinghorse Formation form the base of the Cretaceous succession. Time equivalent to the Lower Buckinghorse Formation, the marine shales of the Wilrich Formation at the base of the Fort St. John Group cap the Bullhead Group continental succession in the south. The thickness of the nonmarine Bullhead Group varies between 0 m in the north and >250 m in the southwest (Figure 30). The top of the Bullhead Group dips southwestward from 50 m to -500 metres above sea level (Figure 31a), and its depth ranges from 600 m to 2300 m below the ground surface (Figure 31b).

4.2 Hydrogeology of the Carboniferous to Lower Cretaceous Bullhead Group

The sedimentary succession from the Carboniferous to the lowermost Cretaceous Bullhead Group is the focus of the regional hydrogeological assessment, because these stratigraphic units contain the targets for the six acid-gas injection operations in the region of northeastern British Columbia.

4.2.1 Hydrostratigraphy

The hydrostratigraphy of the Carboniferous to Lower Cretaceous succession in the regional-scale study area in northeastern British Columbia is presented in Figure 13. The shales and tight carbonates of the Carboniferous Exshaw and Lower Banff formations represent the lower bounding aquitard at the base of the Permo–Carboniferous aquifer. The Permo–Carboniferous aquifer is formed by dolostones and sandstones of the Carboniferous Rundle and Stoddart groups and sandstones of the Permian Belloy Formation. The overlying Montney Formation consists mainly of siltstones and shales

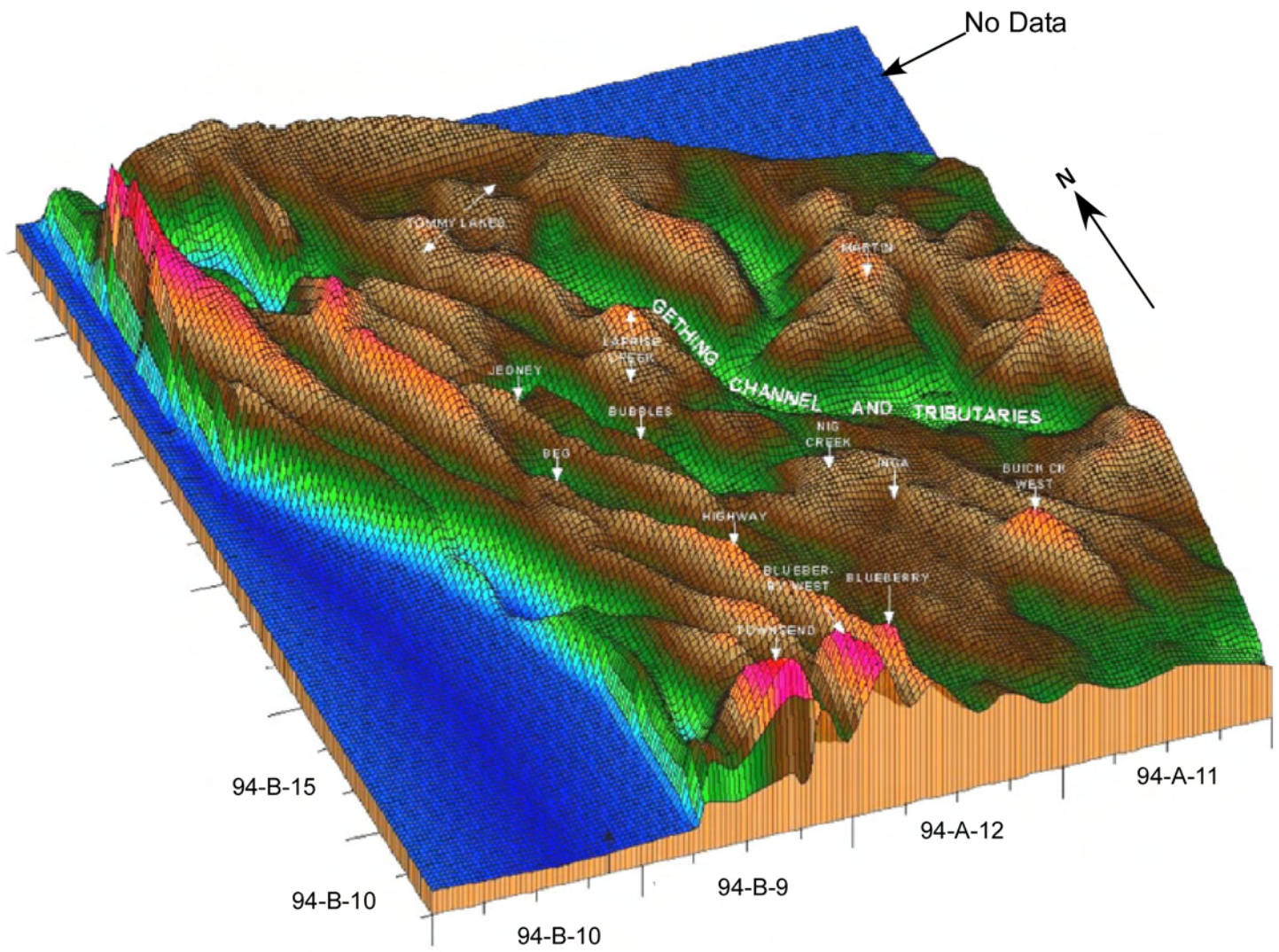

Figure 27. Block diagram of third-order residual structure on Triassic unconformity. The lower southeast corner includes T88 of the Peace River Block. Note the north-northwest linear fold and fault structures of the Beg–Jedney–Bubbles field trend (from Middle and Upper Triassic Baldonnel–Charlie Lake Report, northeastern British Columbia; G.R. Davies and S.W. Donaldson, prepared for GDGC Ltd., 2000).

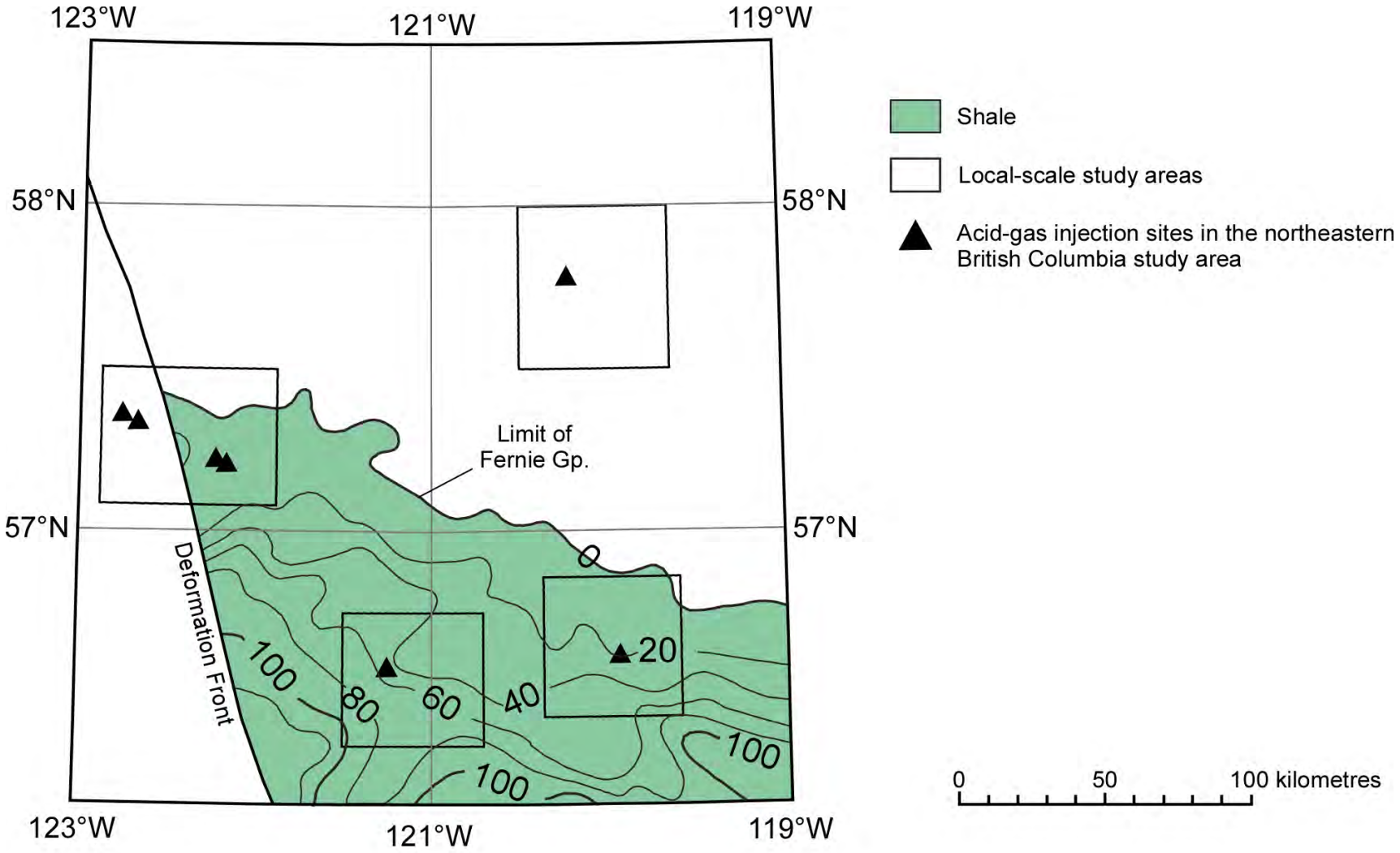

Figure 28. Generalized lithofacies and isopach of the Fernie Group in the regional-scale study area. Injection sites and local-scale study areas are also shown. Contours in metres. Contour interval = 20 m.

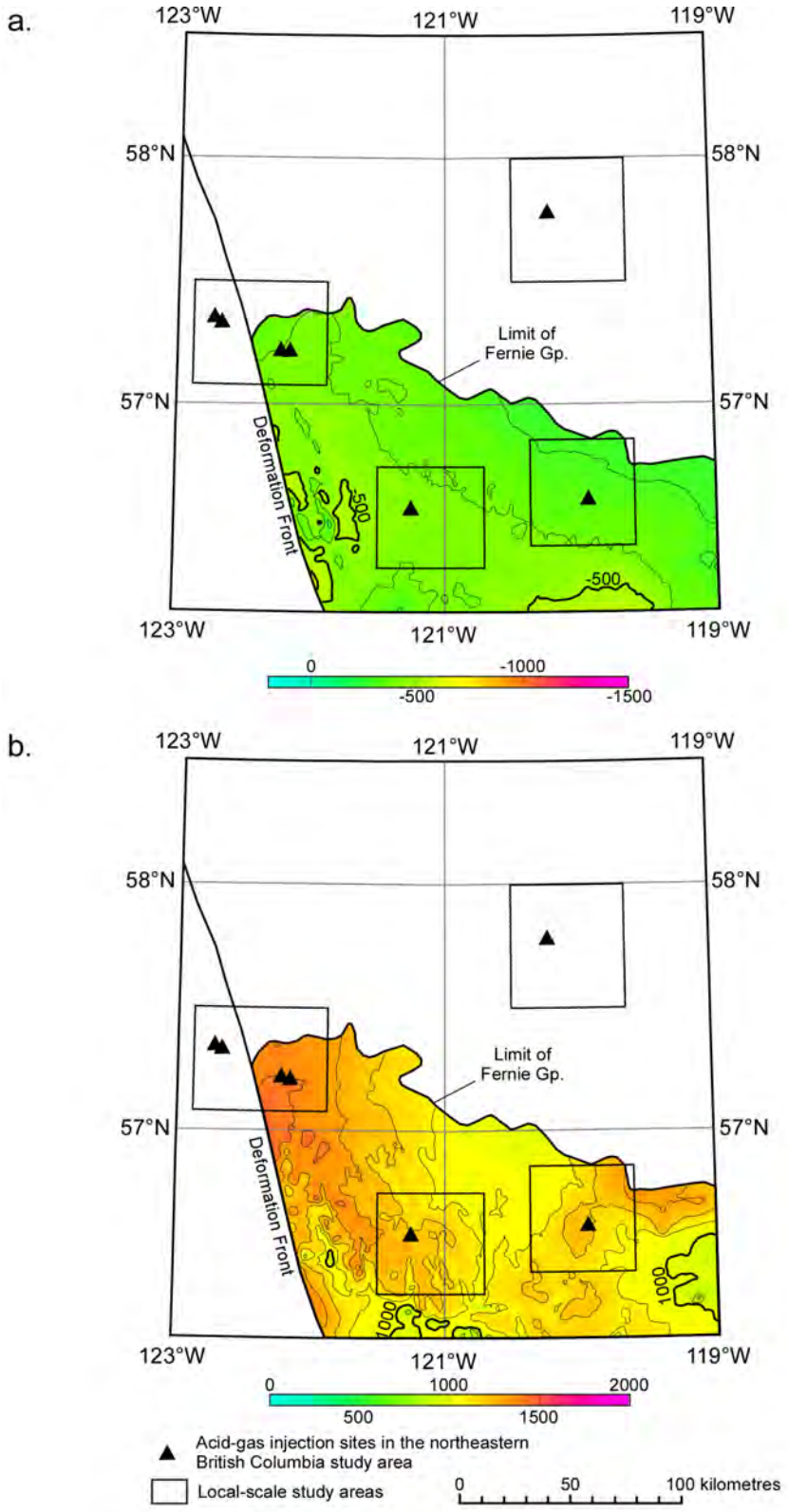

Figure 29. Main geological features of the Jurassic Fernie Group in the regional-scale study area: a) top structure elevation, and b) depth to top. The locations of the injection sites and the local-scale study areas are also shown. Contours in metres. Contour interval = 100 m.

(Edwards et al., 1994), therefore, forming an aquitard in most of the area. Only along its northwestern boundary, thin Montney sandstones are in hydraulic continuity with the underlying Permo–Carboniferous aquifer. The overlying, laterally continuous sandstones of the Halfway Formation form, in conjunction with the channel sandstones of the Upper Doig Formation, the latter cutting into the Montney shales, the Halfway–Doig aquifer. The Halfway–Doig aquifer is confined partly by fine siliciclastics and evaporites of the Charlie Lake Formation. Generally, the Charlie Lake Formation acts as an aquitard between the underlying Halfway–Doig aquifer and the overlying Baldonnel aquifer. Thin, intercalated sandstone units present in the lower to middle part of the Charlie Lake Formation form the relatively discontinuous, mostly isolated Lower Charlie Lake aquifer. The overlying carbonates of the Triassic Baldonnel and Pardonet formations form, in conjunction with the basal limestones of the Nordegg Member at the bottom of the Jurassic Fernie Group, the contiguous Nordegg–Baldonnel aquifer in the southwest of the study area. Large parts of the Carboniferous–Jurassic strata were eroded in the study area, and these sediments subcrop below the Cretaceous Bullhead aquifer. The shales of the Upper Jurassic Fernie Formation in the southwestern half of the study area form an important aquitard, separating the Bullhead aquifer from the underlying Triassic aquifers, where present. The succession of predominantly siltstones and shales of the Cretaceous Smoky and Fort St. John groups, in conjunction with the shales of the Wilrich–Moosebar Formation, form a thick, competent aquitard that overlies and confines the Bullhead aquifer at the top of the studied succession in the south. In the north, the Bullhead aquifer is absent, and marine shales of the Buckinghorse Formation form a continuous aquitard throughout the Lower Cretaceous (Figure 13).

4.2.2 Hydrogeological Observations

Hydrochemical analyses of formation waters and drillstem tests were used to interpret the flow of formation waters in the various aquifers in the regional-scale study area. The data used in this study (Table 1) are in the public domain and available from the Alberta Energy and Utilities Board (EUB) and the Oil and Gas Commission of British Columbia. The data were culled for erroneous analyses and tests, including production influence, and processed according to methods presented by Hitchon and Brulotte (1994), Hitchon (1996) and Michael and Bachu (2002).

Table 1. Number of chemical analyses of formation water and drillstem test (DST) data used in the regional assessment of formation water flow in the regional-scale study area, and estimates of formation water density at in-situ conditions.

Stratigraphic Interval	Number of Chemical Analyses	Number of DSTs	Average Density
Permo–Carboniferous	286	178	1051 kg/m^3
Halfway–Doig	368	325	1079 kg/m^3
Charlie Lake	133	158	1079 kg/m^3
Nordegg–Baldonnel	146	217	1021 kg/m^3
Bullhead	442	270	1026 kg/m^3
Total	1375	1148	1052 kg/m^3

4.2.2.1 Chemistry of Formation Waters

The formation waters in the Carboniferous to Bullhead Group succession in the northwestern part of the Alberta Basin are generally of a Na–Cl type, with the exception of some low-salinity waters in the Bullhead and Nordegg–Baldonnel aquifers that are of a Na–HCO_3–Cl type (Figure 32). The salinity ranges from approximately 5 g/l in the Bullhead aquifer, in recharge areas along the deformation front of the Rocky Mountains, to 225 g/l in the deeper formations and away from the mountains (Figures 33

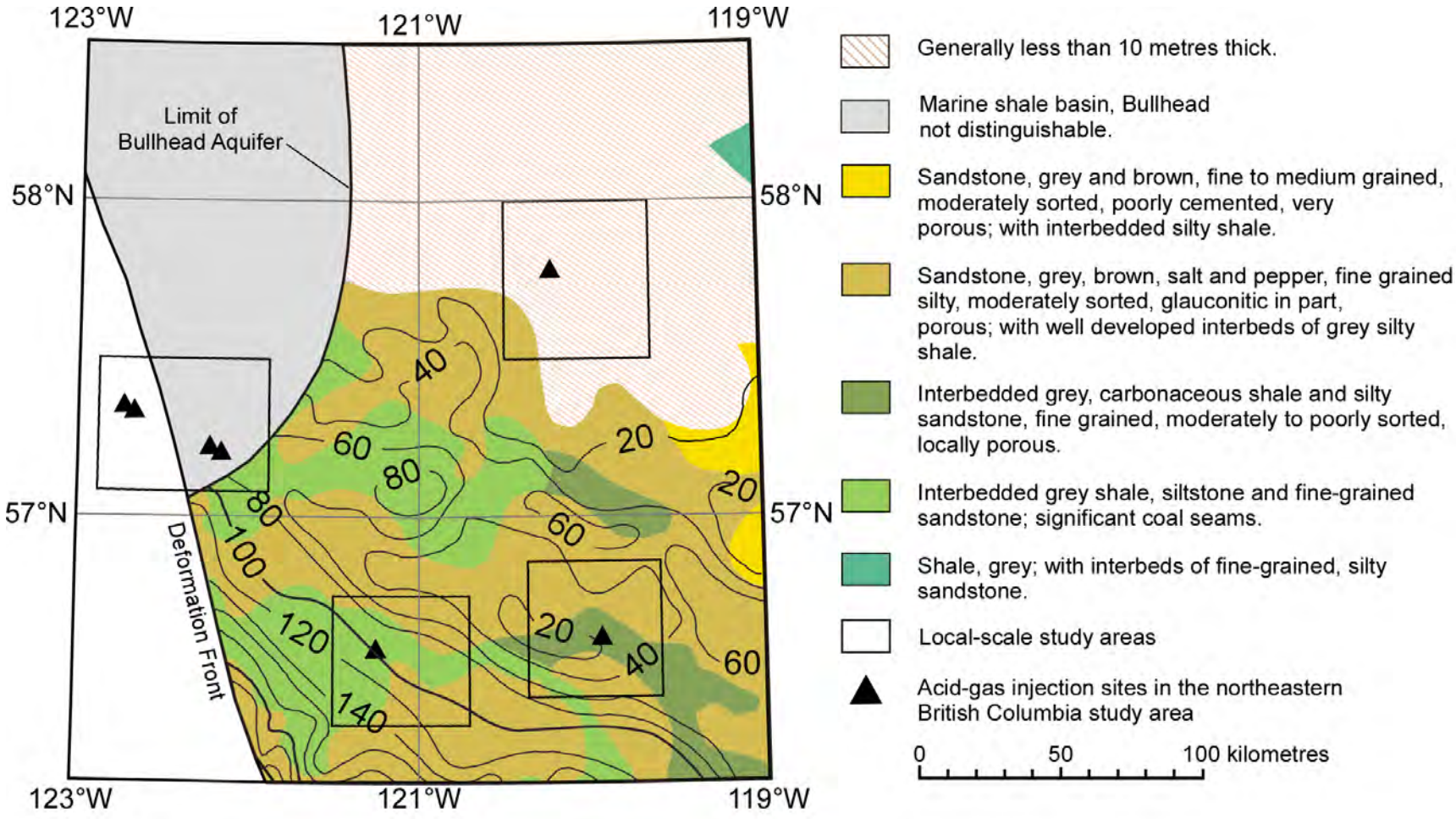

Figure 30. Generalized lithofacies and isopach of the Bullhead Group in the regional-scale study area. Injection sites and local-scale study areas are also shown (modified from Hayes et al., 1994). Contours in metres. Contour interval = 20 m.

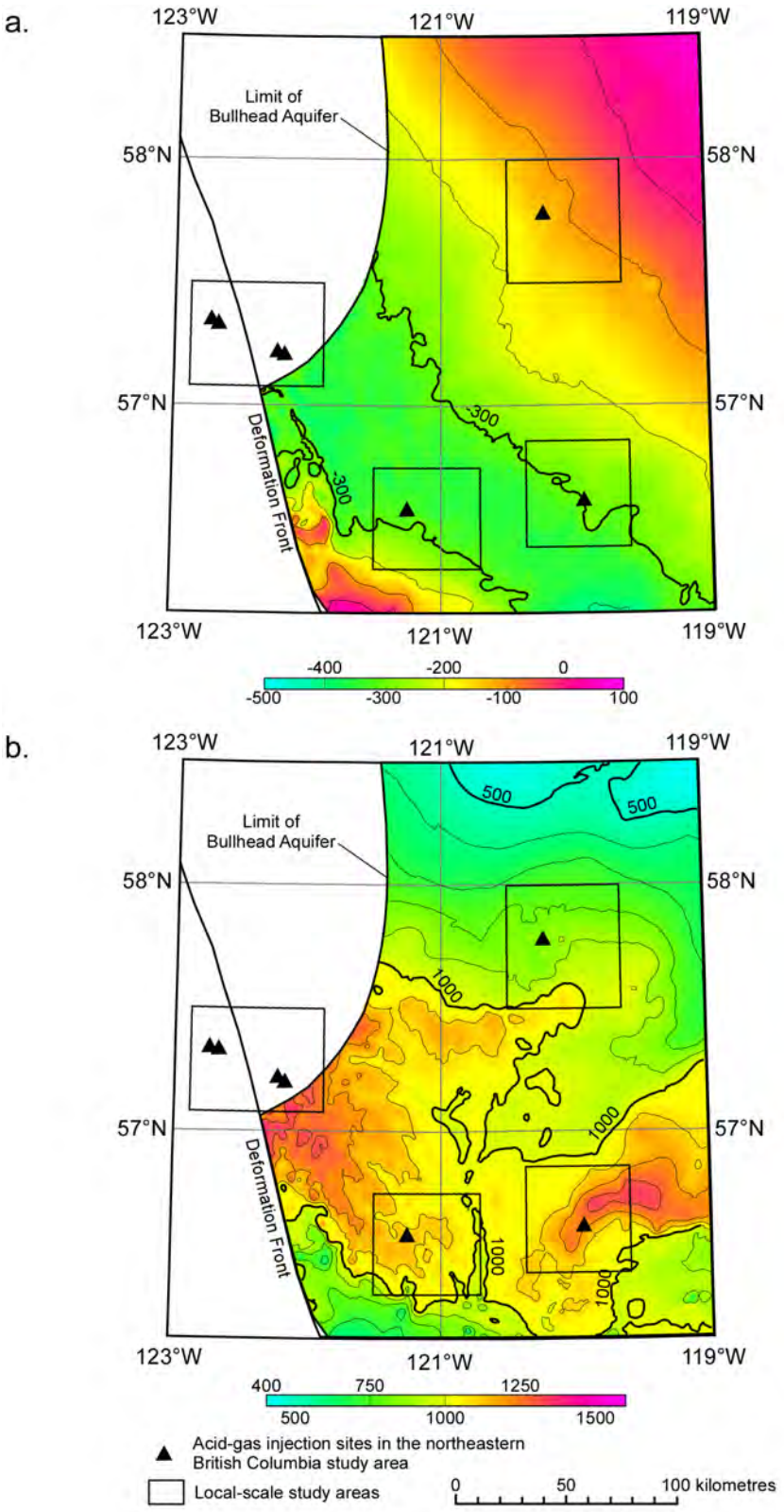

Figure 31. Main geological features of the Cretaceous Bullhead Group in the regional-scale study area: a) top structure elevation, and b) depth to top. The location of the injection sites and the local-scale study areas are also shown. Contours in metres. Contour interval = 100 m.

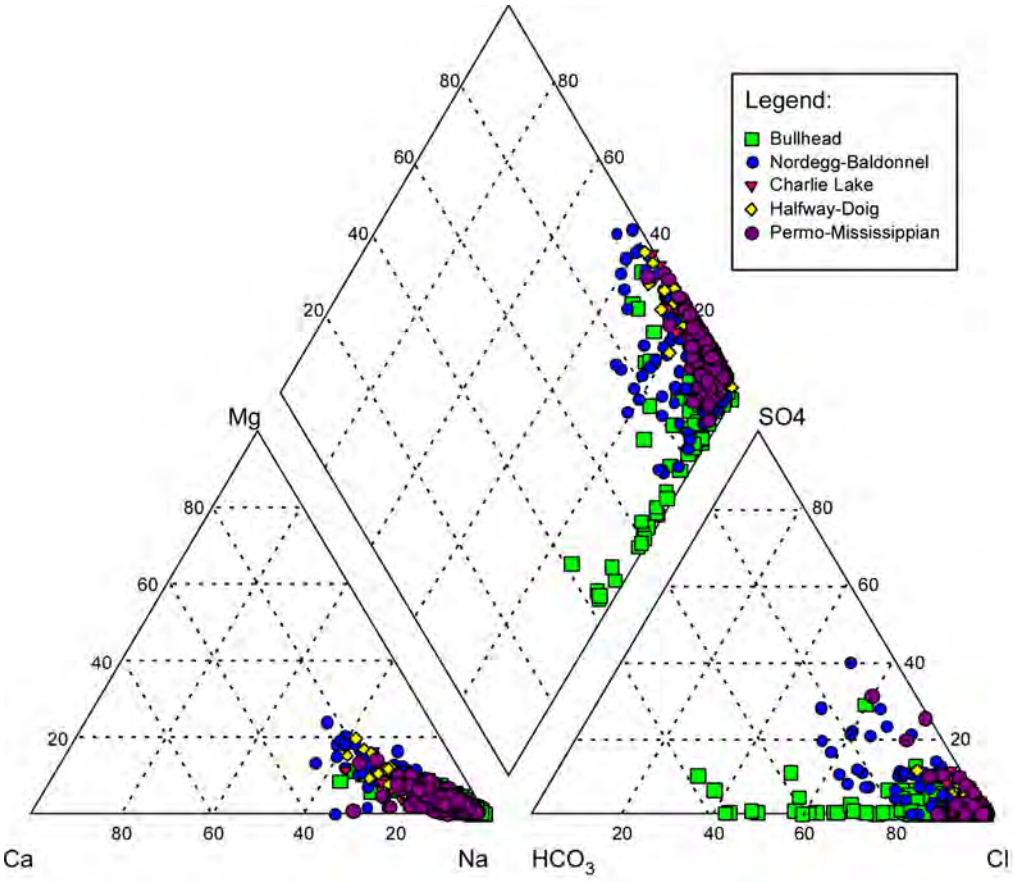

Figure 32. Piper plot of Mississippian to lowermost Cretaceous (Bullhead Group) formation waters in the northwestern part of the Alberta Basin.

to 35). The salinity patterns in the various aquifers are governed by the location of recharge areas, origin and flow of formation water, as well as water-rock interactions.

The salinity in the Permo–Carboniferous aquifer ranges from less than 20 g/l in the north and northeast to 180 g/l in the south (Figure 33a). A tongue of fresher water (~65 g/l) is present in the southwest corner along the deformation front, extending northeastward. The salinity in the overlying Halfway–Doig aquifer is highest in the centre of the aquifer (>140 g/l), decreasing to less than 60 g/l along the deformation front and along the northwestern limit of the aquifer (Figure 33b). Similarly, Total Dissolved Solids (TDS) values in the overlying Charlie Lake aquifer increase from less than 60 g/l along the aquifer boundary in the north to greater than 160 g/l in the south (Figure 34a). Only in the southwest corner, lower salinity values of approximately 60 g/l can be observed. In comparison, salinity in the Nordegg–Baldonnel aquifer is significantly lower, ranging from less than 10 g/l along the deformation front to maximum values greater than 100 g/l in the northern part of the aquifer (Figure 34b). Recharge of freshwater along the Rocky Mountains Front Ranges and Foothills appears to penetrate down to the Bullhead aquifer and is the cause for relatively low TDS in the southeast of the regional-scale study area (Figure 35). Formation water salinity increases successively toward the northeast. Maximum salinity values above 60 g/l can be observed along a northwest-southeast trend in the centre of the study area, subparallel to the limit of the Jurassic Fernie aquitard, where the Bullhead aquifer is in direct hydraulic communication with the underlying Triassic aquifers.

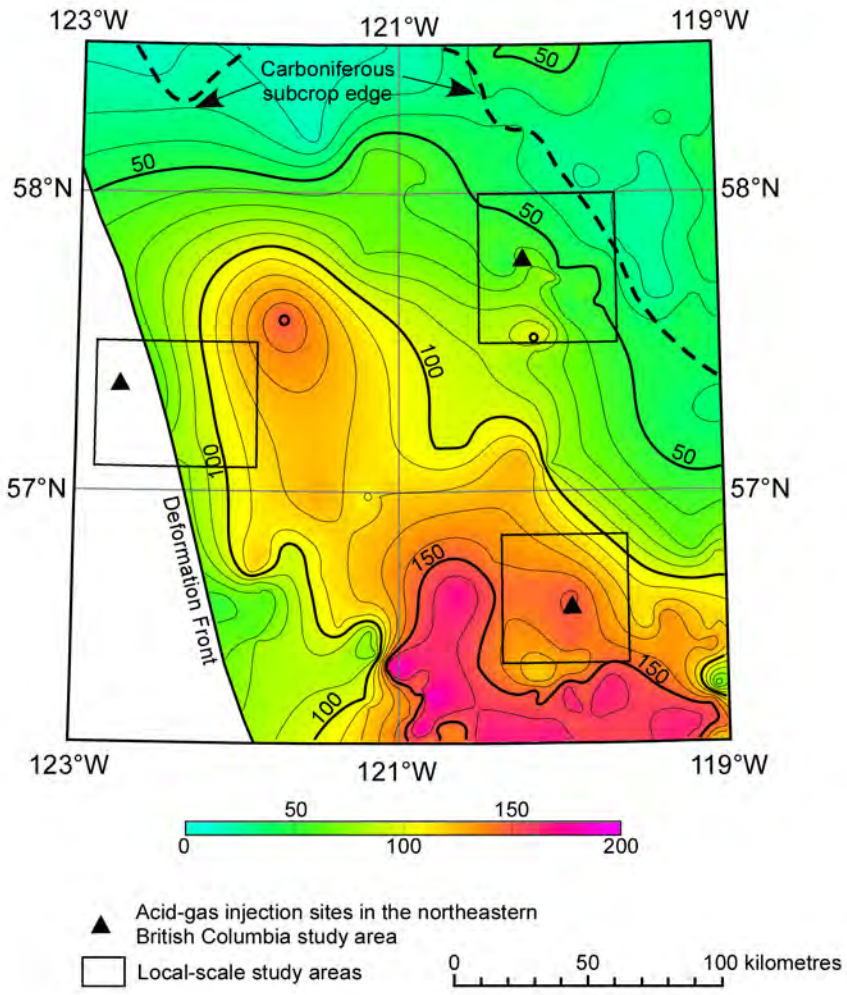

Figure 33. Regional distribution of salinity in the a) Permo–Carboniferous aquifer. Also shown are the Caribou–Debolt, Ring–Debolt and Boundary Lake–Belloy injection sites and the outline of the respective local-scale study areas. Contours in g/l. Contour interval = 10 g/l.

The formation water density was calculated using regression expressions based on measured data in the Alberta Basin and scaling to in-situ pressure, temperature and salinity conditions after Rowe and Chou (1979) (Adams and Bachu, 2002). The in-situ density of formation waters is controlled largely by salinity. Therefore, the average density of formation water is highest in the largely isolated, high-salinity Charlie Lake and Halfway–Doig aquifers that are adjacent to evaporitic beds in the Charlie Lake Formation (1079 kg/m^3) (Table 1). In comparison, the average density of the less saline formation waters in the Nordegg–Baldonnel and Bullhead aquifers is approximately 1025 kg/m^3. The average density of formation water in the Permo–Carboniferous succession is 1051 kg/m^3, which is similar to the overall average density of formation water in the entire Carboniferous–Lower Cretaceous succession (1052 kg/m^3).

4.2.2.2 Flow of Formation Waters

The analysis of the flow of formation waters is based on distributions of hydraulic heads in the Carboniferous to Bullhead Group intervals. The hydraulic heads were calculated with a reference density of 1052 kg/m^3 in order to minimize the errors in representing and interpreting the flow of variable density water near the acid-gas injection sites (Bachu and Michael, 2002). The reference density corresponds to the average brine density at conditions characteristic for the Carboniferous to Bullhead Group succession

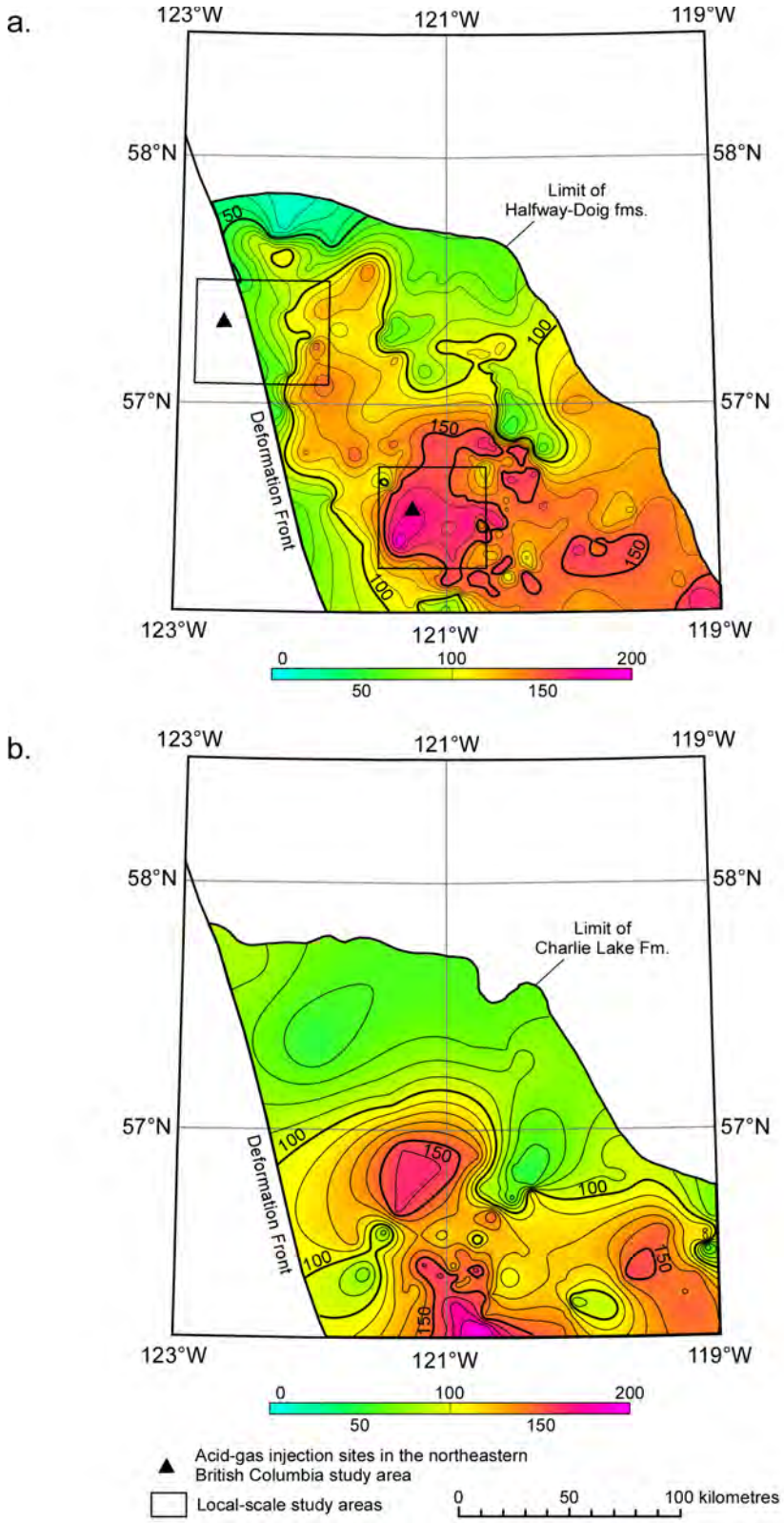

Figure 34. Regional distribution of salinity in the a) Halfway–Doig and b) Charlie Lake aquifers. Also shown are the Caribou–Halfway and Stoddart–Halfway injection sites and the outline of the respective local-scale study area in Figure 34a. Contours in g/l. Contour interval = 10 g/l.

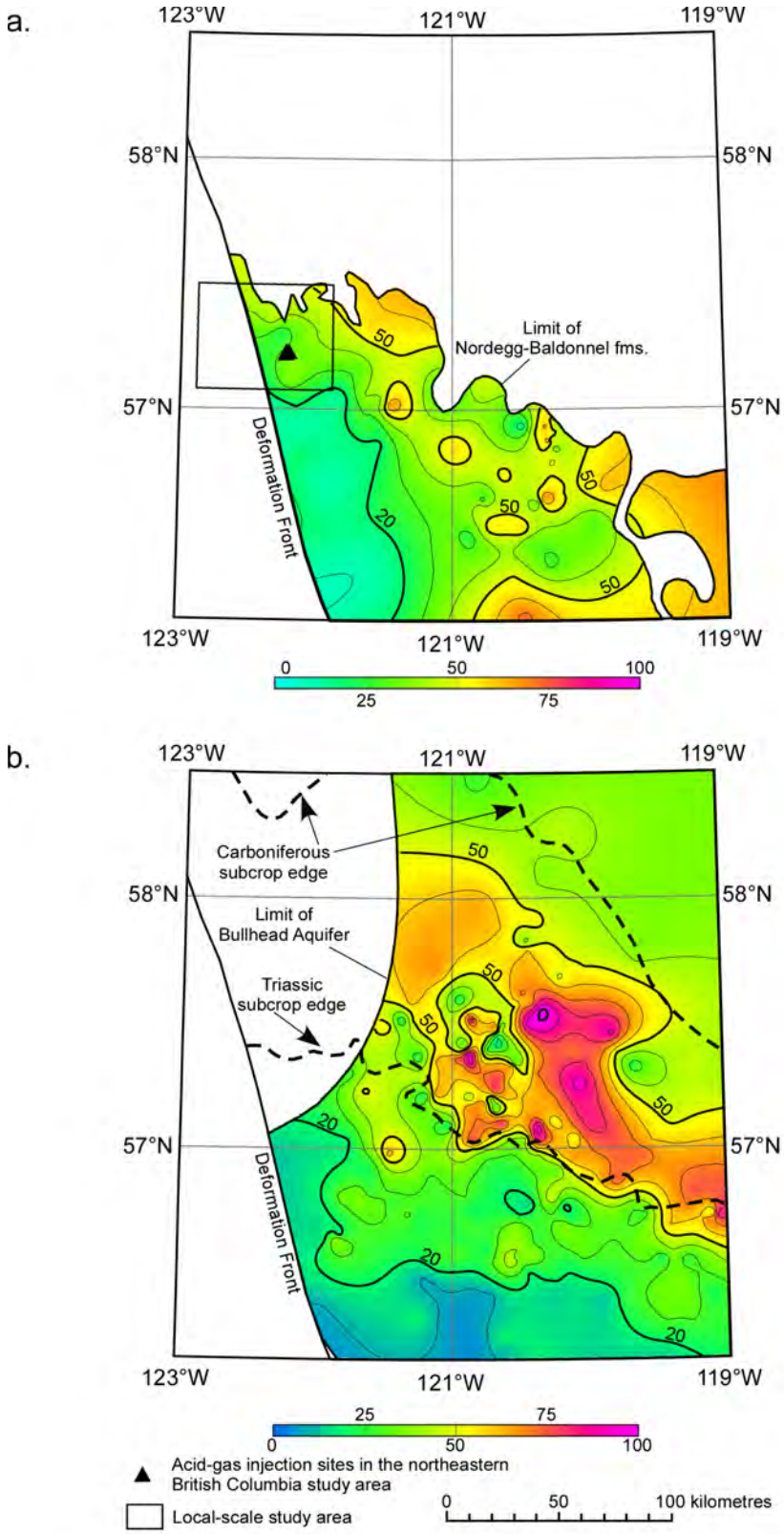

Figure 35. Regional distribution of salinity in the a) Nordegg–Baldonnel and b) Bullhead aquifers. Also shown are the Bubbles–Baldonnel and Jedney–Baldonnel injection sties and the outline of the respective local-scale study area in Figure 35a. Contours in g/l. Contour interval = 10 g/l.

in the regional-scale study area (Table 1). Hydraulic heads were calculated according to

$$H = \frac{p}{\rho_o g} + z \qquad (1)$$

where z (m) is the elevation of the pressure recorder, p (Pa) is pressure, ρ_o (kg/m^3) is the reference density and g is the gravitational constant (9.81 m/s^2).

As discussed previously (Section 3.2.2), flow in the Carboniferous to Cretaceous succession is driven mainly by local to regional-scale topography. In the regional-scale study area, the ground surface elevation generally decreases from >1800 m above sea level (asl) in the northwest in the Rocky Mountains to less than 400 m asl in the north (Figure 36). The Milligan Hills and their westward continuation toward the Rocky Mountains in the centre of the study area, represent a major regional surface water divide, with drainage occurring southwards into the Peace River and northwards into the Sikanni River, respectively. Another important regional topographic high is represented by part of the Clear Hills with elevations >1000 m asl at the southeastern boundary of the study area.

Regional flow in the Permo–Carboniferous aquifer follows the general drop in ground surface topography and is initially toward the northeast from areas with hydraulic heads >600 m along the deformation front, to the limit of Carboniferous subcrop below the Bullhead aquifer, where hydraulic heads are less than 500 m (Figure 37). Subparallel to the subcrop limit, hydraulic heads increase to above 500 m in the area of the Milligan Hills, inferring a northwestward deflection of formation water flow towards the area of the Sikanni River. Northeast of the Milligan Hills, the flow is again northeastward in the direction of decreasing hydraulic heads to values below 350 m in the northeastern corner of the study area. Hydraulic head patterns in the southeast also correspond to ground surface topography, indicating east-northeastward flow from the Rocky Mountains and divergent flow from the area of the Clear Hills towards the north, the west and the Peace River in the south, respectively.

The hydraulic head distribution in the overlying Halfway–Doig aquifer generally suggests north-northwestward flow of formation water, subparallel to the eastern limit of the Halfway Formation (Figure 38a). A significantly underpressured area with hydraulic heads less than 250 m exits in the northwestern part of the Halfway–Doig aquifer, which suggests hydraulic isolation of this area.

Similar to the Halfway–Doig aquifer, hydraulic head values in the overlying Charlie Lake aquifer decrease from >600 m along the deformation front and in the area of the highlands north of the Peace River to <400 m in the north, indicating northward flow of formation water (Figure 38b). Hydraulic head values below 550 m along the southern boundary at the southeast corner of the study area indicate another component of flow in the direction of the Peace River. The hydraulic head distribution in the overlying Nordegg–Baldonnel aquifer suggests northeastward flow from areas of hydraulic heads >600 m along the deformation front of the Rocky Mountains toward the northeastern boundary of the aquifer where hydraulic heads are in the range of 450 m (Figure 39a).

Formation water flow inferred from hydraulic head distributions in the Bullhead aquifer is channelled generally in a northward direction, from areas with hydraulic heads >600 m in the southwest and >500 m in the south, to an area with hydraulic head elevations <400 m in the north (Figure 39b), following the regional drop in ground surface topography (Figure 36). A major flow divide is located approximately along 56.5^{o}N (Rocky Mountain Foothills in the west to Clear Hills in the east), where formation water flows either toward the Peace River Valley in the south or the centre of the study area. Another flow divide with relatively high hydraulic heads (>450 m) is located in the area of the Milligan Hills in the

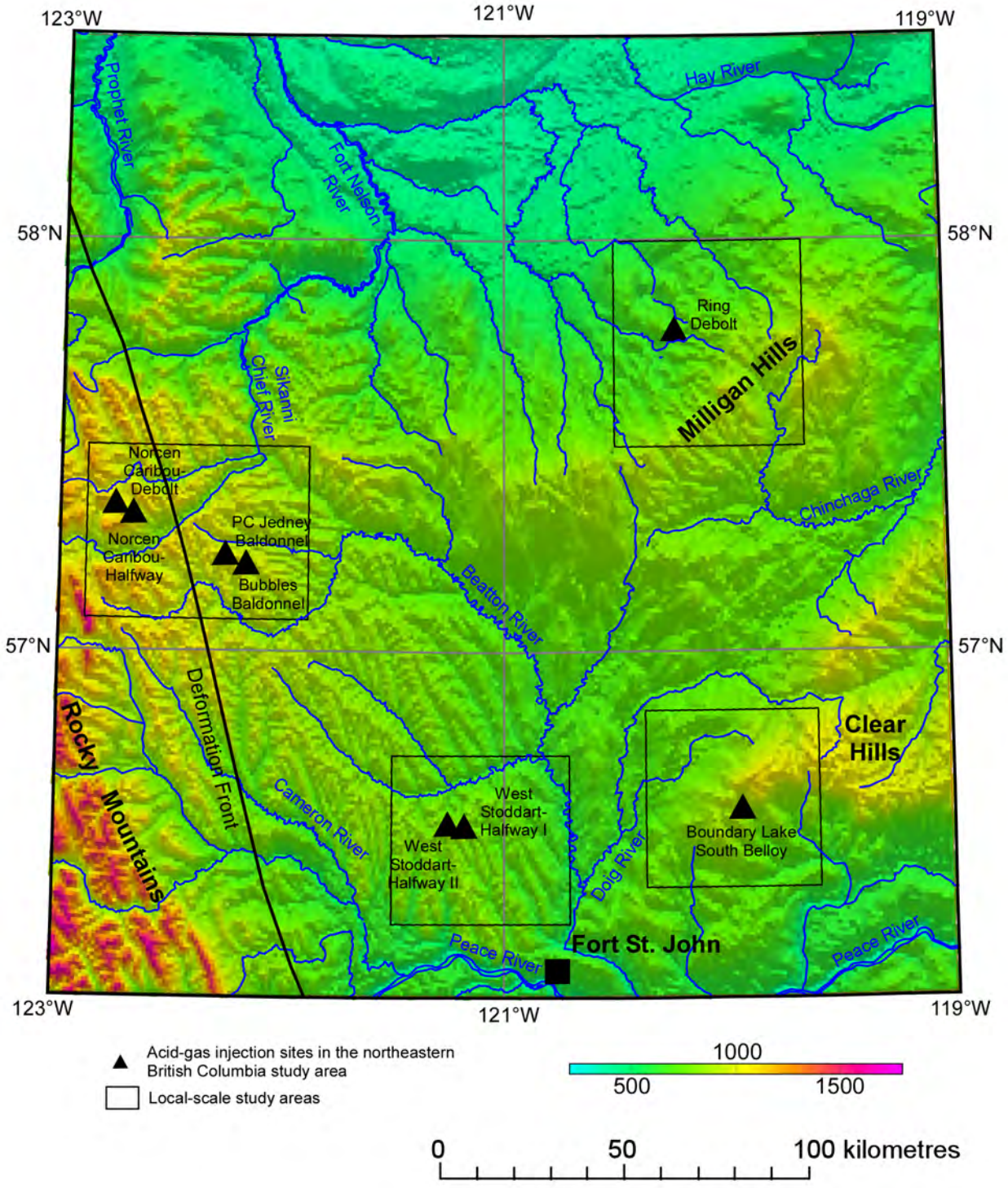

Figure 36. Topographic map of the regional-scale study area showing the location of the acid-gas injection sites and the outline of their respective local-scale study areas.

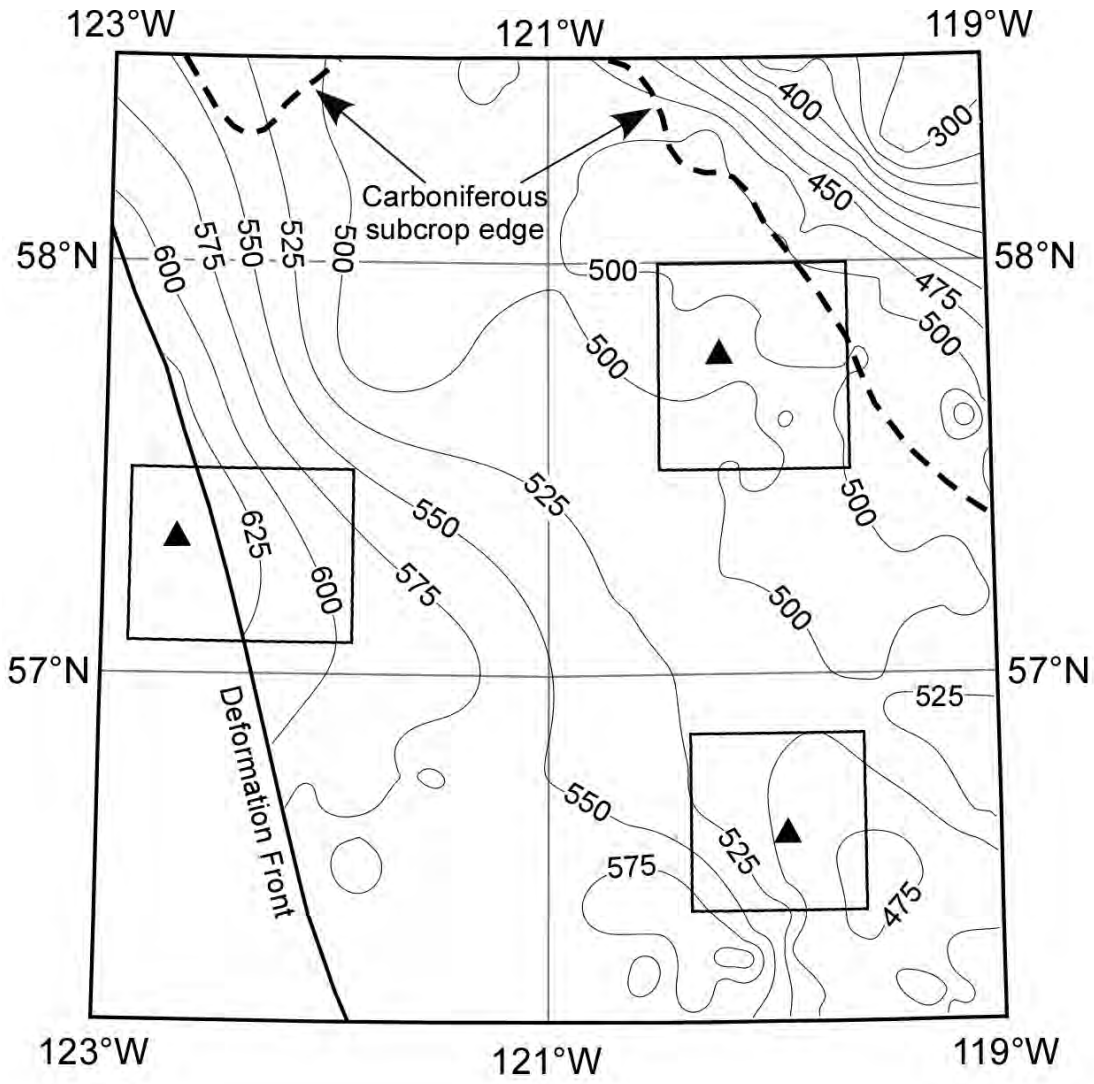

Figure 37. Regional distribution of hydraulic heads in the Permo–Carboniferous aquifer. Also shown are the Caribou–Debolt, Ring–Debolt and Boundary Lake–Belloy injection sites and the outline of the respective local-scale study areas. Contours in metres. Contour interval = 25 m.

east-central part of the study area, the flow of formation water being toward the northeast and southwest, respectively. In the northeastern corner of the study area, the Carboniferous subcrops below the Bullhead aquifer, and hydraulic heads in both aquifers are less than 350 m (Figures 37 and 39b), suggesting good cross-formational hydraulic communication.

All aquifers from the Permo–Carboniferous to the Bullhead show a similar generalized flow pattern. Combining the analysis of formation water flow and salinity distribution in the various aquifers, the hydrogeology and flow pattern in the regional-scale study area can be summarized as follows:

- Five aquifers can be distinguished in the study area: Permo–Carboniferous, Halfway–Doig, Lower Charlie Lake, Nordegg–Baldonnel and Bullhead.
- The bounding and intervening aquitards are Exshaw–Lower Banff, Montney, Doig (lower part), Upper and Lower Charlie Lake, Fernie, and Fort St. John–Wilrich.

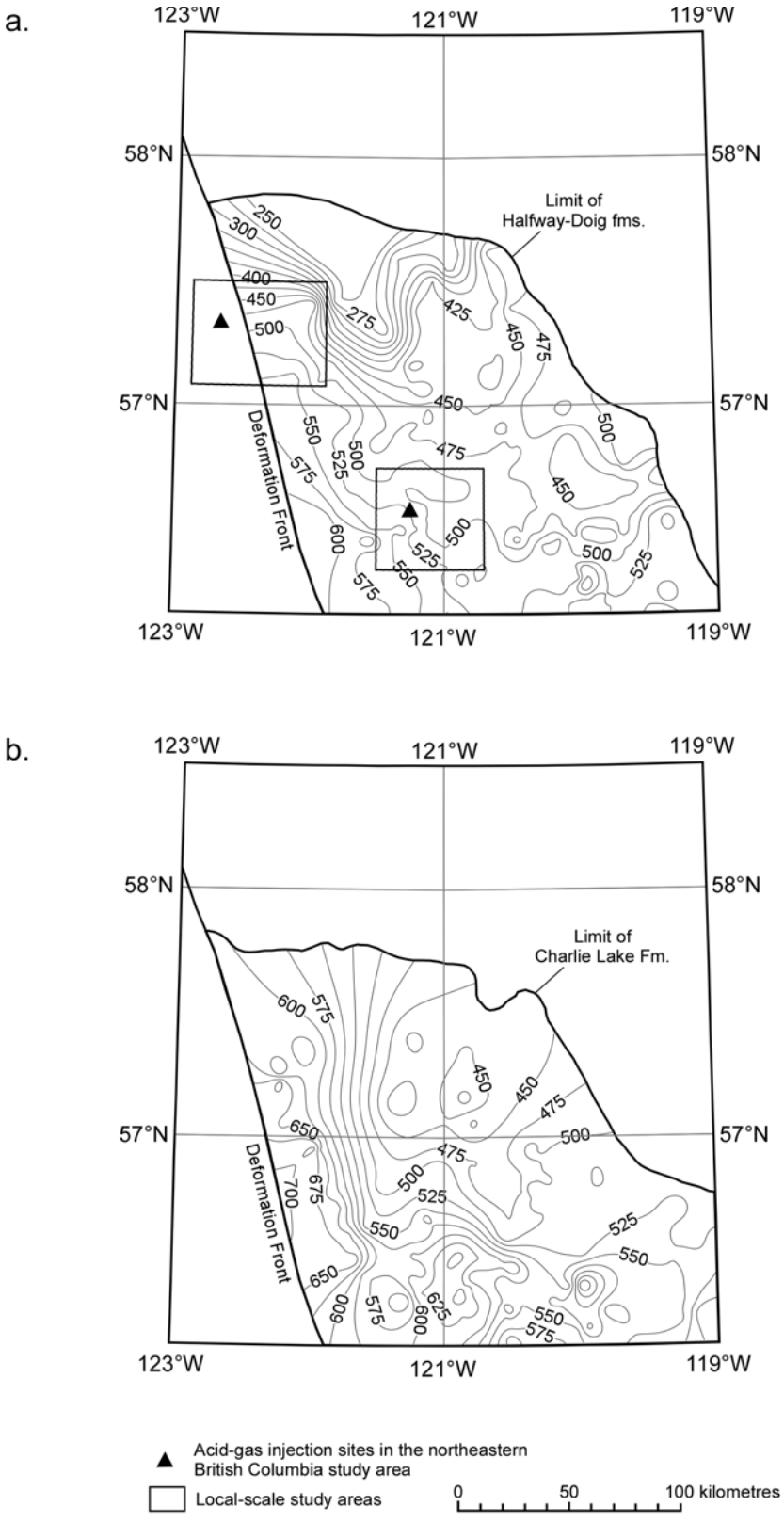

Figure 38. Regional distribution of hydraulic heads in the a) Halfway–Doig and b) Charlie Lake aquifers. Also shown are the Caribou–Halfway and Stoddart–Halfway injection sties and the outline of the respective local-scale study area in Figure 38a. Contours in metres. Contour interval = 25 m.

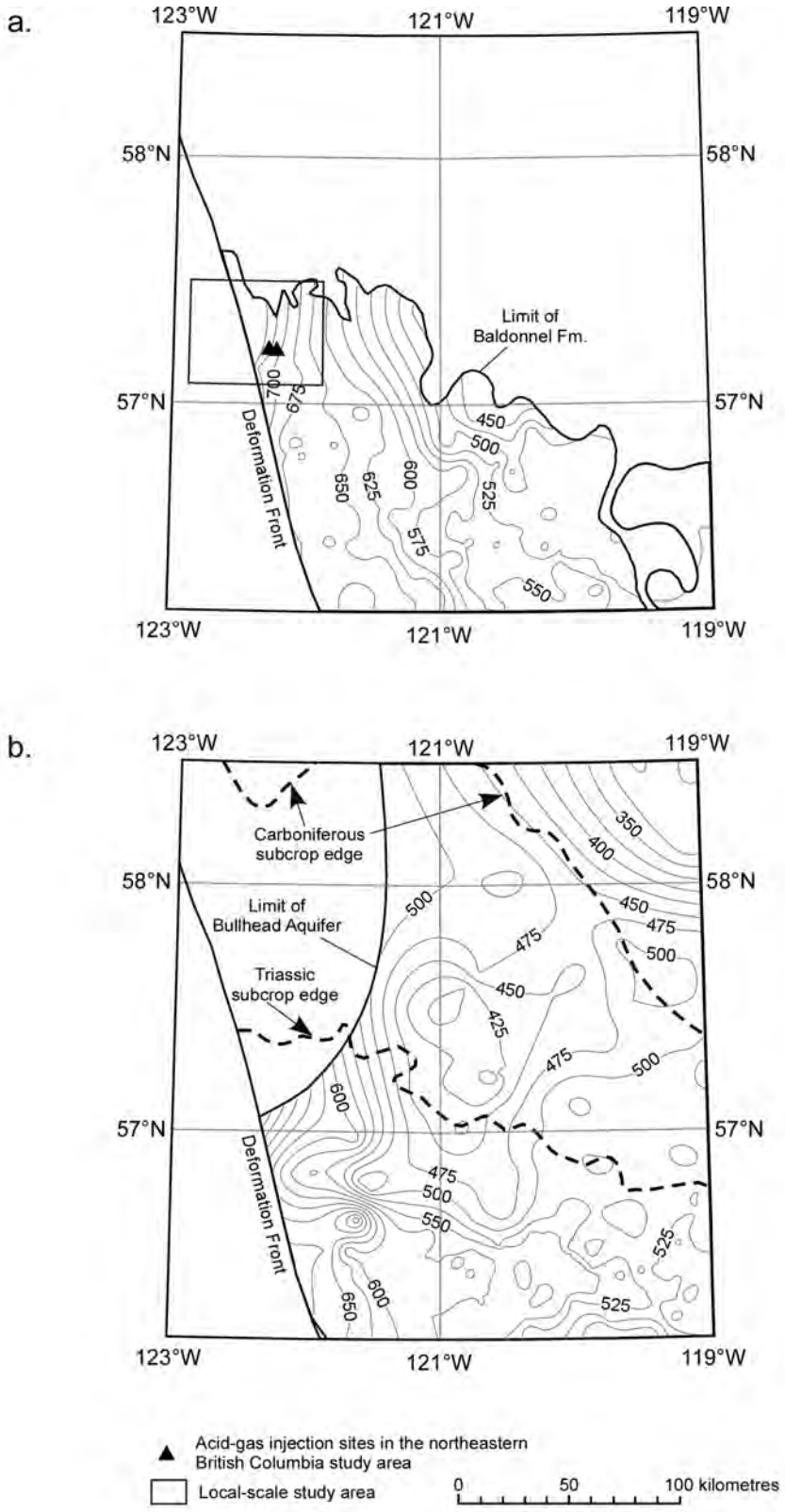

Figure 39. Regional distribution of hydraulic heads in the a) Nordegg–Baldonnel and b) Bullhead aquifers. Also shown are the Bubbles–Baldonnel and Jedney–Baldonnel injection sites and the outline of the respective local-scale study area in Figure 39a. Contours in metres. Contour interval = 25 m.

- The salinity of formation waters varies over a wide range, from approximately <10 g/l in the shallowest aquifer in the southwest to >225 g/l in the centre of the regional-scale study area.
- Where the Fernie aquitard is absent, brines from the various Triassic to Carboniferous aquifers mix along their subcrops with fresher formation water from the Bullhead aquifer.
- Relatively fresher formation water enters the various aquifers from the Rocky Mountain Foothills in the southwest, and flow is generally updip in a north-northeastward direction in the southwestern half of the study area.
- In the northeastern half of the study area, flow of formation water is driven by the local topography of the Milligan and Clear Hills, partly counteracting the updip flow from the Rocky Mountains.

4.2.3 Flow Interpretation

Present-day formation water flow in the regional-scale study area is mainly driven by gravity, through a regional-scale flow system originating in the southwest, at topographic highs in and along the Front Ranges and Foothills of the Rocky Mountains (Figure 40). Generally, flow is toward areas with low ground surface elevation in the north and northeast, corresponding to the regional interpretation of formation water flow in the northern Alberta Basin by Bachu (1997), with the exception of the southernmost part, where flow is southward toward the Peace River Valley. Relatively fresh water originating from recharge in the Rocky Mountains penetrates vertically down to the Bullhead, Triassic and Permo–Carboniferous aquifers, becoming increasingly more saline with depth because of mixing with older formation water and increasing dissolution with increasing temperatures. Away from the deformation front, the fresher water is in the process of displacing the original high-salinity brines in the Triassic to Carboniferous aquifer northeastward, thereby pushing the original brines updip. Past the limit of the Fernie aquitard, which separates the Bullhead from the Triassic aquifers in the south, the slowly updip-moving brines from the Triassic mix(ed) with Bullhead formation water, forming a plume of high-salinity brine in the latter. The flow pattern in northeastern British Columbia is the result of superposition of local, intermediate and regional-scale flow systems driven by topography. The flow in the deep Carboniferous to Triassic aquifers is regional scale from recharge at high elevation in the Rocky Mountains Thrust and Fold Belt to discharge at the northeastern basin edge (Bachu, 1997). Local topographic highs, like the Clear and Milligan hills, are the origin of local and intermediate-scale flow systems, which are most evident in the Bullhead aquifer, superimposed on and partly counteracted in places the regional-scale updip flows (Figures 40 and 41). The interplay between regional, intermediate and local-scale flow systems in northeastern British Columbia is in good agreement with the concept of topographically driven flow in sedimentary basins developed by Tóth (1963).

The similarity of hydraulic head and salinity distribution in the three Triassic aquifers indicates that there is some degree of vertical hydraulic communication between these aquifers, and that the intervening Lower and Upper Charlie Lake aquitards are discontinuous. An area where there apparently is no hydraulic communication between the Halfway–Doig and adjacent aquifers is the northwestern corner of the Halfway–Doig aquifer, where hydraulic head values in the overlying Charlie Lake and underlying Permo–Carboniferous aquifers are significantly higher than in the Halfway–Doig aquifer. The severe underpressures, probably the result of erosional rebound, indicate that the Halfway–Doig aquifer is relatively isolated in this area. In addition to the vertical isolation, the Halfway–Doig aquifer pinches out northward against the marine shales of the Fort St. John Group that probably are the source of the erosional underpressuring.

Only marginally affecting formation water flow in the study area, the downdip flow component in the southeastern corner of the Bullhead aquifer is attributed to re-imbibement of formerly gas-saturated areas (i.e., Elmworth Field) by formation water (Thompson, 1989; Michael and Bachu, 2001), and

underpressuring created by the erosional rebound of overlying shales (Bachu, 1995).

With respect to the regional hydrostratigraphy and hydrogeology, the acid-gas injection targets in the northeastern British Columbia area are in ascending stratigraphic order: a) the Permo–Carboniferous aquifer (Boundary Lake, Ring, Caribou II), b) the Triassic Halfway–Doig aquifer (West Stoddart, Caribou I), and c) the Nordegg–Baldonnel aquifer (Bubbles, Jedney).

4.3 Stress Regime and Rock Geomechanical Properties

4.3.1 Stress Regime

Knowledge of the stress regime at any injection site is important for establishing the potential for hydraulic rock fracturing as a result of injection, and for setting limits for operational parameters. A comprehensive assessment of the stress regime at all the acid-gas injection operations in the Alberta Basin can be found in another report (Stress Regime at Acid-Gas Injection Operations in Western Canada, S. Bachu et al., prepared for the Acid Gas Management Committee, 2004). Given its tensorial nature, the stress regime in any structure, including the Earth, is defined by the magnitude and orientation of the three principal stresses, which are orthogonal to each other. In consolidated rocks, the fracturing threshold is greater than the smallest principal stress, σ_3, but less than the other two principal stresses, σ_1 and σ_2. If fracturing is induced, fractures will develop in a plane and direction perpendicular to the trajectory of the smallest principal stress. Basin-scale studies of the stress regime suggest that in most of the Alberta Basin the smallest principal stress, σ_3, is horizontal (Bell and Babcock, 1986; Bell et al., 1994; Bell and Bachu, 2003). Due to the orthogonality of the stress tensor, this means the smallest stress is the minimum horizontal stress ($\sigma_3=S_{Hmin}$). Rock fracturing occurs at pressures P_b that are greater than the minimum horizontal stress and can be estimated using the equation:

$$P_b = 3S_{H\min} - S_{H\max} + P_0 + T_0 \qquad (2)$$

where S_{Hmax} is the maximum horizontal principal stress, P_0 is the pressure of the fluid in the pore space, and T_0 is tectonic stress. In the case of injection, the fluid pressure at the well is the bottomhole injection pressure. This equation demonstrates that the fracturing pressure is related to the effective stress (stress less fluid pressure), beside the tensile strength of the rock.

The minimum horizontal stress, S_{Hmin}, can be evaluated using a variety of tests. The most accurate method for estimating the magnitude of the S_{Hmin} is through micro-fracture testing, but mini-fracturing, leak-off tests and Fracture Breakdown Pressure tests are also used (Bell, 2003; Bell and Bachu, 2003). The maximum horizontal stress cannot be directly measured, but it can be calculated according to the

relation $$S_{H\max} = \frac{\mu}{1-\mu}(S_V - P_0) \qquad (3)$$

where S_V is the vertical stress and μ is Poisson's ratio, which is determined through laboratory tests on rock samples. The magnitude of the vertical stress S_V at any depth coincides with the pressure exerted by the rocks above that point (weight of the overburden), and can be calculated by integrating the values recorded in density logs. Unfortunately, there are no methods for estimating the tectonic stress, $T_{0;}$ hence, it is not possible to estimate the rock fracturing pressure. However, previous studies have shown that in the regional-scale study area the S_{Hmax} is less than S_V (Bell and Babcock, 1986; Bell et al., 1994). Thus, estimation of S_{Hmin} and S_V in a well provides loose lower and upper bounds for the fracturing pressure in that well.

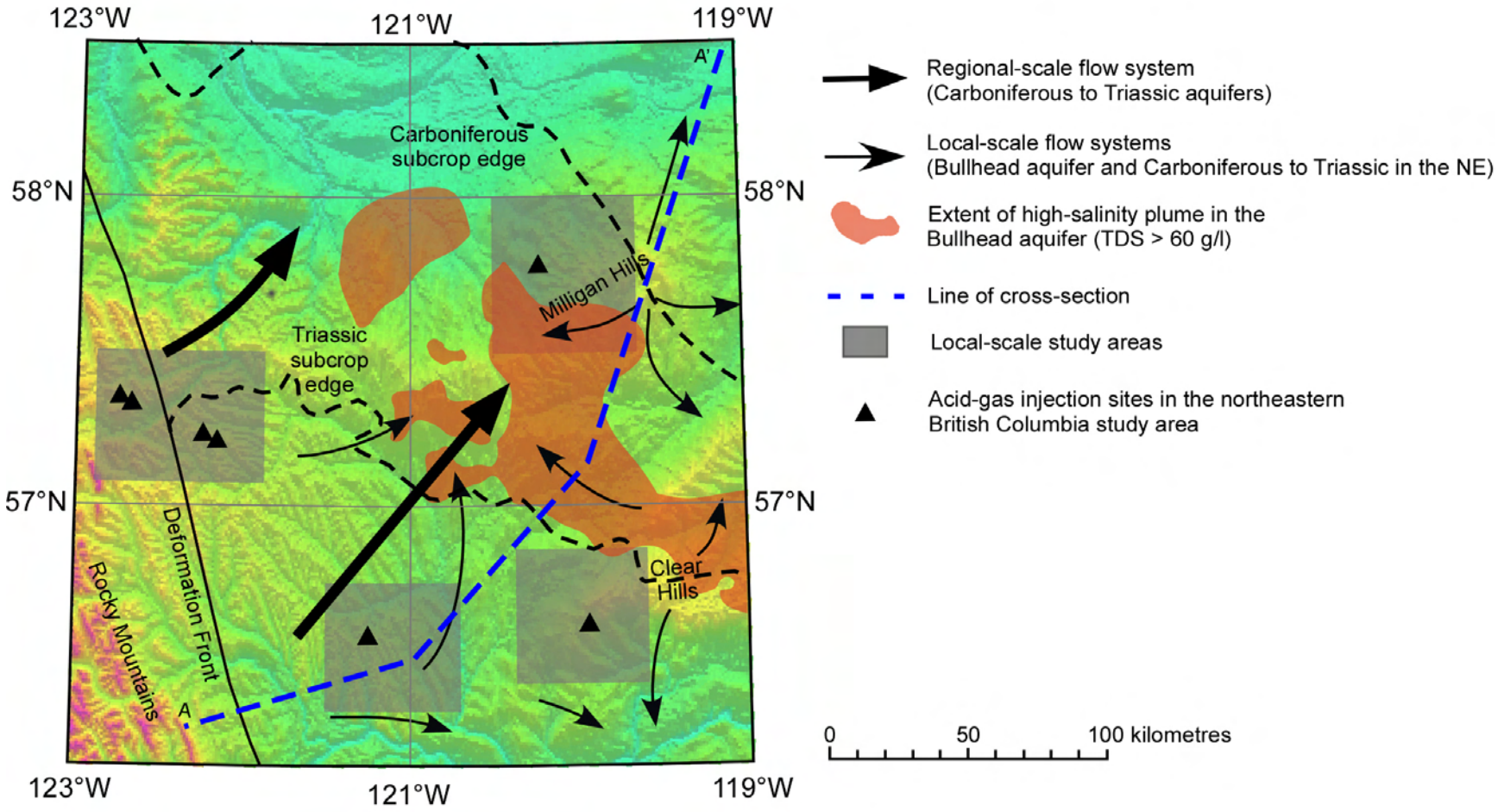

Figure 40. Generalized flow patterns in the northeastern British Columbia regional-scale study area.

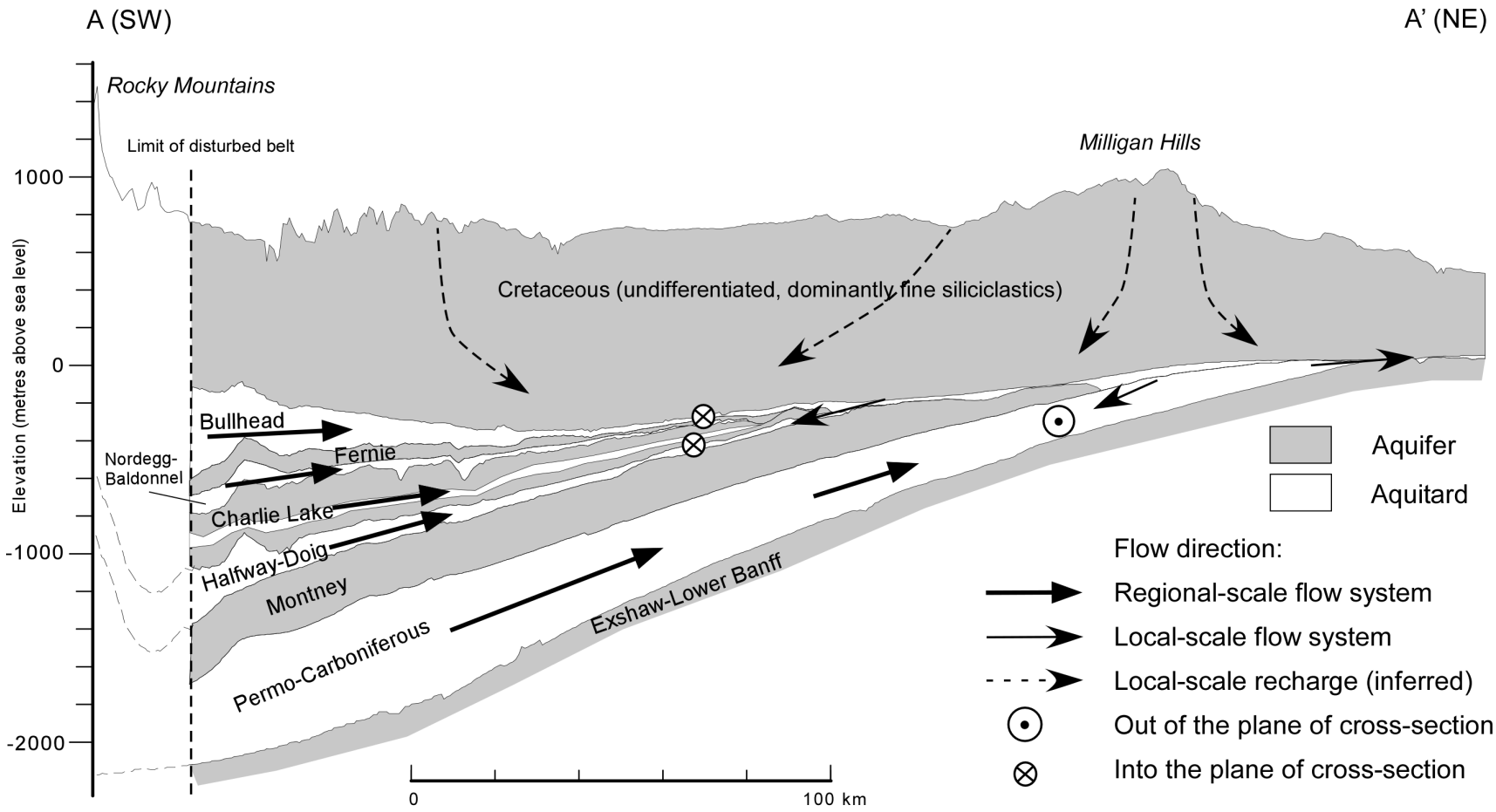

Figure 41. Diagrammatic representation in cross-section of the flow systems in the Carboniferous to Bullhead sedimentary succession in the regional-scale study area. The location of the cross-section is shown in Figure 40.

If fractures occur, they will develop perpendicular to the plane of the minimum horizontal stress; hence, the need to know the principal directions of the stress field. Horizontal stress orientations can be determined from breakouts, which are spalled cavities occurring on opposite walls of a borehole (Bell, 2003). They form because the well distorts and locally amplifies the far-field stresses, producing shear fracturing on the borehole wall. If the horizontal principal stresses are not equal, the wallrock of a quasi-vertical well is anisotropically squeezed. Caving occurs preferentially aligned with the axis of the smaller S_{Hmin}. More detailed description of the methods used for estimating stress magnitude, gradient and orientation are found in Bell (2003).

Orientations of the minimum horizontal stress S_{Hmin} were determined from breakouts in six wells in the regional-scale study area (Table 2 and Figure 42). The direction of the minimum horizontal stress varies between 104.6° and 148.3° (average 131.4°), in a general southeast-northwest direction. This means fractures will form and propagate in a vertical plane in a southwest-northeast direction (14.6°-58.3°; average 41.4°), perpendicular to the Rocky Mountain deformation front and along the direction of the tectonic stress induced by the Laramide Orogeny (Figure 42). This preferential fracturing direction was observed previously in coal mines in Alberta (Campbell, 1979) and was similarly determined for Cretaceous rocks in southern and central Alberta (Bell and Bachu, 2003).

Table 2. Orientations of the minimum and maximum horizontal stresses determined from breakouts in wells in the British Columbia regional-scale study area.

Well Location	Stratigraphic Age	S_{Hmin} Azimuth	S_{Hmax} Azimuth
00/03-08-083-08W6/0	Cretaceous	104.6	14.6
00/09-27-089-12W6/0	Lower Cretaceous	143.8	53.8
00/09-27-089-12W6/0	Triassic	141.8	51.8
00/12-34-095-11W6/0	Cretaceous	148.3	58.3
00/12-34-095-11W6/0	Permian	132.8	42.8
00/12-34-095-11W6/0	Triassic	133.3	43.3
00/D-053-B/094-A-13/0	Cretaceous	125.8	35.8
00/07-12-087-17W6/0	Cretaceous	133.2	43.2
00/07-12-087-17W6/0	Jurassic	120.9	30.9
00/07-29-083-15W6/0	Cretaceous	129.7	39.7

Magnitudes and gradients of the vertical stress S_V were calculated at 1 m intervals for each acid-gas injection site based on density logs. In some cases, density logs were taken in the injection well itself, although in a few instances the log had to be extrapolated to the injection depth. In other cases, no density log exists for the injection well, and logs from nearby wells had to be used. However, because the density of sedimentary rocks varies in a narrow range, the stress magnitude and gradient obtained at a nearby well is representative for the acid-gas injection well.

No records of stress and/or geomechanical testing in the acid-gas injection wells in the northeastern British Columbia area exist in the public domain (i.e., operator applications to the Oil and Gas Commission). Microfrac, minifrac, leak-off and hydraulic fracturing tests from wells in the various local-scale study areas were used to estimate the gradient of the minimum horizontal stress, ∇S_{Hmin}. These gradients were used to infer the value of the minimum horizontal gradient at the acid-gas injection sites based on stress gradient and depth (Bell, 2003; Bell and Bachu, 2003).

The vertical and horizontal stress data for the individual acid-gas injection sites are presented and discussed in the site-specific characterization of injection operations (Section 5.6).

4.3.2 Rock Geomechanical Properties

Knowledge of the geomechanical properties of rocks in formations affected by acid gas injection is an essential part of the subsurface characterization of any injection site, including the acid-gas injection operations in northeastern British Columbia. These properties, in combination with the stress regime, are important in evaluating the safety of the operation and avoiding rock fracturing and acid gas leakage into overlying formations. Two parameters are essential to understand the rock mechanics of an injection site: Young's modulus and Poisson's ratio. A literature review of geomechanical properties provided general values for Poisson's ratio and Young's modulus from rock samples in as well as outside of the regional-scale study area. Measurements in each case covered a number of samples and a range of values. The value closest to the average of that particular set of measurements was considered as representative and is provided in Table 3. Three of the values given represent parameters measured in Mississippian carbonates. Shale and chert cap rock values are represented by measurement taken in the Jurassic Fernie Group and Nordegg Member, respectively. No data for Triassic and Permian strata were available. Therefore, the sandstone injection interval is characterized by sandstone from the Basal Quartz Formation, which is a Lower Cretaceous Bullhead Group equivalent.

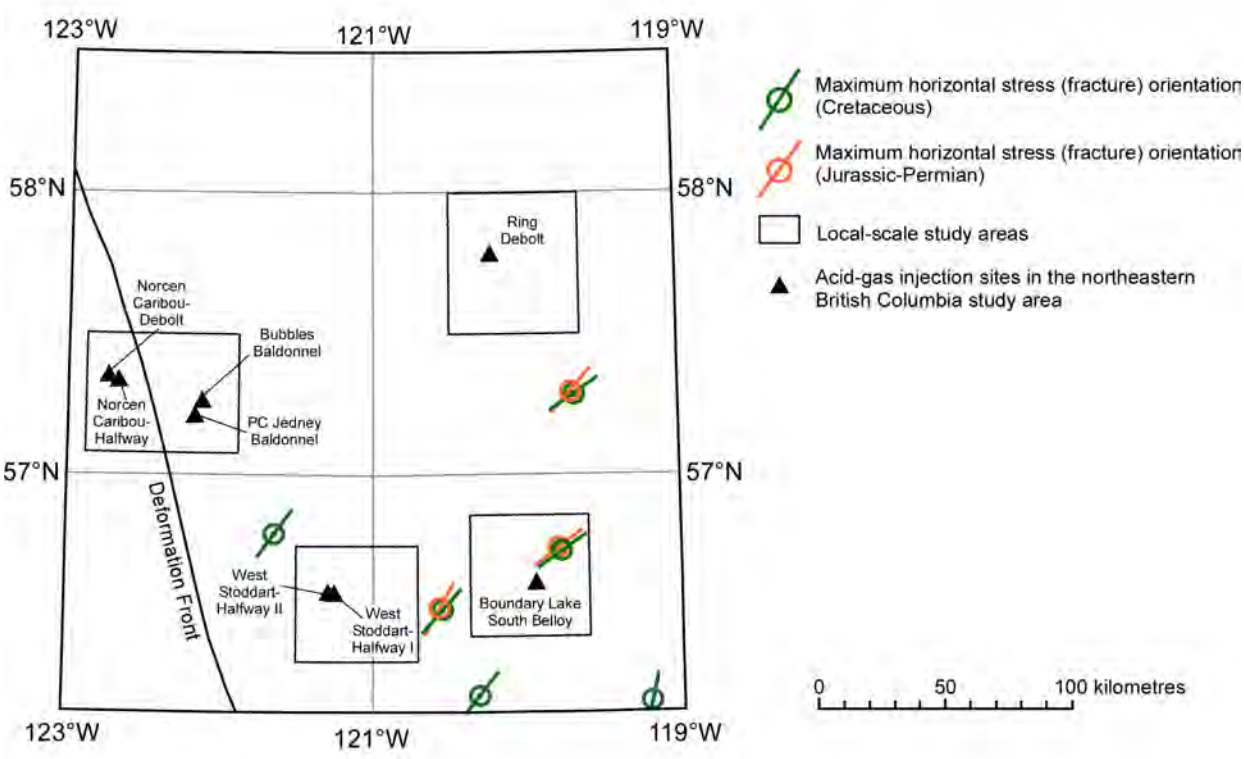

Figure 42. Orientation of horizontal stresses in Permian to Cretaceous strata in the regional-scale study area. The location of the injection sites and the local-scale study areas are also shown.

Table 3. Geomechanical properties of rocks of interest from the Alberta Basin (based on data from McLennan et al., 1982; Miller and Stewart, 1990; Wang et al., 1991; McLellan and Cormier, 1996).

Formation	Rock Type	Latitude	Longitude	Depth (m)	Poisson's Ratio	Young's Modulus (GPa)
Fernie Formation	shale	55.4557	-122.2174	—	0.28	28.3
Debolt (?)	carbonate	56.4753	-119.9095	—	0.29	54.2
Debolt (?)	carbonate	58.2941	-119.2714	—	0.34	54.3
Pekisko Formation	limestone	52.3611	-114.4178	2195	0.31	63.8
Basal Quartz	sandstone	51.9863	-114.8608	3030	0.19	44.9
Nordegg Member	Ss, ls, chert	52.3575	-114.4358	2196	0.24	54.03

Young's modulus, E, is defined as the amount of strain (deformation) caused by a given stress and is a function of the stiffness of the material. Young's modulus is used as an indication of the possible width of fractures. A high Young's modulus correlates to a narrower fracture width. In general, typical Young's modulus values for rocks range from 20 to 82.5 GPa (Jumikis, 1983; Haas, 1989). The Young's modulus values for Mississippian carbonates range from 47 GPa to 72 GPa (Miller and Stewart, 1990; Wang et al., 1991), compared with values of 30 GPa to 63 GPa for the Basal Quartz sandstone (McLennan et al., 1982) and 13 GPa to 45 GPa for the Fernie shale (McLellan and Cormier, 1996).

Poisson's ratio, υ, is defined as the ratio of the strain perpendicular to an applied stress, to the strain along the direction of that stress. It is a measure of the deformation perpendicular to and along the stress being applied to the rock, and indicates the plasticity of the rock. The rock plasticity, expressed by Poisson's ratio and S_{Hmin}, has a significant effect in determining the rock fracture threshold (see equations 2 and 3). A formation with high S_{Hmin} and Poisson's ratio would likely be an effective barrier to fracture propagation. In general, values for Poisson's ratio for carbonates range from 0.15 to 0.35, for sandstones 0.1 to 0.3, and for shales from 0.1 to 0.4 (Lambe and Whitman, 1979; Jumikis, 1983; Haas, 1989). The Poisson's ratio for Mississippian carbonates ranges from 0.23 to 0.34 (Miller and Stewart, 1990; Wang et al., 1991), compared with values of 0.13 to 0.33 for the Basal Quartz sandstone (McLennan et al., 1982) and 0.14 to 0.44 for the Fernie shale (McLellan and Cormier, 1996).

5 Local-Scale Setting Of the Acid-Gas Injection Sites in Northeastern British Columbia

Because the acid-gas injection sites in northeastern British Columbia are distributed over a large area and various stratigraphic intervals, which have variable characteristics, the geological and hydrogeological characteristics of the these injection sites are described at a local scale in individual specific areas (each defined broadly by the respective oil or gas field they are located in and proximity to each other). The six injection operations (seven sites) were therefore studied in four local-scale study areas (Table 4).

Table 4. Location of acid-gas injection wells in local-scale study areas.

Local-Scale Study Area	Site Name	Injection Well Location	Latitude	Longitude
Stoddart	W. Stoddart–Halfway	00/01-33-087-21W6/0	56.58458	-121.2755
		00/07-34-087-21W6/0	56.58547	-121.2532
		00/15-11-088-13W6/0	—	—
Ring	Ring Debolt	d-049-B/094-H-16	57.79554	-120.2255
Boundary Lake	Boundary Lake S–Belloy	00/15-11-088-13W6/0	56.62443	-119.9492
Bubbles	PC Jedney–Baldonnel	b-88-J/94-G-1	57.2344	-122.2219
		a-79-J/94-G-1	57.22663	-122.2277
	Bubbles Baldonnel	b-19-A/94-G-8	57.25917	-122.1113
	Caribou–Debolt	a-30-G/94-G-7	57.35279	-122.7389
	Caribou–Halfway	c-4-G/94-G-7	57.33836	-122.671

The local-scale study areas encompass all or a large part of the Stoddart, Ring, Boundary Lake–South, Bubbles, Jedney or Caribou gas fields, after which the acid-gas injection operations were named (Figure 12). At Bubbles, Jedney and Caribou, acid gas is actually injected into depleted pools of the main gas-producing horizon. At the other operations, acid gas is injected into aquifers that underlie or overlie currently producing horizons. The geology in these specific areas is moderately well known and understood because drillcore, albeit in restricted numbers, is available due to exploration for and production of hydrocarbons from Carboniferous, Permian and Triassic strata. Maps showing the depth to and the structure top of the respective injection units are not presented at the local scale. This information is available from corresponding regional-scale maps (Figures 16, 18, 22 and 26). In turn, isopach maps and/or local-scale cross-sections are presented, since information about the thickness of the injection unit is relevant at the local scale.

The actual in-situ formation water density in the local-scale study areas generally differs from the regional average. However, for the calculation of hydraulic head values at the regional scale, a reference density of 1052 kg/m^3 was used (see Section 4.2.2), and this value will be used at the local scale as well. This allows for the comparison between contour maps of hydraulic heads on the regional and local scales, but will not significantly affect the accuracy of the flow analysis (Bachu and Michael, 2002).
Rock properties relevant to the flow of formation fluids and injected acid gas used in the local-scale characterization are porosity and permeability. The core-scale porosity values were up-scaled to the well scale using the weighted arithmetic average. Permeability values were up-scaled to the well scale using a power-law average with a power of ω=0.8 (Desbarats and Bachu, 1994). Representative values presented in tables in the following sections present the statistics of the well-scale averaged porosity and permeability values.

5.1 Stoddart–Halfway

The local-scale study area is defined around the Stoddart gas field between 56.34°N to 56.75°N and 120.71°W to 121.50° W. It includes two injection wells supplied with acid gas by the West Stoddart Gas Processing Facility (WSGPF) located at section 34- Township 87- Range 21W6 (Figure 12), approximately 40 km west-northwest of Fort St. John. Acid gas injection takes place into clastic sediments of the Halfway Formation, which is the lowermost unit of the Triassic Schooler Creek Group (Figure 13, Appendix 1). Due to the continuous nature of the beach/barrier and shoreface of the Halfway

Formation, stratigraphic traps are rare and hydrocarbon accumulations occur only in anticlinal structures. No traps are evident near the WSGPF. The closest Halfway gas production occurs at Cache Creek 14 kilometres to the northeast and at the West Stoddart Halfway C pool 10 kilometres to the south. Within the Triassic there is also production from the Charlie Lake as well as the Doig Formation, with the latter being the source of the injected acid gas. Furthermore, there is production from sandstones of the underlying Permian Belloy Formation, as well as the overlying Cretaceous Gething sandstone.

5.1.1 Geology

The sandstones of the Halfway Formation form a widespread, continuous and porous aquifer and the sands were deposited in a north-northwest–trending beach/barrier complex that prograded westward. The injection horizon within the Halfway Formation in the study area is about 27 m thick, although the Halfway Formation thickness varies between 10 and 70 m over the entire local-scale study area (Figure 43). The rocks of the Halfway Formation at the injection site are mainly composed of quartz (80%), with additional fine-grained carbonate cements (10%), as well as peloids, quartz overgrowths, chert, plagioclase feldspar (together 10%) (Figure 44). Subangular to round grains form a grain-supported texture with intergranular porosity.

The Halfway Formation is overlain by the Charlie Lake Formation, also part of the Schooler Creek Group. The Charlie Lake Formation generally consists of a variable sequence of yellowish brown to yellow-pale grey dolomitic to calcareous sandstone, siltstone, sandy limestone, dolostone and lesser amounts of intraformational and/or solution breccia. In the study area, the formation is dominated by massive anhydrites, red dolomitic siltstones, evaporitic dolomites and minor halite. The Charlie Lake Formation displays a transition from evaporitic facies in the east to sandstone and carbonate facies in the west. In the subsurface, several oil and gas producing members have been defined: the Coplin, Inga, Boundary Lake and Nancy (Armitage, 1962; Hess, 1968; Fitzgerald and Peterson, 1968;), which are productive in the general area, for instance in the Cache Creek Coplin, Inga Inga and West Stoddart North Pine fields. However, the Lower Charlie Lake Formation in the local-scale study area consists of anhydrites, silty dolomitic mudstones and fine quartzitic sandstones, which were deposited on a broad flat sabkha environment and reach thicknesses up to 65 m, albeit the thickness of the entire formation varies between 60 to over 300 m (Figure 45). These units within the Charlie Lake are generally impermeable and are considered a good seal to the underlying Halfway Formation.

The Halfway Formation is underlain by impermeable shales of the Doig Formation, which is part of the Triassic Diaber Group. It consists of mainly fine-grained, grey, argillaceous siltstone and dark grey, calcareous shale. Interbedded nodular phosphates and bitumen staining increase toward the base of the formation. Sand content increases in a north-northwesterly direction. Anomalously thick, fine-grained, porous sands occur locally as ‘bars’ or ‘channel’ fills in the upper units of the formation. These are the main producing units at West Stoddart, as well as the source of the injected acid gas. In the local-scale study area, the Doig is about 35 m thick (Figure 46).

5.1.2 Hydrogeological Characteristics and Rock Properties

5.1.2.1 Chemistry of Formation Waters

Forty-four chemical analyses of Halfway–Doig formation water exist in the local-scale study area. The major constituents are sodium (55 g/l) and chloride (90 g/l), making up 95% of the total dissolved solids (TDS) (Table 5). Magnesium, calcium, sulphate and bicarbonate are present in minor concentrations (Figure 47a). Salinity ranges from less than 130 g/l along the northern and southern boundary of the study area to 175 g/l in the centre (Figure 48a). The average in-situ density of formation water in the Halfway–Doig aquifer/reservoir in the local-scale study area was estimated to be 1100 kg/m^3 using the methods presented in Adams and Bachu (2002).

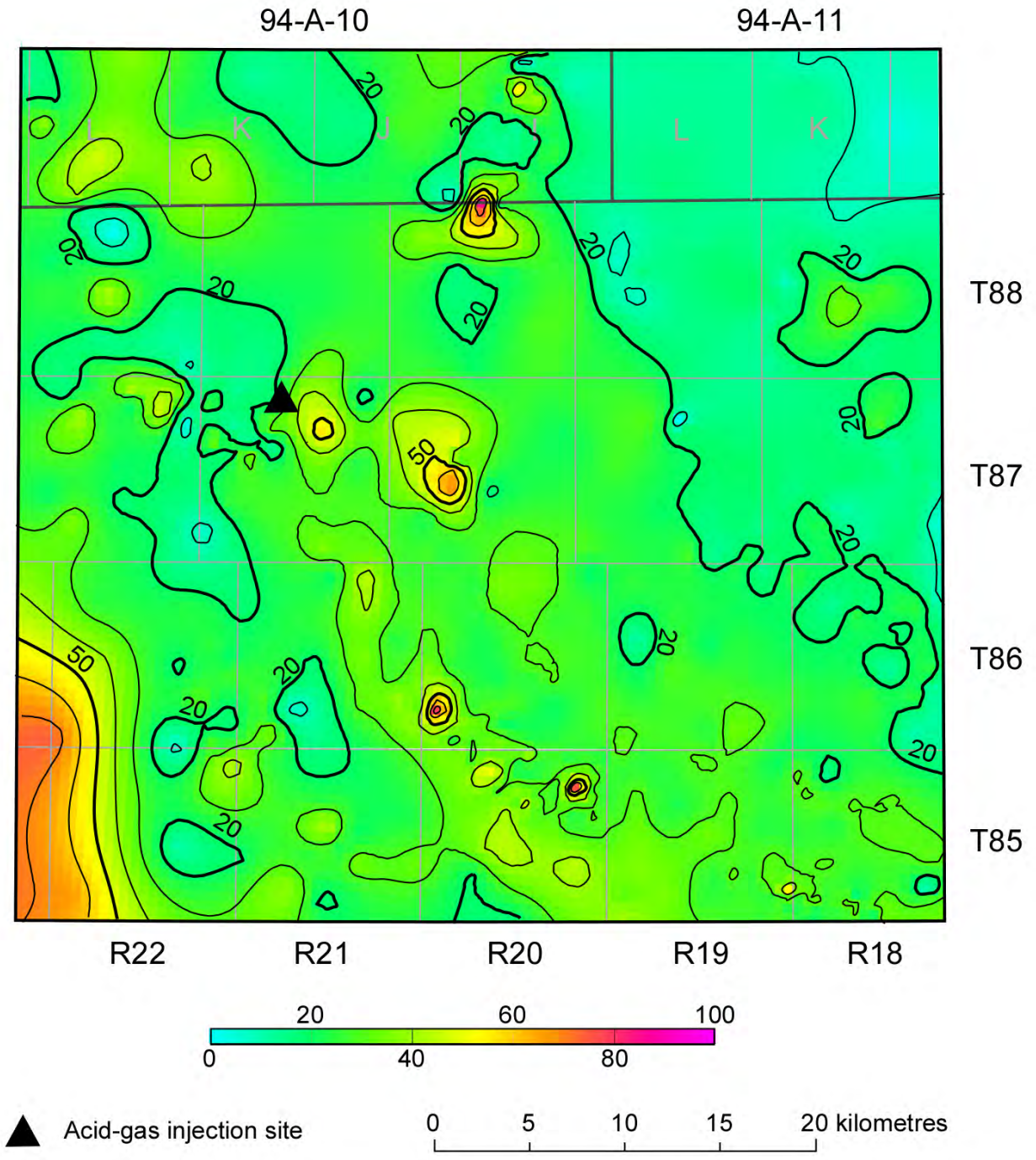

Figure 43. Isopach map of the Halfway Formation in the Stoddart local-scale study area. Contours in metres. Contour interval = 10 m.

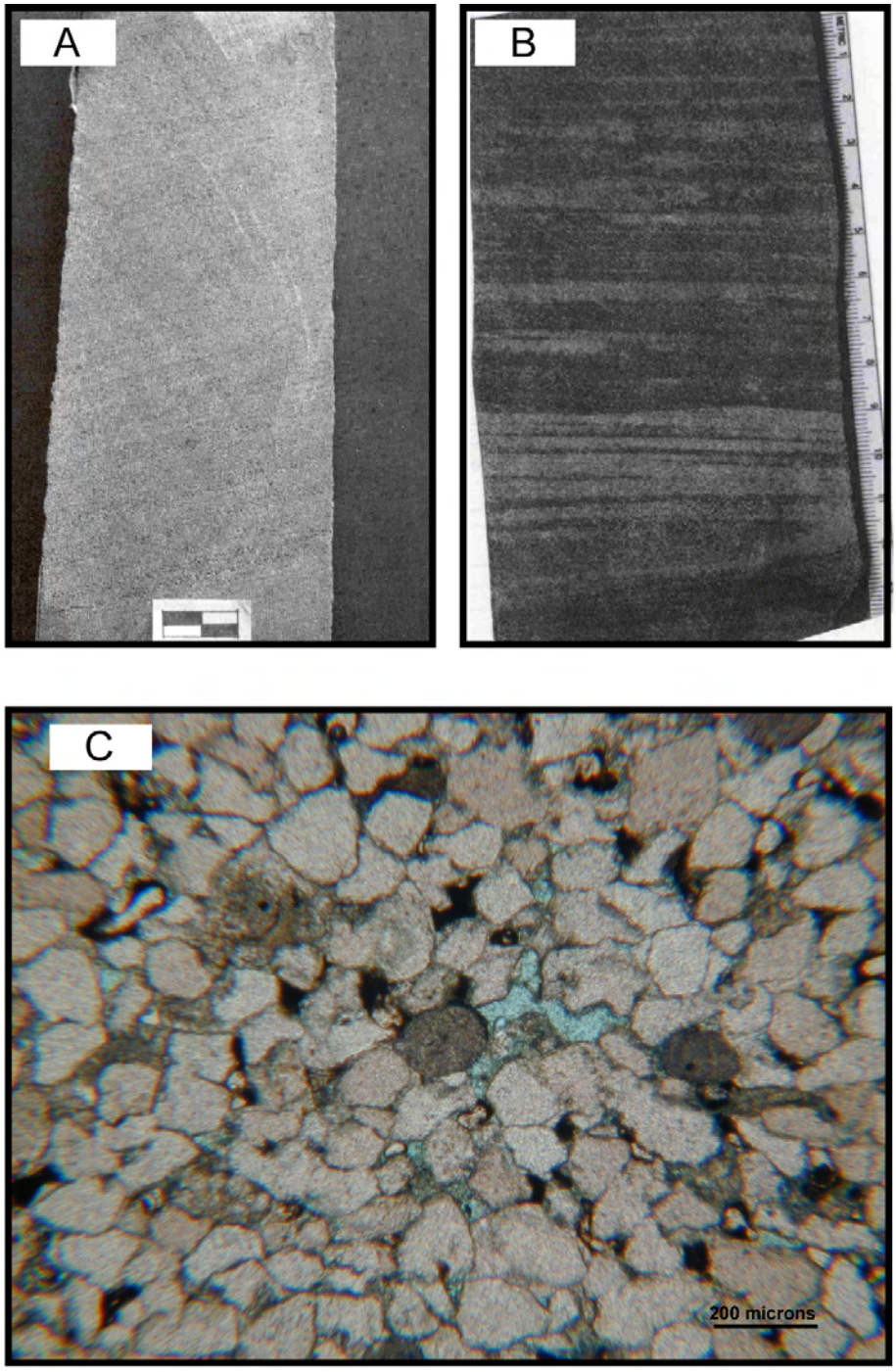

Figure 44. Core and thin section photographs of the Halfway Formation sandstone in the Stoddart area. Cross-laminated sandstones (Photo A; from Norgard, 1997) change to flat, planar-laminated sandstones (Photo B; from Young, 1997), which consist mainly of quartz. The intergranular porosity can best be seen on the blue-stained pores in the centre of the thin section photo (Photo C).

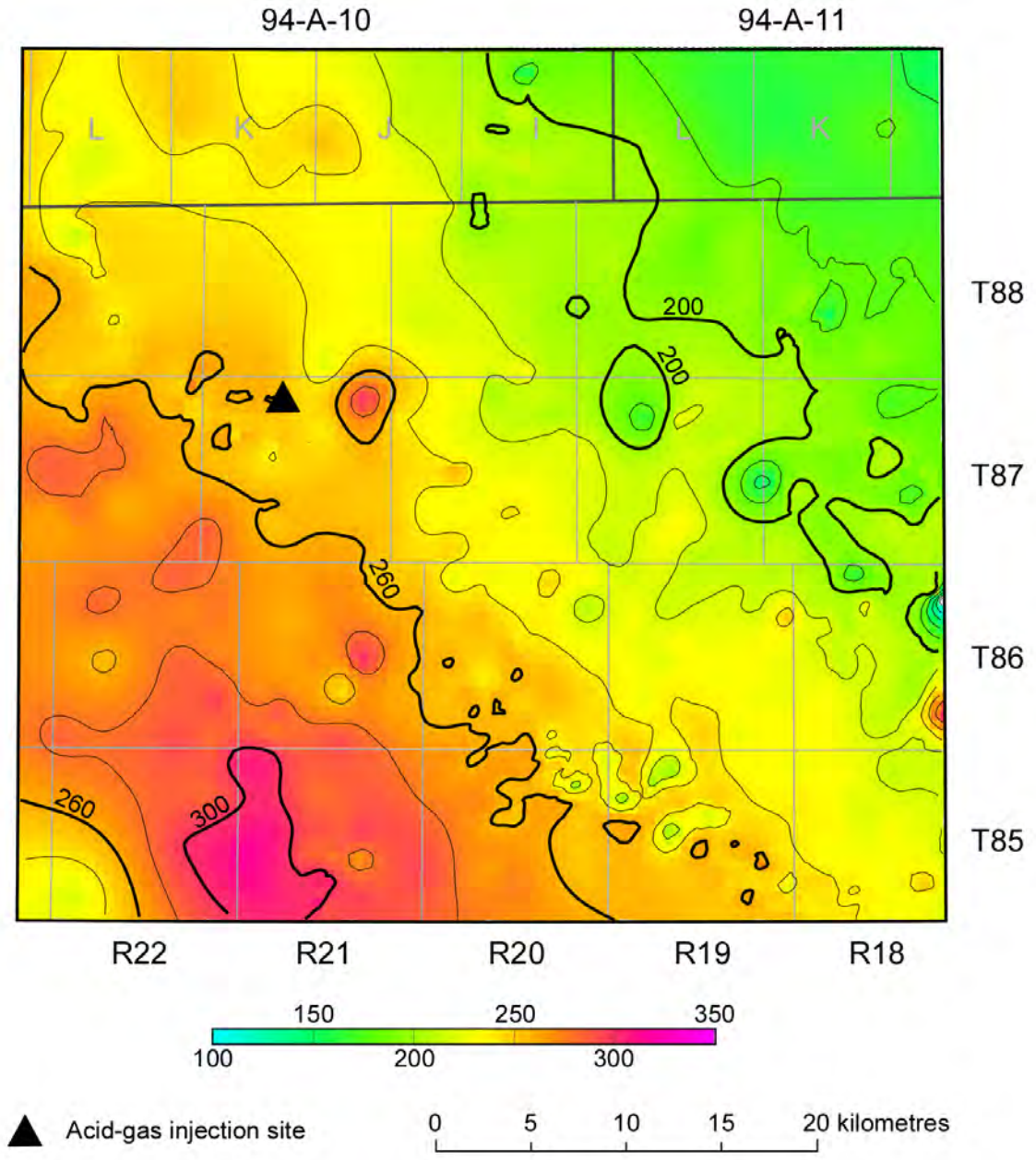

Figure 45. Isopach map of the Charlie Lake Formation in the Stoddart local-scale study area. Contours in metres. Contour interval = 20 m.

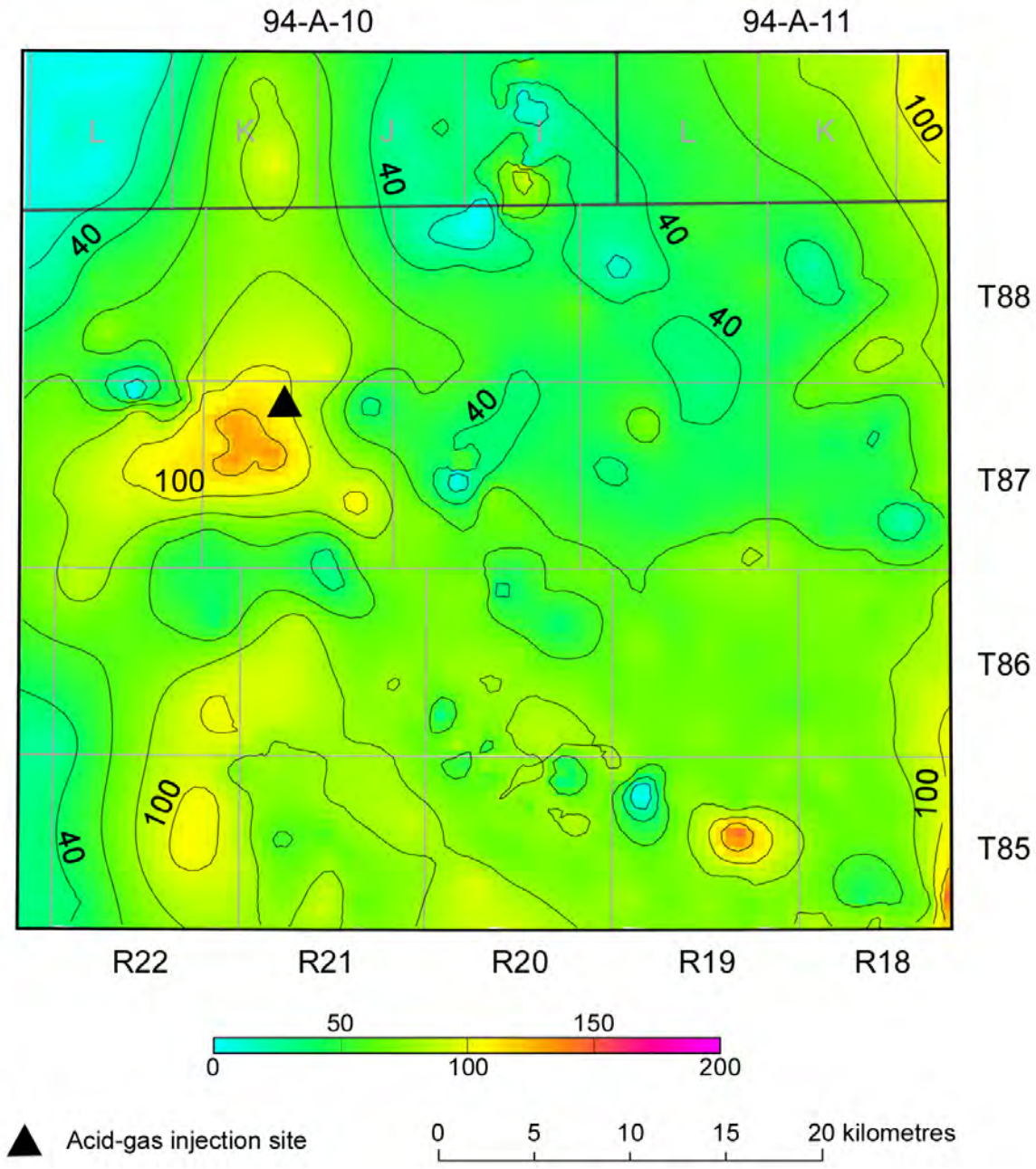

Figure 46. Isopach map of the Doig Formation in the Stoddart local-scale study area. Contours in metres. Contour interval = 20 m.

Table 5. Major ion chemistry of Halfway–Doig brines in the Stoddart area (concentrations in g/l).

Location	Na	K	Ca	Mg	Cl	SO_4	HCO_3	TDS
06-22-088-22-W-6	57.0	2.2	2.2	0.6	91.1	3.0	3.7	156.9
d-038-K/094-A-11	56.6	—	2.4	0.2	88.1	4.4	2.3	153.1
a-029-K/094-A-10	50.6	1.2	2.7	0.3	83.2	4.1	0.2	142.6
16-22-087-18-W-6	60.2	1.6	3.0	1.2	98.3	2.8	1.4	165.9
16-32-086-19-W-6	55.7	—	2.5	0.3	87.6	4.6	0.3	150.8
04-07-087-18-W-6	56.4	1.4	6.7	2.3	104.3	2.0	0.5	172.3
d-086-I/094-A-11	51.9	1.3	2.3	0.6	88.3	4.0	2.2	152.5
d-087-K/094-A-10	47.9	1.1	2.3	0.9	80.3	3.8	1.5	138.1
06-07-085-20-W-6	51.8	—	1.6	0.2	79.2	3.5	2.5	137.4
c-016-L/094-A-11	27.7	—	1.4	0.4	43.0	1.9	3.3	76.0
05-08-088-18-W-6	49.5	3.1	2.5	1.1	84.0	2.5	1.6	142.1
16-06-085-18-W-6	49.1	1.2	2.2	0.5	71.9	5.0	1.1	126.0
10-12-086-22-W-6	65.0	2.2	10.0	3.1	128.5	0.5	0.2	208.6
11-15-085-21-W-6	51.5	—	3.5	0.8	84.9	2.2	2.5	144.1
13-13-086-18-W-6	62.1	1.6	2.7	0.8	101.0	2.9	1.2	170.7
10-19-087-19-W-6	61.5	1.0	2.2	1.0	98.3	3.0	1.6	166.7
06-26-087-21-W-6	66.5	2.1	2.4	0.6	101.0	2.8	2.3	171.8
12-02-086-18-W-6	41.0	1.1	2.2	0.5	69.7	3.9	1.4	121.1
16-36-086-20-W-6	54.2	1.6	2.0	0.6	92.7	2.6	1.3	156.8
01-04-087-18-W-6	61.5	1.6	2.9	0.7	105.1	2.8	1.1	177.4
11-10-085-21-W-6	45.3	—	1.4	0.6	70.0	3.2	3.1	122.0
16-17-085-19-W-6	61.9	—	2.5	0.2	97.2	3.0	1.7	165.7
11-15-088-22-W-6	52.5	—	1.9	0.8	85.3	2.7	3.5	146.6
04-26-087-18-W-6	60.1	1.4	4.8	1.5	102.0	2.6	0.7	170.6
10-19-087-19-W-6	55.3	2.1	2.0	0.8	90.2	3.5	0.3	153.1
11-08-086-21-W-6	57.4	3.3	2.2	0.5	92.5	3.3	3.4	159.5
04-23-086-21-W-6	63.1	—	2.2	0.1	96.8	3.5	3.8	167.6
11-03-088-18-W-6	62.0	1.7	2.1	1.0	103.0	2.5	0.7	172.8
11-13-087-18-W-6	61.4	1.5	3.5	1.8	102.9	2.4	1.0	172.1
02-34-088-19-W-6	49.5	1.7	3.2	0.2	86.3	2.5	1.6	146.6
04-23-086-19-W-6	63.7	—	2.3	0.6	101.4	2.7	1.2	171.3
d-087-K/094-A-10	49.8	0.8	2.5	0.8	91.2	3.4	1.6	155.6
15-11-086-18-W-6	55.4	1.3	2.6	0.6	97.5	3.2	1.1	165.5
09-14-087-18-W-6	41.6	1.2	6.9	1.5	81.3	2.5	0.3	135.6
14-12-087-18-W-6	57.0	1.5	2.8	0.6	97.6	2.9	1.2	165.3
13-18-087-17-W-6	61.4	1.5	3.6	1.1	100.6	0.02	1.1	165.3
11-03-088-18-W-6	48.6	1.1	2.8	0.9	83.5	3.7	0.9	142.6
11-13-087-18-W-6	58.2	1.4	3.2	1.2	99.9	2.6	1.1	168.1
06-22-088-22-W-6	57.1	2.1	2.1	0.6	91.2	3.0	3.6	157.0
12-23-088-19-W-6	54.9	1.7	2.5	0.6	82.0	2.7	2.0	140.0
06-26-087-21-W-6	64.0	—	2.9	0.4	101.8	2.4	2.4	172.7
07-02-087-18-W-6	—	—	2.6	0.6	62.7	1.9	1.0	106.1
01-04-088-18-W-6	57.9	1.5	2.8	0.8	100.2	2.8	1.3	169.3
04-18-088-18-W-6	54.6	1.5	3.2	0.9	92.6	2.9	1.6	156.9
Average	**55.1**	**1.6**	**2.9**	**0.8**	**90.7**	**2.9**	**1.6**	**154.1**

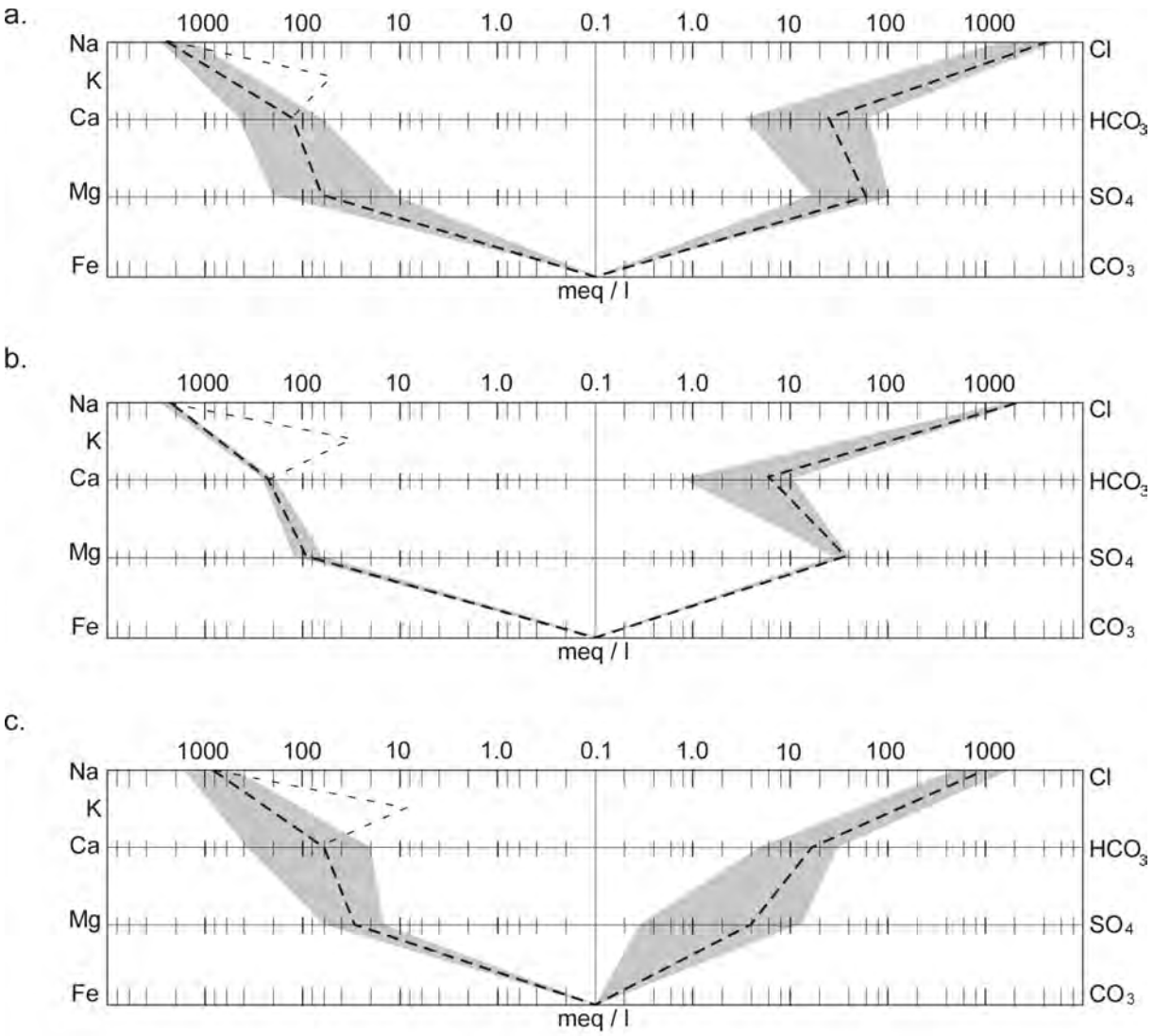

Figure 47. Stiff diagrams of formation waters in the a) Stoddart area (Halfway–Doig aquifer, 44 analyses), b) Ring area (Permo–Carboniferous aquifer, 5 analyses) and c) Boundary Lake area (Permo–Carboniferous aquifer, 15 analyses). The grey-shaded area shows the range, the bold dashed line represents the average concentration in meq/l. The thin dashed line represents the potassium concentration.

5.1.2.2 Pressure Regime

Hydraulic heads, calculated with a reference density of 1052 kg/m^3, decrease from 550 m in the west to 480 m in the east-central part of the area (Figure 48b), generally indicating eastward flow. The pattern of hydraulic head contours suggests channelling of formation flow along the paths indicated by the arrows in Figure 48b. The high hydraulic gradient as expressed by the relatively rapid decrease of hydraulic head values from >530 to 490 m in the vicinity of the Stoddart injection site and to the south is a sign for a lateral permeability change or a thinning of the aquifer in this area. The Stoddart acid-gas injection site pressure is located just east of this lateral barrier in the aquifer. The relatively low hydraulic-head value of 486 m was estimated from the initial reservoir pressure, and the very low hydraulic gradient east of the injection site implies a low-flow velocity of formation water toward the east.

The recorded pressures are plotted against elevation in Figure 49 and compared to pressures in over and

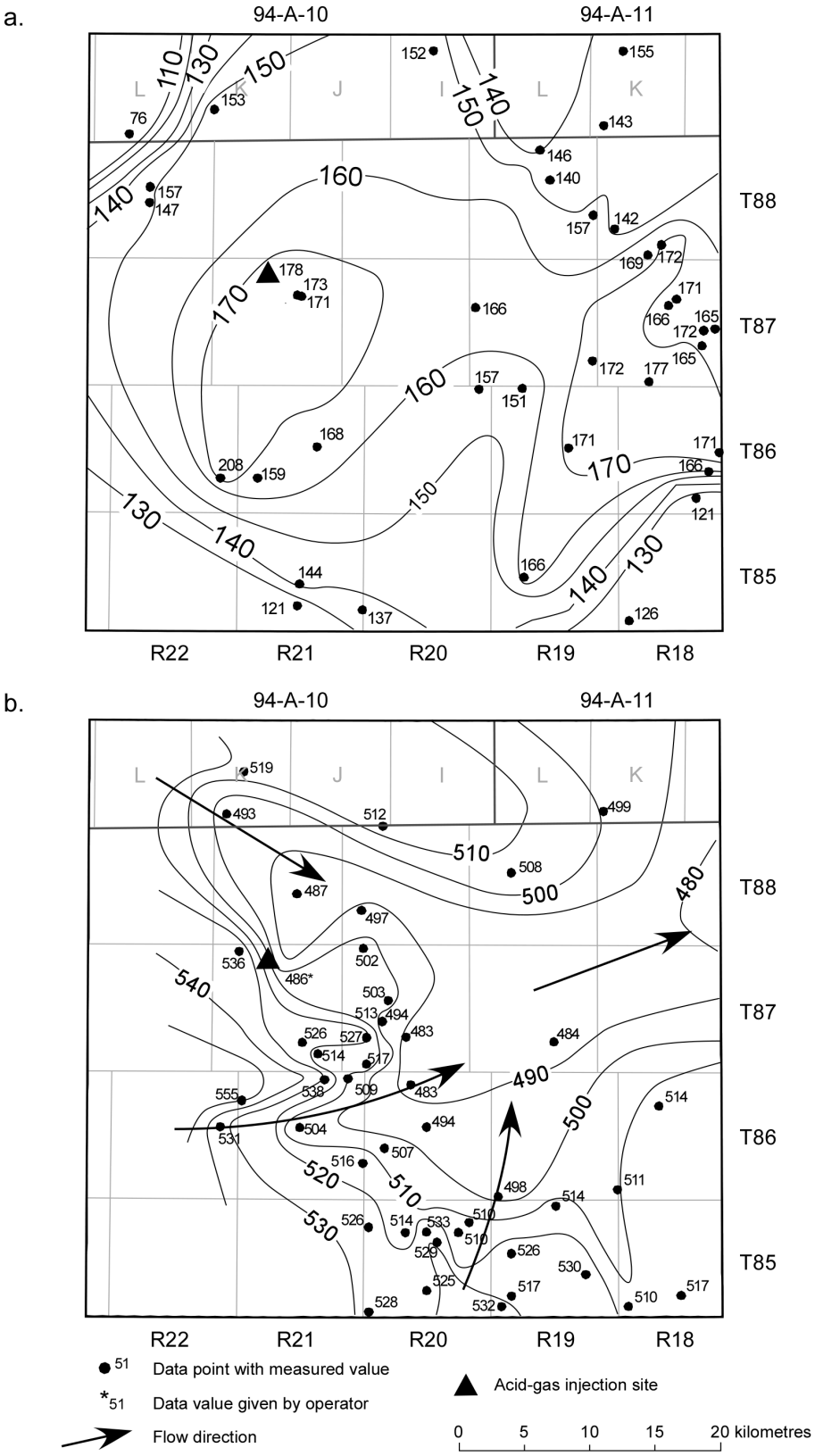

Figure 48. Distribution of a) salinity (g/l) and b) hydraulic heads (m) in the Halfway–Doig aquifer in the Stoddart local-scale study area.

underlying formations. Pressures in the Halfway–Doig aquifer plot along a linear trend representative of the pressure distribution in an underpressured static column of brine. Pressure-elevation trends in the overlying Charlie Lake, Nordegg–Baldonnel and Bullhead aquifers are shifted toward higher pressures. This offset in the pressure distribution indicates no, or only weak, vertical hydraulic communication across the Lower Charlie Lake aquitard, and the potential for vertical flow is downward from the overlying aquifers into the Halfway–Doig aquifer. Pressures in the underlying Permo–Carboniferous aquifer plot along a similar pressure-elevation trend as pressures in the Halfway–Doig aquifer, which suggest that these aquifers might be in vertical hydraulic communication. However, the intervening Montney aquitard is up to 200 m thick in the area of the Stoddart site, and the continuous trend in pressure distribution between the Halfway–Doig and Permo–Carboniferous aquifers is probably due to similar lateral boundary conditions to formation water flow.

5.1.2.3 Rock Properties

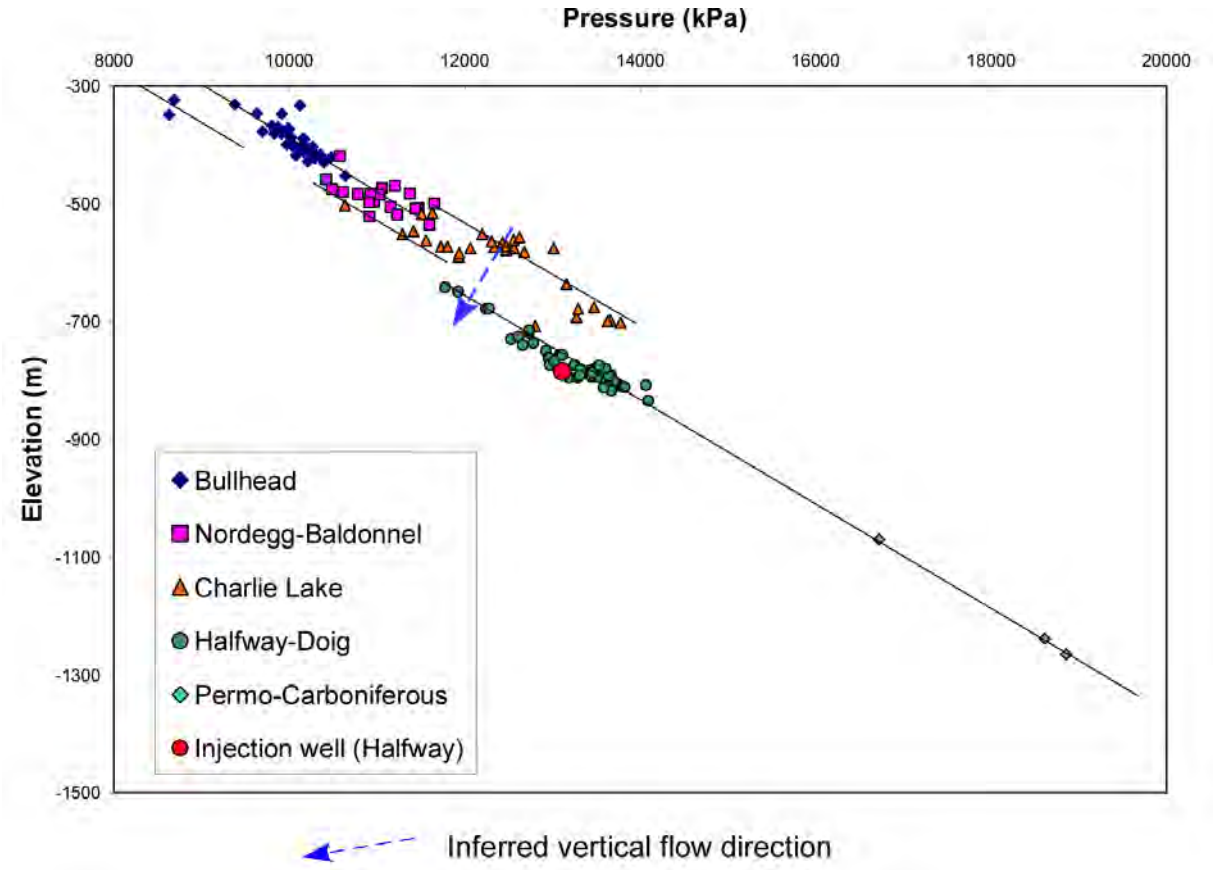

Figure 49. Distribution of pressure versus elevation in the injection stratum (Halfway Fm.) and adjacent formations in the local-scale study area of the West Stoddart acid-gas injection operation.

The well-scale porosity and permeability values for the Halfway and Doig formations, which form the aquifer/reservoir and the over/underlying Charlie Lake and Montney formations are shown in Table 6. Also shown are permeability values calculated from drillstem tests that were performed in the Halfway–Doig aquifer, which range between 0.1 and 210 mD, with a median value of approximately 5 mD. Core plug measurements generally are biased toward higher porosity and permeability values. The average values of porosity (11%) and horizontal permeability (23 mD) are highest in the Halfway Formation, which is the main aquifer unit. In comparison, porosity and horizontal permeability values in the over and underlying formations range from 6% to 7% and from 2 to 5 mD, respectively. Besides the

producing channel sandstones, the Doig Formation appears to have dominantly aquitard characteristics in the Stoddart area. The average vertical permeability (12 mD) is highest in the Lower Charlie Lake Formation, compared to 3 to 7 mD in the Halfway–Doig formations and 0.13 mD in the Montney Formation, confirming the good aquitard characteristics of the Montney Formation. However, missing values from low-permeability cores in the Lower Charlie Lake Formation skew its average toward permeability values that are too high.

Table 6. Well-scale porosity and permeability values obtained from measurements in core plugs from the Montney (24 wells), Doig (57 wells), Halfway (83 wells) and Lower Charlie Lake (28 wells) formations, and permeability values calculated from 50 drillstem test analyses in the Stoddart local-scale study area.

	Porosity (%)			Horiz. Perm. (mD)			Vert. Perm. (mD)			DST Perm. (mD)		
Formation	Min	Max	Avg	Min	Max	Median	Min	Max	Median	Min	Max	Median
L. Ch. Lk.	0.5	16	7	0.01	443	5.09	0.01	76.1	11.9	—	—	—
Halfway	0.7	18	11	0.5	253	23.3	0.01	137	7.0	0.1	210	4
Doig	0.8	19	6	0.01	446	5.61	0.02	74	3.31	0.5	69	5
Montney	1.4	14	6	0.04	390	1.7	0.02	61	0.13	—	—	—

5.1.2.4 Flow of Formation Water

The hydraulic head distribution in the Halfway–Doig aquifer suggests the flow of formation water is eastward in the Stoddart area, being slightly deviated from the general regional northeastward direction of flow. Generally, the Halfway Formation in the Stoddart area has relatively low-permeability strata (Section 5.1.1), and the change in hydraulic gradient in the Halfway–Doig aquifer coincides approximately with the outline of the West Stoddart gas field. The main reservoir rocks in the West Stoddart Field are deltaic/shoreface sandstones in the upper part of the Doig Formation that form stratigraphic-diagenetic traps (Harris and Bustin, 2000). Therefore, the channelling of formation water flow in the Halfway–Doig aquifer appears to be governed by the location of Doig sandstone bodies. However, high salinity of formation water (< 170 g/l) in the area of the West Stoddart and Buick Creek fields, compared to salinities less than 140 g/l along the boundary of the local-scale study area, suggests these fields have been insignificantly diluted by fresher water of meteoric origin, and that this part of the Halfway–Doig aquifer is fairly isolated hydraulically. Hydraulic isolation within the aquifer is supported by the trapping of gas in the West Stoddart and Buick Creek gas fields.

5.2 Ring–Debolt

The Ring local-scale study area is defined around the Ring hydrocarbon field, which extends from 57.5°N to 58.00°N and 119.64°W to 120.5°W (Townships 98, R11W6 to L-94-H-16) (Figure 12). The Ring–Debolt injection site is located about 180 km northeast of the city of Fort St. John (Figure 36) within the Ring–Pedigree Fields of British Columbia and Alberta, respectively. Acid gas injection takes place in the Carboniferous Debolt Formation of the Rundle Group (Figure 13, Appendix 1). Production in the Ring Field is mainly from the overlying Montney Formation, especially from the top 30 m, which tend to contain gas-bearing sandstones.

5.2.1 Geology

The Debolt Formation has been divided into a lower and an upper member. In the Ring local-scale study area, the Lower Debolt consists mainly of brown, cherty, massive bioclastic, partly crinoidal limestone becoming increasingly dolomitic eastward, whereas the upper Debolt is light brown, consisting of mainly microcrystalline to finely crystalline dolomite with some anhydrite and micritic limestone. In the Ring

local-scale study area, the Debolt carbonates have a general thickness of 200 m (Figure 50); however, the injection unit consists of zones of high permeability interspersed with zones of low/tight permeability with a net pay of only 3.6 m. The rocks of the Debolt Formation are mineralogically composed of varying degrees of dolomite and calcite, 89% to 78%, respectively, with minor amounts of quartz and fossil material. Porosity is mainly intercrystalline and vuggy (Figure 51).

Shales and sandstones of the Permian Belloy Formation and the Triassic Montney Formation overlie the Debolt carbonates with a thickness of about 90 m (Figure 52). The Montney Formation consists of a sequence of shoreface sands, silts and shales, with the sands being of reservoir quality and the shales

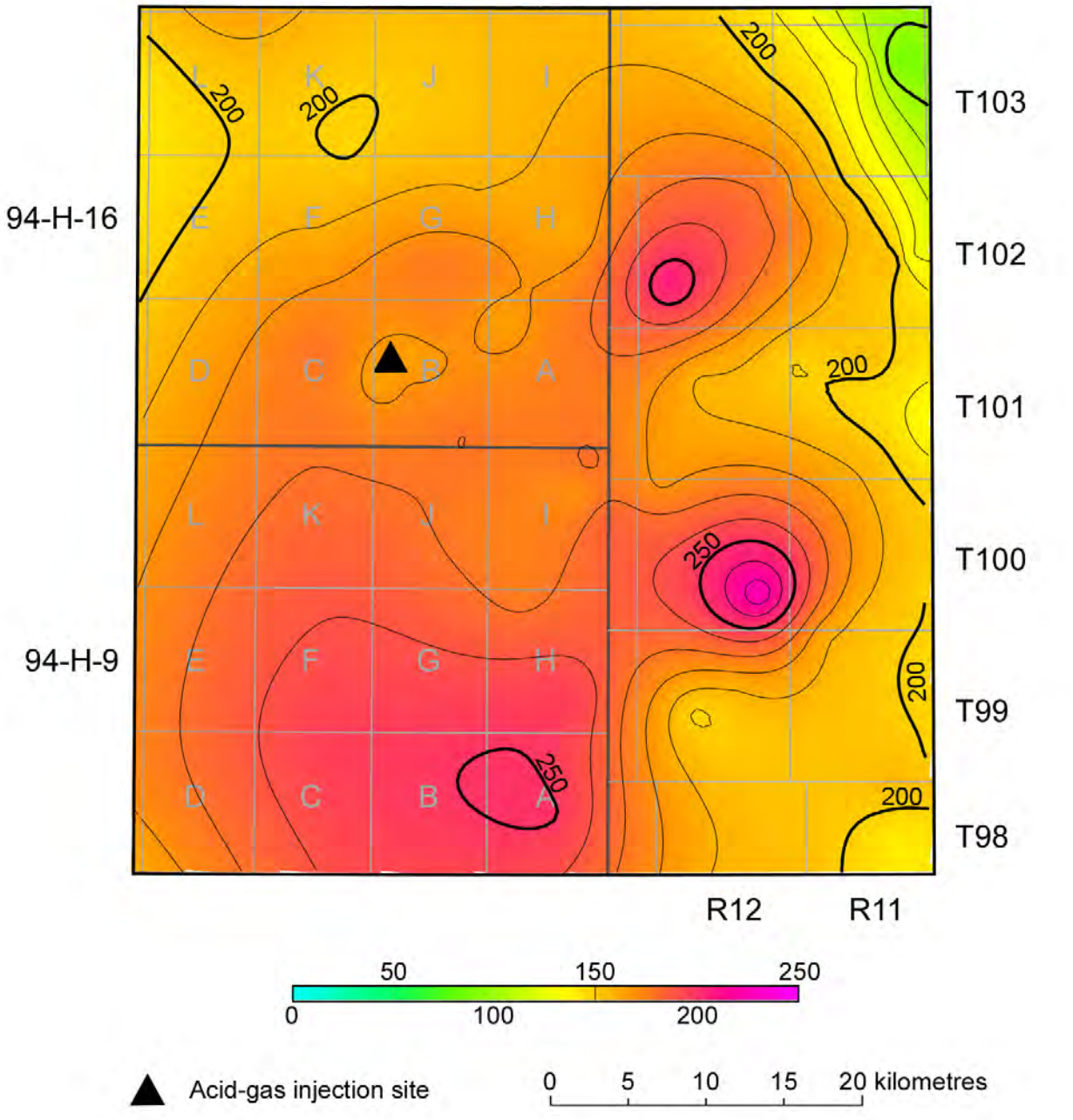

Figure 50. Isopach map of the Debolt Formation in the Ring local-scale study area. Contours in metres. Contour interval = 10 m.

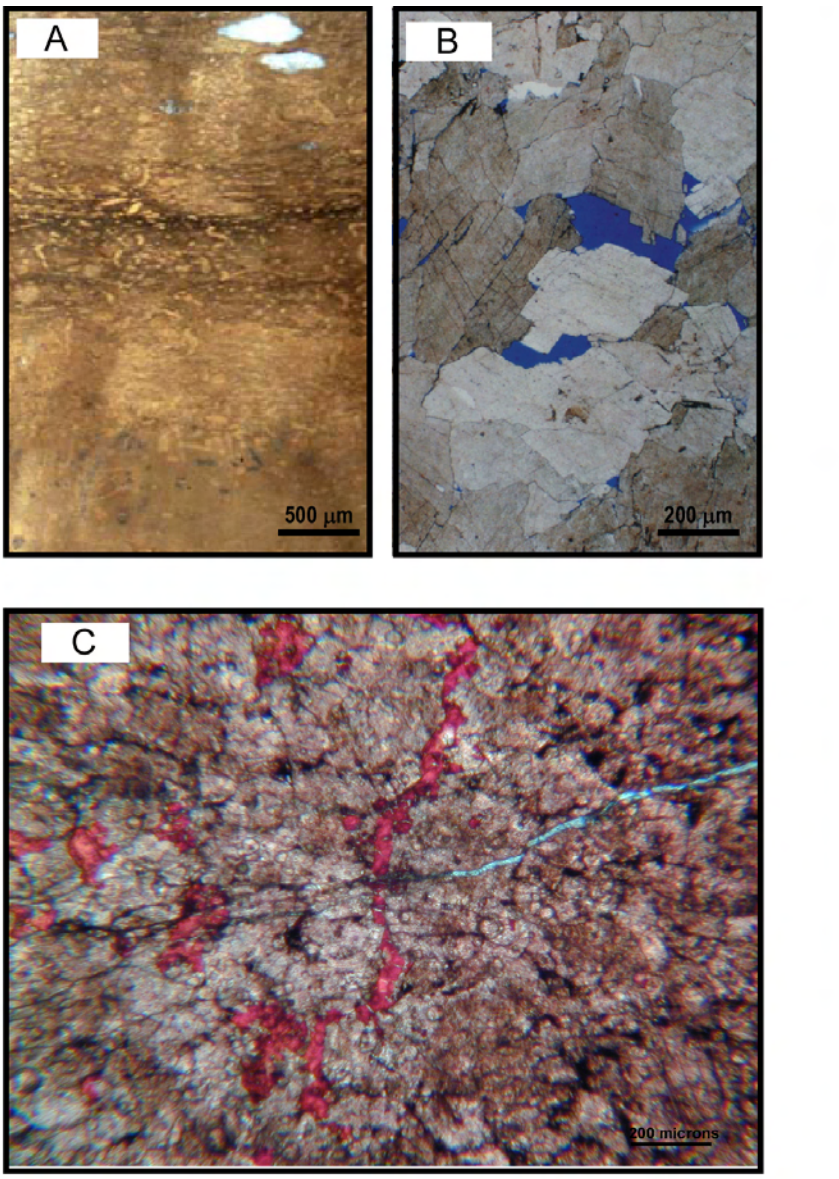

Figure 51. Core and thin section photographs of the Debolt Formation carbonate in the Ring and Caribou areas. Burrowed dolomudstones (Photo A) change to porous, coarse-grained dolostone (Photo B). The intercrystalline and fracture porosity can best be seen on the blue-stained pores in the centre of the thin section photo (Photos B and C). (Photo A from Packard et al., 2004; Photo B from Davies et al., 2004)

acting as aquitards (Sturrock and Dawson, 1991) (Figure 53). The interbedded shale and siltstones are representative of distal sediments of a large westward-prograding sequence. Cretaceous Gething channels have eroded into the Montney and are productive at Ring. The Gething sandstones are overlain by clastic sediments of the Bluesky Formation. However, in the study area, the Bluesky Formation seems to be quite shaly. Shaly and nodular limestones of the Banff Formation underlie the Debolt carbonates with a total thickness of more than 200 m (Figure 54).

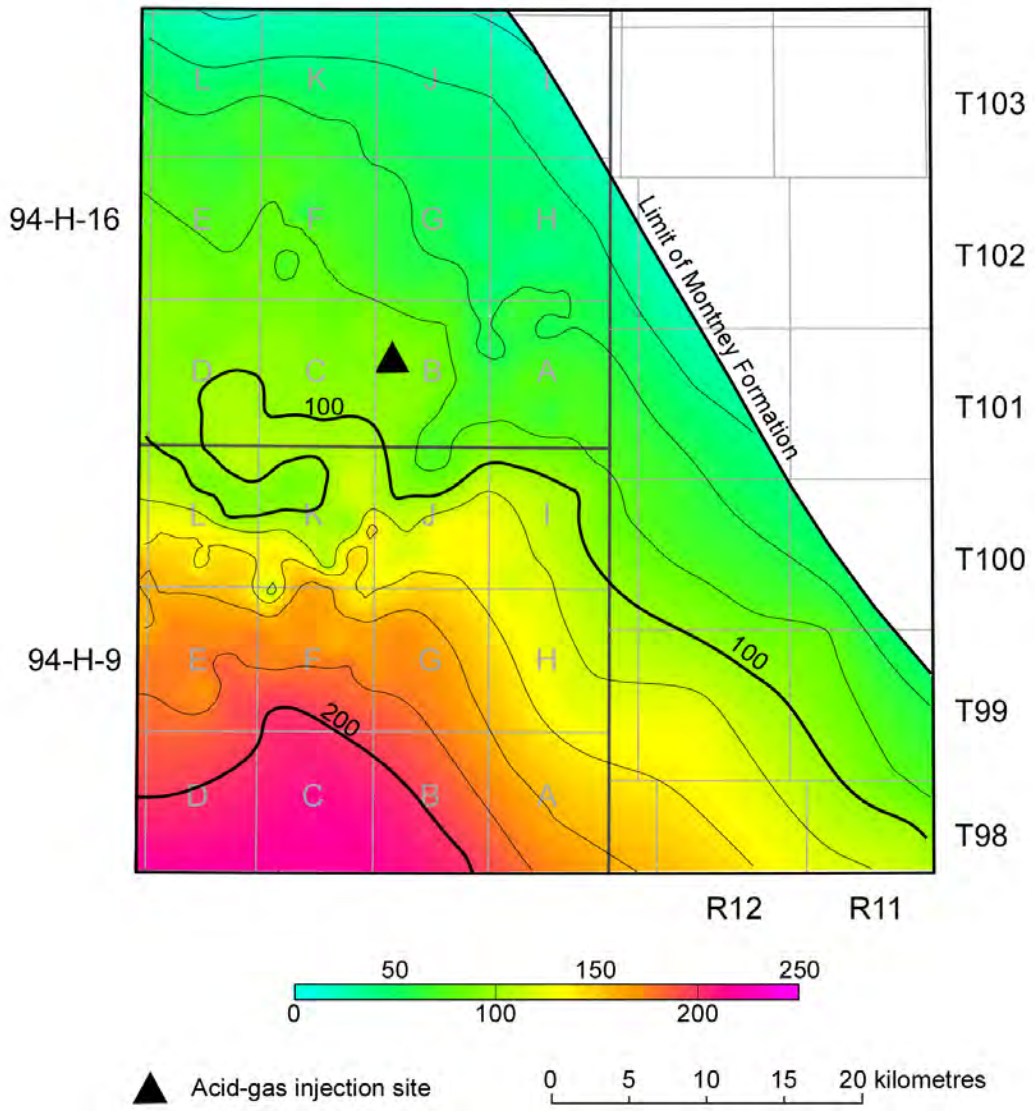

Figure 52. Isopach map of the Montney Formation in the Ring local-scale study area. Contours in metres. Contour interval = 10 m.

5.2.2 Hydrogeological Characteristics and Rock Properties

5.2.2.1 Chemistry of Formation Waters

The major constituents of Permo–Carboniferous formation water, as determined from 15 analyses, are sodium (20 g/l) and chloride (33 g/l), making up 95% of the total dissolved solids (Table 7). Magnesium, calcium, sulphate and bicarbonate are present in minor concentrations (Figure 47). Note the sulphate concentrations <0.8 g/l, which are low compared to other areas and aquifers. In the Ring area, the salinity of formation water decreases from >100 g/l in the south to approximately 30 g/l in the northeast. The low salinity values are observed mainly in the area of Mississippian subcrop below the Bullhead aquifer (Figure 55a). The average in-situ density of formation water in the Halfway–Doig aquifer in the local-scale study area was estimated to be 1037 kg/m^3 using the methods presented in Adams and Bachu (2002).

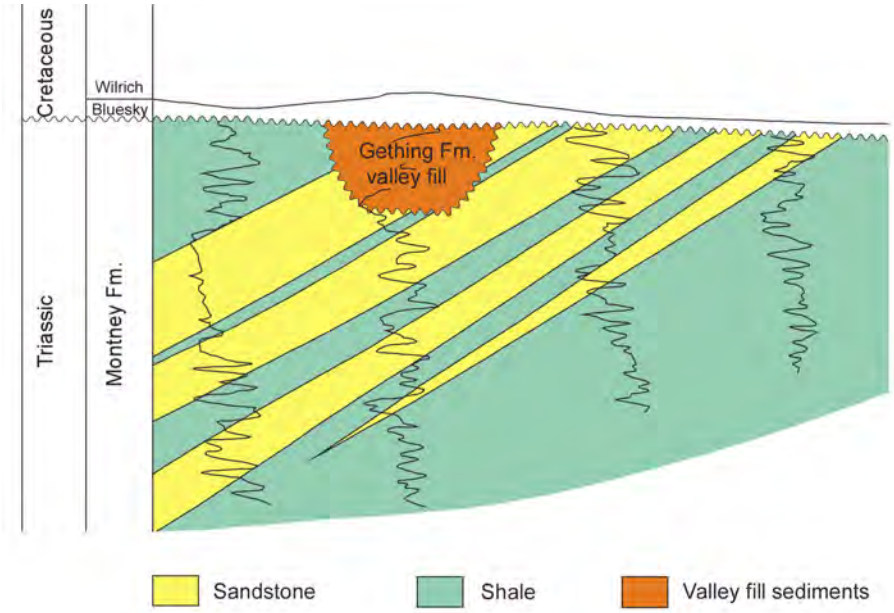

Figure 53. Stratigraphic dip cross-section in the Ring–Pedigree Field area, illustrating the sub-Cretaceous unconformity and hydrocarbon bearing sandstones. Note the Cretaceous Gething Formation valley fill (after Sturrock and Dawson, 1991). Only the sandstones have aquifer characteristics, whereas the shales are seals.

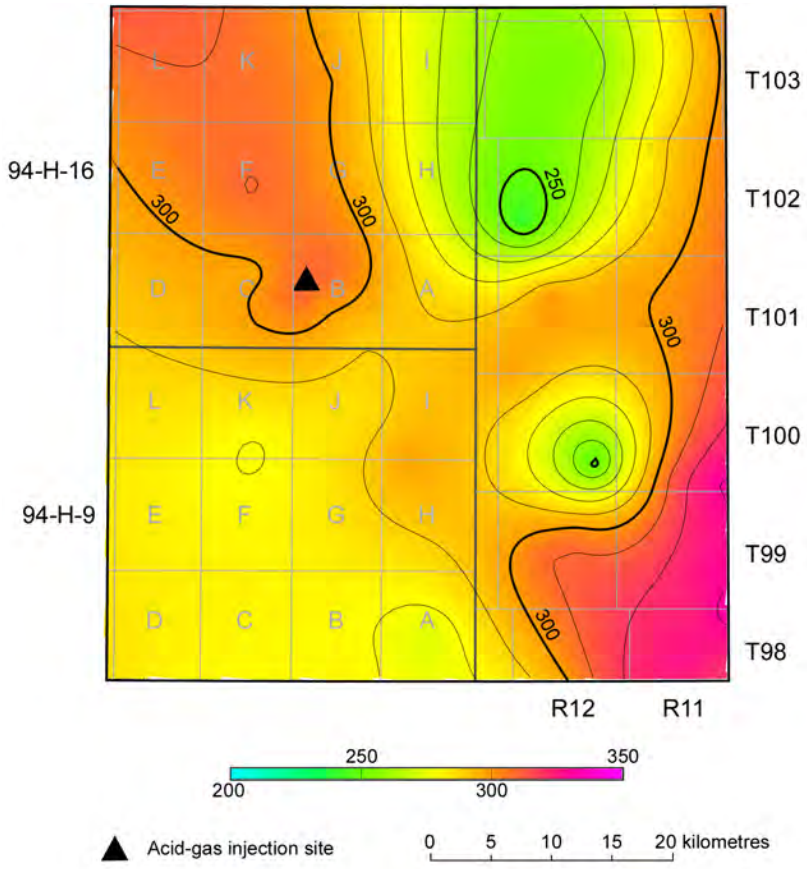

Figure 54. Isopach map of the Banff Formation in the Ring local-scale study area. Contours in metres. Contour interval = 10 m.

Table 7. Major ion chemistry of Permo–Carboniferous brines in the Ring area (concentrations in g/l). * Indicates analysis from the acid-gas injection well.

Location	Na	K	Ca	Mg	Cl	SO_4	HCO_3	TDS
D-076-B/094-H-16	20.8	0.3	1.6	0.4	35.4	0.1	0.9	58.8
B-064-C/094-H-16	18.4	—	0.8	0.6	30.6	0.7	0.6	51.4
D-049-B/094-H-16*	28.3	0.6	1.6	0.5	47.6	0.001	0.6	78.3
D-076-B/094-H-16	21.9	0.2	1.6	0.4	37.2	0.1	0.8	61.7
04-22-101-11-W-6	18.3	—	1.1	0.3	30.4	0.0	1.1	50.6
C-002-B/094-H-09	39.9	—	2.8	0.8	68.2	0.4	0.7	112.5
D-076-B/094-H-16	13.3	0.2	0.9	0.3	22.3	0.1	0.8	37.4
C-014-C/094-H-16	15.5	—	0.8	0.3	24.7	0.5	2.1	42.9
06-15-102-11-W-6	9.5	—	0.4	0.2	14.9	0.02	2.0	26.0
B-044-A/094-H-09	32.6	—	3.0	0.3	56.0	0.03	0.5	92.1
05-32-103-11-W-6	12.6	0.1	0.4	0.2	19.6	0.2	1.8	33.9
05-32-103-11-W-6	12.6	0.1	0.4	0.2	19.6	0.2	1.8	33.9
12-23-102-11-W-6	12.1	0.1	0.5	0.3	19.3	0.1	1.8	33.1
D-019-L/094-H-16	17.8	0.2	0.9	0.8	30.6	0.3	0.5	50.6
06-12-100-12-W-6	23.6	0.3	1.6	0.5	40.2	0.2	0.3	66.2
Average	**19.8**	**0.2**	**1.2**	**0.4**	**33.1**	**0.2**	**1.1**	**55.3**

5.2.2.2 Pressure Regime

Hydraulic heads, calculated with a reference density of 1052 kg/m^3, range from >530 m in the northeast to <450 m in the southeastern part of the area (Figure 55b). The hydraulic-head contours indicate the convergence of a northeastward and southwestward-directed flow system in the centre of the study area, southwest of the Carboniferous subcrop edge, resulting in a deflection of the regional formation water flow toward the northwest and southeast.

The recorded pressures in the Permo–Carboniferous aquifer are plotted against elevation in Figure 56 and compared to pressures in the overlying Bullhead aquifer. Pressures in the Permo–Carboniferous aquifer plot along a linear trend representative of the pressure distribution in an underpressured static column of brine. Pressure-elevation trends in the overlying Bullhead aquifer are shifted toward lower pressures. This offset in the pressure distribution indicates weak vertical hydraulic communication across the Montney aquitard, and that the potential for vertical flow is upward from the Permo–Carboniferous into the Bullhead aquifer. Pressures at elevations between -150 m to -250 m in the Permo–Carboniferous aquifer, including pressures measured in the injection well, plot slightly below the regional trend, reflecting a downward flow component from shallower parts of the aquifer in the northeast and an upward component of flow from deeper parts in the southwest.

5.2.2.3 Rock Properties

The average of well-scale porosity and permeability values for the injection horizon, the Debolt Formation and the overlying Montney Formation are shown in Table 8. Also shown are permeability

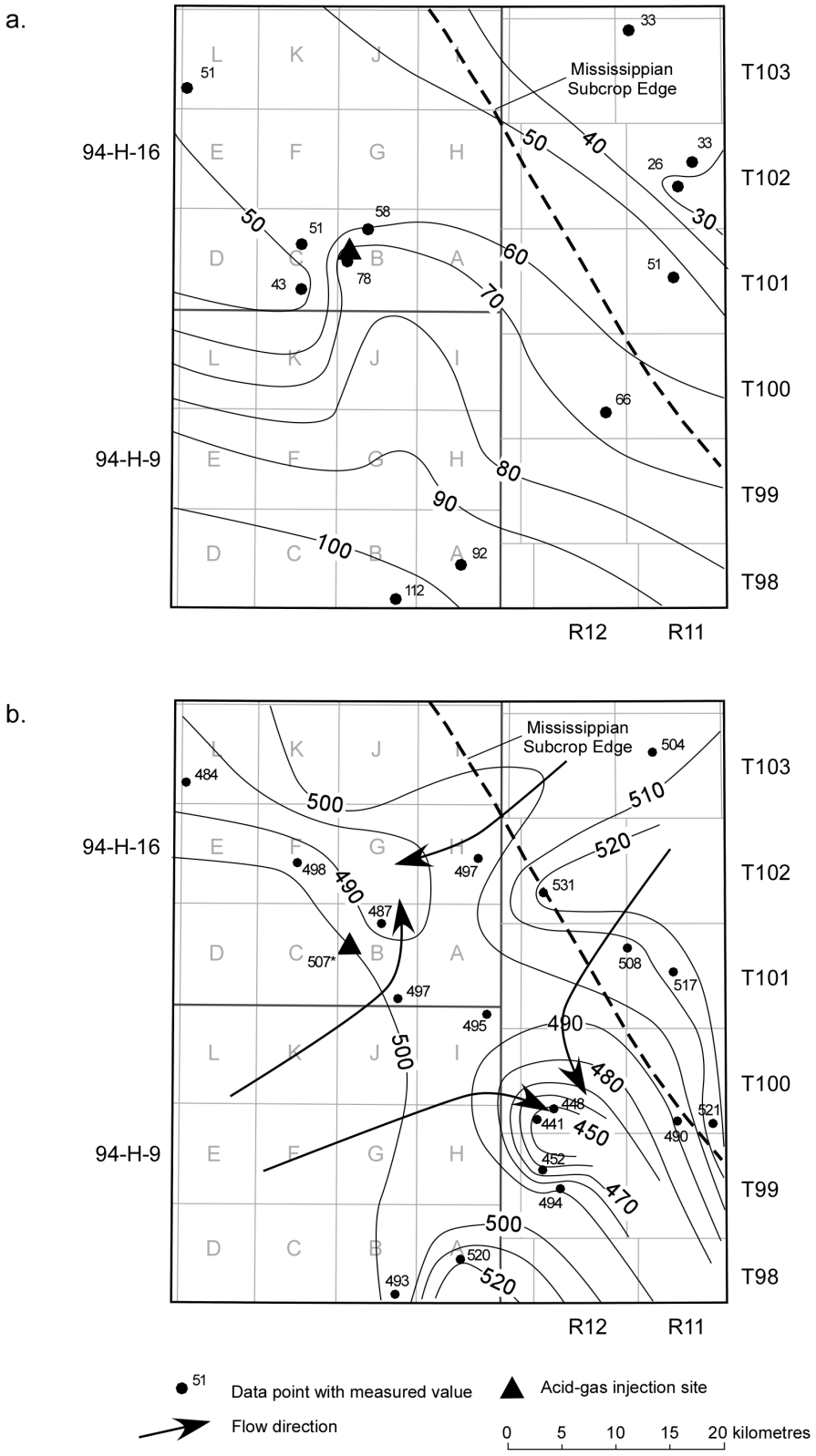

Figure 55. Distribution of a) salinity (g/l) and b) hydraulic heads (m) in the Permo–Carboniferous aquifer in the Ring local-scale study area.

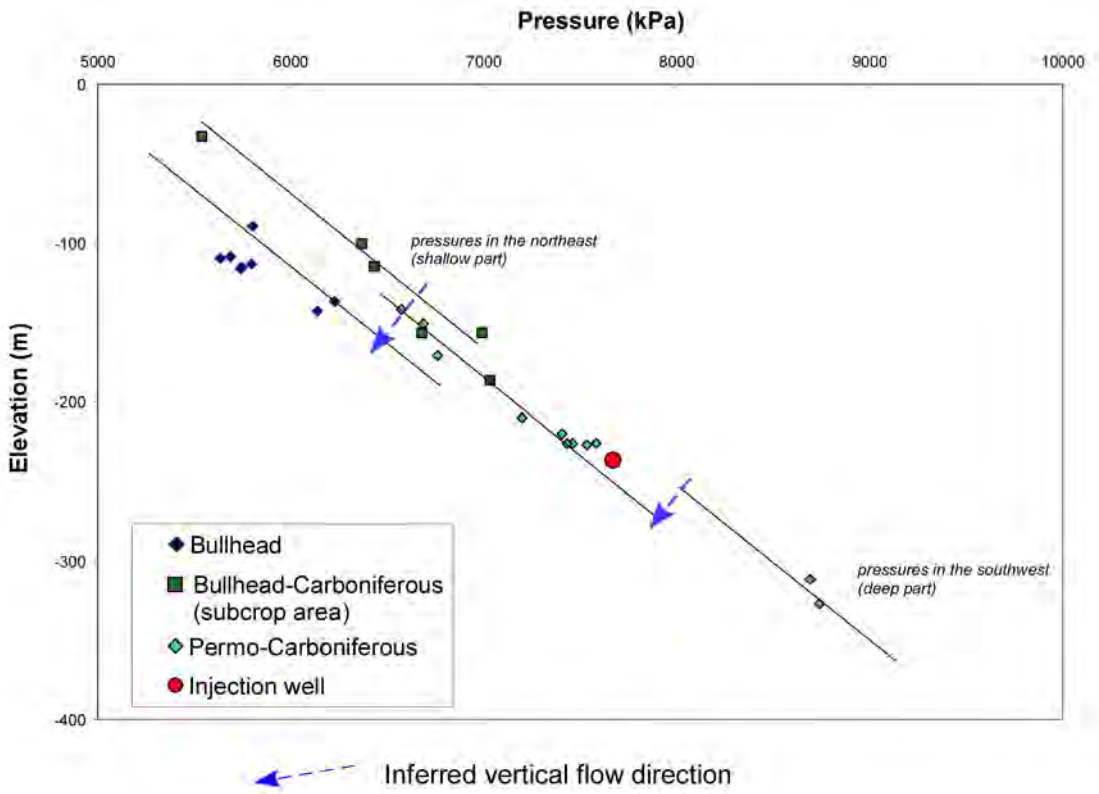

Figure 56. Distribution of pressure versus elevation in the injection strata and adjacent formations in the local-scale study area around the Ring acid-gas injection operation.

values calculated from drillstem tests performed in the Permo–Carboniferous aquifer, which range between 5 and 733 mD, with a median value of 275 mD. The average values of porosity (10%), horizontal permeability (21 mD) and vertical permeability (2 mD) in the Debolt Formation are of the same order of magnitude as respective values in the supposedly confining Montney Formation. The Montney Formation in the Ring area, being located along the edge of the Montney zero edge, contains a more variable range of lithologies than the otherwise shale and siltstone-dominated lithofacies deposited toward the southwest (Figure 19).The majority of the core analyses originated from the Ring–Border Field, where gas is produced from very fine, well-sorted sandstones and siltstones in the upper part of the Montney Formation, with an average permeability of 10 mD over an average of 10 m of net pay (Sturrock and Dawson, 1991. The reservoir rocks exist only in thin layers embedded in layers of shale (Figure 53), and the entire Montney Formation still acts as a vertical-flow barrier between the Permo–Mississippian aquifers.

Table 8. Well-scale porosity and permeability values obtained from measurements in core plugs from the Montney (66 wells) and Debolt (6 wells) formations, and permeability values calculated from 5 drillstem test analyses in the Ring local-scale study area.

	Porosity (%)			Horiz. Perm. (mD)			Vert. Perm. (mD)			DST Perm. (mD)		
Formation	Min	Max	Avg	Min	Max	Median	Min	Max	Median	Min	Max	Median
Montney	5	20	13	0.3	180	4.7	0.07	107	2.5	—	—	—
Debolt	2	13	10	6	94	21	0.15	20	1.9	5	733	275

5.2.2.4 Flow of Formation Water

The distributions of hydraulic heads and salinity in the Permo–Carboniferous aquifer suggest two flow systems meet in the Ring area. One flow system, following the northeastward direction of the regional-scale updip flow of high-salinity (>70 g/l) formation water, converges with the downdip, southwestward flow of less saline formation water. The decrease in relative bicarbonate concentration with increasing salinity (Figure 57) in the less saline brine follows the typical evolution of meteoric water along its flow path according to the Chebotarev sequence (Freeze and Cherry, 1979). At higher salinity values (>70 g/l), the relative bicarbonate content stays constant with further increase in salinity, suggesting the presence of older, possibly connate formation water. Therefore, the less saline formation water probably originates from local recharge in the area of the Milligan Hills. Downward flow of water of meteoric origin into the Permo–Carboniferous aquifer is facilitated by the absence of the Montney and Fernie aquitards and direct hydraulic communication between the Bullhead and Permo–Carboniferous in the northeast corner of the Ring area. Acid gas injection at the Ring site occurs a few kilometres to the southwest, downdip of the line of convergence of the two flow systems, and formation water salinity has an intermediate value of 78 g/l. The horizontal hydraulic gradient at the site is approximately 3 m/km. The Ring injection site is also located approximately 20 km southwest of the Carboniferous subcrop edge and 5 km southwest of the Ring–Border gas field, in an area where the Montney aquitard is more than 80 m thick and forms an effective barrier to vertical flow of formation water.

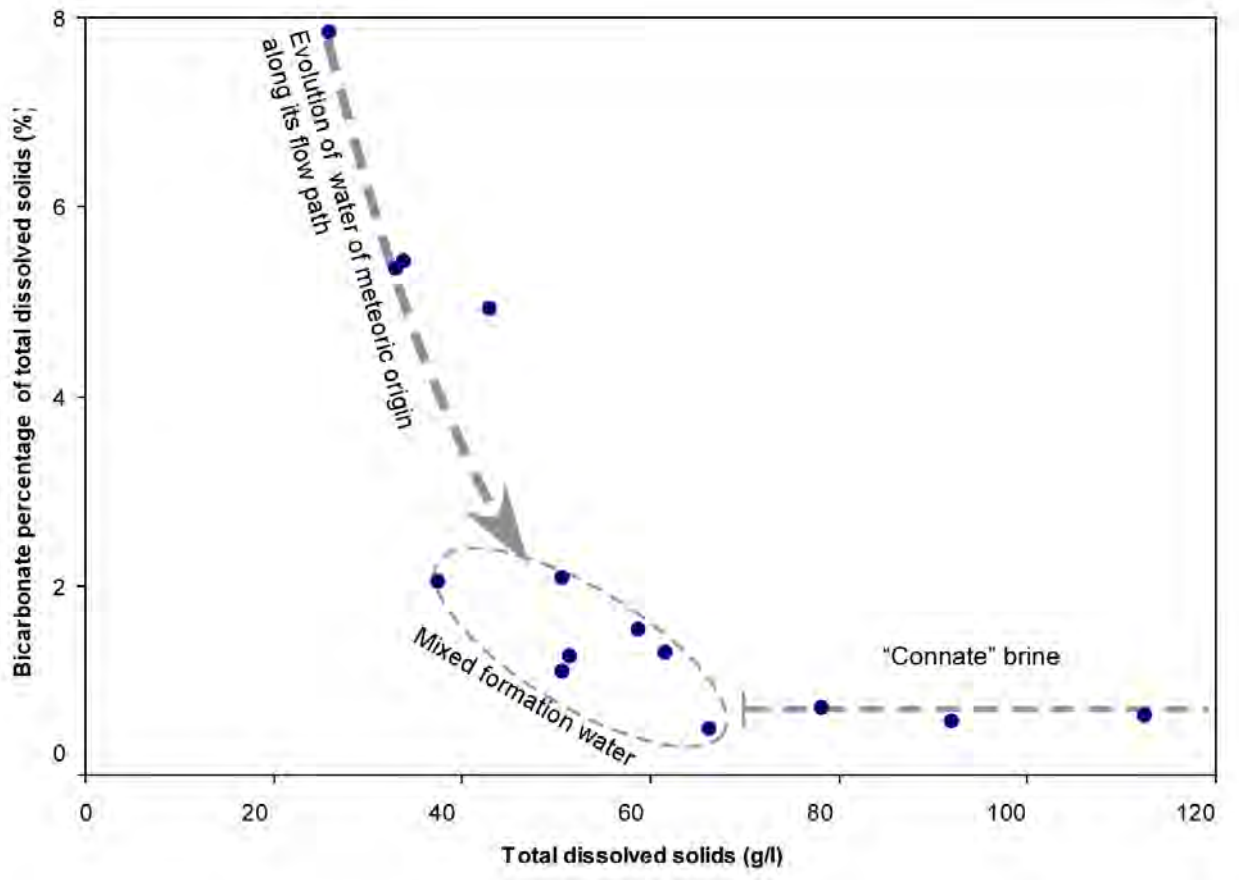

Figure 57. Plot showing relative bicarbonate concentrations versus total dissolved solids in Permo–Carboniferous formation water in the Ring local-scale study area.

5.3 Boundary Lake–South Belloy

The Boundary Lake–South local-scale study area is defined around the Boundary Lake–South Field, which extends from 56.43°N to 56.86°N and 119.6°W to 120.37°W (Townships 86 to 90 and Ranges 11 to 15W6) (Figure 12). It spans the British Columbia–Alberta border about 80 km east-northeast of Fort St. John (Figure 36). Injection takes place in Alberta at 15-11-88-13W6 within the Permian Belloy Formation, a water-wet, nonproducing unit, with sufficient porosity and permeability for injection. Production in the Boundary Lake–South Field is mainly from the Carboniferous Kiskatinaw and the Triassic Halfway and Baldonnel formations; there are no wells producing from the Belloy for several townships near the injection well. The closest production from the Belloy Formation is at Osborn in J/94-A-9, about 15 kilometres to the northeast from the injector.

5.3.1 Geology

The sandstones of the Belloy Formation range in thickness from 0 m to 55 m within the local-scale study area (0 m in the northwest corner due to erosion), and they are on average about 30 m thick in the injection area (Figure 58) with a net pay of 10 m. The Belloy thickens toward the southeast due to increased accommodation space in the Peace River Embayment/Dawson Creek Graben Complex. In addition, Barclay (2000) showed that faults that caused disruption of the underlying Stoddart Group rarely appear to cause offset of Belloy Formation units at the northern rim of the graben complex (Figure 59 and 60). Within the study area, the Belloy Formation is predominantly a sandstone facies. The rocks consist of quartz, chert, glauconite and traces of feldspar and mica. Porosity is mainly intergranular; however, it varies and can be up to 18% (Figure 61). Correlations suggest these sandstones represent a shoreline-related basin margin facies. Dissolution textures and influx of chert within the upper part of the Belloy Formation are related to exposure at the Triassic–Permian unconformity (Barclay, 2000).

The Belloy Formation is consistently overlain by approximately 240 m of dense Montney shales (Figure 62) and unconformably underlain by dense Mississippian Debolt Formation dolomites, which are more than 150 m thick (Figure 63).

5.3.2 Hydrogeological Characteristics and Rock Properties

5.3.2.1 Chemistry of Formation Waters

The major constituents of Permo–Carboniferous formation water, as determined from six analyses, are sodium (52 g/l) and chloride (91 g/l), making up 94% of the total dissolved solids (Table 9). Magnesium, calcium, sulphate and bicarbonate are present in minor concentrations (Figure 47c). In the Boundary Lake area, formation water chemistry is relatively invariable, salinity ranging from less than 138 g/in the southwest to 160 g/l in the centre (Figure 64a). The average in-situ density of formation water in the Permo–Carboniferous aquifer in the local-scale study area was estimated to be 1094 kg/m^3 using the methods presented in Adams and Bachu (2002).

Table 9. Major ion chemistry of Belloy brines in the Boundary Lake area (concentrations in g/l). * Indicates analysis from the acid-gas injection well; [C] indicates analysis of Carboniferous formation water.

Location	Na	K	Ca	Mg	Cl	SO_4	HCO_3	TDS
15-24-088-13-W6	52.3	1.0	4.4	1.7	93.0	1.9	0.3	154.2
11-27-086-13-W6	53.0	1.0	4.2	0.1	92.8	1.6	0.04	154.8
15-24-088-13-W6	55.5	1.1	5.4	1.5	96.5	1.7	0.2	159.7
15-11-088-13-W6*	54.5	1.2	5.2	1.0	93.5	1.1	0.7	156.7
06-27-086-13-W6[C]	48.1	1.0	5.1	1.0	89.0	1.7	0.5	148.0
07-21-087-15-W6[C]	47.1	—	4.7	1.0	82.7	1.6	0.7	137.8
Average	**51.8**	**1.1**	**4.9**	**1.0**	**91.3**	**1.6**	**0.3**	**151.9**

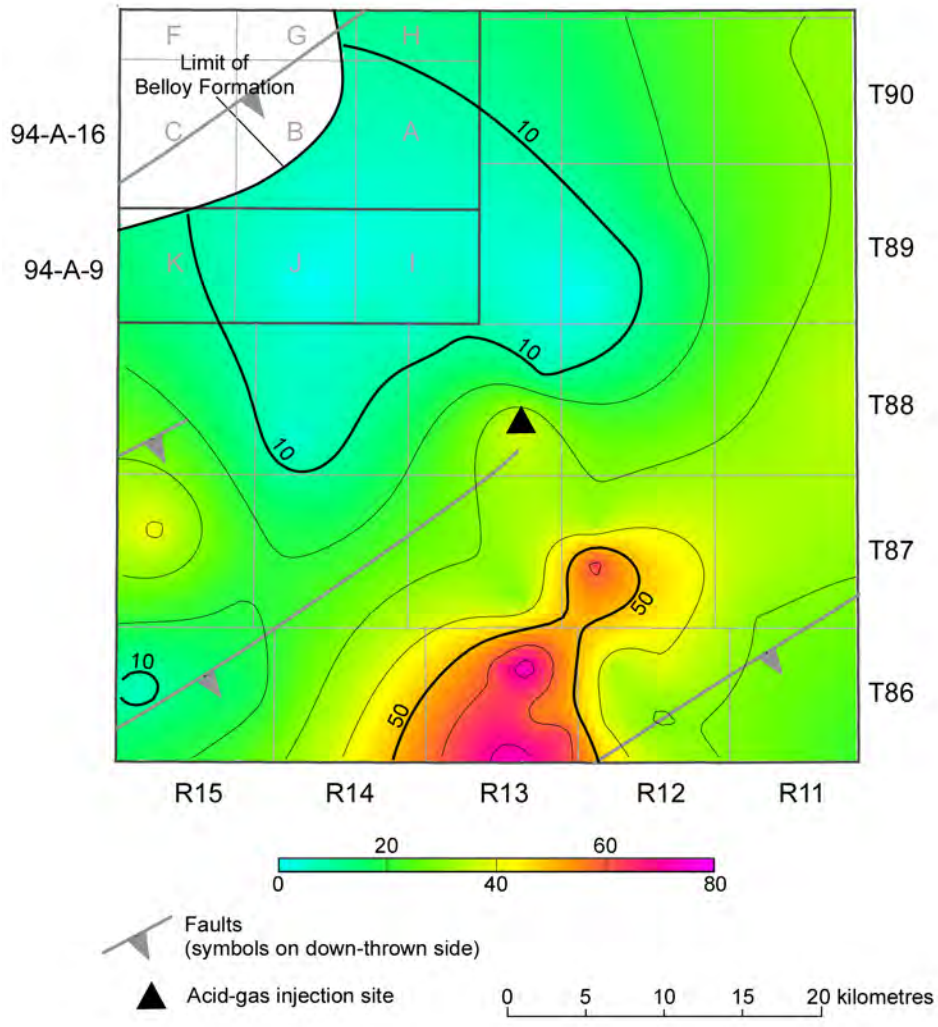

Figure 58. Isopach of the Belloy Formation in the Boundary Lake–South local-scale study area. Contours in metres. Contour interval = 10 m.

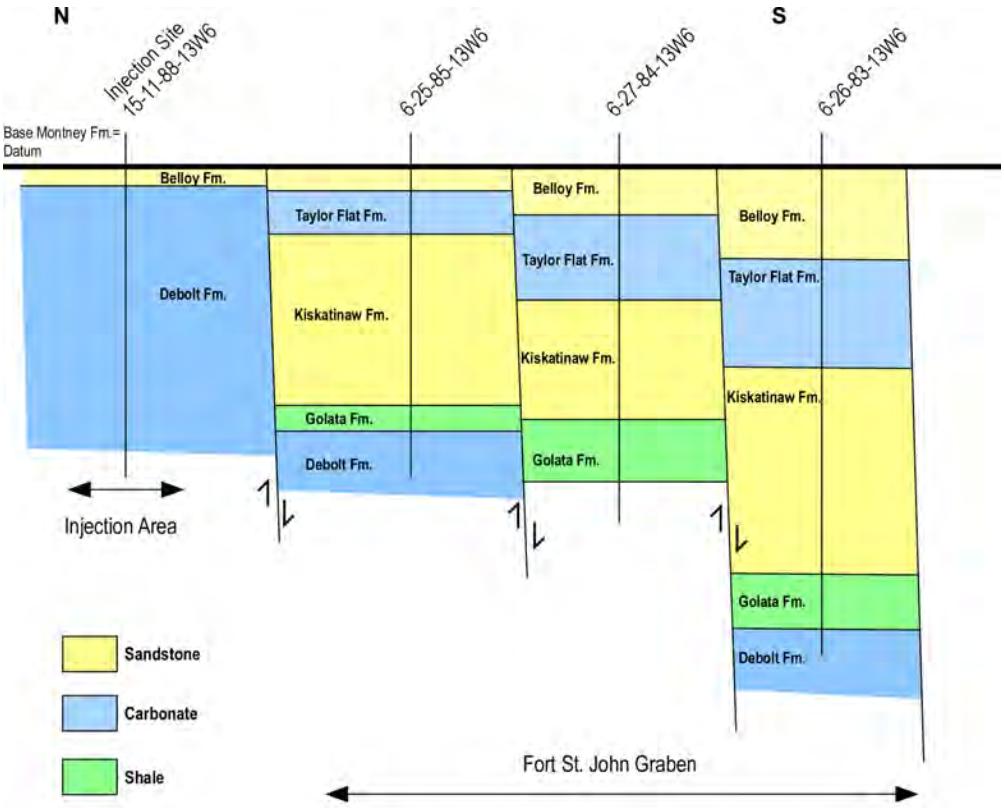

Figure 59. Schematic cross-section from the injection site at Boundary Lake to the south into the Fort St. John Graben, showing the thickening of the Belloy Formation to the south. At the injection sites, the Belloy sandstones are directly underlain by the Debolt Formation carbonate (modified after Barclay et al., 1990).

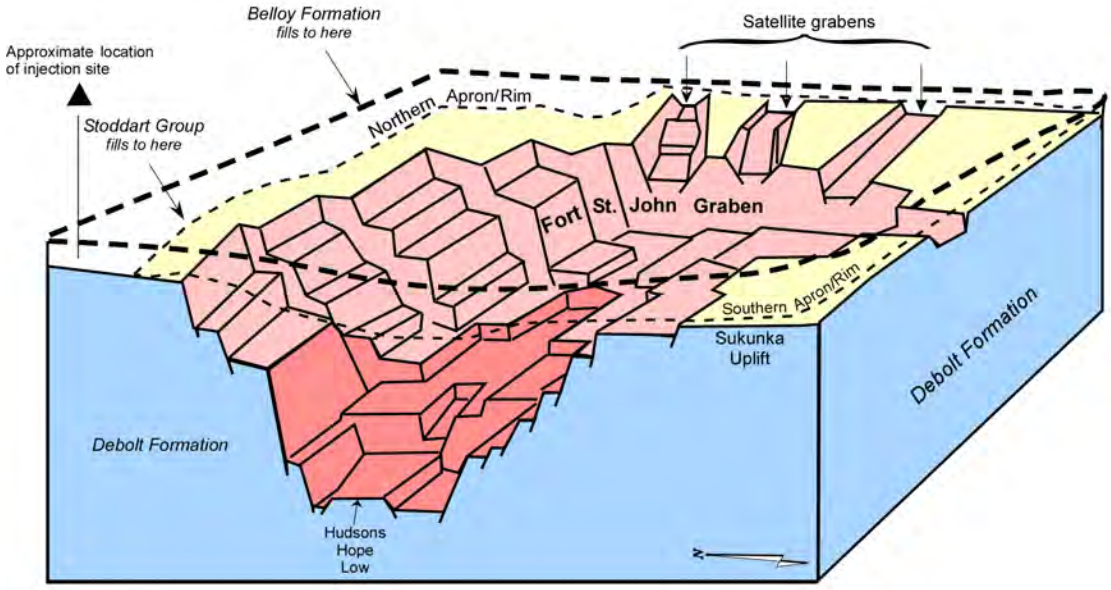

Figure 60. Schematic sketch of Carboniferous–Permian Peace River Embayment. The graben was successively filled by the Golata, Kiskatinaw, Taylor Group (Golata Group) and Belloy formations. Acid gas injection takes place on the upper northern flank of the complex where the Belloy is directly underlain by the Debolt Formation (modified from Barclay, 2000).

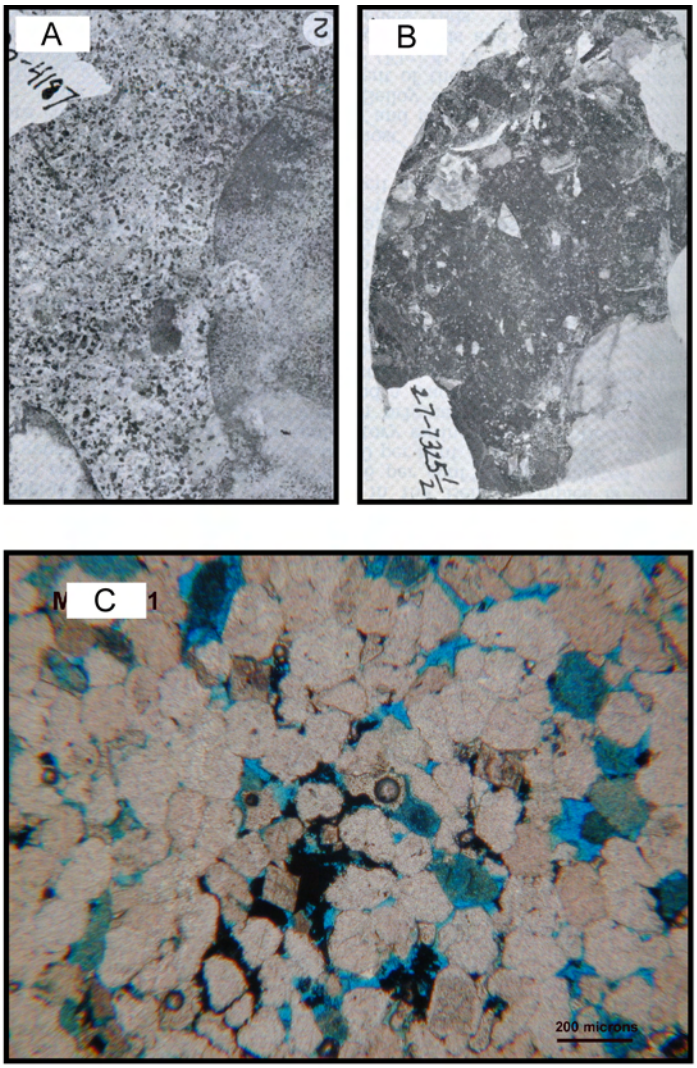

Figure 61. Core and thin section photographs of the Belloy Formation sandstone in the Peace River area. Grainy dolomitic sandstones (Photo A) are inter-layered with chert and sandy dolostones (Photo B) (Photo A and B, Naqvi, 1972). The intergranular porosity can best be seen on the blue-stained pores throughout the thin section photo (Photo C).

5.3.2.2 Pressure Regime

Hydraulic heads, calculated with a reference density of 1052 kg/m^3, decrease from about 550 m in the south and north to 480 m in the eastern part of the area (Figure 64b). The contour pattern indicates an eastward-channelled flow of formation water. The flow direction is parallel to the Permian Fault lineaments, and flow apparently is focused into the area of increased thickness of the Belloy Formation (Figure 58).

The recorded pressures are plotted against elevation in Figure 65 and compared to pressures in overlying formations. Pressures in the Permo–Mississippian aquifer plot along a linear trend representative of the pressure distribution in an underpressured static column of brine. Pressures in the overlying Halfway–Doig aquifer plot along a similar trend, which is probably due to similar lateral boundary conditions to formation water flow. The lack of data points between elevations of approximately -600 to -750 m corresponds to the interval of the intervening Montney aquitard, suggesting that at this depth the

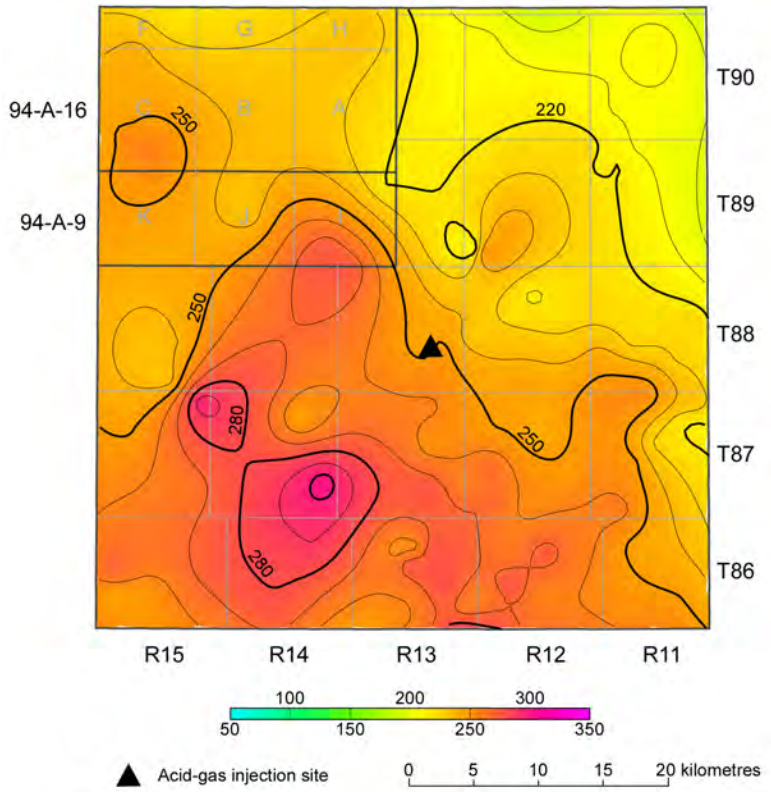

Figure 62. Isopach of the Montney Formation in the Boundary Lake–South local-scale study area. Contours in metres. Contour interval = 10 m.

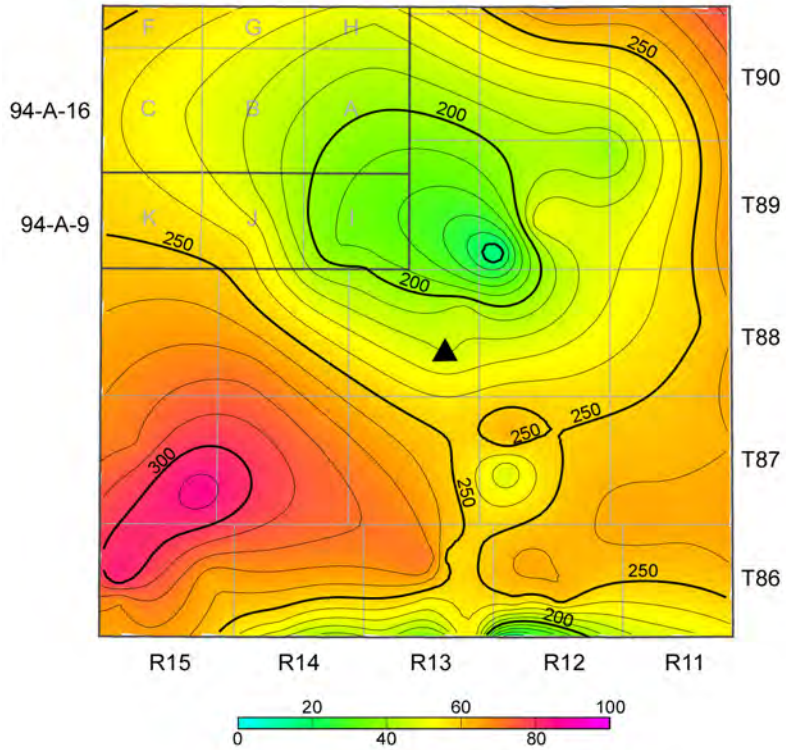

Figure 63. Isopach of the Debolt Formation in the Boundary Lake–South local-scale study area. Contours in metres. Contour interval = 10 m.

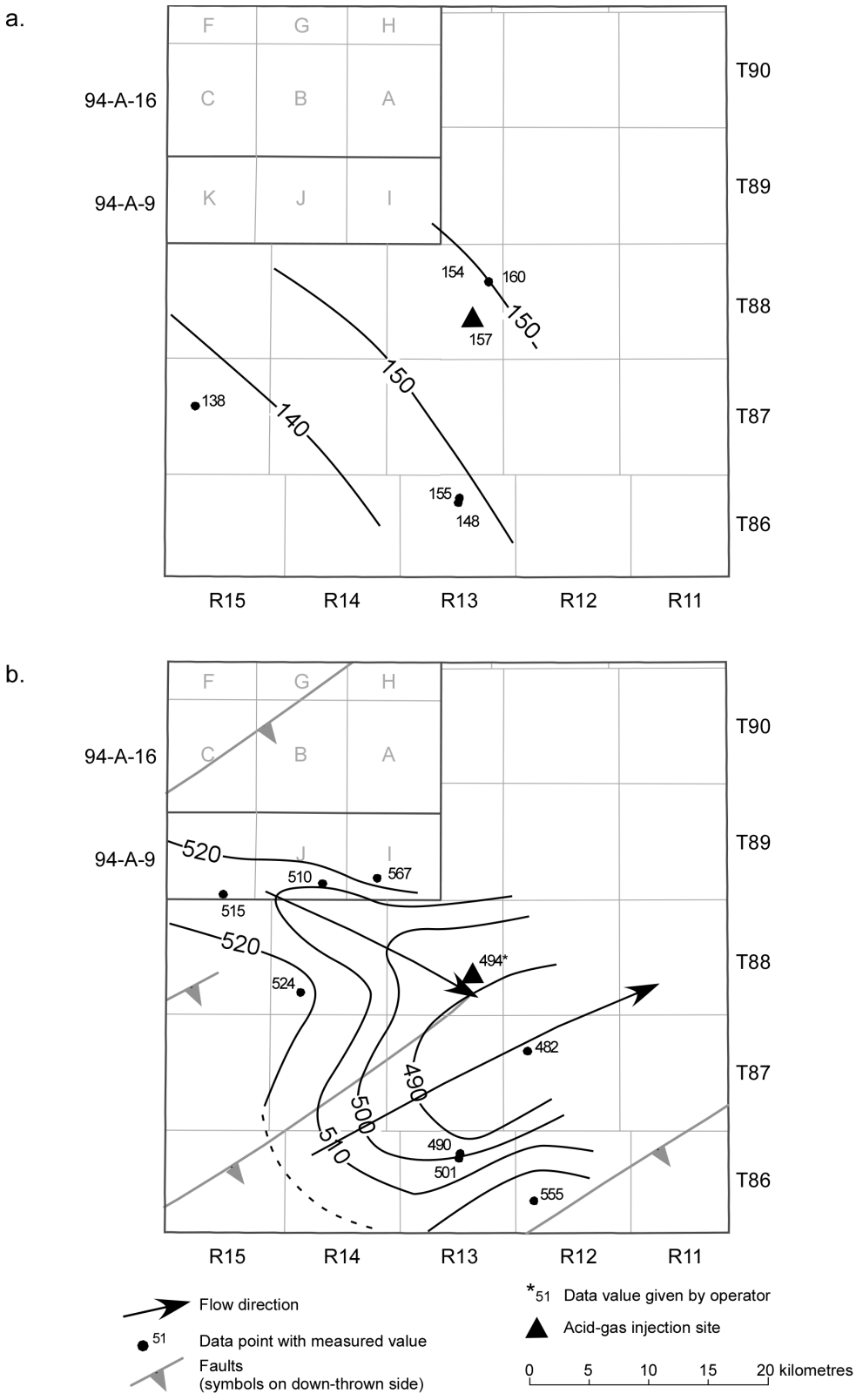

Figure 64. Distribution of a) salinity (g/l) and b) hydraulic heads (m) in the Permo–Carboniferous aquifer in the Boundary Lake–South local-scale study area.

strata are of low permeability and that cross-formational communication is unlikely. Pressure-elevation trends in the overlying Charlie Lake, Nordegg–Baldonnel and Bullhead aquifers are shifted toward higher pressures. This offset in the pressure distribution indicates there is no or only weak vertical hydraulic communication across the Lower Charlie Lake aquitard, and the potential for vertical flow is downward from the overlying aquifers into the Permo–Mississippian aquifer. Pressures in the underlying Permo–Carboniferous aquifer plot along a similar pressure-elevation trend as pressures in the Halfway–Doig aquifer, which suggest these aquifers might be in vertical hydraulic communication.

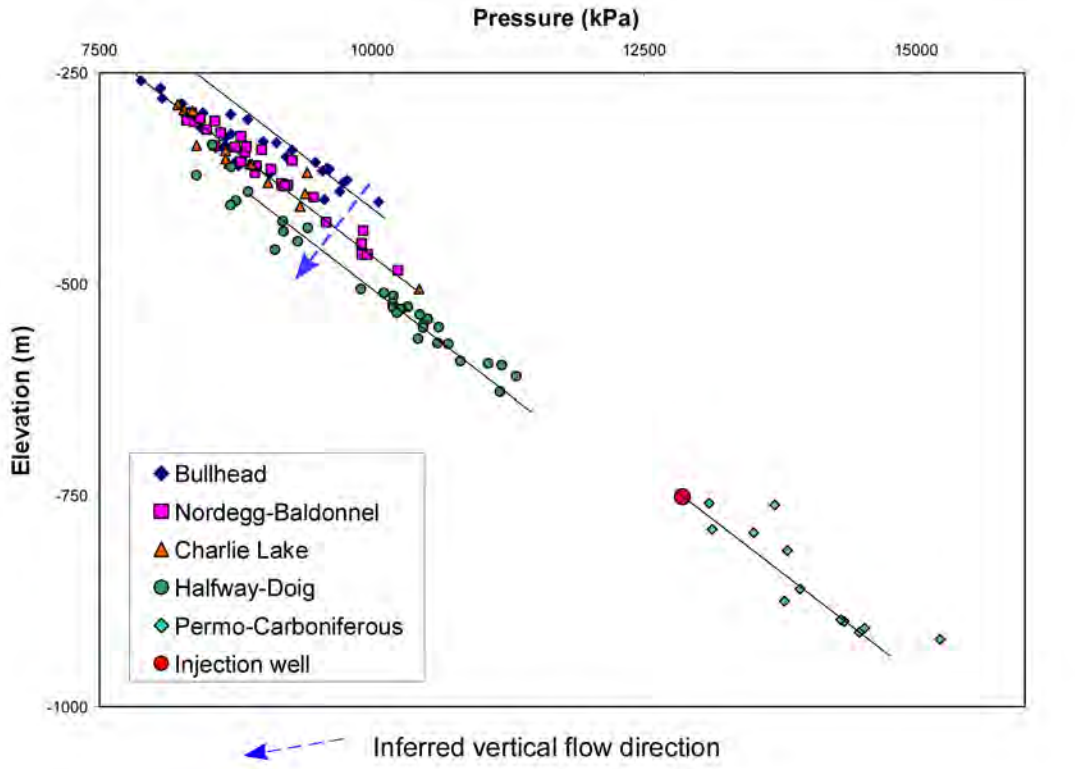

Figure 65. Distribution of pressure versus elevation in the injection strata and adjacent formations in the local-scale study area around the Boundary Lake–South acid-gas injection operation.

5.3.2.3 Rock Properties

The average of well-scale porosity and permeability values for the injection horizon, the Belloy Formation, and the overlying Montney Formation are shown in Table 10. Also shown are permeability values calculated from drillstem tests that were performed in the Permo–Carboniferous aquifer, which range between 0.1 and 100 mD, with a median value of approximately 0.25 mD. Core plug measurements generally are biased toward higher porosity and permeability values. The average values of porosity (15%), horizontal permeability (212 mD) and vertical permeability (70 mD) in the Belloy Formation are noticeably higher than respective values in the confining Montney Formation, confirming the flow-retarding characteristics of the Montney aquitard in the area.

Table 10. Well-scale porosity and permeability values obtained from measurements in core plugs from the Montney (five wells) and Belloy (three wells) formations, and permeability values calculated from five drillstem test analyses in the Boundary Lake local-scale study area.

	Porosity (%)			Horiz. Perm. (mD)			Vert. Perm. (mD)			DST Perm. (mD)		
Formation	Min	Max	Avg	Min	Max	Median	Min	Max	Median	Min	Max	Median
Montney	0.4	14	7	0.17	0.9	0.5	0.02	0.11	0.08	—	—	—
Belloy	11.7	19	15	113	222	212	2.3	118	70	0.10	100	0.25

5.3.2.4 Flow of Formation Water

The similarity in pressure versus elevation trends in the Belloy Formation and Carboniferous strata in the Boundary Lake area confirm the previous regional hydrostratigraphic assignment of a contiguous Permo–Carboniferous aquifer. The flow direction of formation water inferred from the distribution of hydraulic heads is northeastward, subparallel to the Permian tectonic lineaments; syn-depositional vertical movement along these faults caused a thickening of Permian strata (Figure 58). The increase in the thickness of Permian sediments and concurrent increase in aquifer transmissivity is probably the cause for the northeastward channelling of formation water flow in the southern part of the Boundary Lake area. The horizontal hydraulic gradient at the Boundary Lake–South injection site is approximately 2 m/km.

5.4 Bubbles/Jedney/Caribou–Baldonnel, Halfway, Debolt

The injection operations at Bubbles, Jedney and Caribou have been summarized in one local-scale study area, due to their proximity to each other. The injection horizon at Bubbles and Jedney is the Triassic Baldonnel Formation, whereas injection at Caribou takes place in the Triassic Halfway Formation and the Carboniferous Debolt Formation. The local-scale study area for all three operations was defined between 57.08°N to 57.5°N and 121.88°W to 122.88°W (E-94-H-4 to L-94-G-8) and includes the Caribou, Bubbles and Jedney gas fields (Figure 12, 36).

5.4.1 Geology

5.4.1.1 Baldonnel Formation (and Bounding Formations)

The injection zone in the Bubbles and Jedney fields is within the Triassic Baldonnel Formation of the Schooler Creek Group. The carbonates of the Baldonnel Formation have an average thickness of approximately 40 m (Figure 66; Appendix 1), with a net pay zone of 25 m. Evaporitic brine pan and high-stress peritidal environments of the upper Charlie Lake gave way to restricted marine facies of the Baldonnel, with the actual contact often recorded by an erosional disconformity with clasts of saline dolomudstone floating in crinoidal, bioclastic wackestones of the basal Baldonnel transgression. The middle and upper Baldonnel were deposited as more open-marine facies in a (slightly) more pronounced low-relief shelf or distally steepened ramp. Deposition occurred in numerous high-order cycles or sequences that resulted in a high degree of reservoir heterogeneity (Davies, et al., 2004). Compositionally, the Baldonnel is an intermixture of carbonate grains, carbonate mud, siliciclastics and phosphate. The most common skeletal (bioclastic) components are bivalve molluscs, with variable contributions by crinoids, brachiopods, gastropods, rare bryozoans and corals, ammonoids, foraminifera, sponge spicules, and conodonts. Nonskeletal carbonate grains include micritic peloids, micritized grains, algal-coated grains, clusters of large fecal pellets (‘pelcluster’ fabric), and ooids. The dissolution of these primary calcitic components contributed to the early diagenetic moldic porosity. The majority of the Baldonnel traps in the area north of the Peace River Block in northeastern British Columbia are influenced by north-

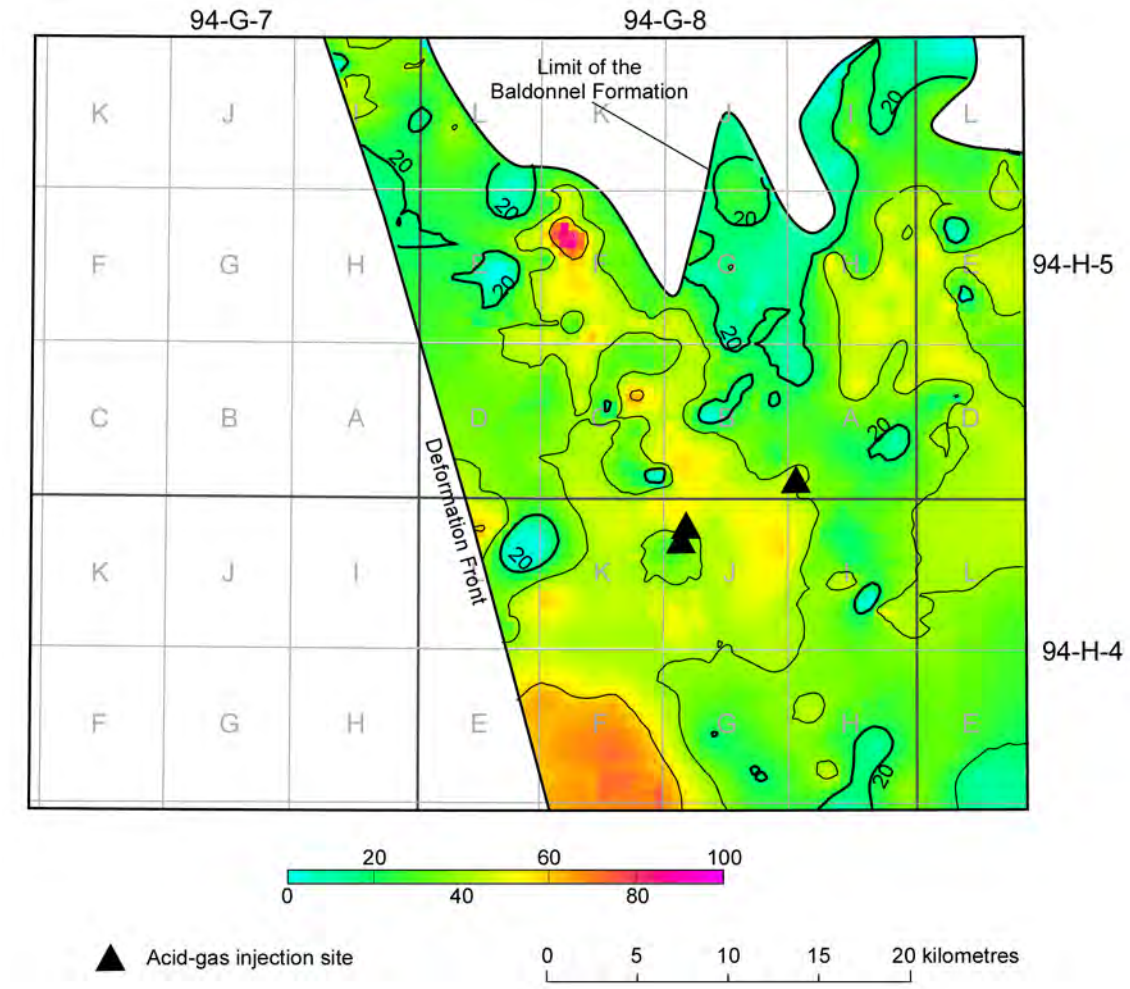

Figure 66. Isopach of the Baldonnel Formation in the Bubbles/Jedney local-scale study area. Contours in metres, Contour interval = 10 m.

northwest–trending folds and faults (as previously shown in Figure 27), which may have been initiated in Jurassic time. In addition, these folds can be seen in the local-scale cross-section (Figure 67), which also shows the thickening and thinning of the Baldonnel Formation.

The Baldonnel Formation in the local-scale study area is composed of 87% to 94% dolomite, with minor amounts of quartz, calcite, anhydrite and opaque material. Porosity is well developed and includes intercrystalline, moldic and vuggy porosity (Figure 68). The Baldonnel is overlain unconformably throughout most of the local-scale study area by the Jurassic Nordegg Member of the Fernie Group, which consists of hard, platy to medium-bedded, cherty and phosphatic limestones, with 40% to 90% chert, dark grey to black with blue tints, occurring as layers exhibiting pinch and swell, lenticular beds and nodules. Interbeds of platy, dark grey and black silty shales and papery black shales are also present in small amounts. A thin (30 cm) band of slightly phosphatic chert conglomerate often forms the lowermost bed of this unit. The Nordegg has a thickness of about 20 m in the injection area (Figure 69). The Baldonnel is gradationally underlain by medium grey dolostone, siltstone and limestone of the Charlie Lake Formation. The Charlie Lake reaches a maximum thickness of 200 m in the study area (Figure 67).

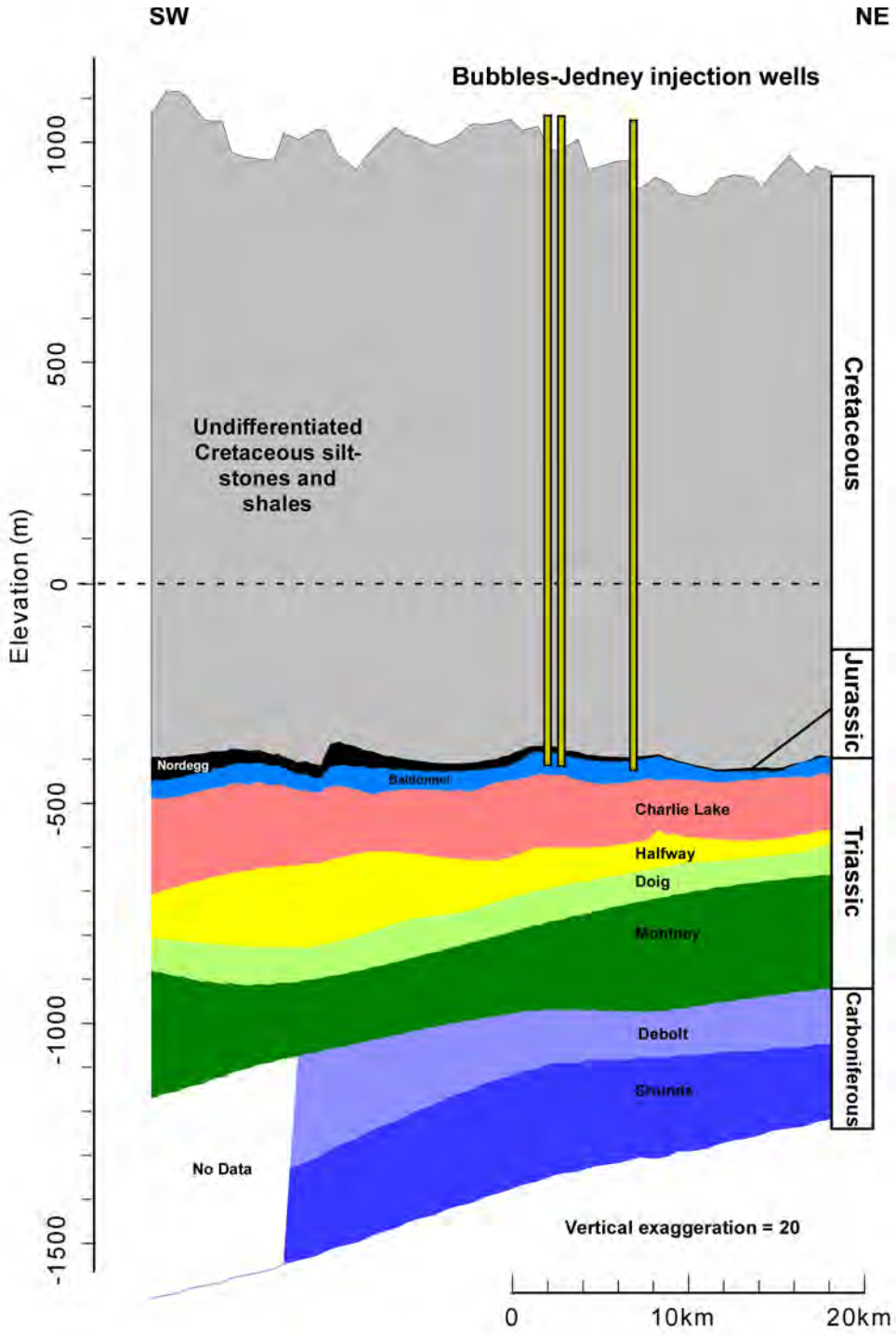

Figure 67. Local-scale cross-section through the Bubbles/Jedney acid-gas injection area. Note the tectonic undulation of the Baldonnel Formation, resulting in changing thickness of the formation and tectonic trapping of the injected acid gas in anticlinal structures.

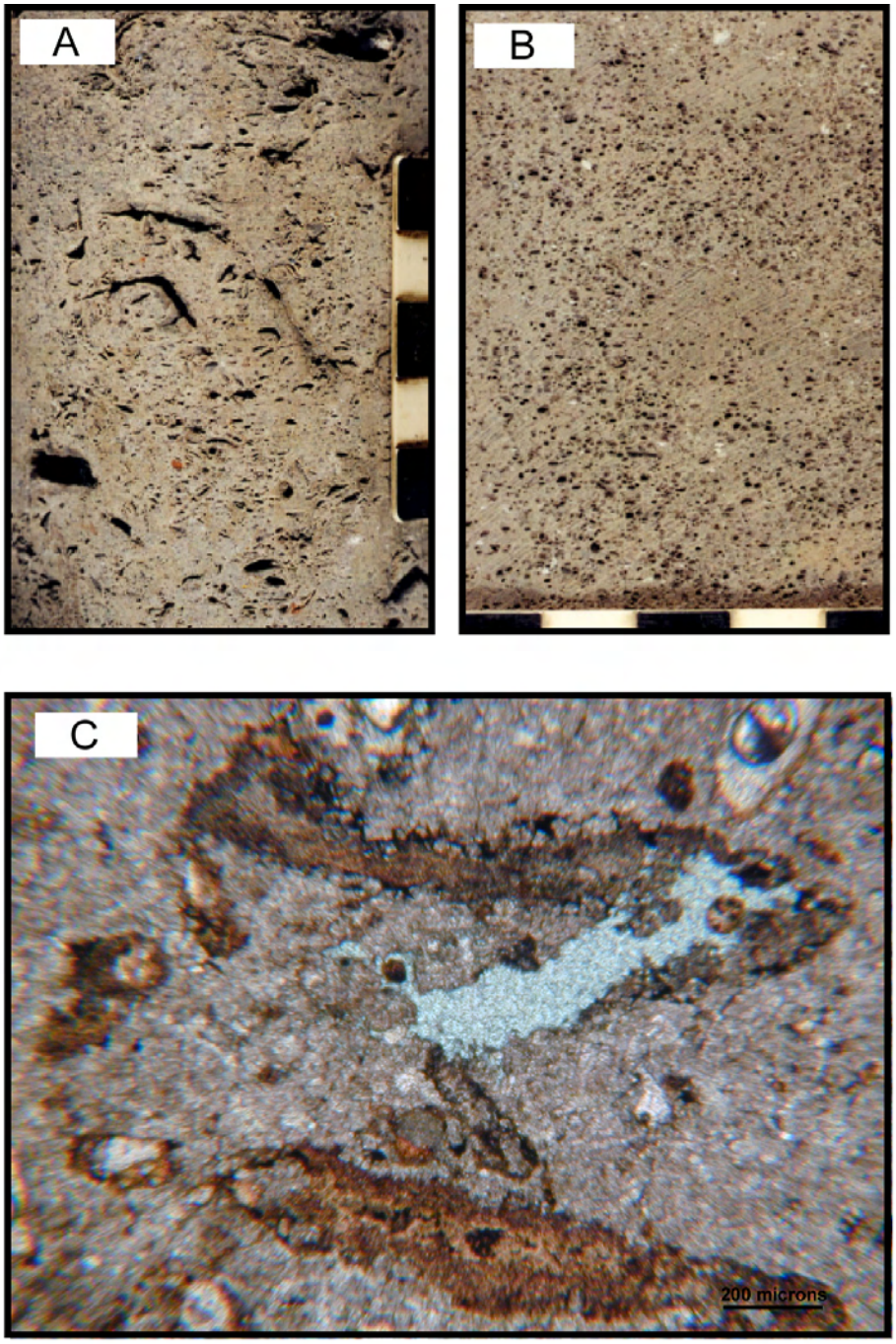

Figure 68. Core and thin section photographs of the Baldonnel Formation carbonate in the Bubbles/Jedney areas. Moldic to vuggy dolostones with abundant intercrystalline porosity (Photo A and B, Davies, 2004) are dominant (Photo B). The porosity can best be seen on the blue-stained pores in the centre of the thin section photo (Photo C).

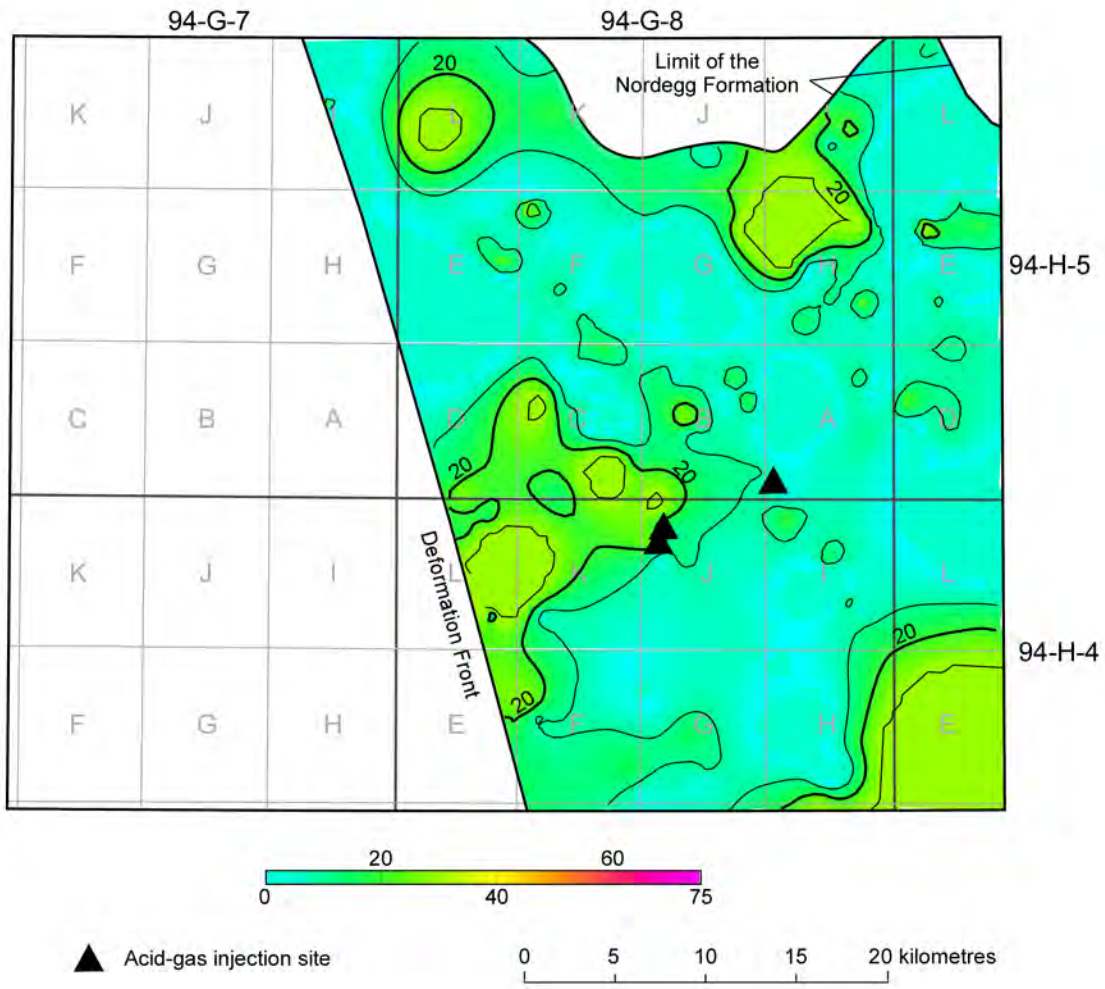

Figure 69. Isopach of the Nordegg Formation in the Bubbles/Jedney local-scale study area. Contours in metres. Contour interval = 10 m.

5.4.1.2 Debolt Formation

At the Caribou–Debolt site, acid gas is injected through the a-30-G/94-G-7 well into the Loomis Member of the Debolt Formation. The injection well was drilled on an anticline; therefore, the acid gas is structurally trapped (Figure 70).

The Mississippian Debolt Formation in the Caribou area consists of a series of stacked, extensive, low-relief carbonate ramps that prograded from east to west. These ramps developed moderate to good primary-depositional porosity in low-relief shoal, patch reef and carbonate grainstone belts proximal to ramp break in slope. In the Caribou area, the Debolt Formation can be subdivided into four members based on work by Law (1981) and Davies (The Mississippian Debolt Project, northeastern British Columbia, phase I, prepared for GDGC Ltd., 1990). In ascending order, these members are the Turner Valley, Salter, Loomis and Opal members. Progressive erosional truncation of the Debolt Formation by Permian and Triassic age deposits resulted in broad northwest-southeast–trending subcrop belts for each of these members. The principal productive reservoir zones are within the Loomis Member, where Laramide–age thrusting and folding formed structural/diagenetic traps. Porosity within the Loomis

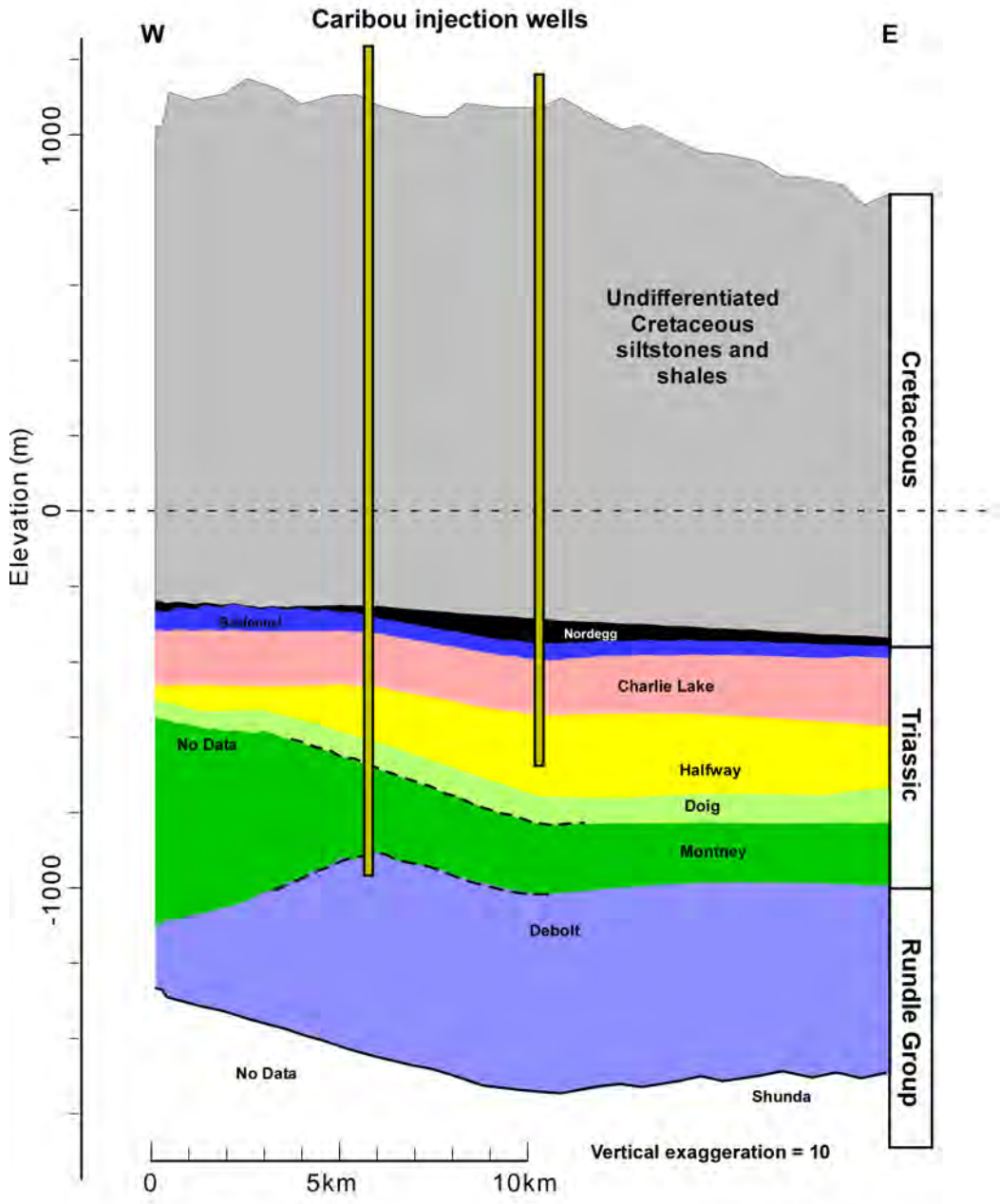

Figure 70. Local-scale cross-section through the Caribou acid-gas injection area. Note the anticlinal structure in the Debolt injection horizon and the synclinal feature in the Halfway injection horizon.

Member is generally developed through fault and unconformity-related dolomitization and associated porosity enhancement of ramp margin to ramp interior grainstones and packstones. The lower Opal and upper Loomis members in the Caribou area typically contain 20 to 30 metres of dolomite (90% dolomite and 10% fossil fragments), of which approximately 50% exhibit porosity in excess of 3%; the effective pay cut-off for many carbonate reservoirs in Western Canada.

The Debolt Formation is overlain by about 150 m shale packages of the Montney Formation and underlain by carbonates of the Shunda Formation (Figure 70).

5.4.1.3 Halfway Formation

The Halfway Formation in the Caribou area consists of a series of stacked, extensive, fine-grained shoreface sandstones that prograded from east to west over deeper water deposits of the Doig and Montney formations. In addition, the sandstone package of the Halfway Formation at the Caribou–Halfway site sits in a synclinal low, resulting in a structural position of over 80 metres lower than two offsetting wells (Figure 70). The Halfway Formation sandstones at the Caribou site have higher dolomite contents than their counterparts at West–Stoddart, but in general are composed of well-sorted quartzose sandstones. The Halfway Formation is overlain by 80 to 90 m of evaporites of the Charlie Lake Formation and underlain by thick shale packages of the Montney Formation (Figure 70).

5.4.2 Hydrogeological Characteristics and Rock Properties

The three aquifers that correspond to the injection units in the Caribou–Jedney–Bubbles area are the Permo–Mississippian, the Halfway–Doig, and the Nordegg–Baldonnel. Distribution of salinity and hydraulic heads, calculated with a reference density of 1052 kg/m^3, in these aquifers are shown in Figures 71 to 73.

5.4.2.1 Chemistry of Formation Waters

The major constituents of Permo–Carboniferous formation water, as determined from six analyses, are sodium (19.2 g/l) and chloride (35.2 g/l), compared to 35.9 g/l sodium and 58.4 g/l chloride in brine from the Halfway–Doig aquifer, and 11.3 g/l sodium and 19.9 g/l chloride in the Nordegg–Baldonnel aquifer. Sodium and chloride make up approximately 95% of the total dissolved solids in the three aquifers (Table 11). Magnesium, calcium, sulphate and bicarbonate are present in minor concentrations. A relative increase of sulphate and decrease of bicarbonate concentrations can be observed from the Nordegg–Baldonnel to the Permo–Mississippian aquifer (Figure 74), which is due to dissolution of sulphate minerals and diminishing penetration of bicarbonate-rich meteoric water with depth.

In the Caribou–Jedney–Bubbles area, chemical analyses of Permo–Carboniferous formation water are restricted to the area west of the deformation front of the Rocky Mountains. Salinity values in the northern and north-central parts are low, ranging from 13.5 g/l to 20 g/l at the Caribou injection site (Figure 71a). In the southern part, salinity of Permo–Carboniferous formation water is significantly higher, with values between 50 to 100 g/l. In comparison, the only two chemical analyses of formation water in the overlying Halfway–Doig aquifer west of the deformation front show salinity values of approximately 23 g/l (Figure 72a). However, salinity increases east of the deformation front up to 150 g/l at the eastern boundary of the study area. In the Nordegg–Baldonnel aquifer, salinity values of formation water are noticeably lower than in the underlying aquifers, ranging from 12 g/l east of the Rocky Mountains deformation front to 45 g/l in the west (Figure 73a).

The average in-situ densities of formation water in the Permo–Carboniferous, Halfway–Doig and Nordegg–Baldonnel aquifers in the local-scale study area were estimated to be 1011 kg/m3, 1045 kg/m3, and 1020 kg/m3, respectively, using the methods presented in Adams and Bachu (2002).

5.4.2.2 Pressure Regime

In the Permo–Carboniferous aquifer, pressures exist only in the area west of the deformation front, with corresponding hydraulic-head values ranging from 640 to 750 m. The hydraulic head distribution suggests the convergence of a southward and a northward-directed flow system in the west-central part of the study area, resulting in eastward flow of formation water from the Rocky Mountains into the undeformed part of the basin. Contour lines of hydraulic heads east of the deformation front are

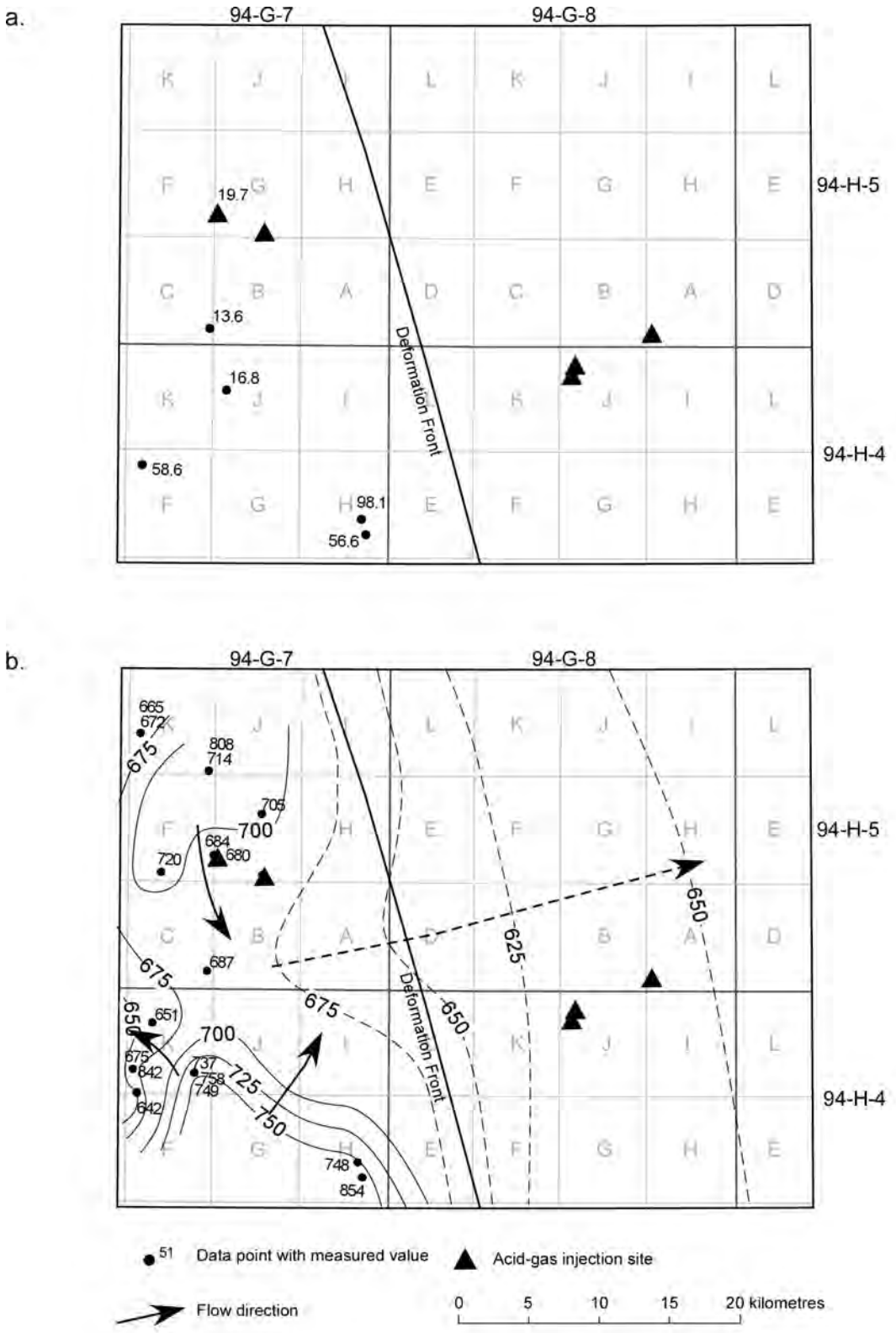

Figure 71. Flow patterns in the Bubbles–Jedney–Caribou area: a) salinity (g/l) and b) hydraulic heads (m) in the Permo–Carboniferous aquifer. Interpolated hydraulic-head contours from regional hydraulic-head distribution and respective inferred flow directions are shown as dashed lines/arrows.

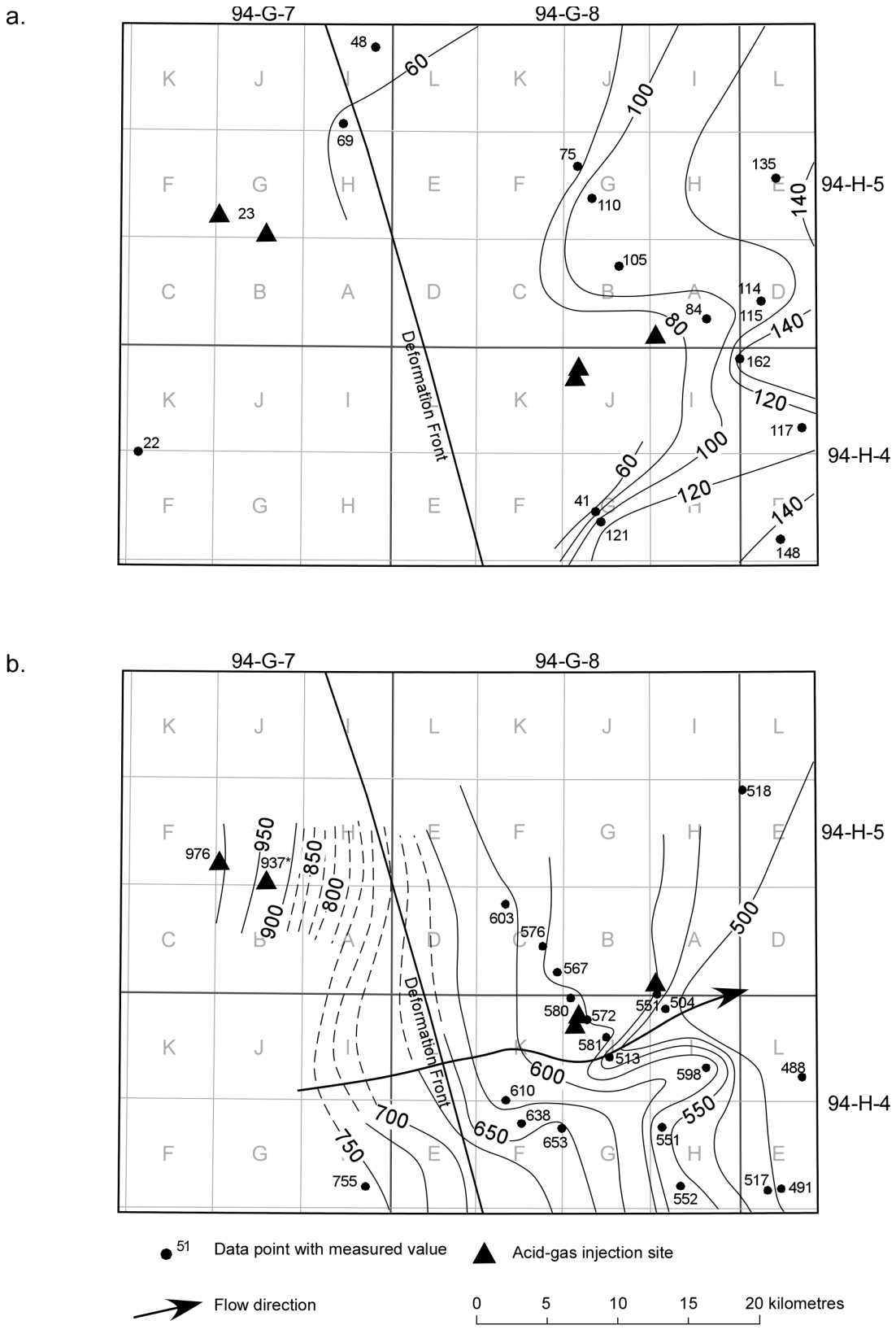

Figure 72. Distribution of a) salinity (g/l) and b) hydraulic heads (m) in the Halfway–Doig aquifer in the Bubbles–Jedney–Caribou local-scale study area.

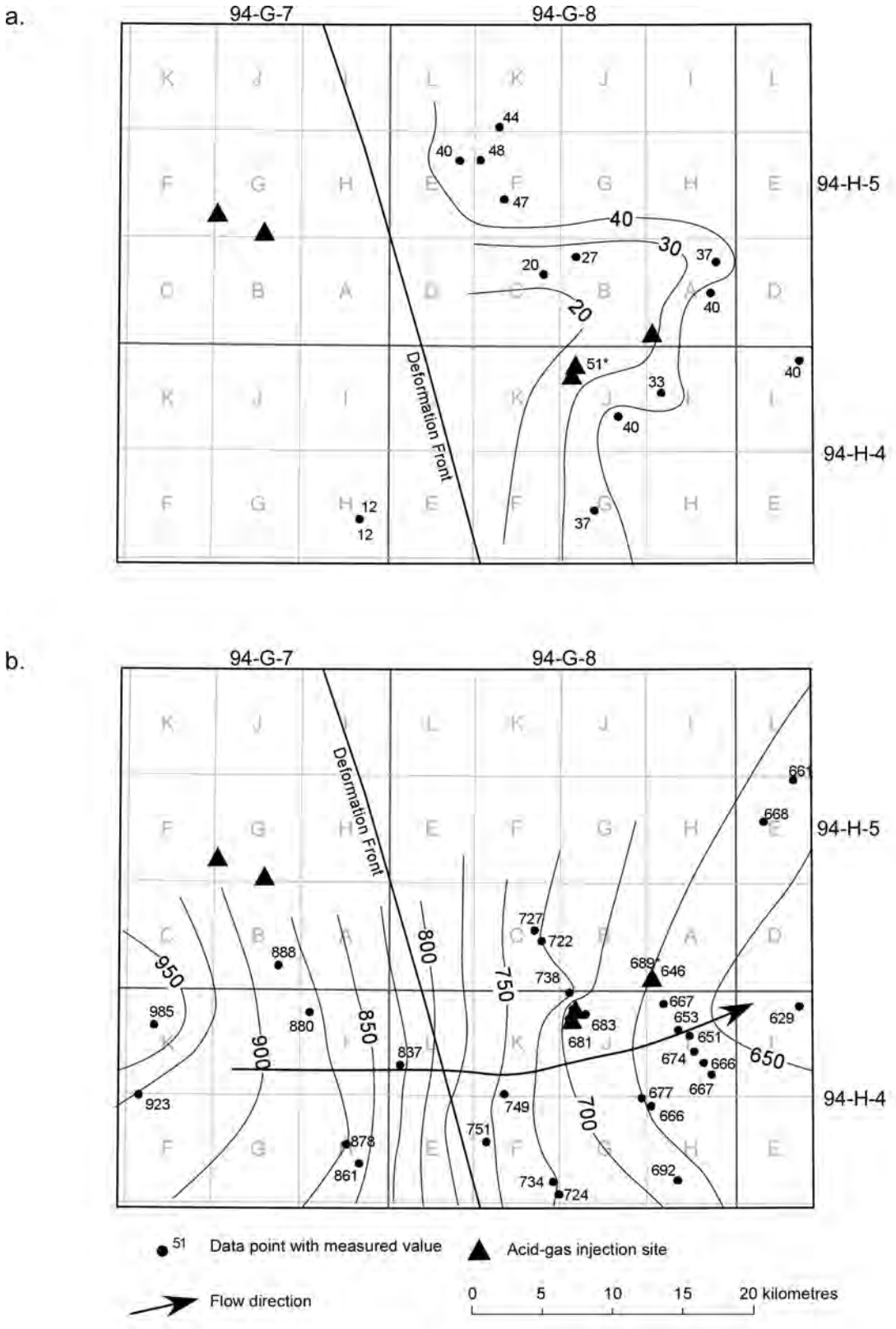

Figure 73. Distribution of a) salinity (g/l) and b) hydraulic heads (m) in the Nordegg–Baldonnel aquifer in the Bubbles–Jedney–Caribou local-scale study area.

Table 11. Major ion chemistry of brines from the injection units in the Caribou–Jedney–Bubbles area (concentrations in g/l). * Indicates analysis from the acid-gas injection well.

Location	Na	K	Ca	Mg	Cl	SO_4	HCO_3	TDS
Carboniferous								
d-033-H/094-G-02	33.2	1.5	7.6	1.0	67.2	0.4	0.4	109.6
d-033-H/094-G-02	29.6	1.5	6.8	1.0	60.1	0.4	0.4	98.1
c-020-B/094-G-07	3.6	0.1	1.0	0.4	7.2	1.2	0.7	13.7
c-058-J/094-G-02	6.2	0.1	0.2	0.1	8.3	1.4	1.3	16.8
b-022-H/094-G-02	20.7	1.4	0.9	0.3	34.0	0.3	0.6	56.6
d-088-F/094-G-02	22.1	1.0	0.6	0.2	34.7	0.8	0.5	58.6
Average	**19.2**	**0.9**	**2.8**	**0.5**	**35.2**	**0.7**	**0.6**	**58.9**
Halfway								
d-071-I/094-G-07	17.3	0.7	0.8	0.5	27.8	0.8	2.0	48.2
a-047-D/094-H-05	42.8	—	1.7	0.4	69.0	1.2	0.2	115.2
c-089-L/094-H-04	61.3	2.6	1.7	0.5	98.1	1.2	0.2	162.9
c-055-E/094-H-05	47.8	3.2	3.8	0.9	81.6	1.2	0.7	135.6
c-035-G/094-G-01	42.0	1.3	3.6	1.2	73.3	1.5	0.5	121.9
b-073-B/094-G-08	38.0	1.5	1.9	0.9	63.5	0.8	0.9	105.5
d-015-E/094-H-04	56.0	0.0	1.8	0.3	88.9	0.9	1.5	148.6
b-022-L/094-H-04	43.6	1.8	1.6	0.5	69.5	1.6	1.3	117.5
d-068-G/094-G-08	28.3	0.9	0.8	0.3	44.7	0.5	1.4	75.1
a-047-D/094-H-05	40.4	2.9	2.8	1.1	69.1	1.4	0.4	114.9
c-023-A/094-G-08	30.9	1.6	1.6	0.4	49.1	1.8	1.7	84.6
d-005-I/094-G-07	26.7	0.9	0.4	0.2	40.5	0.1	3.4	69.7
b-008-K/094-G-02	7.1	—	1.0	0.3	10.8	2.1	2.2	22.4
c-036-G/094-G-08	41.3	—	1.4	0.4	66.0	0.3	1.9	110.3
d-046-G/094-G-01	14.5	0.6	0.9	0.4	24.4	0.7	0.6	41.2
Average	**35.9**	**1.5**	**1.7**	**0.5**	**58.4**	**1.1**	**1.3**	**98.2**
Nordegg–Baldonnel								
c-058-I/094-G-01	12.6	0.6	0.3	0.1	19.4	0.3	1.0	33.2
b-033-J/094-G-01	15.5	0.3	0.3	0.1	23.1	0.01	3.0	40.6
a-018-K/094-G-08	15.8	0.2	0.9	0.5	25.5	0.1	2.8	44.1
d-072-A/094-G-08	10.2	—	2.5	1.3	22.6	0.1	2.1	37.7
d-072-E/094-G-08	15.6	0.3	0.2	0.1	23.5	0.2	2.1	40.6
c-042-A/094-G-08	9.6	1.0	3.3	1.7	24.4	0.3	1.8	40.3
a-098-B/094-G-08	5.7	0.2	2.6	1.6	17.0	0.1	1.7	27.8
b-082-L/094-H-04	15.1	0.6	0.6	0.02	22.8	0.2	2.5	40.0
a-061-C/094-G-08	6.7	0.1	0.8	0.5	11.6	0.2	2.3	20.9
c-068-F/094-G-08	14.8	0.3	2.2	1.2	28.8	0.1	2.5	48.5
d-033-H/094-G-02	3.7	—	0.8	0.3	5.6	0.8	3.1	12.6
d-046-G/094-G-01	14.7	0.3	0.2	0.1	20.7	0.01	4.5	37.9
c-036-F/094-G-08	14.5	0.4	2.0	1.3	28.0	0.1	2.6	47.1
d-033-H/094-G-02	3.5	—	0.8	0.3	5.4	0.7	3.1	12.2
Average	**11.3**	**0.4**	**1.3**	**0.7**	**19.9**	**0.2**	**2.5**	**34.5**

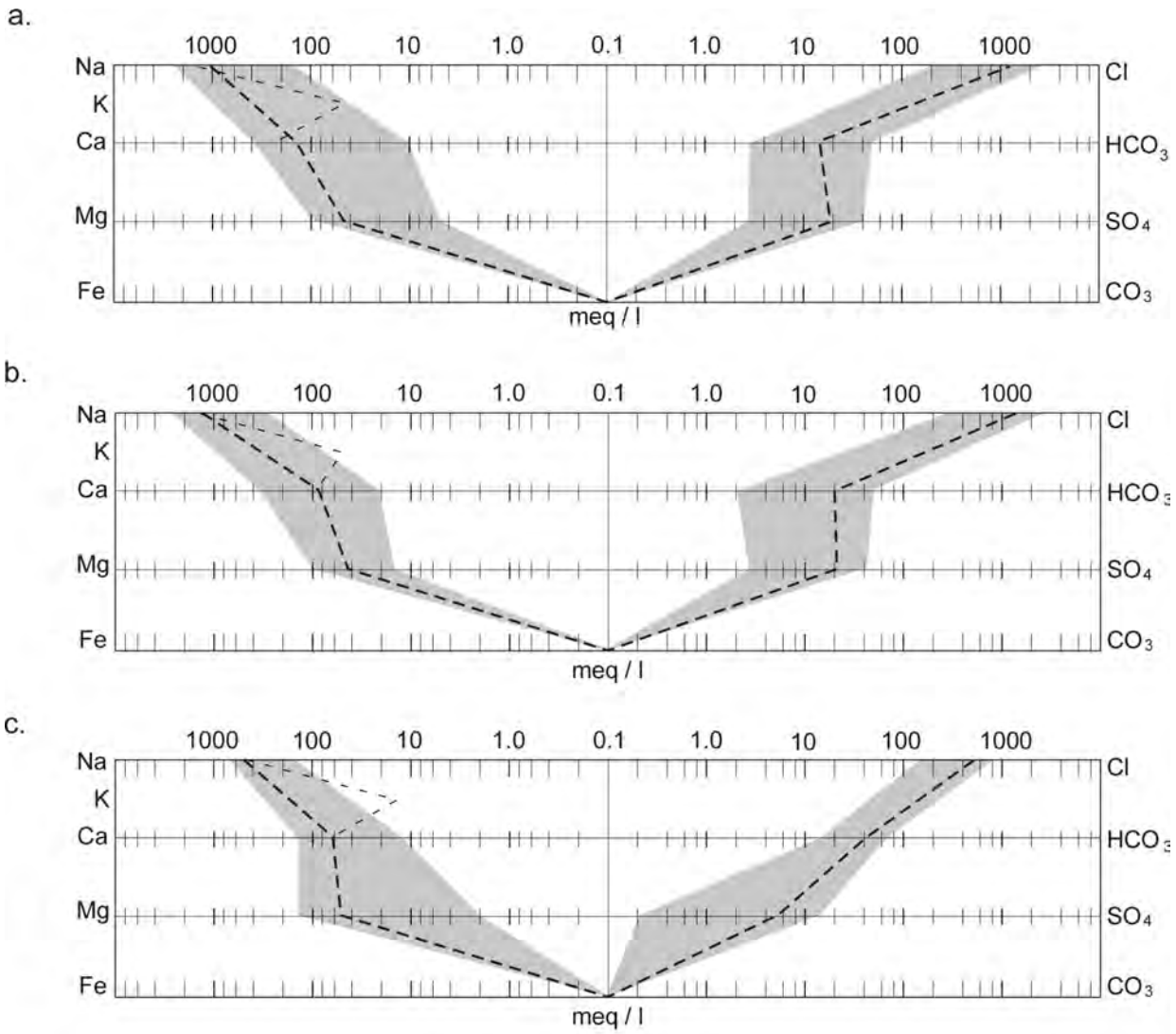

Figure 74. Stiff diagrams of formation waters in the Bubbles–Caribou–Jedney area: a) Permo–Carboniferous aquifer (5 analyses), b) Halfway–Doig aquifer (15 analyses), and c) Nordegg–Baldonnel aquifer (14 analyses). The grey-shaded area shows the range, the bold, dashed-line represents the average concentration in meq/l. The thin, dashed-line represents the potassium concentration.

interpolated from the regional hydraulic-head distribution (Figure 71b). In the overlying Halfway–Doig aquifer, hydraulic heads decrease eastward from 975 m in the west, at the Caribou injection site, to 490 m along the eastern boundary of the area (Figure 72b), indicating basinward flow of formation water originating in the Rocky Mountains. The high hydraulic gradient inferred from the high density of hydraulic-head contour lines near and subparallel to the deformation front implies a lateral barrier to flow, either in the form of a permeability change or a decrease in aquifer thickness. Similarly to the patterns in the Halfway–Doig aquifer, hydraulic heads in the Nordegg–Baldonnel aquifer decrease eastward from >950 m west of the deformation front to <650 m at the eastern boundary (Figure 73b), indicating eastward flow of formation water.

The recorded pressures in the Permo–Carboniferous to Nordegg–Baldonnel aquifers are plotted against elevation and compared to linear trends representative of the pressure distribution in underpressured

static columns of brine with a density of 1025 kg/m^3 (Figure 75). Generally, the wide spread of data between and within the various aquifers suggests a strong potential for vertical flow. A noticeable offset between pressure trends east and west of the deformation front indicates a certain degree of lateral hydraulic disconnect between the area of the Rocky Mountains and undeformed parts of the basin.

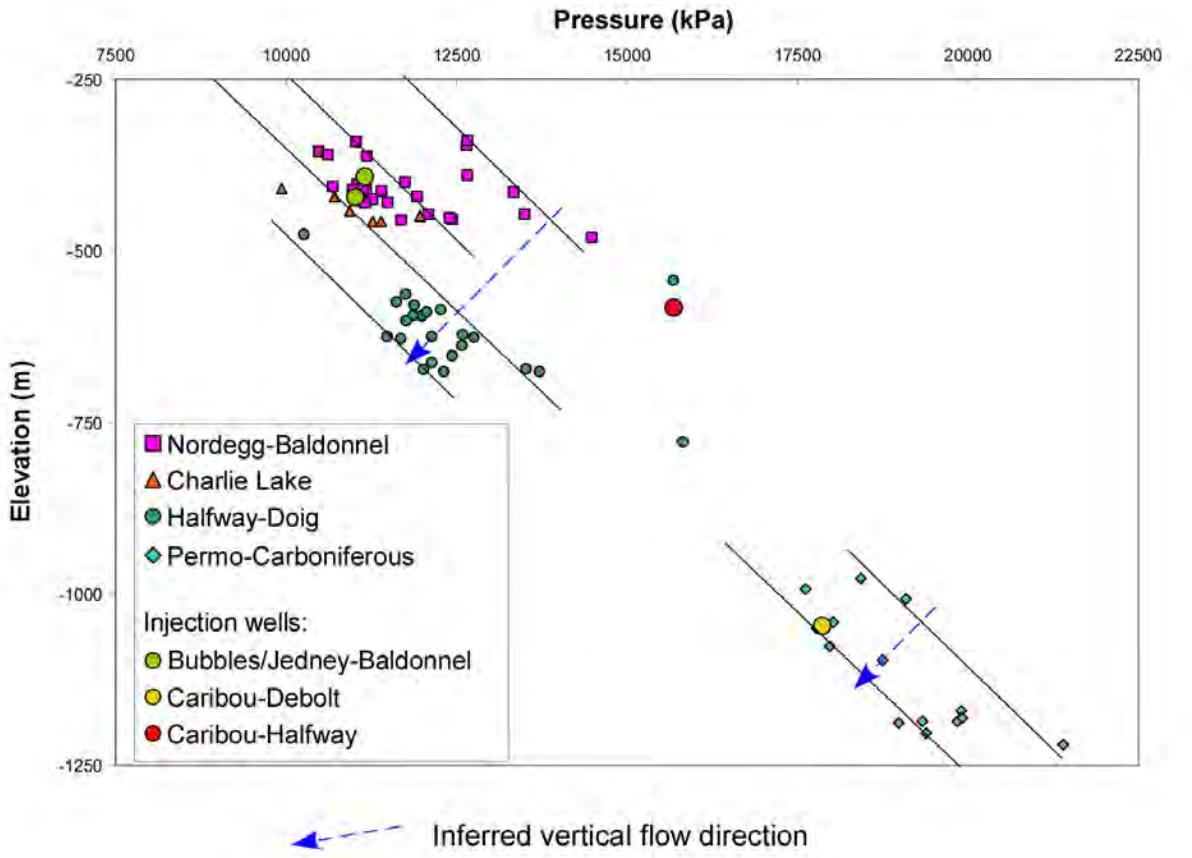

Figure 75. Distribution of pressure versus elevation in the injection strata and adjacent formations in the local-scale study area of the Bubbles, Jedney and Caribou acid-gas injection operations.

5.4.2.3 Rock Properties

The ranges and averages of well-scale porosity and permeability values for the injection horizons and bounding strata are shown in Table 12. Porosity values for the siliciclastic Jurassic and Triassic formations range between 6% and 8%. Only the average porosity of the carbonates in the Debolt Formation is comparably low (2%). The median horizontal permeability is highest in the Debolt Formation (11.5 mD), compared to 7.9 mD in the Baldonnel Formation and 1.2 – 3.8 mD in the Nordegg, Charlie Lake, Halfway and Doig formations. Vertical permeability values are comparably low for all formations, ranging on average between 0.4 mD in the Debolt Formation and 1.4 mD in the Baldonnel Formation. Also shown are permeability values calculated from drillstem tests that were performed in the Permo–Carboniferous, Halfway–Doig, Charlie Lake and Nordegg–Baldonnel aquifers. The median permeability in the Debolt Formation of 4.9 mD is approximately one order of magnitude higher than the permeability in the other formations (0.3 – 0.7 mD).

Table 12. Well-scale porosity and permeability values obtained from measurements in core plugs from the injection horizons; Baldonnel (54 wells), Halfway (36 wells), Debolt (5 wells), and intervening formations, Charlie Lake (61 wells), Doig (4 wells), Nordegg (11 wells), in the Caribou–Jedney–Bubbles area. Also shown are permeability values calculated from 48 drillstem test analyses.

	Porosity (%)			Horiz. Perm. (mD)			Vert. Perm. (mD)			DST Perm. (mD)		
Formation	Min	Max	Avg	Min	Max	Median	Min	Max	Median	Min	Max	Median
Nordegg	2.2	13	7	0.01	138	2.9	0.48	14	0.9	0.2	100	0.7
Baldonnel	2.6	11	8	0.23	219	7.9	0.03	42	1.4	0.1	15	0.6
Charlie Lake	1.0	13	6	0.01	135	3.8	0.01	15	0.9	0.1	1	0.3
Halfway	2.9	10	7	0.05	100	1.2	0.06	2.4	0.5	0.2	3	0.5
Doig	1.6	9	6	0.014	4	1.8	0.96	1.2	1.1	—	—	—
Debolt	0.9	3	2	0.15	44	11.5	0.03	1.9	0.4	0.4	1309	4.9

5.4.2.4 Flow of Formation Water

The increase of salinity and the vertical downward hydraulic gradient from the Nordegg–Baldonnel (~12 g/l) to the Halfway–Doig (20 g/l) to the Permo–Carboniferous aquifer (<100 g/l) in the western part of the Caribou–Jedney–Bubbles area suggests that, in the Rocky Mountains, meteoric recharge infiltrates into the Jurassic to Carboniferous strata, successively dissolving more solids and mixing with older formation water with depth. Lateral hydraulic gradients and a concurrent increase in salinity indicate east-northeastward flow of formation water within the individual aquifers. Less saline formation water of meteoric origin displaces and mixes with connate Jurassic to Mississippian brines with differential advancement of the mixing front in the different aquifers. While salinities less than 30 g/l can be observed in the Nordegg–Baldonnel aquifer up to 20 km east of the deformation front, similar concentrations in the underlying Halfway–Doig and Permo–Carboniferous aquifers are found only west of the deformation front. Although data are sparse, increased hydraulic gradients suggest the existence of a lateral barrier to flow subparallel to the Rocky Mountain deformation front. As the style of deformation in this part of the Rocky Mountains is dominated by the folding of strata, the existence of displacement faults that could obstruct flow is unlikely. Instead, the folding of strata probably caused the thinning of some parts of the aquifers (Figure 70), resulting in a decrease of aquifer transmissivity (hydraulic conductivity x aquifer thickness). Also, the folding of aquifer strata, possibly inducing fractures, could have resulted in the increase of permeability west of the deformation front, as permeability values measured on the core plug scale are rather low (Table 12). The highest permeability values determined from drillstem test actually originate from the Debolt Formation from the western part of the study area.

5.5 Summary of the Local-Scale Hydrogeological Analysis

The acid-gas injection sites in northeastern British Columbia area target Triassic carbonates and sandstones (West Stoddart, Caribou, Jedney and Bubbles), Permian sandstones (Boundary Lake–South) and Carboniferous carbonates (Ring, Caribou). Overall, the general vertical hydraulic gradient in the injection horizons is downwards, except for the Ring site. However, the flow is controlled by permeability distribution and does not necessarily occur if vertical permeability barriers exist, such as aquitards. The local-scale hydrogeological analyses in the northeastern British Columbia area show the injection units at the various acid-gas injection sites are overlain by thick aquitards forming effective barriers to cross-formational flow; i.e., the Montney aquitard at Ring and Boundary Lake–South, the Lower Charlie Lake

aquitard at Caribou and West Stoddart, and the Fernie aquitard at Bubbles and Jedney. Cross-formational flow occurs across the sub-Cretaceous unconformity, where the Bullhead aquifer is in direct hydraulic communication with the Halfway–Doig or Permo–Carboniferous aquifers. However, acid-gas injection sites that target horizons in the Halfway–Doig or Permo–Carboniferous aquifers are located southwest of the respective aquifer subcrop edges, so that in each case at least one aquitard (Fernie and/or Montney) separates the injection horizon from the Bullhead aquifer.

Typical, undiluted Triassic to Carboniferous brines are a Na–Cl type with relatively low bicarbonate concentrations and have salinity values >100 g/l, like the formation waters from the Permo–Carboniferous aquifer at Boundary Lake–South (157 g/l), and from the Halfway–Doig aquifer at West Stoddart (112 – 178 g/l) (Figure 76). In contrast, formation waters from areas that are affected by the dilution of connate brines in any aquifer due to mixing with less saline waters of meteoric origin are of Na–Cl or Na–Cl–HCO_3 type with relatively high bicarbonate concentrations and salinity values <80 g/l (Figure 76). The sites at which formation waters possibly have been diluted by freshwater from meteoric recharge in the Rocky Mountains are Bubbles–Baldonnel (40 g/l), Jedney–Baldonnel (52 g/l), Caribou–Halfway (24 g/l) and Caribou–Debolt (20 g/l). At Ring–Debolt (78 g/l), formation water chemistry has been influenced by mixing with local meteoric recharge from the Milligan Hills.

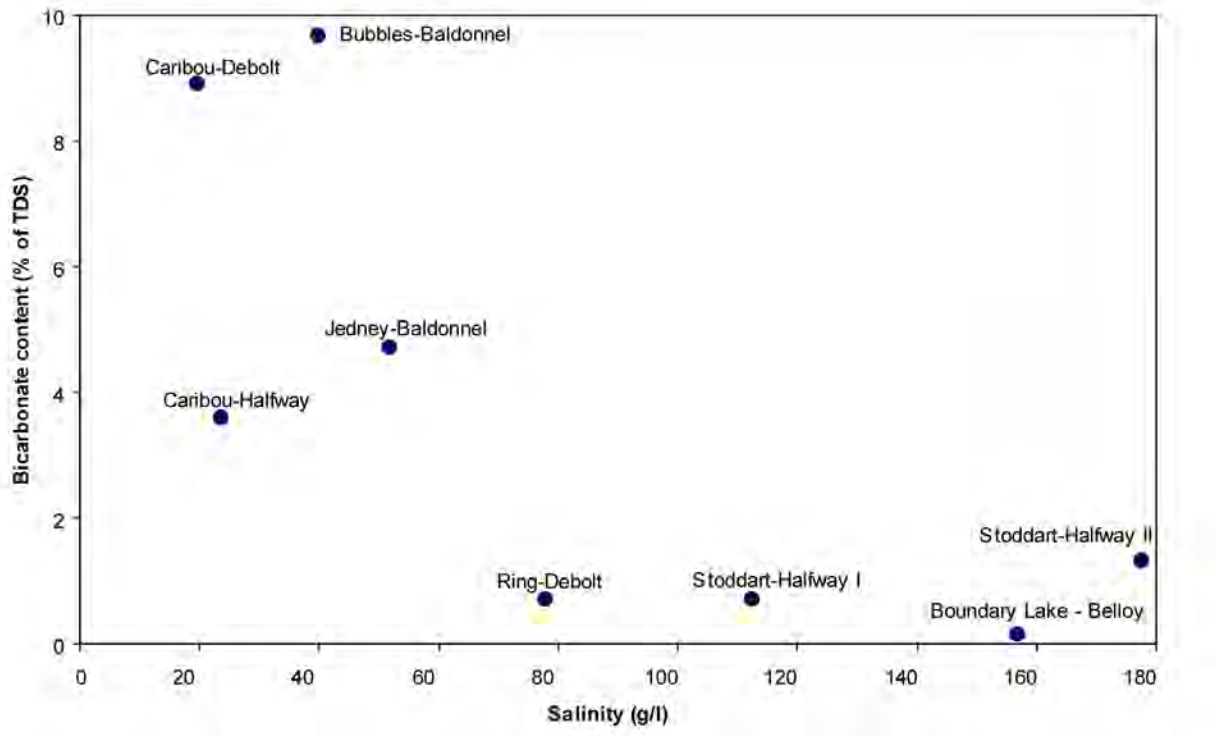

Figure 76. Plot showing relative bicarbonate content versus salinity of formation waters from the various acid-gas injection sites.

Evidence for faulting affecting the flow of formation water can be seen in the Boundary Lake area. Normal, syn-depositional faults in the Permian strata, associated with the tectonic history of the Peace River Arch, have caused a displacement and thickening of aquifer strata, creating a preferential flow path parallel to the fault lineaments. The Caribou–Jedney–Bubbles area, being located within and near the Rocky Mountains deformation front, was affected by the Laramide Orogeny. The dominant

deformation style is the folding of strata, creating traps, as with the Caribou, Jedney and Bubbles gas fields. However, no significant displacement can be observed within the hydrostratigraphic framework, and the advancement of less saline formation water in the Triassic to Carboniferous aquifers beyond the deformation front indicates that the lateral continuity of aquifers has not been compromised.

5.6 Site Specific Characteristics of the Acid Gas Operations

The site-specific characteristics of the acid gas operations in the northeastern British Columbia area are summarized in Table 13. This information has been compiled from many sources, including approval applications submitted by operators to the British Columbia Oil and Gas Commission (OGC) or the Alberta Energy and Utilities Board (EUB).

Regarding reservoir geology, operators usually identify the first stratigraphic unit that overlies the injection horizon as cap rock. However, at some sites this cap rock is directly overlain by other low-permeability strata, potentially adding to the vertical sealing capacity. In the Bubbles–Baldonnel and Jedney–Baldonnel operations, the chert horizon in the Nordegg Member is identified as the cap rock, which is directly overlain by shales of the Fernie Group, resulting in a combined cap rock thickness of approximately 70 m. Detailed downhole stratigraphic models for each injection site are shown in Appendix 1. The operators indicate site-specific porosity and permeability values for the injection horizon that are within the range of the average local-scale values (Tables 6, 8, 10, 12 and 13).

Vertical stresses, S_V, at the top of the various injection intervals vary between 22.7 MPa at 987.5 m depth and 52.0 MPa at 2154 m depth, reflecting the thickness and density of the strata that overlie the injection interval (Table 13). The gradient of the vertical stress was determined from density logs of the injection well, or where this was incomplete or unavailable, combined with wells near the injection well. The gradient varies between 22.9 kPa/m and 25.2 kPa/m, reflecting variations in rock density. Minimum horizontal stresses, S_{Hmin}, in the five injection intervals vary between 15.2 MPa and 35.7 MPa (Table 13) and corresponding gradients between 16.0 kPa/m to 19.5 kPa/m, reflecting variations in the rock properties, injection depth and stress distribution. The rock fracturing threshold in each well is between S_{Hmin} and S_V, but generally closer to S_{Hmin}. If the bottomhole injection pressure (BHIP) reaches the S_{Hmin} value, pre-existing fractures, if present, may open up. If no fractures exist, (except maybe around the wellbore), the pressure has to increase beyond S_{Hmin} to overcome the compressive strength of the rocks to create a fracture. However, fractures may be limited to reservoir rocks only and may not propagate into the cap rock. In order to avoid reservoir fracturing, OGC and EUB regulations require that the maximum BHIP be less than 90% of the fracturing threshold. Maximum BHIPs set for the studied acid-gas injection operations are safely below the S_{Hmin} (Figure 77); thus, if the maximum BHIP is reached, there is no danger of opening pre-existing fractures.

Because the injected acid gas may react with the formation rocks and fluids, it is important to know the geochemical composition of the rocks at each site. The results of mineralogical analyses and modelling of potential geochemical reactions between the injected acid gas and formation water and rocks will be in a companion report (Geochemistry of acid gas injection operations in Western Canada, S.J. Talman and B.E. Buschkuehle, work in progress, 2006).

Table 13. Characteristics of acid-gas injection operations in northeastern British Columbia.

	Operation Description	Boundary Lake S	Bubbles-Baldonnel	Caribou-Debolt	Caribou-Halfway	Jedney-Baldonnel	Ring-Debolt	W. Stoddart-Halfway I	W. Stoddart-Halfway II
Injection Operations	Gas Plant	Clear Hills Gas Plant	Jedney Expansion Plant	Caribou Gas Plant	Caribou Gas Plant	Jedney Sour Gas Plant	Slave Point Gas Plant	W. Stoddart Gas Processing Facility	W. Stoddart Gas Processing Facility
	Current Operator	Canadian Natural Resources Ltd.	Duke Energy Midstream	Anadarko Petroleum Corp.	Anadarko Petroleum Corp.	Petro Canada	Burlington Resources	Williams Energy Canada	Williams Energy Canada
	Approval Date	19-Dec-95	25-Jun-97	30-Mar-98	23-Apr-97	31-Oct-96	1-Dec-98	30-Apr-98	18-Sep-98
	Status	active	active	active	active	active	active	active	active
	Location (DLS)	16-11-088-13-W6	d-77-J/94-G-01	c-04-G/94-G-07	c-04-G/94-G-07	b-88-J/94-G-01	d-049-B/94-H-16	34-087-21W6	34-087-21W6
	Latitude (N)	56.624	57.231	57.338	57.338	57.227	57.788	56.585	56.585
	Longitude (W)	-119.946	-122.204	-122.671	-122.671	-122.228	-120.226	-121.253	-121.253
	KB Elevation (m AMSL)	910.0	905.0	1120.0	1069.0	1057.0	715	805	811
	Depth of Injection Interval (m)	1661-1673	1297-1355	2086-2222	1652-1713	1487-1535	950-1025	1590-1617	1590-1618
	Average Injection Depth (m)	1667	1326	2154	1682.5	1511	987.5	1603.5	1603.5
Reservoir Geology	Injection Formation Name	Belloy Fm.	Baldonnel Fm.	Debolt Fm.	Halfway Fm.	Baldonnel Fm.	Debolt Fm.	Halfway Fm.	Halfway Fm.
	Injection Formation Lithology	Sandstone	Dolostone	Carbonates	Sandstone	Limestone	Carbonates	Sandstone	Sandstone
	Injection Formation Thickness (m)	12.0	58.0	136.0	61.0	48.0	75	27	27
	Net Pay (m)	10	25	15	9	30	4	13	13
	Caprock Formation	Montney Fm.	Nordegg Fm.	Stoddart Gp.	Charlie Lake Fm.	Nordegg Fm.	Montney Fm.	Charlie Lake Fm.	Charlie Lake Fm.
	Caprock Formation Lithology	Shale	Chert	Siltstone	Dolostone	Limestone & chert	Shale	Anhydrite	Anhydrite
	Caprock Thickness (m)	240	20	20	185	25	83	59	60
	Underlying Formation	Debolt Fm.	Charlie Lake Fm.	Banff Fm.	Doig Fm.	Charlie Lake Fm.	Banff Fm.	Doig Fm.	Doig Fm.
	Underlying Formation Lithology	Dolostone	Anhydrite	Limestone	Shale	Dolostone	Carbonates	Shale	Shale
	Underlying Thickness (m)	200	35	250	189	110	200	35	35
Rock Properties	Porosity (fraction)	0.18	0.10	0.04	0.12	0.09	0.1	0.12	0.12
	Permeability (md)	186.00	21.00	2.00	9.00	5.00	346	13	32
	SV (MPa)	38.1	32.7	52.0	41.0	37.4	22.7	37.8	37.6
	SV Gradient (kPa/m)	22.9	25.2	25.0	24.8	25.2	23.9	23.8	23.6
	SHMIN (MPa)	26.7	25.3	35.7	28.9	29	15.2	29.7	29.7
	SHMIN Gradient (kPa/m)	16.1	19.5	17.1	17.5	19.5	16	18.7	18.6
Reservoir Properties	Original Formation Pressure (kPa)	16700	11154	17956	15685	11133	7670	13113	15459
	Formation Temperature (°C)	57.0	64.0	76.0	64.0	68.0	53	61	70
	Reservoir Volume (1000 m3)	396	n/a	1141	n/a	n/a	379.2	n/a	480.9
Formation Water	TDS Calculated (mg/L)	156804	39807	19737	23742	51797	77800	177691	112398
	Na (mg/L)	54500	13793	7219	8549	16533	26900	66490	29600
	Ca (mg/L)	5240	173	164	110	1512	1620	2442	1420
	HCO3 (mg/L)	257	3853	1757	854	2440	555	2330	807
Licensed Injection Operations	Injected Gas - CO2 (mole fraction)	0.51	0.45	0.44	0.50	0.45	0.53	0.17	0.17
	Injected Gas - H2S (mole fraction)	0.43	0.40	0.45	0.44	0.50	0.41	0.77	0.77
	Maximum Approved H2S (mole fraction)	0.70	0.55	0.4	0.4	0.50	0.37	0.85	0.85
	Maximun Approved WHIP (kPa)	10000	9760	10500	10500	9760	8000	10500	10500
	Maximum Approved Injection Rate (1000 m3/d)	21	228	69	69	114	22.5	391	391
	Total Approved Injection Volume (103 m3)	94200	416000	380000	16600	416000	82000	1876000	
	EPZ (km)	1.30	1.40	1.8	2	5.20	1.57	1.6	3.5

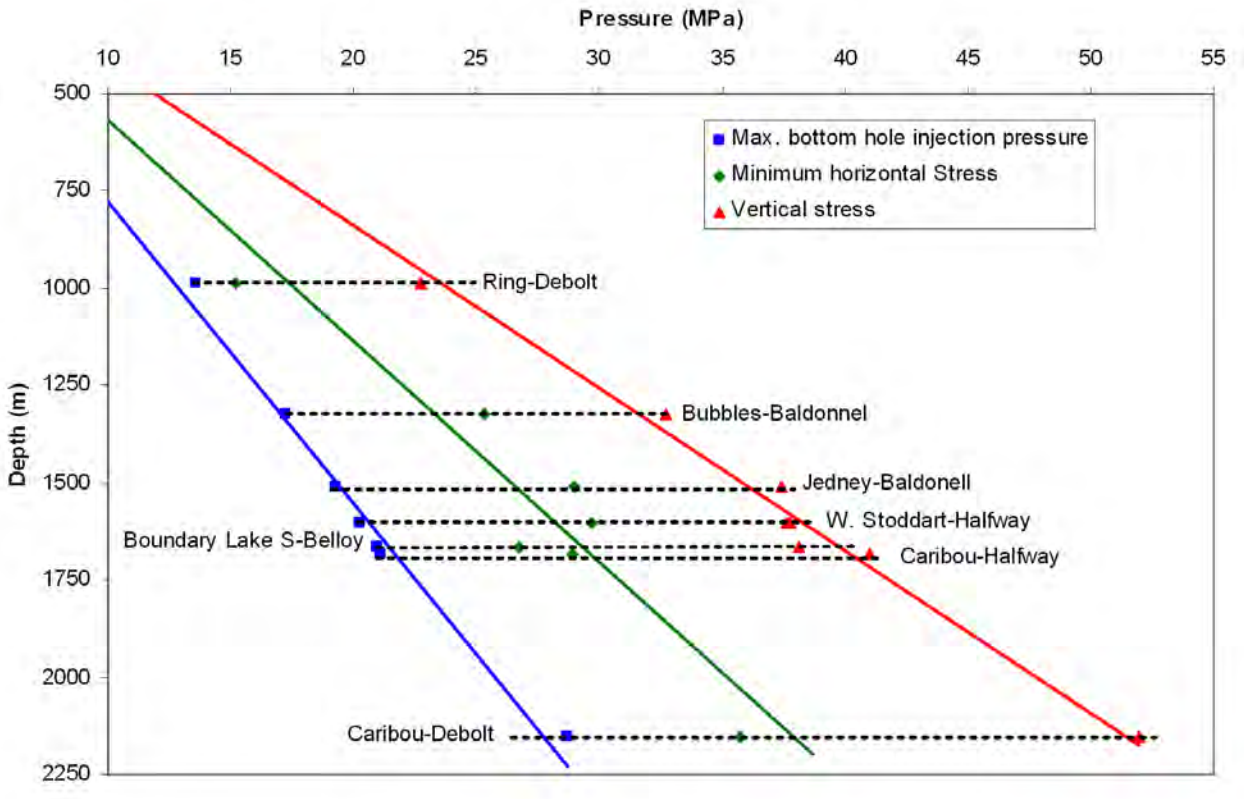

Figure 77. Maximum bottomhole injection pressure in relation to minimum horizontal stress and vertical stress at the various acid-gas injection sites in northeastern British Columbia.

6 Discussion

Based on the hydrogeological analysis of the acid-gas injection sites at local, regional and basin scales presented in the preceding chapters, the potential for acid gas migration and/or leakage from the injection sites in the northeastern British Columbia study area can be qualitatively assessed. Migration is defined in this report as flow along bedding within the same formation (reservoir or aquifer). Leakage is defined as upward flow to overlying formations and possibly to the surface. Both are considered in the context of the natural hydrogeological setting and of manufactured features, such as pressure drawdown, wells and induced fractures.

The fate of the injected acid gas in all seven cases is controlled by the in-situ properties of the gas and native fluid (reservoir gas or formation water). Table 14 presents the density and viscosity of the injected acid gas and native reservoir gas or formation water calculated for the initial in-situ conditions given in Table 13 (Adams and Bachu, 2002 Bachu and Carroll, 2004).

Table 14. Properties of native fluids and injected acid gas at in-situ conditions at the six acid-gas injection operations in the northeastern British Columbia area.

Fluid Property	Boundary	Bubbles		Caribou			Jedney		Ring	Stoddart
				Halfway	Debolt					
Native fluid	Water	Gas	Water[1]	Water	Gas	Water[1]	Gas	Water[1]	Water	Water
ρ (kg/m^3)	1096.3	91.6	1010.2	1001.5	120.1	992.7	93.9	1016.6	1040	1106.6
μ (mPa s)	0.66	0.015	0.48	0.46	0.017	0.39	0.016	0.46	0.6	0.65
ρ_{ag} (kg/m^3)	634.83	381.8		571.81	506.62		434.67		204.44	655.41
μ_{ag} (mPa s)	0.059	0.031		0.052	0.045		0.036		0.02	0.073
[2]max ρ_{ag} (kg/m^3)	691.1	579.7		656.6	647		655.3		615.2	709.5
[2]max μ_{ag} (mPa s)	0.069	0.053		0.064	0.065		0.063		0.055	0.084

[1] Water properties from the water leg underlying the gas cap in the reservoir.

[2] Values calculated for maximum approved bottomhole injection pressures.

The containment characteristics of the injected acid gas in the case of the seven injection sites in the northeastern British Columbia study area can be split into two categories:

1. injection into a deep saline aquifer: at Boundary Lake–South, Ring and Caribou–Debolt into the Permo–Carboniferous aquifer, and at West Stoddart and Caribou–Halfway into the Halfway–Doig aquifer.
2. injection into depleted gas reservoirs at Bubbles and Jedney in the Baldonnel Formation.

Although gas was produced intermittently for approximately one year at the Caribou–Debolt site before start-up of acid gas injection, production from the relatively small gas pool could not be maintained because the reservoir structure is mostly water-flushed. Therefore, the cumulative injected acid-gas is expected to take up more volume than the original gas cap, and the assessment of acid gas migration at the Caribou–Debolt site will be handled like migration in a regional aquifer.

The containment of the injected acid gas has to be assessed differently for aquifers and depleted hydrocarbon reservoirs. Depleted reservoirs usually have well defined vertical and lateral boundaries, within which the hydrocarbons were trapped initially and, after hydrocarbon production, the injected acid gas will be confined. Aquifers, although confined vertically by aquitards, generally have a large areal extent (defined in reservoir engineering as an infinite aquifer), and there are no lateral physical constraints to the flow of the injected acid gas.

6.1 Mathematical Expressions for the Lateral Migration of Acid Gas

In an aquifer, acid gas flows because of the interplay between the hydrodynamic drive imposed by injection, the natural hydrodynamic drive in the aquifer and buoyancy. The flow velocity of acid gas in a sloping aquifer can be written with respect to a reference density ρ_0 as (Bachu, 1995):

$$v = \frac{q}{\Phi} = -\frac{k_{rag}\rho_0 g}{\mu_g}\left(\nabla H_0 + \frac{\Delta\rho}{\rho_0}\nabla E\right) \qquad (1)$$

Where q is the specific discharge or Darcy flow velocity, Φ is porosity, g is the gravitational constant,

μ_g is acid gas viscosity, k_{rag} is the relative permeability of the acid gas, ρ_0 is the reference density (that of formation water), $\Delta\rho$ is the density difference between the acid gas and formation water, ∇H_0 is the hydraulic head gradient, and ∇E is the slope of the aquifer. The first term in brackets in relation (1), ∇H_0, represents the hydrodynamic drive, and the second term represents buoyancy. The relative importance of the two driving forces is expressed by the driving force ratio (Bachu, 1995):

$$DFR = \frac{\Delta\rho}{\rho_0} \cdot \frac{|\nabla E|}{|\nabla H_0|_h} \qquad (2)$$

where subscript *h* denotes the horizontal component of the hydraulic gradient.

The hydrodynamic drive in turn has two components, the first induced by injection and/or production (if present), and the second corresponding to the natural flow of formation water. The hydraulic gradient created by injection decreases logarithmically with distance from the well, such that in the vicinity of the well (near field) the hydrodynamic drive induced by injection dominates the flow, while away from the injection well (far field) it becomes negligible.

During injection of a nonaqueous fluid into an aquifer, the flow of the injected fluid in the near field of the well is driven by injection hydrodynamics and by the density contrast between the two fluids (buoyancy), and is controlled by the viscosity contrast (mobility) between the two fluids. The following dimensionless parameter

$$\Gamma = \frac{2\pi\Delta\rho\, g k k_{rb} B^2}{\mu_b Q} \qquad (3)$$

represents the ratio of buoyant versus viscous and pressure forces, and is an indication of the importance of buoyancy (density differences) in driving the flow of the injected acid gas (Nordbotten et al., 2004). In the above expression, porosity ϕ, permeability k (m^2) and thickness B (m) are aquifer characteristics, k_{rb} and μ_b (Pa·s) are, respectively, the relative permeability and viscosity of the formation water (brine) and express mobility (including viscous forces). Q (m^3/s) is the injection rate and expresses injection forces, and $\Delta\rho$ (kg/m^3) is the density contrast between the injected acid gas and formation water, expressing buoyant forces.

For Γ <0.5 hydrodynamic and viscous forces dominate and buoyancy can be neglected in the near field (Nordbotten et al., 2004). In this case, the maximum spread of the plume can be estimated by

$$r_{max}(t) = \sqrt{\frac{\mu_b V(t)}{\mu_g \Phi\pi B}} \qquad (4)$$

This situation will happen for 1) high injection rate (strong hydrodynamic force); 2) small density difference between the injected gas and formation water (low buoyancy); and 3) injection into a thin and/or low porosity and permeability aquifer. At the other end of the spectrum, buoyancy totally dominates for Γ >10. Such cases will occur for a combination of the following factors: 1) large density differences between the injected fluid and formation water; 2) injection into a thick aquifer characterized by high porosity and permeability; and 3) low injection rate (small hydrodynamic force). This estimate of r_{max} is based on a set of simplifying assumptions, such as no mixing and diffusion between the acid gas and aquifer brine, no gas dissolution in the brine, full saturation with either acid gas or brine in their

respective domains, no capillary effects, and a sharp interface between the two fluids (Nordbotten et al., 2004). These assumptions mostly lead to overestimates of the plume spread because, in reality, some plume mass will be lost through dissolution, diffusion and mixing. In addition, saturations less than 100% and capillary effects will retard the gravity override and plume spread. On the other hand, in a sloping aquifer buoyancy will distort the plume, which will advance faster updip and slower downdip. As a result, the plume will become elongated along dip, with the downdip edge of the plume closer to and the updip edge of the plume farther from the injection well than the radial plume for a horizontal aquifer.

For $0.5 < \Gamma < 10$, buoyancy, hydrodynamic and viscous forces are comparably important (Nordbotten et al., 2004). The change from one flow regime to another is not sharp, but gradual. These results are intuitive, because the injected acid gas will rise to the top of the aquifer (gravity override) if the aquifer has large enough permeability, porosity and thickness, and if the density difference is large enough; otherwise the plume will spread mostly laterally as a result of the strong hydrodynamic drive, being controlled by the mobility contrast between the two fluids.

After injection has ceased, the migration of acid gas is governed by the natural hydrodynamics in the aquifer and buoyancy according to Equation 1. The relative importance between hydrodynamic and buoyancy driving forces can be assessed with Equation 2. Solving Equation 1 estimates the lateral migration velocity and direction of acid gas in the aquifer. The velocity is a force vector from the vectorial summation of the hydrodynamic and buoyancy force vectors for homogeneous aquifer and fluid properties. Due to the naturally occurring variations in permeability and porosity, as well as local changes of aquifer slope and hydrodynamic gradient, which are difficult to fully capture over a large area, Equation 1 represents only an order of magnitude assessment of the regional direction and velocity of acid gas migration. Furthermore, during plume migration, acid gas will continuously encounter formation water, leading to the dissolution, diffusion and mixing of acid gas. As acid gas dissolves in formation water, it becomes heavier than unsaturated brine, and a process of brine-free convection will be set in motion (Lindeberg and Wessel-Berg, 1997). The heavier brine will drop to the bottom of the aquifer and migrate downdip, while brine not saturated with acid gas will replace it and encounter the acid gas plume. This process will continue as the plume migrates, ultimately leading to the total dissolution of the acid gas plume (McPherson and Cole, 2000). Also, acid gas will collect along the migration path in traps created by the uneven aquitard base at the top of the respective aquifer. In addition, not all of the injected acid gas will exist in a mobile phase, but some amounts will remain fixed in the pore space in the reservoir and along the flow path due to the effects of residual phase saturation (Holtz, 2003). As a result of all these processes (dissolution, dispersion, mixing, traps along the migration path and residual saturation) the acid gas plume will migrate a finite distance from the injection well. Modelling studies of the migration of CO_2 in the subsurface have shown that the maximum distance of plume migration is in the order of a few tenths of kilometres (Ennis-King et al., 2004).

In the following, the lateral migration of acid gas is assessed for the near and far fields of the various acid-gas injection sites that inject into aquifers, as well as the potential for acid gas leakage through overlying aquitards and wells along the flow path.

6.2 Injection into Regional Aquifers

Acid gas is injected into the Permo–Carboniferous aquifer at Boundary Lake–South, Ring, Caribou–Debolt and into the Halfway–Doig aquifer at West Stoddart and Caribou–Halfway. In the near field (injection well and its vicinity), pressures are actually higher than the initial aquifer pressure. Since water is only very slightly compressible, and its density is affected mostly by temperature and salinity and very little by pressure (Adams and Bachu, 2002, the density values presented in Table 14 for formation water are valid, even if pressure increases as a result of injection. However, for acid gas, whose properties are

strongly dependent on pressure, the density is highest at the well and decreases away from the well as pressure drops, toward the values presented in Table 14. The bottomhole injection pressure, although not measured, can be estimated based on the hydrostatic weight of the acid gas column in the well, assuming average gas density. As an upper limit, pressures always have to be below 90% of the fracturing pressure. Using this upper limit for pressure, the maximum acid-gas density at the injection well would be 691 kg/m^3 at Boundary Lake–South, 657 kg/m^3 at Caribou–Halfway, 710 kg/m^3 at West Stoddart and 615 kg/m^3 at Ring. Thus, at each site, the density contrast between the injected acid gas and formation water will likely vary from approximately 1:1.5 at the injection well to 1:2.5 at the boundary of the area of influence, and the viscosity contrast will vary correspondingly from 1:8 to 1:12. The Ring site is an exception, because under initial reservoir p/T conditions the injected acid gas exists in a vapour phase with a relatively low density and viscosity. Therefore, the density and viscosity contrast (1:5 and 1:30, respectively) between acid gas and formation water; hence, the effect of buoyancy can be expected to be large.

The average injection rates at surface pressure/temperature conditions to the end of 2003 were ~11 200 m^3/day at Boundary Lake–South, ~33,300 m^3/day at Caribou–Halfway, 29,100 m^3/day at Caribou–Debolt, ~82 500 m^3/day at West Stoddart and ~6500 m^3/day at Ring. Considering full saturation in the regions occupied respectively by the injected gas and formation water (i.e., $k_{rb}=k_{rag}=1$), values of $\Gamma = 2.7$, $\Gamma = 0.04$, $\Gamma = 0.03$, $\Gamma = 0.05$ and $\Gamma = 0.8$, respectively, are calculated (Equation 3, Table 15).

Table 15. Injection characteristics of acid-gas injection operations in aquifers.

Operation	Q (m^3/day)	V_{max} in-situ (10^{3}m^3)	Γ	R_{max}(m)	R_{op} (m)
Boundary Lake	11200	244	2.34	692	937
Caribou–Halfway	33300	1079	0.04	1684	4000
Caribou–Debolt	29100	1193	0.03	2343	3600
West Stoddart	82500	4337	0.04	2807	4400
Ring	6500	666	0.77	4016	2000

Q = average injection rate; V_{max} in-situ = maximum approved injection volume at reservoir conditions; R_{max} = maximum spread of acid gas plume during injection calculated by Equation 4; R_{op} = radius of influence gas plume given by operator.

Injection hydrodynamics and viscous forces dominate in acid gas injection at the Caribou–Debolt, Caribou–Halfway and West Stoddart sites, and Equation 4 gives an accurate estimate of the maximum plume spread. Low-injection rates at Boundary Lake–South and Ring and low acid-gas density at Ring are the main reasons why buoyancy cannot be neglected in estimating the plume spread. Comparing results from Equation 4 with more elaborate, semi-analytic solutions indicates that Equation 4 underestimates the plume spread by up to 15% for cases where $0.5 < \Gamma < 3.0$ (Characteristics of Acid-Gas Injection Operations in Western Canada, Final Report, S. Bachu et al., prepared for the Acid Gas Management Committee, 2004). Considering uncertainties in other parameters that affect plume spread, like permeability distribution, porosity and acid-gas properties, a 15% error due to the neglect of buoyancy effects is deemed acceptable in an order-of-magnitude analysis of long-term acid-gas migration. For maximum volumes of acid gas at the end of injection, the respective maximum radii of plume spread estimated using Equation 3 at the various injection sites ranged from 690 to 4000 m. Values for the maximum radius of influence calculated by the various operators using various methods are shown for comparison. With the exception of the Ring operation, the values given by operators are actually more conservative and up to 50% higher. The maximum extent of plume spread during injection will be used as a starting point for the assessment of acid gas migration in the far field of the respective injection wells at each injection site.

6.2.1 Boundary Lake–South

Injection of acid gas at Boundary Lake–South commenced in 1996. In the far field, away from the injection well, the natural flow in the aquifer becomes dominant over the hydrodynamic drive caused by injection. In the Boundary Lake–South area the hydraulic gradient in the Permo–Carboniferous aquifer is approximately ∇H_0 = 0.23% (2.3 m/km), changing from 100° SE at the injection site to 120° SE at the regional scale (Figure 78). The slope of the top of the aquifer is ∇E = 0.75% (7.5 m/km) at 28° to the northeast. Considering the density contrast between the injected acid gas and formation water (Table 14), the driving force ratio (DFR) is 1.4, which indicates that buoyancy is slightly stronger than the natural hydrodynamic drive in the aquifer. This means the plume of acid gas will migrate generally to the northeast at ~70°. On the basis of the permeability and porosity values for the Permo–Carboniferous aquifer (Table 8) and of acid gas and brine properties (Table 14), an order-of-magnitude analysis shows that, once outside the cone of influence around the injection well, the velocity of the updip migrating acid gas is on the order of 25 m/year or less, depending on relative permeability of acid gas k_{rag}. The limit of the Montney aquitard, beyond which the Permo–Carboniferous aquifer subcrops below the Bullhead aquifer, is located at a distance of 100 km from the injection well along the potential acid-gas migration path. Even in the unlikely case that the acid gas plume was not reduced by dissolution, dispersion, residual gas saturation and trapping of the acid gas along the migration path, it would take in the order of 5000 years before acid gas could be detected in the Bullhead aquifer. Once in the Bullhead aquifer, the acid gas theoretically would have to move farther updip along the top of the aquifer for another 300 km (~15 000 years) before it would reach the ground surface in the outcrop area of the Bullhead aquifer.

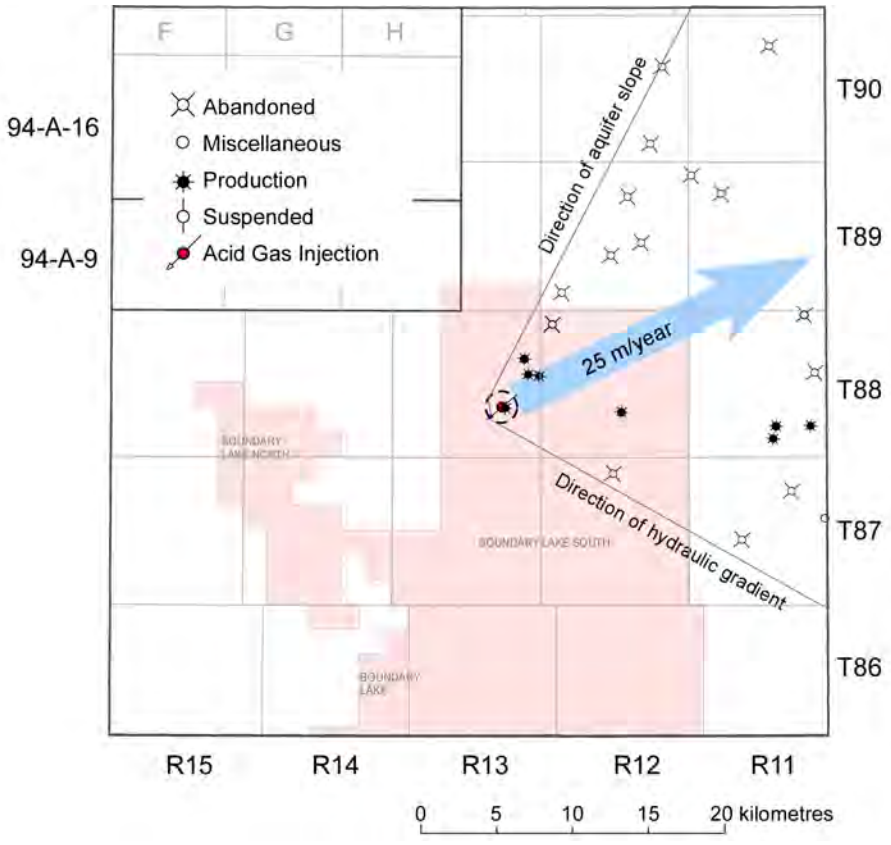

Figure 78. Assessment of long-term acid-gas migration at Boundary Lake–South, showing location and status of wells along the potential migration path and administrative boundaries of gas fields (in red). The blue arrow represents the inferred flow direction of separate-phase acid-gas from the vectorial summation of buoyancy and hydrodynamic drive (Equation 1).

The potential vertical migration of acid gas into formations overlying the Belloy Formation are upward leakage through a) windows, natural faults and/or fractures in the Montney aquitard, or b) induced fractures and/or improperly completed and/or abandoned wells. The Boundary Lake–South injection site is on the northern flank of the Fort St. John Graben structure, and there are faults that caused thickening of Permian strata near the injection well. However, there is no indication that any of these syn-sedimentary faults continue into the Montney aquitard. The hydrogeological assessment has shown that the Montney aquitard acts as an effective barrier to vertical flow on a local and regional scale. The succession of additional regional aquitards (Charlie Lake, Fernie, Wilrich–Fort St. John) farther up in the stratigraphic column would effectively prevent any leakage to shallow aquifers or the ground surface, even if the Montney aquitard were weakened locally by production-induced geomechanical stress.

As with acid gas injection into depleted reservoirs, wells that penetrate the injection horizon along the potential flow path of the acid gas in the Permo–Carboniferous aquifer (Figure 78) represent possible leakage conduits to overlying formations. Figure 79 shows histograms of status, age and time of abandonment for these well. Of the 34 wells, almost half were drilled in the last four years. Eight wells currently produce from the overlying Triassic and one from the Upper Cretaceous Belly River Group. There is no production from the Permo–Carboniferous in this area. There are 18 abandoned wells located along the potential migration path and seven wells are characterized as 'miscellaneous,' which in this case mostly refers to 'spudded and cased.' The wells were abandoned relatively evenly over the past decades, seven in the last four years.

6.2.2 West Stoddart

At West Stoddart, acid gas is injected through two closely spaced wells into the Halfway–Doig aquifer since 1998. With an anticipated maximum injection volume of 1876 x 10^6 m^3, it is the largest acid-gas injection operation in the Alberta Basin.

The direction of formation water flow in the Halfway–Doig aquifer is east-northeastward at 80° (Figure 80), and the hydraulic gradient is approximately ∇H_0 = 0.23% (2.6 m/km). The slope of the top of the aquifer is ∇E = 0.5% (5 m/km) at 40° to the northeast. The driving force ratio of DFR = 0.75 indicates that the natural hydrodynamic drive in the aquifer is slightly stronger than buoyancy. As a result, acid gas will migrate northeastward at approximately 65°. Based on the porosity and permeability values for the Halfway–Doig aquifer (Table 6) and of acid gas and brine properties (Table 14), an order-of-magnitude analysis shows that the velocity of the updip migrating acid-gas in the far field of the injection well is approximately 4 m/year or less.

The subcrop edge of the Halfway–Doig aquifer, beyond which it is in direct hydraulic communication with the Bullhead aquifer, is located at a distance of approximately 100 km from the injection well along the potential acid-gas migration path. Dissolution, dispersion, residual gas saturation and trapping of the acid gas along the migration path make it unlikely that the extent of the acid gas plume would reach the Bullhead aquifer. The Halfway transitions from a regionally extensive, relatively continuous tighter sand in the west and southwest to more discontinuous and segregated higher porosity accumulations in the east and northeast, which would inhibit lateral migration prior to reaching the Halfway subcrop edge. Also, the Buick Creek and Rigel oil fields, which are located along the potential migration path approximately 20 km northeast of the injection wells (Figure 80), currently produce from the Halfway Formation. Therefore, most of the updip-migrating acid gas in the Halfway–Doig aquifer would be captured in the production wells. After depletion of the Buick Creek and Rigel oil fields, it would hypothetically take in the order of 25 000 years before acid gas reaches the subcrop edge. Once in the Bullhead aquifer, the acid gas will have to move farther updip along the top of the aquifer for another 350 km (~90 000 years)

a.

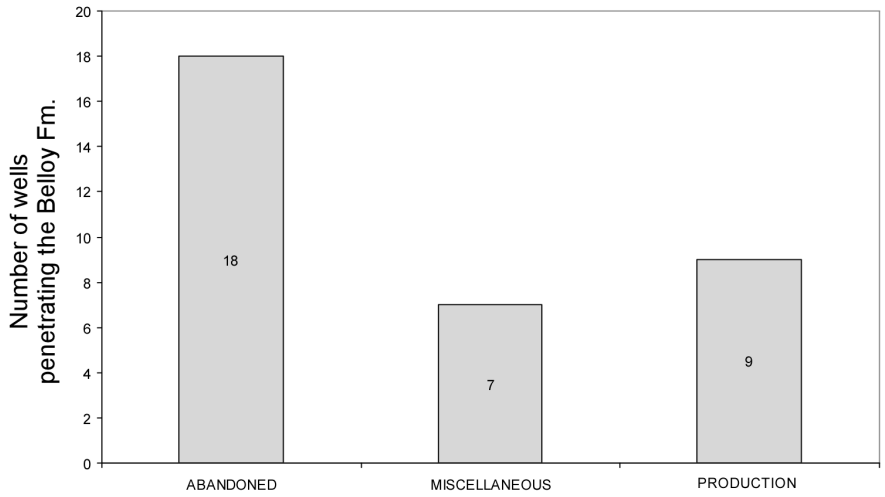

b.

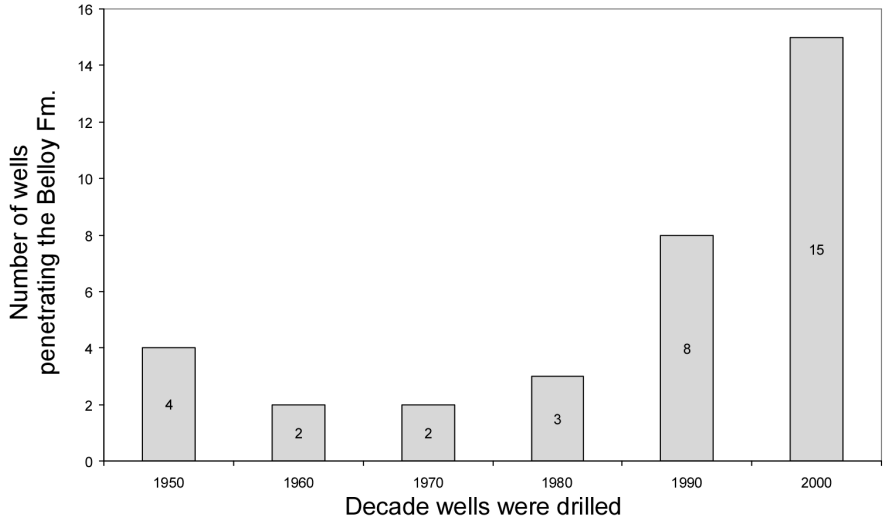

c.

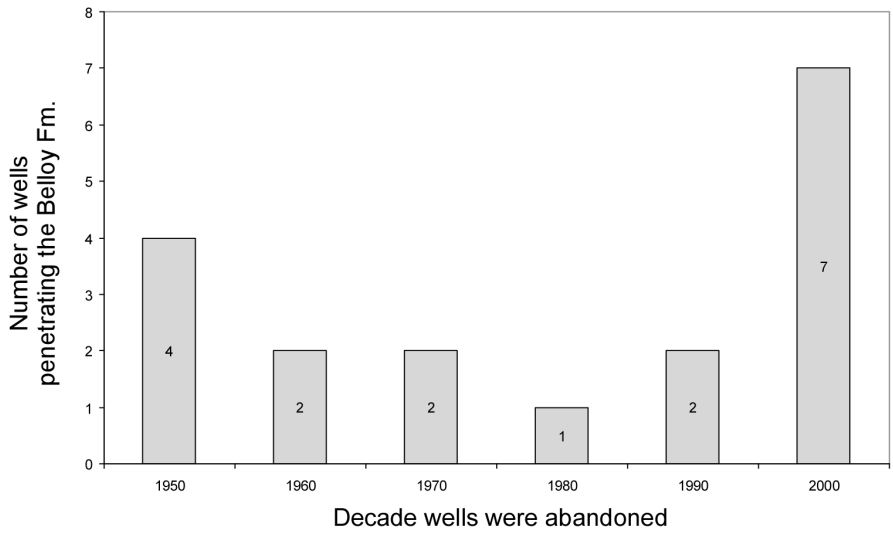

Figure 79. Histograms for wells that penetrate the Permo–Carboniferous aquifer in the Boundary Lake–South area, showing a) well status, b) time of drilling, and c) time of abandonment.

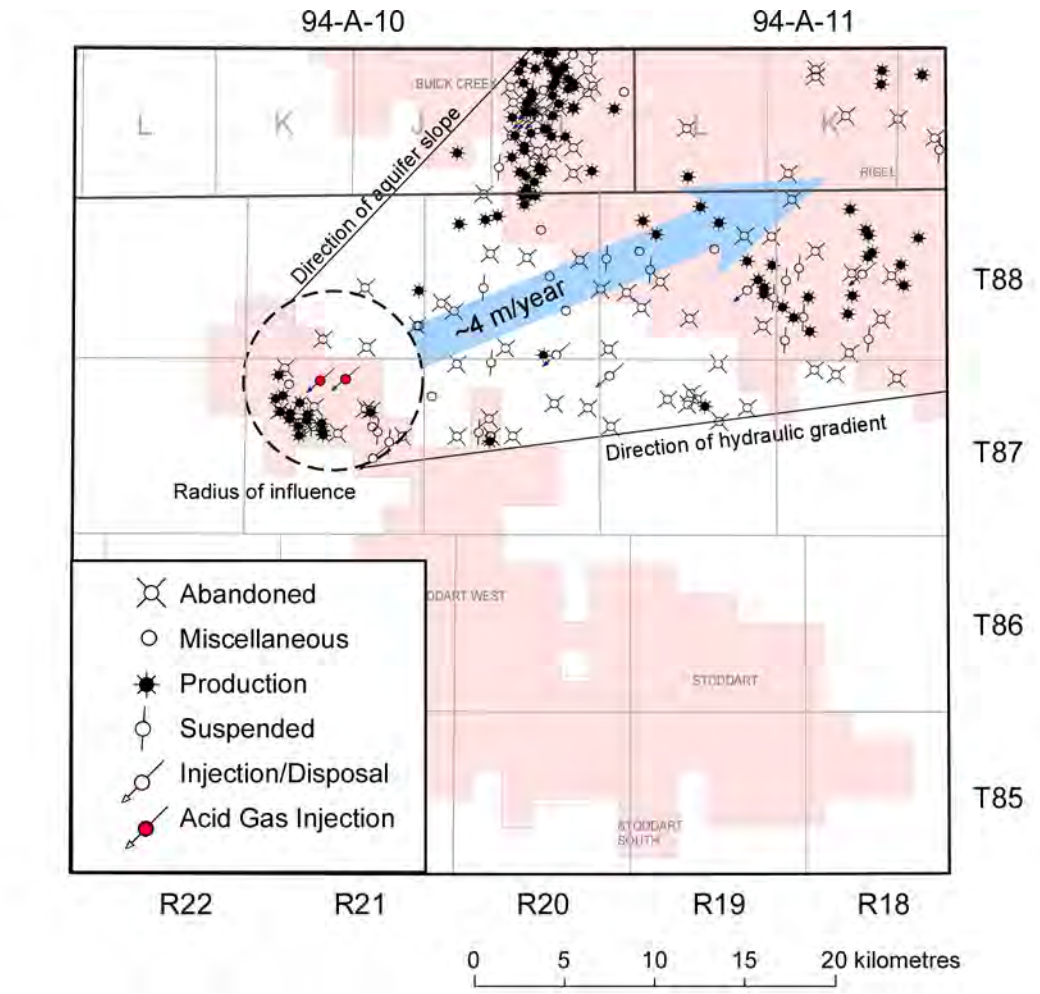

Figure 80. Assessment of long-term acid-gas migration at Stoddart, showing location and status of wells along the potential migration path and administrative boundaries of gas fields (in red). The blue arrow represents the inferred flow direction of separate-phase acid-gas because of the vectorial summation of buoyancy and hydrodynamic drive (Equation 1).

before it will reach the ground surface in the outcrop area of the Bullhead aquifer. It is not realistic that this long migration path will ever be completed because of dissolution, dispersion, residual gas saturation and trapping of the acid gas along the migration path.

There are no known major faults propagating through the sedimentary succession in the Stoddart area. Therefore, the only possibility of vertical migration of acid gas into aquifers overlying the Halfway Formation through the natural system is upward leakage through windows in the Lower Charlie Lake aquitard. Evaporites and siltstones in the Lower Charlie Lake aquitard act as an effective barrier to vertical flow, as shown in the local and regional-scale hydrogeological assessments. The succession of additional regional aquitards (Fernie and Wilrich–Fort St. John) farther up in the stratigraphic column would effectively prevent any leakage to shallow aquifers or the ground surface, even if the Lower Charlie Lake aquitard were breached by production-induced fractures.

More than 200 wells, the majority drilled in the last 15 years, penetrate the injection horizon along the potential flow path of the acid gas in the Halfway aquifer (Figure 80), which represent possible leakage conduits to overlying formations. Figure 81 shows the well statistics for status, age and time

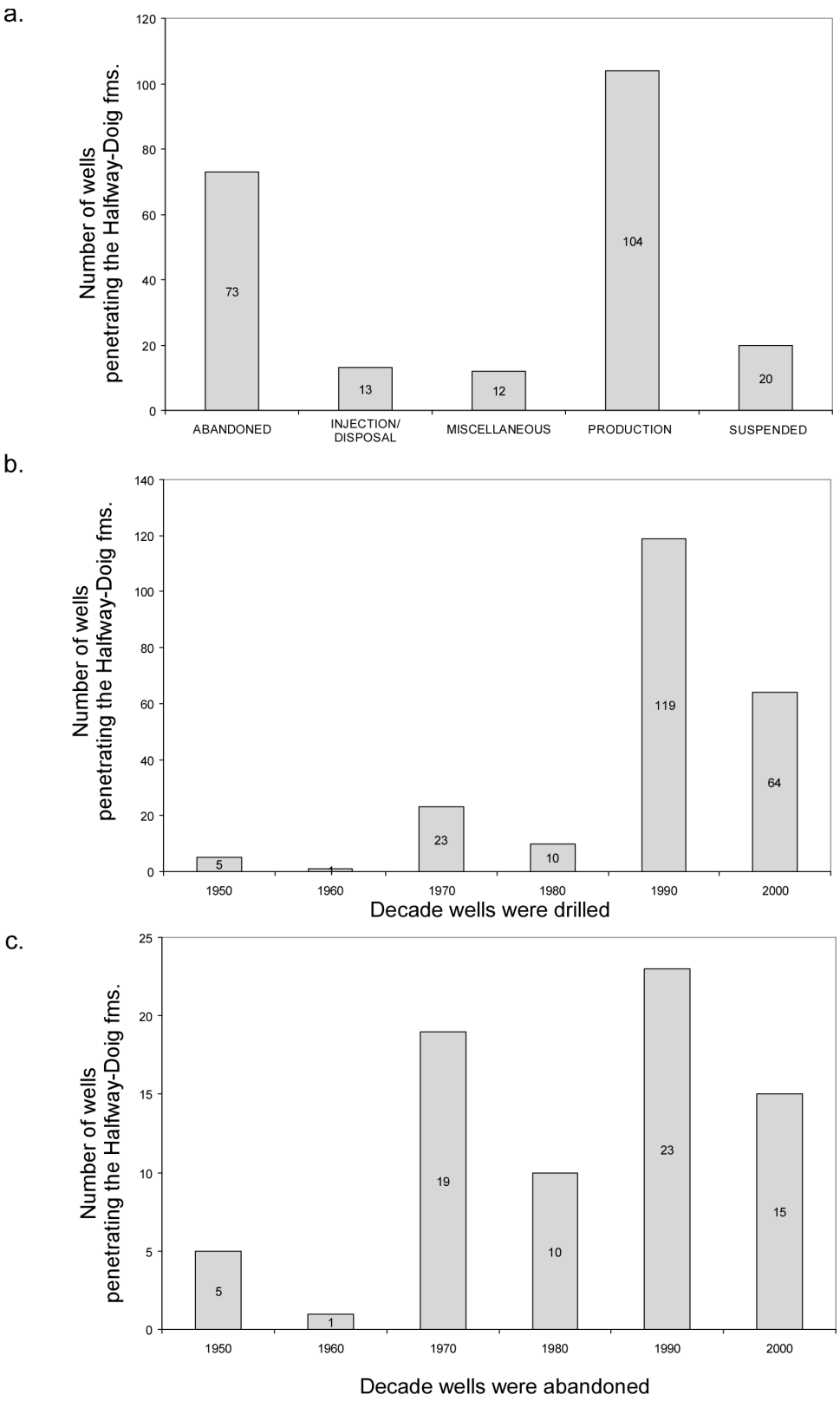

Figure 81. Histograms for wells that penetrate the Halfway–Doig aquifer along the potential migration path of acid gas from the Stoddart–Halfway site, showing a) well status, b) time of drilling, and c) time of abandonment.

of well abandonment. Of the 104 producing wells, 15 wells, located within a radius of 4 km from the injection wells, currently produce oil from 'channel' sands in the upper part of the Doig Formation. On a regional scale, these sandstones are in contact with sandstones of the overlying Halfway Formation, and together form the Halfway–Doig aquifer. Locally, however, siltstones form a seal above the Doig channel sandstones, thereby forming a stratigraphic trap for the oil reservoirs in the West Stoddart Field (Harris and Bustin, 2000). Currently there are insufficient data to assess whether acid gas injection into the Halfway Formation at Stoddart will affect oil production from the Doig Formation. The oil-producing wells represent potential pressure sinks for the injected acid gas, and only chemical analyses of the produced oil could show a change in acid gas content with time, indicating breakthrough of the injected acid gas. The remainder of the producing wells are located in the Buick Creek (Lower Halfway/Doig) and Rigel oil fields, mainly producing from the Halfway Formation as discussed above. Besides the 2 acid-gas injection wells, there are 11 other wells that dominantly dispose of or inject water into the Halfway Formation in the Buick Creek and Rigel fields. Additional production occurs from the overlying Charlie Lake Formation, Bullhead Group and Notikewin Formation. Six of the 73 abandoned wells along the potential acid-gas migration path were abandoned in the 1950s and 1960s. The majority of wells were abandoned between 1979 and 2004 when more stringent well abandonment regulations were in place.

6.2.3 Ring

At Ring, acid gas mixed with water has been injected into the Permo–Carboniferous aquifer since 1999. Due to the pressure-temperature conditions in the reservoir, the injected acid gas exists in a gaseous phase and will form initially a gas cap at the top of the aquifer. The injection interval is located near the convergence of two counteracting flow systems, one northeastward (updip), the other southwestward (downdip). As a result, formation water flow at the Ring site is toward the northwest at 58°, with a relatively low hydraulic gradient ∇H_0 = 0.02% (0.2 m/km) (Figure 82). The slope of the aquifer is∇E = 0.63% (6.3 m/km) at 77° to the northeast. The fact that the acid gas is in gaseous phase results in a large density difference between acid gas and formation water. Consequently, buoyancy will be the dominant flow-driving mechanism for acid gas migration (DFR = 25), and the flow direction of the acid gas plume will be approximately 75° to the northeast, at a velocity in the order of 17 m/year.

Although the migration distance of the acid gas plume is limited by dissolution, dispersion, residual gas saturation and trapping of the acid gas along the migration path, it is possible that the plume will reach the Carboniferous subcrop edge, 30 km northeast of the injection site, and migrate into the Cretaceous Bullhead aquifer. The thick Wilrich–Fort St. John aquitard that overlies the Bullhead aquifer will prevent any vertical leakage of acid gas to shallower aquifers. Currently, there is production from the Debolt Formation from seven wells in the Fontas Field (Figure 82) in the subcrop area. These wells, as long as they are actively producing, would gather the largest part of any updip-migrating acid gas. Farther lateral updip migration within the Bullhead aquifer will only lead to further dissolution/trapping/dispersion of the acid gas, and it is unlikely that significant concentrations of acid gas will be detected more than 50 km away from the injection site. The nearest outcrop of the Bullhead aquifer in the updip direction is approximately 300 km to the northeast and covering that distance theoretically would take an acid gas plume in the order of 50 000 years.

Sixty-six wells, the majority drilled in the 1990s, penetrate the injection horizon along the potential flow path of the acid gas in the Permo–Carboniferous aquifer (Figures 82 and 83), and represent possible leakage conduits to overlying formations. Figure 83 shows the well statistics for status, age and time of well abandonment. Except for the seven wells in the Fontas Field in the northern corner of the study area, there are no wells producing from the Debolt Formation in the Ring–Pedigree Field. Production in the Ring–Pedigree Field is mainly from the overlying Bullhead Gething–Montney interval (19 wells) and

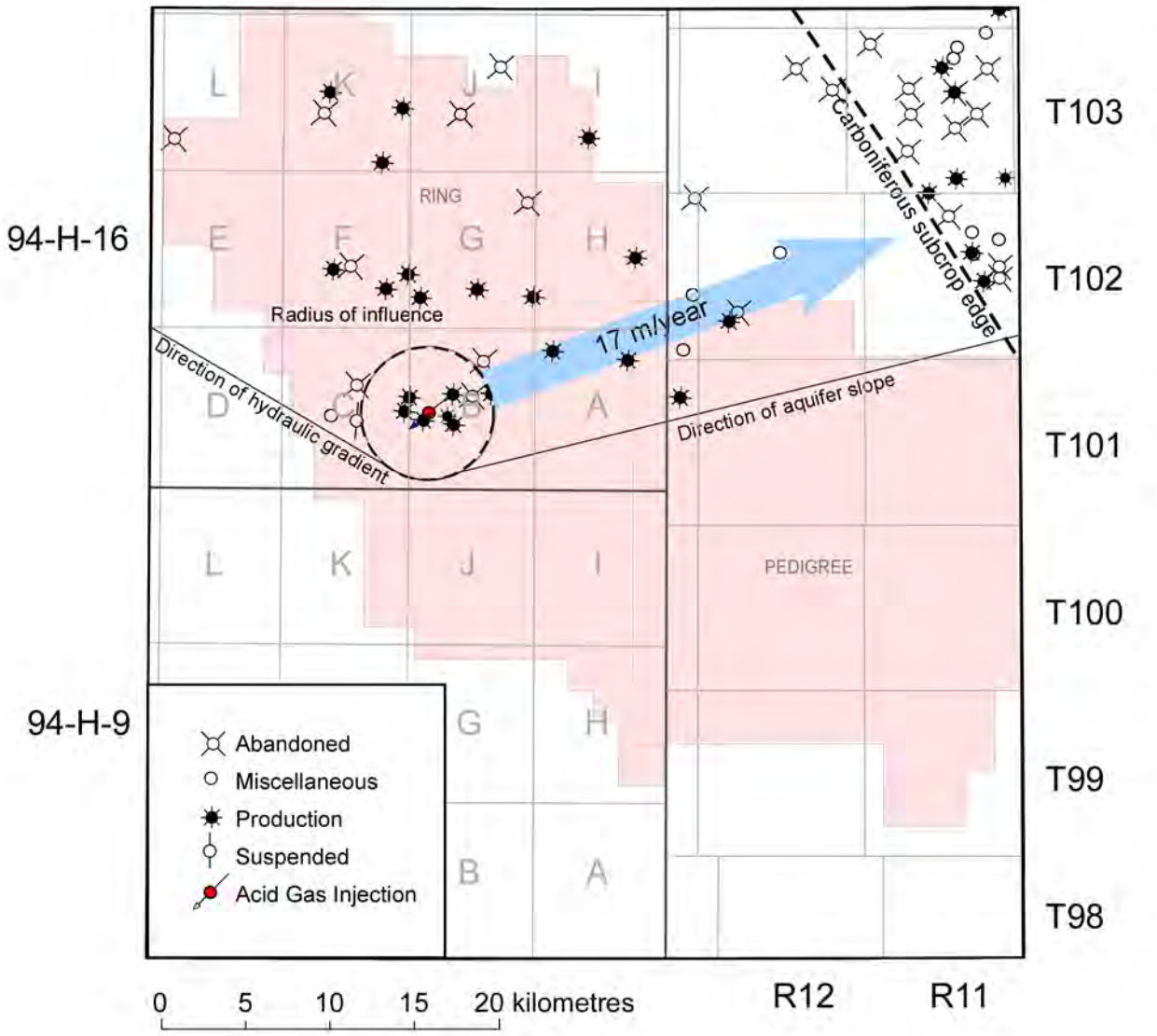

Figure 82. Assessment of long-term acid-gas migration at Ring, showing location and status of wells along the potential migration path and administrative boundaries of gas fields (in red). The blue arrow represents the inferred flow direction of separate-phase acid-gas as a result of the vectorial summation of buoyancy and hydrodynamic drive (Equation 1).

from the underlying Devonian Slave Point Formation (two wells). More than half of the 25 abandoned wells were abandoned in the last 15 years, when stringent well abandonment regulations were in place.

6.2.4 Caribou

At Caribou, acid gas injection into the Halfway Formation commenced in 1997. A second injection well was added in 1998, injecting into the Debolt Formation.

The direction of formation water flow in the Halfway–Doig aquifer is east-southeastward at 85°, and the hydraulic gradient is approximately ∇H_0 = 1.35% (13.5 m/km) (Figure 84). The slope of the top of the aquifer is ∇E = 0.74% (7.4 m/km) at 45° to the northwest. The hydraulic gradient is relatively large due

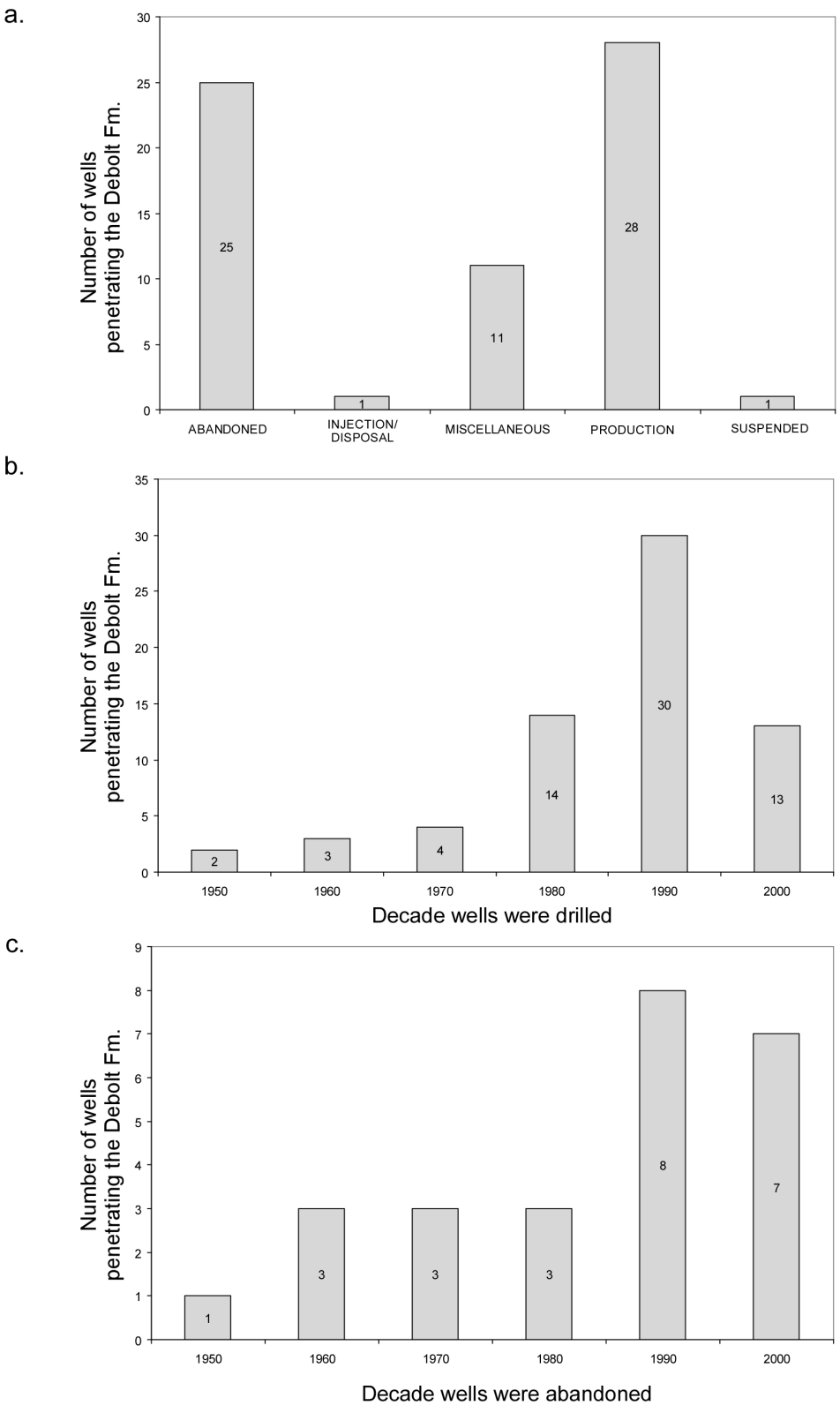

Figure 83. Histograms for wells that penetrate the Permo–Carboniferous aquifer in the Ring area, showing a) well status, b) time of drilling, and c) time of abandonment.

to the strong topographic drive on formation water flow exerted by the drop-in, ground surface elevation from the Rocky Mountains toward the east. Consequently, the driving force ratio of DFR = 0.23 indicates that the natural hydrodynamic drive in the aquifer is stronger than buoyancy, and acid gas will migrate dominantly east-southeastward at approximately 75° at a velocity in the order of 1 m/year (Figure 84). It would take approximately 100 000 years for any acid gas to reach the subcrop of the Halfway–Doig aquifer, which is located at a distance of approximately 100 km from the injection well. Besides dissolution, dispersion and residual saturation, the undulating surface of the top of the Halfway–Doig aquifer forms many traps along the potential flow path of the acid gas, making it improbable that any acid gas will ever reach the subcrop edge.

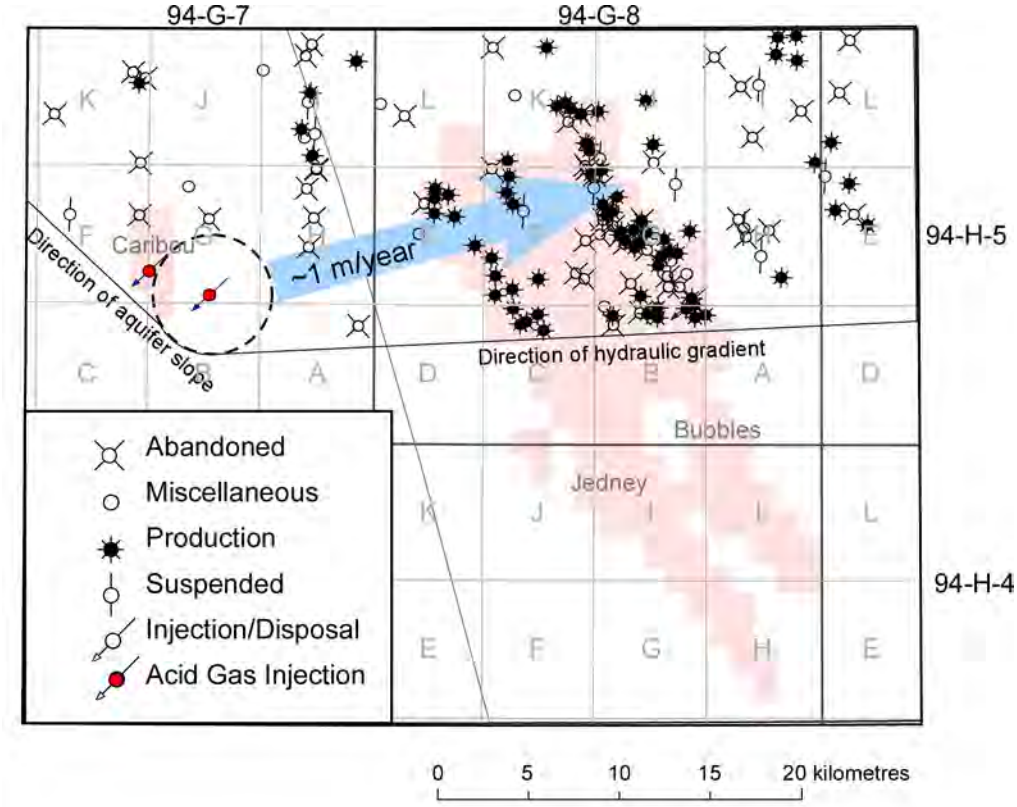

Figure 84. Assessment of long-term acid-gas migration at Caribou–Halfway, showing location and status of wells along the potential migration path and administrative boundaries of gas fields (in red). The blue arrow represents the inferred flow direction of separate-phase acid-gas as a result of vectorial summation of buoyancy and hydrodynamic drive (Equation 1).

The local and regional hydrogeological assessment has shown that the lower part of the Charlie Lake Formation forms an effective aquitard at the top of the Halfway–Doig aquifer, preventing natural vertical leakage to overlying aquifers. Low-permeability sediments in the Fernie Group and Fort St. John Group provide additional vertical barriers to flow to shallow aquifers containing potable groundwater or the ground surface.

There are 155 wells in the vicinity and along the potential migration path for the injected gas, of which the majority (89 wells) was drilled in the last 5 years (Figures 85 a, b). Most of these wells are within the Jedney and Bubbles gas fields, approximately 20 km from the injection well in the general migration path of the injected acid gas. Of the 76 currently producing wells (Figures 84, 85), 41 wells produce from

a.

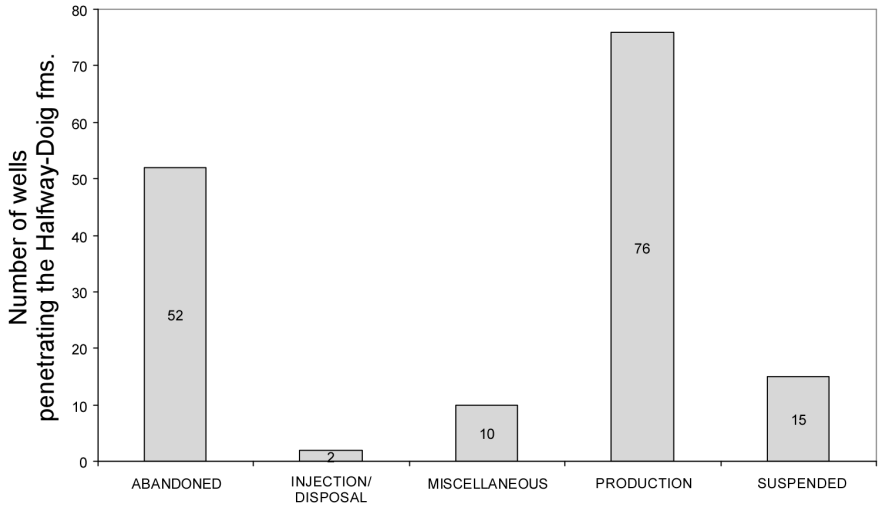

b.

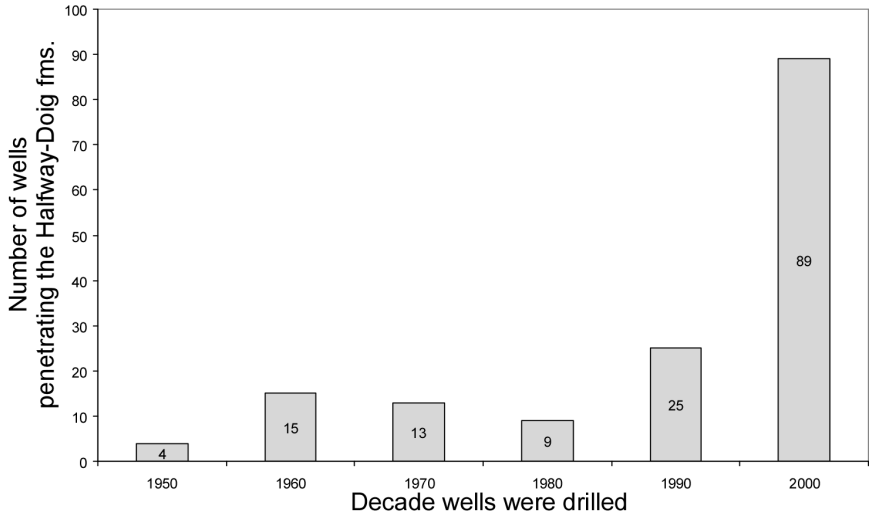

c.

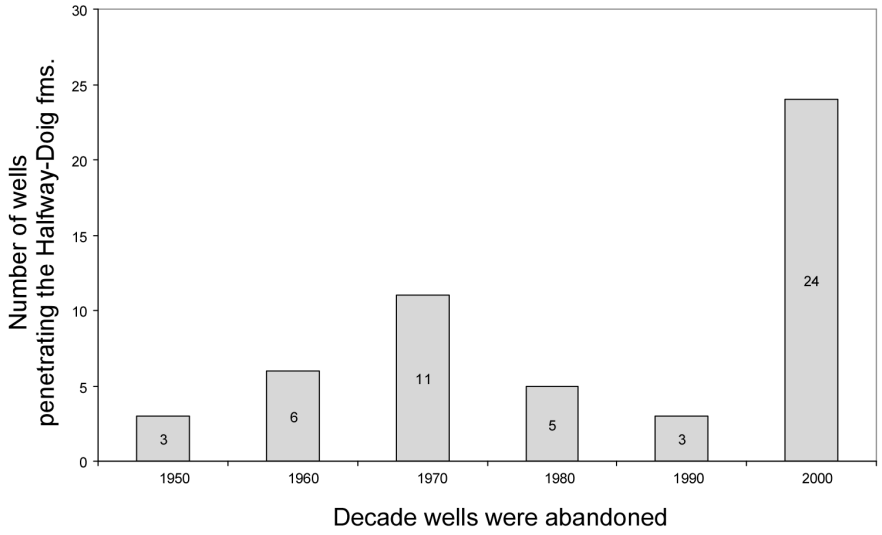

Figure 85. Histograms for wells that penetrate the Halfway–Doig aquifer along the potential migration path of acid gas from the Caribou–Halfway site, showing a) well status, b) time of drilling, and c) time of abandonment.

the Halfway–Doig interval (4 wells in Jedney, 31 wells in Bubbles and 5 wells in other areas). If the acid gas plume has not dissolved by then, increased acid-gas concentrations should be first detected in the Jedney production wells, which present a sink for migrating fluids due to the production-induced pressure drawdown around the well. There are also 15 suspended wells, 10 miscellaneous wells and 52 abandoned wells within the potential migration path of the injected gas. Abandonment occurred mainly in the 1970s and after 2000 (Figure 85c).

It is difficult to establish the exact flow direction in the Permo–Carboniferous aquifer in the vicinity of the Caribou–Debolt injection site because data are sparse and hydraulic head gradients had to be interpolated from the regional-scale interpretations for flow west of the deformation front. The a-30-G well (acid-gas injection well) produced from November 1988 to November 1990. An increase in water production led to the shut-in of the well. The increasing water content after continuous production and the fact that reservoir pressures recovered relatively fast after production stopped, indicates that the reservoir interval in the Debolt Formation is in good hydraulic communication with underlying Permo–Carboniferous aquifer. In terms of migration, the acid gas at Caribou in the Debolt Formation will be confined initially to the injection reservoir by the small fold structures. After the reservoir is filled beyond its spill point, acid-gas migration will be governed by the hydrodynamics in the Permo–Mississippian aquifer and buoyancy. Near the injection site the flow of formation water is initially toward the southeast, but changes after approximately 10 km to the regional 85° east-northeastward flow direction. The magnitude of the hydraulic gradient is approximately $\nabla H_0 = 0.3\%$ (3 m/km) (Figure 86). The slope of the top of the aquifer is $\nabla E = 0.9\%$ (9 m/km) at 35° to the northeast. The driving force ratio (DFR) is 1.5 indicating that buoyancy is 50% stronger than the natural hydrodynamic drive in the aquifer, and acid gas will migrate dominantly northeastward at approximately 55°. The migration velocity based on local porosity and permeability values in the Permo–Carboniferous is in the order of 14 m/year. The migration velocity is probably significantly less toward the northeast along the potential migration path, because geological and hydrogeological data indicate the permeability of the Debolt Formation is relatively low in the area of the Rocky Mountain deformation front. Therefore, lateral migration of acid gas along the Permo–Carboniferous aquifer up to the Carboniferous subcrop edge (approximately 150 km from the injection well) is very unlikely considering the low aquifer permeability and processes like dissolution, dispersion, residual saturation and trapping of acid gas.

The Montney Formation forms a thick, confining aquitard at the top of the Permo–Carboniferous aquifer, and the hydrogeological assessment showed no indications for the possibility of leakage to overlying aquifers. Additional barriers preventing vertical leakage to shallow aquifers or the ground surface are formed by the succession of the Lower Charlie Lake, the Fernie and the Wilrich–Fort St. John aquitards. Only one other well, 3.75 km north of the injection well and abandoned in 2002, penetrates the Debolt Formation in the Caribou Field and is close to the predicted radius of influence of acid gas injection (Figure 86). Thirteen additional wells, mainly drilled in the last 20 years and half of them abandoned, penetrate the Debolt Formation along the potential migration path of the injected acid gas, including the Caribou–Halfway injection well that was plugged back and re-completed in the Halfway Formation (Figures 86 and 87). The nearest well along the potential acid-gas migration path that actively produces from the Debolt Formation is located within the area of the Bubbles gas field, approximately 30 km east of the injection well.

6.3 Injection into Depleted Gas Reservoirs

In the case of the two gas reservoirs, Bubbles and Jedney, since the pressure at injection start-up (6000 kPa and 8000 kPa, respectively) was, and the current pressure is still below the initial reservoir pressure (~11 000 kPa in both cases), the actual density and viscosity of the native gas and injected acid gas are

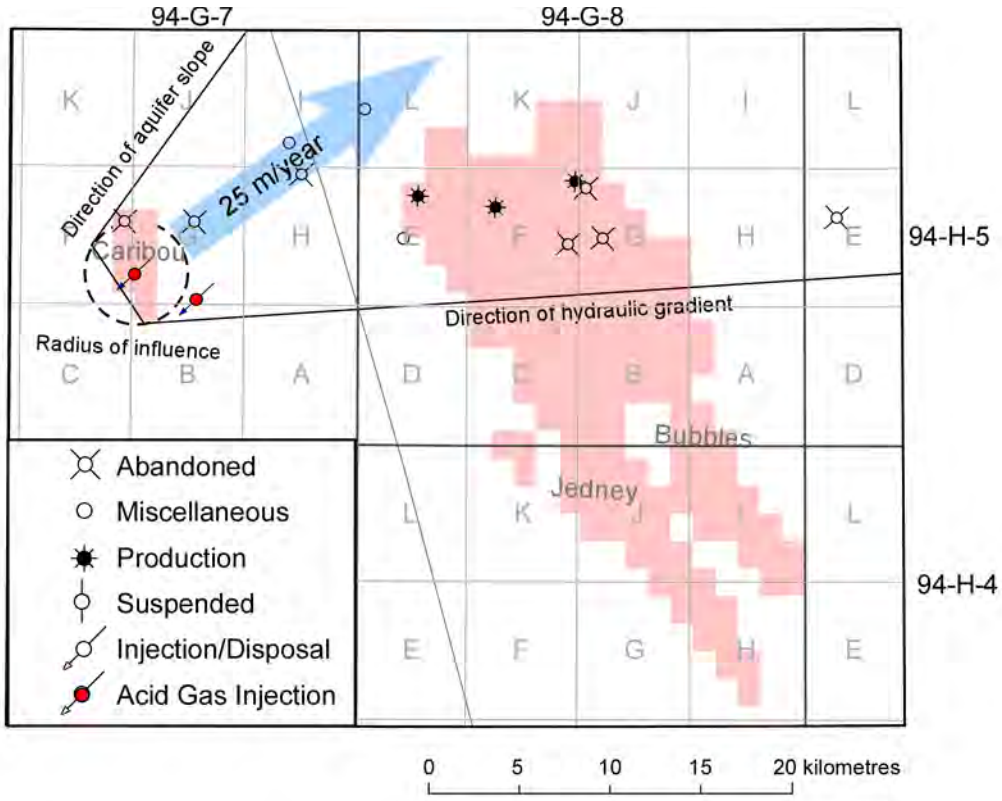

Figure 86. Assessment of long-term acid-gas migration at Caribou–Debolt, showing location and status of wells along the potential migration path and administrative boundaries of gas fields (in red). The blue arrow represents the inferred flow direction of separate-phase acid-gas as a result of the vectorial summation of buoyancy and hydrodynamic drive (Equation 1).

lower than the values presented in Table 14. For all of these gases they will continue to increase toward the values presented in Table 14 as the reservoir is pressured up during injection. However, the gases compress directionally in the same way (although not proportionally), such that the values presented in Table 14 are a good indication of the large density and viscosity contrast between them. The injected acid gas is about four times heavier and twice more viscous than the reservoir gas. If the acid gas is injected at the bottom of the reservoir, it will stay there and will gradually fill up the reservoir, chasing the residual natural gas to the top of the reservoir. Since both gases are nonwetting fluids, no capillary forces affect the flow of the two gases. This method can actually be used to produce additional gas (enhanced gas recovery), but some acid gas would be recovered at the producing well and would have to be stripped out. If the acid gas is injected at a level higher than the bottom of the reservoir, the acid gas will flow to the bottom of the reservoir, with a similar effect. There will be some gas dissolution in the underlying formation water at the gas-water contact, but the amount of acid gas that will dissolve is going to be small since the formation water has already a very high salinity. In addition, once the top water layer is saturated with acid gas no additional dissolution will occur.

Acid gas injection at Jedney and Bubbles started in 1996 and 1997, respectively. In terms of migration, the acid gas at these sites will be confined initially to the injection reservoir by the fold structures that originally trapped the natural gas. Lateral, updip migration would only be possible, if the reservoir is filled beyond its spill point. The respective reservoirs that are the target for acid gas injection are gas pools that are part of the larger Jedney and Bubbles gas fields (Figure 88). Currently, there is still production from the Baldonnel Formation in these fields (28 wells in Bubbles, 40 wells in Jedney).

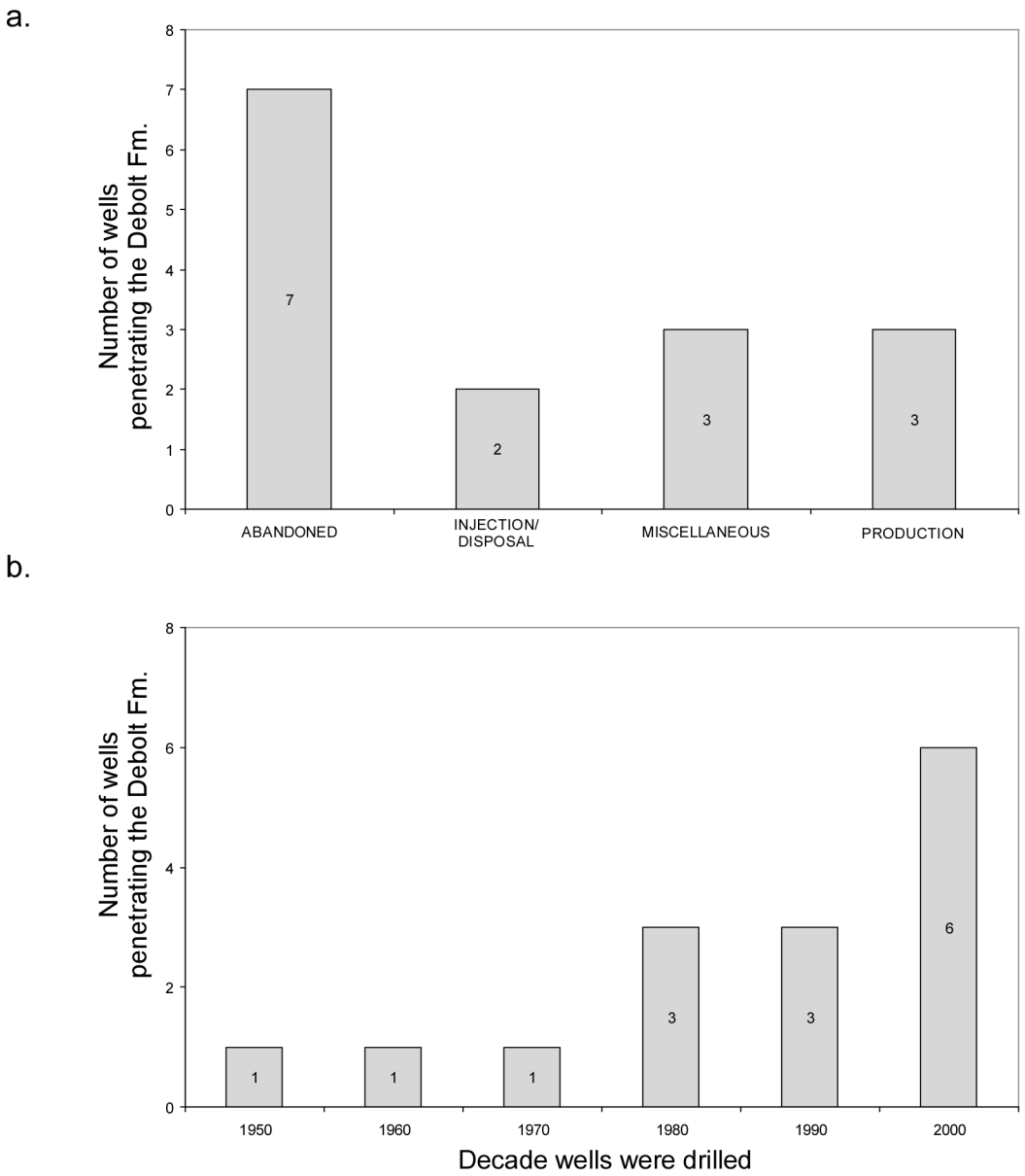

Figure 87. Histograms for wells that penetrate the Permo–Carboniferous aquifer along the potential migration path of acid gas from the Caribou–Debolt site, showing a) well status and b) time of drilling.

Production from the Baldonnel Formation started in 1959 (Figure 89). According to interpretations of production and pressure drawdown data by the operator of the Bubbles and Jedney acid-gas injection operations, the Bubbles and Jedney gas fields consist of different pools in the Baldonnel Formation, which are hydraulically separated from each other by lateral permeability barriers (Figure 88). The decline in reservoir pressure, due to gas production from the Baldonnel Formation in the Bubbles and Jedney gas fields, is shown in Figure 89. Hydrogeological data suggest that the Baldonnel gas pools are pressure-supported, at least partially, by an underlying aquifer. Consequently, the acid gas may migrate toward producing wells in the vicinity of the injection well as a result of the hydrodynamic drive created between an injecting well (high pressure) and producing wells (low pressure). Results of a reservoir modelling study submitted by the operator of the Bubbles injection site, Westcoast Gas Services

(WCGS), predicts that a concentration of 10 per cent acid gas will be detected in the nearest well, d-88-I/94-G-1 (Figure 88), producing from the Baldonnel Formation (2.5 km southeast of the injection well) after 7 years of injection. As stated in the approval by the OGC, WCGS is required to monitor and report acid gas concentrations in the offsetting wells for increases in the acid gas content. No increases in acid gas concentration were detected until the end of 1999, and there is no further information on acid gas concentration in offsetting wells in progress reports submitted by WCGS to the OGC after 1999. Similarly, at Jedney, the operator predicted breakthrough of injected acid gas at two nearby producing wells, d-77-J/94-G-1 and d-99-J/94-G-1 (Figure 88), by the year 2000 and 2002, respectively. With the currently available data, it is impossible to determine whether breakthrough of acid gas actually has occurred because the operator of Jedney is not required to submit data on the composition of produced gas from the neighbouring wells. In the future, more data on the acid gas content in producing offsetting wells is needed to confirm the extent of the injected acid-gas plume and its effect on gas production from the Baldonnel Formation in the Bubbles and Jedney fields. Ultimately, the anticlinal structure of the gas fields and the hydraulic sink created by producing wells make it unlikely that injected acid gas will migrate laterally beyond the boundaries of the Bubbles and Jedney fields, even if breakthrough of acid gas will be detected in offsetting wells within these gas fields.

The possibilities for the potential vertical migration of acid gas into formations overlying the Baldonnel Formation are upward leakage through a) windows, natural faults and/or fractures in the Nordegg aquitard, or b) induced fractures and/or improperly completed and/or abandoned wells. There are no known major faults in the area of the Bubbles and Jedney gas fields that propagate upward through the sedimentary succession. Natural leakage through the overlying aquitards is very unlikely because the regional and local-scale (hydro) geological assessments have shown that the Baldonnel Formation is capped by an effective aquitard that is formed by a thick, competent succession of Nordegg Formation chert, Fernie Group shale and Bullhead Group siltstone. Farther up, the thick shales of the Fort St. John Group form another strong aquitard. These barriers to vertical leakage of the acid gas in the natural system exist not only at the site and local scales in the northeastern British Columbia area, but also at the regional and even basin scales (Bachu, 1999). Diffusion of gas through the sedimentary succession is an extremely slow process, approximately hundreds of thousands of years and more, depending on the thickness of the intervening shale layers (Gurevich et al., 1993). Thus, acid gas leakage through the natural system at the Jedney and Bubbles injection sites is considered highly unlikely.

Leakage of the injected acid gas through local fractures induced in the cap rock because of injection would be possible if the cap rock is fractured or weakened by geomechanical and/or geochemical processes. The licensed bottomhole injection pressure is below the fracturing pressure; hence, injection-induced fracturing should not occur. However, even if the immediate cap rock layer may have been weakened, the large thickness of the overlying aquitards ensures no leakage will occur. No leakage farther up is possible because of the overlying succession of aquifers and aquitards.

While leakage of acid gas through the natural system is very unlikely, leakage through wells is a very distinct possibility, now or in the future. Figure 90 shows the status, time of drilling and time of well abandonment for the wells that penetrate the Baldonnel Formation in the Bubbles and Jedney gas fields. More than half of the wells were drilled between 1990 and 2004, and currently many are still under production. In addition to the 68 wells producing from the Baldonnel Formation, the other main target in the Bubbles and Jedney fields is the underlying Halfway Formation with 51 producing wells. Minor production occurs from the overlying Bluesky (seven wells), underlying Charlie Lake (four wells), Shunda (one well) and Slave Point (one well) formations. Two wells inject or dispose of water into the Charlie Lake and Baldonnel formations, respectively. The well disposing of water in the Baldonnel Formation is located only 1 km south of the Jedney acid-gas injection well, and well interference can be expected. Less

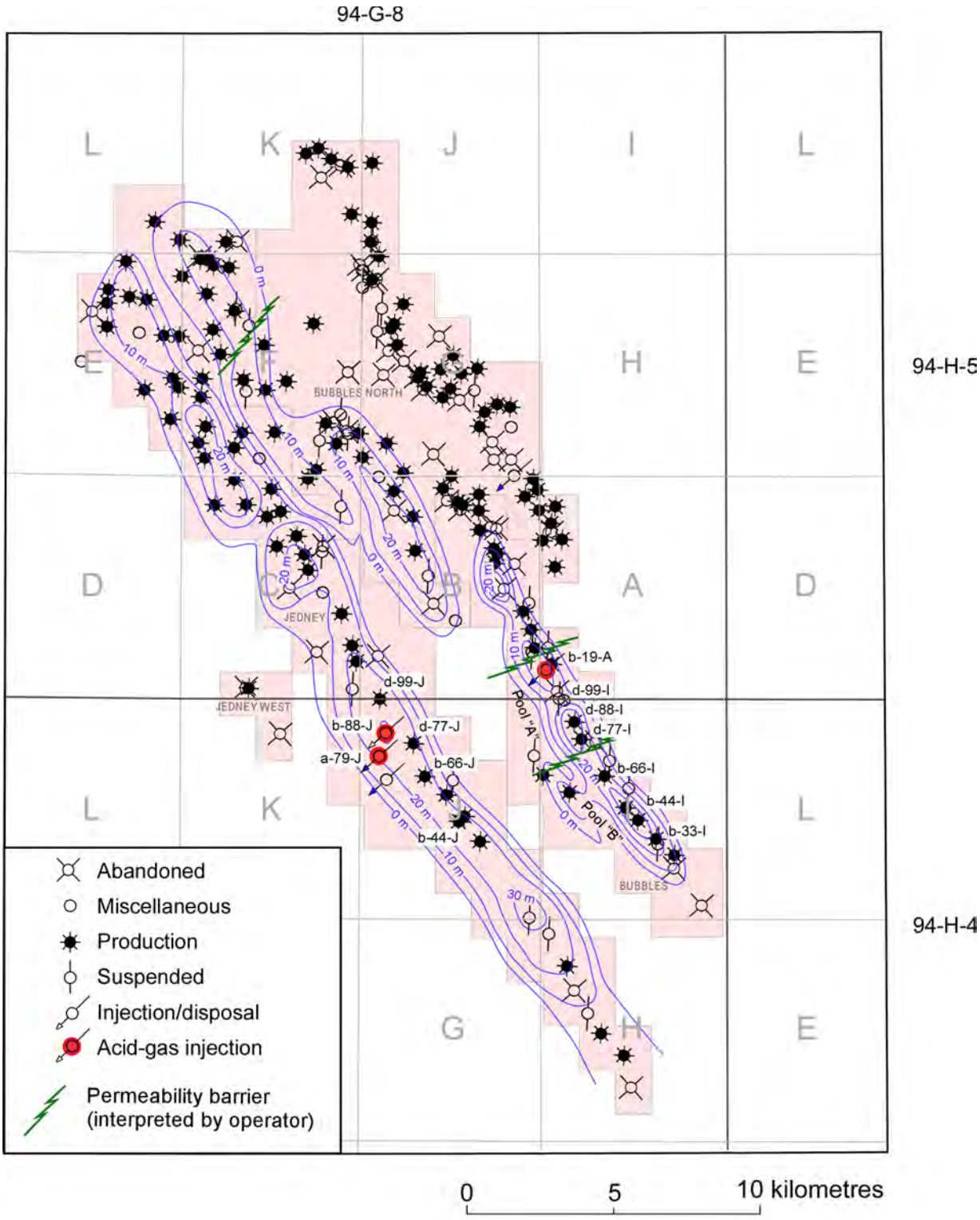

Figure 88. Map showing location and status of wells within administrative boundaries of the Bubbles and Jedney gas fields (in red). Individual gas pools producing from the Baldonnel Formation are delineated by the closed contour lines of net pay (in blue; after net pay maps provided in the application for acid gas injection).

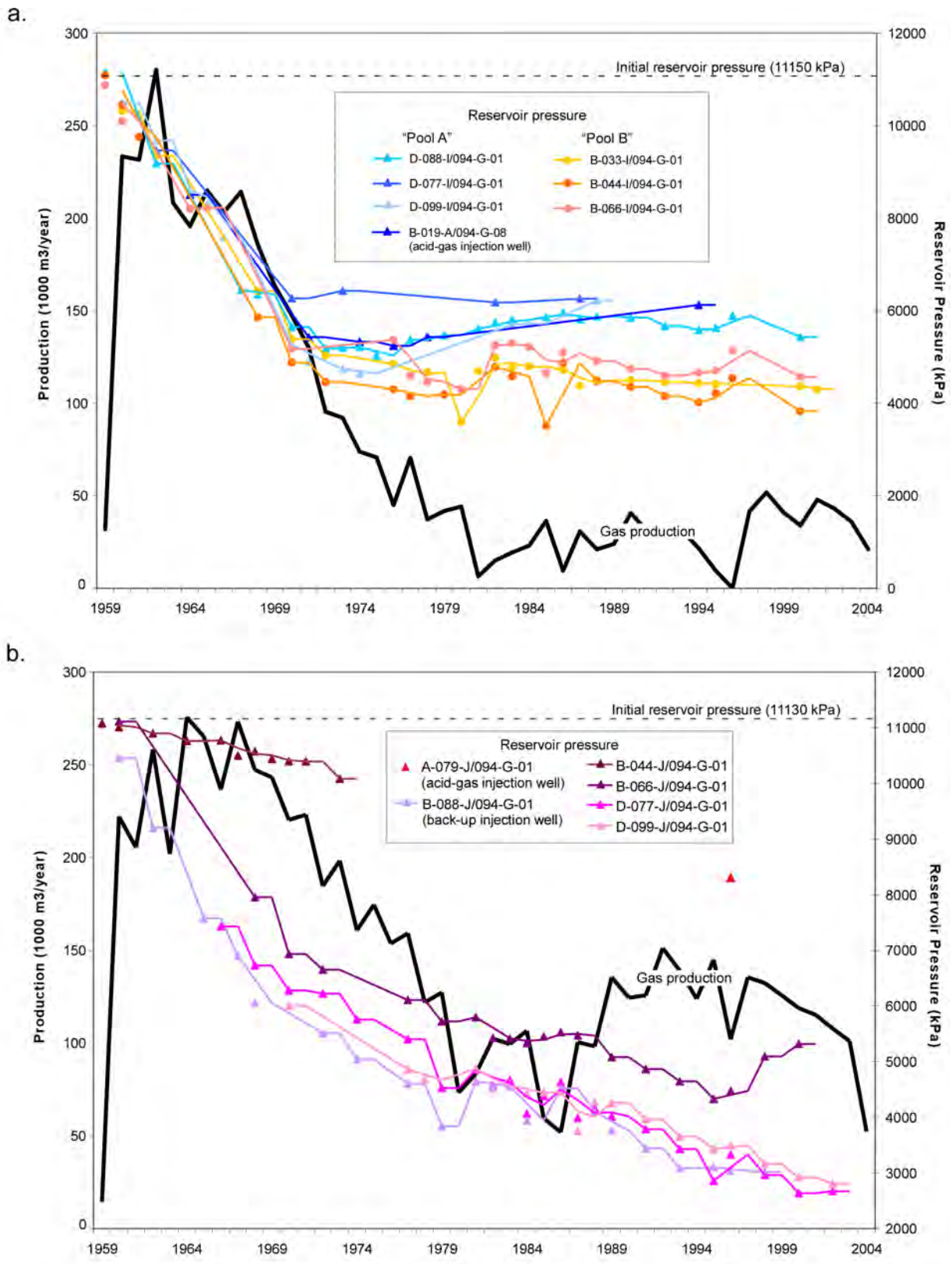

Figure 89. History of reservoir pressure and hydrocarbon production from the Baldonnel Formation at a) Bubbles and b) Jedney (central part of the gas field). Well locations are shown in Figure 88.

than 25% of the wells are already abandoned, most of them in the last 10 years, when more stringent well abandonment regulations than in the 1950s and 1960s were in place.

6.4 Comments on Well Abandonment and Potential Leakage through Wells

Open-hole wells are abandoned by plugging every aquifer and producing formation in the succession above perforations, to avoid cross-formational flow, such that further leakage through these wells is unlikely unless cement plugs are completely degraded. In open-hole abandoned wells, further leakage of acid gas is stopped by the succession of plugs. Cement degradation takes place in the presence of both formation water and acid gas; if the acid gas forms an isolating layer at the bottom of the plug that stops any contact between cement and formation water, then further degradation will not occur (Scherer et al., 2004). Any leaked acid gas will likely spread into the aquifer that is isolated by that plug, where it will dissolve. The rate of leakage is relatively small (flow through porous media) and likely decreases from one aquifer to another, similar to the 'elevator model' in the case of water leakage. Cased wells are abandoned by usually emplacing a plug just above perforations and another one close to surface. If acid gas corrodes the casing and leaks inside, and then degrades the cement plug, it will migrate upwards to the top plug. Along the way, the acid gas will decompress and reach gaseous phase at the top. Accumulation of acid gas with water present will have a corrosive effect on the casing, such that acid gas leakage may subsequently occur directly into shallow groundwater close to the surface. In this case, the well tubing provides an open-flow conduit that bypasses the entire succession of aquifers and aquitards above the injection unit with their retarding effect. From this point of view, leaky cased wells represent a greater risk than open-hole abandoned wells.

In all cases, poor-quality completion in existing or future wells may provide a pathway for upward leakage from the injection reservoir or from any place an acid gas plume may reach in the future. However, the time scale and magnitude of the degradation cannot be assessed with the current data, knowledge and methods. Furthermore, leakage to the surface through abandoned wells at the seven acid-gas injection sites, now or in the future, should not be a concern, even if some wells are improperly abandoned, for the following reasons

- Leaky wells affect each other (pressure interference), such that the leakage rate per well is significantly reduced (Nordbotten et al., 2005);
- The leakage rate is again significantly reduced when other aquifers containing high-salinity brine overlies the injection unit, because these aquifers serve as receptors for most of the leaked gas (Nordbotten et al., 2005) before it can reach shallow freshwater aquifers or the ground surface;
- Any acid gas that would leak from the injection horizon into overlying or underlying aquifers will disperse, diffuse and mix further with the formation water in that aquifer; and
- The injection reservoir in Bubbles and Jedney is underpressured. Thus, the injected acid gas will not have enough pressure drive to reach the surface, at least not in the earlier phases of injection.

7 Conclusions

The experience gained since the start of the first acid-gas injection operation in Canada in 1989 shows that, from an engineering point of view, acid gas disposal is a well-established technology. By the end of 2004, close to 2.5 Mt CO_2 and 1.8 Mt H_2S have been successfully injected into deep hydrocarbon reservoirs and saline aquifers in Alberta and British Columbia. A major issue that has not been addressed is the containment and long-term fate of the injected acid gas.

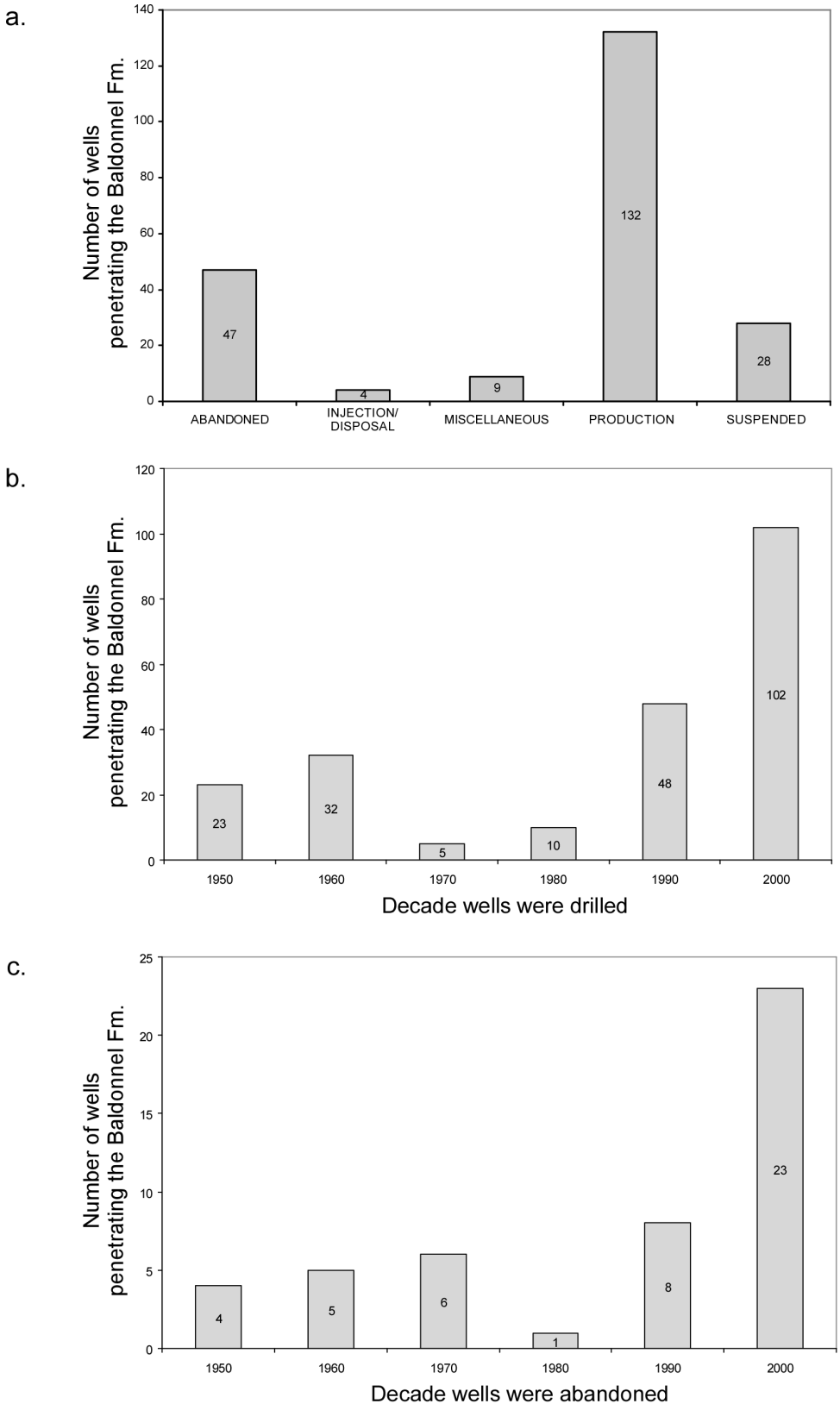

Figure 90. Histograms for wells that penetrate the Baldonnel Formation in the Bubbles and Jedney gas fields, showing a) well status, b) time of drilling, and c) time of abandonment.

Injection of acid gas in northeastern British Columbia region takes place at seven sites into four different stratigraphic intervals. Dry acid gas is injected into the deep saline Permo–Carboniferous aquifer at Boundary Lake–South, Caribou–Debolt and mixed with water at Ring. At West–Stoddart and Caribou–Halfway, dry acid gas is injected into the Triassic Halfway–Doig aquifer. At Bubbles and Jedney, the acid gas is injected into depleted gas reservoirs in the Triassic Baldonnel Formation. Boundary Lake–South and Bubbles, operating since 1996, are the oldest acid-gas injection operations in British Columbia. By the end of 2004, more than 890 kt of acid gas have been injected into deep geological formations in the northeastern British Columbia region.

If only the natural setting is considered, including geology and flow of formation waters, the basin and local-scale hydrogeological analyses indicate that injecting acid gas into these deep geological units in northeastern British Columbia is basically a safe operation, with no potential for acid gas migration to shallower strata, potable groundwater and the surface. The acid gas plume will likely be reduced by dissolution, dispersion, residual gas saturation and trapping along the migration pathway and therefore not reach the overlying aquifers. In the unlikely event of further migration, it would take in the order of 5000 years before acid gas could be detected in the Bullhead aquifer at Boundary Lake–South. Once in the Bullhead aquifer, the acid gas theoretically would have to move farther updip along the top of the aquifer for another 300 km (~15 000 years) before it would reach the ground surface in the outcrop area of the Bullhead aquifer. At West Stoddart, updip-migrating acid gas will be captured in neighbouring production wells. However, once production ceases, it will take hypothetically in the order 90 000 years before acid gas will reach the ground surface. Finally, it is not realistic that this long migration path will ever be completed because of dissolution, dispersion, residual gas saturation and trapping of the acid gas along the migration path. At Ring, acid gas is injected mixed with water into the Permo–Carboniferous aquifer, and will initially form a gas cap at the top of the aquifer due to pressure–temperature conditions. If the acid gas would reach the Cretaceous Bullhead aquifer, further migration would be impeded by the overlying thick and tight shales of Wilrich–Fort St. John aquitard. At Caribou–Halfway, vertical migration will be prevented by the effective aquitard characteristics of the Charlie Lake Formation. In, addition low-permeability sediments of the Fernie Group and Fort St. John Group provide additional vertical barriers to flow to shallow aquifers. At Caribou–Debolt, the Montney Formation forms a thick, confining aquitard at the top of the Permo–Carboniferous aquifer, and the hydrogeological assessment showed no indications for the possibility of leakage to overlying aquifers. Additional barriers preventing vertical leakage to shallow aquifers or the ground surface are formed by the succession of the Lower Charlie Lake, Fernie and Wilrich–Fort St. John aquitards. At Bubbles and Jedney, where acid gas is injected into depleted reservoirs, density and viscosity values show that if the acid gas is injected at the bottom of the reservoir, it will stay there and gradually fill up the reservoir, displacing the residual natural gas to the top of the reservoir. Since both gases are nonwetting fluids, no capillary forces affect the flow of the two gases. This method can be actually used to produce additional gas (enhanced gas recovery). If the acid gas is injected at a level higher than the bottom of the reservoir, the acid gas will flow to the bottom of the reservoir with a similar effect. There will be some gas dissolution in the underlying formation water at the gas–water contact, but the amount of acid gas that will dissolve is going to be small since the formation water has already a very high salinity. Also, once the top water layer is saturated with acid gas, no additional dissolution will occur.

The entire stratigraphic interval from the Debolt Formation to the Baldonnel Formation is overlain by thick shales within the Fernie, Bullhead and Fort St. John groups. There are many barriers to acid gas migration from an injection zone into other strata, and the flow process, if it will ever happen, would take an extremely long time on a geological time scale. Any acid gas plume would disperse and dissolve in formation water during flow on such large time and spatial scales.

Based on available data, it seems there is no potential for acid gas leakage through fractures. However, the possibility for upward leakage of acid gas exists along wells that were improperly completed and/or abandoned, or along wells whose cement and/or tubing have degraded or may degrade in the future as a result of chemical reactions with formation brine and/or acid gas. A review of the status and age of wells that penetrate the respective injection unit at each site shows that most wells were drilled in the 1990s, and that less than 25% of the wells are abandoned. Therefore, no leakage has been detected and reported to date, however, the potential for this occurring in the future should be considered by both operators and regulatory agencies.

These conclusions are based on a qualitative hydrogeological analysis in the sense that the geological and hydrogeological data were interpreted within the framework of the most current knowledge about the Alberta Basin and its contained fluids. No quantitative analysis based on numerical modelling was performed because, to the best knowledge of the authors, no such models are available. Predictive numerical models of acid gas injection and flow, if not already in existence, should be developed and used to validate the qualitative hydrogeological analysis presented in this report. Geochemical and geomechanical effects on reservoir rock and cap rock should be assessed to confirm integrity. The potential for and risk of leakage through existing wells should be better assessed. In addition, a monitoring program would support and provide feedback to the analysis and modelling, and greatly enhance the confidence in the safety of the operation.

Extension of this analysis to other current and future disposal sites will lower risk and increase the public trust in the potential and safety of geological sequestration of acid and greenhouse gases. Ideally, a thorough program for predicting the long-term fate of the injected acid gas should contain the following major components

- a hydrogeological analysis of the injection site at various scales, from site-specific to regional, to provide the context, understanding and necessary data for a qualitative assessment;
- numerical modelling for predicting possible migration and/or leakage paths and corresponding time scales for the injected acid gas;
- monitoring of the acid gas plume to validate and update the numerical model; and
- continuous updating of the hydrogeological and numerical models as new data are acquired.

Currently, no adequate numerical models exist to properly simulate the fate of the acid gas injected in deep geological formations. Furthermore, monitoring programs are expensive, and in the absence of forward-simulating models, may not provide the necessary information. However, the hydrogeological analysis, the first step for understanding the fate of the acid gas, can be easily implemented for all acid-gas injection sites, particularly in basins with a wealth of data such as the Alberta Basin.

8 References

Adams, J.J. and Bachu, S. (2002): Equations of state for basin geofluids: algorithm review and intercomparison for brines; Geofluids, v. 2, p. 257–271.

Alberta Energy and Utilities Board (2000): Guide 65: resources applications for conventional and gas reservoirs; Alberta Energy and Utilities Board, p. 113–136.

Anfort, S.J., Bachu, S. and Bentley, L.R. (2001): Regional-scale hydrogeology of the Upper Devonian-Lower Cretaceous sedimentary succession, south-central Alberta Basin, Canada; American Association of Petroleum Geologists Bulletin, v. 85, p. 637–660.

Armitage, J.H. (1962): Triassic oil and gas occurrences in northeastern British Columbia, Canada; Journal of Alberta Society Petroleum Geology., v. 10, p. 35–36.

Bachu, S. (1995): Synthesis and model of formation water flow in the Alberta Basin, Canada; American Association of Petroleum Geologists Bulletin, v. 79, p. 1159–1178.

Bachu, S. (1997): Flow of formation waters, aquifer characteristics, and their relation to hydrocarbon accumulations, northern Alberta Basin; American Association of Petroleum Geologists Bulletin, v. 81, no. 5, p. 712–733.

Bachu, S. (1999): Flow systems in the Alberta Basin: Patterns, types and driving mechanisms; Bulletin of Canadian Petroleum Geology, v. 47, p. 455–474.

Bachu, S. and Carroll, J.J. (2004): In-situ phase and thermodynamic properties of resident brine and acid gases (CO_2 and H_2S) injected in geological formations in Western Canada; *in* Proceedings, 7th International Greenhouse Gas Technologies Conference, Vancouver, B.C., September 5–9, 2004, pp.9.

Bachu, S. and Michael, K. (2002): Flow of variable-density formation water in deep sloping aquifers: minimizing the error in representation and analysis when using hydraulic head distributions; Journal of Hydrology, v. 259, p. 49–65.

Bachu, S. and Michael, K. (2003): Hydrogeology and stress regime of the Upper Cretaceous–Tertiary coal-bearing strata in the Alberta Basin: toward coalbed methane producibility; American Association of Petroleum Geologists Bulletin, v. 87, p. 1729–1754.

Bachu, S. and Underschultz, J.R. (1993): Hydrogeology of formation waters, northeastern Alberta Basin; American Association of Petroleum Geologists Bulletin, v. 77, p. 1745–1768.

Bachu, S. and Underschultz, J.R. (1995): Large-scale erosional underpressuring in the Mississippian-Cretaceous succession, southwestern Alberta Basin; American Association of Petroleum Geologists Bulletin, v. 79, p. 989–1004.

Bachu, S., Michael, K. and Buschkuehle, B.E. (2002): The relation between stratigraphic elements, pressure regime, and hydrocarbons in the Alberta deep basin (with emphasis on select Mesozoic units): discussion; American Association of Petroleum Geologists Bulletin, v. 86, p. 525–528.

Barclay, J.E., Krause, F.F., Campbell, R.I. and Utting, J. (1990): Dynamic casting and growth faulting: Dawson Creek Graben Complex, Carboniferous-Permian Peace River Embayment, Western Canada; Bulletin of Canadian Petroleum Geology, v. 38A, p. 115–145.

Barclay, J.E. (2000): Estuarine deposition, valley incision and soil development controlled by tectonic evolution of a growth-faulted coastal graben embayment, Stoddart Group–Belloy Formation, Carboniferous–Permian, Western Canada Basin; Ph.D. thesis, University of Calgary, 650 p.

Bell, J. S. (2003): Practical methods for estimating in-situ stresses for borehole stability applications in sedimentary basins; Journal of Petroleum Science and Engineering, v. 38:3–4, p. 111–119.

Bell, S.J. and Babcock, E. A. (1986): The stress regime of the Western Canada Sedimentary Basin and implications for hydrocarbon production; Bulletin of Canadian Petroleum Geology, v. 34, p. 364–378.

Bell, S.J. and Bachu, S. (2003): In situ stress magnitude and orientation estimates for Cretaceous coal-bearing strata beneath the plains area of central and southern Alberta; Bulletin of Canadian Petroleum Geology, v. 51, p. 1–28.

Bell, S.J., Price, P.R. and McLellan, P.J. (1994): In-situ stress in the Western Canada Sedimentary Basin; *in* Geological Atlas of the Western Canada Sedimentary Basin, G.D. Mossop and I. Shetsen (comp.), Canadian Society of Petroleum Geologists and Alberta Research Council, Special Report 4, p. 439–446.

Bennion, D.B., Thomas, F.B., Bennion, D.W. and Bietz, R.F. (1996): Formation screening to minimize permeability impairment associated with acid gas or sour gas injection/disposal; *in* 47th Annual Technical Meeting of the CIM Petroleum Society, Calgary, Alberta, June 10–12, 1996, CIM Paper 96–93.

Burrowes, O.G. and Krause, F.F. (1987): Overview of the Devonian system: subsurface Western Canada Basin; *in* Devonian lithofacies and reservoir styles in Alberta, F.F. Krause and O.G. Burrowes (ed.), 2nd International Symposium of the Devonian System, 13th CSPG Core Conference, Calgary, p. 1–52.

Buschkuehle, B.E. and Machel, H.G. (2002): Diagenesis and paleofluid flow in the Devonian Southesk-Cairn carbonate complex in Alberta, Canada; Marine and Petroleum Geology, v. 19, p. 219–227.

Bustin, R.M. (1991): Organic maturation of the Western Canadian Sedimentary Basin; International Journal of Coal Geology, v. 19, p. 319–358.

Campbell, J. D. (1979): Major cleat trends in Alberta Plains coals; Canadian Institute of Mining Bulletin, v. 72, p. 69–75.

Carroll, J. J. (1998a): Phase diagrams reveal acid-gas injection subtleties; Oil and Gas Journal, v. 96:9, p. 92–96.

Carroll, J. J. (1998b): Acid gas injection encounters diverse H_2S, water phase changes; Oil and Gas Journal, v. 96:10, p. 57–59.

Carroll, J.J. and Lui, D.W. (1997): Density, phase behavior keys to acid gas injection; Oil and Gas Journal, v. 95:25, p. 63–72.

Davies, G.R. (1997): The Triassic of the Western Canada Sedimentary Basin: tectonic, structural and stratigraphic framework, paleoenvironment, paleoclimate and biotic evolution; Bulletin of Canadian Petroleum Geology, v. 45, p. 434–460.

Davies, G.R., Spencer, R. and Berger, Z. (2004): Early burial reflux (?) dolomitization of the Upper Triassic Baldonnel Formation, northeast British Columbia: gas giant (6+TCF) and youngest major carbonate reservoir in the WCSB; *in* CSPG Seminar and core conference, Calgary, Alberta, Abstracts, CD-ROM.

Davison, R.J., Mayder, A., Hladiuk, D.W. and Jarrell, J. (1999): Zama acid gas disposal/miscible flood implementation and results; Journal of Canadian Petroleum Technology, v. 38:2, p. 45–54.

Deming, D. and Nunn, J.A. (1991): Numerical simulations of brine migration by topographically driven recharge; Journal of Geophysical Research, v. 96:B2, p. 2485–2499.

Desbarats, A. J. and Bachu, S. (1994): Geostatistical analysis of aquifer heterogeneity from the core scale to the basin scale: a case study; Water Resources Research, v. 30:3, p. 673–684.

Edwards, D.E., Barclay, J.E., Gibson, D.W., Kvill, G.E. and Halton, E. (1994): Triassic strata of the Western Canada Sedimentary Basin; *in* Geological Atlas of the Western Canada Sedimentary Basin, G.D. Mossop and I. Shetsen (comp.), Canadian Society of Petroleum Geologists and Alberta Research Council, Special Report 4, p. 259–276.

Ennis-King, J., Bradshaw, J., Gibson-Poole, C., Hennig, A., Lang, S., Paterson, L., Root, R., Sayers, J., Spencer, L., Streit, J. and Undershultz, J. (2004): Long-term numerical simulation of a portfolio of possible sites for geological storage of carbon dioxide in Australia; *in* Proceedings of 7th International Conference on Greenhouse Gas Control Technologies, IEA Greenhouse Gas Programme, Cheltenham, UK, pp.9.

Fitzgerald, E.L. and Peterson, D.J. (1967): Inga oil field, British Columbia; Bulletin of Canadian Petroleum Geology, v. 15, p. 65–81.

Freeze, R.A. and Cherry, J.A. (1979): Groundwater; Prentice-Hall Inc., Inglewood Cliffs, 604 p.

Gibson, D.W and Barclay, J.E. (1989): Middle Absaroka sequence: the Triassic stable craton; *in* The Western Canada Sedimentary Basin – A Case History, B.D. Ricketts (ed.), Canadian Society of Petroleum Geologists, Special Publication 30, p. 219–232.

Gibson, D.W. and Edwards, D.E. (1990): An overview of Triassic stratigraphy and depositional environments in the Rocky Mountain Foothills and western Interior Plains, Peace River Arch area, northeastern British Columbia; Bulletin of Canadian Petroleum Geology, v. 38A, p. 146–158.

Grasby, S. and Hutcheon, I. (2001): Controls on the distribution of thermal springs in the southern Canadian Cordillera; Canadian Journal of Earth Sciences, v. 38:3, p. 427–440.

Gunter, W.D., Perkins, E.H. and Hutcheon, I. (2000): Aquifer disposal of acid gases: modeling of water-rock reactions for trapping acid wastes; Applied Geochemistry, v. 15, p. 1085–1095.

Gurevich, A.E., Endres, B.L., Robertson Jr., J.O. and Chilingar, G.V. (1993): Gas migration from oil and gas fields and associated hazards; Journal of Petroleum Science and Engineering, v. 9, p. 223–238.

Haas, C. J. (1989): Static stress-strain relationships; *in* Physical properties of rocks and minerals, Y.S. Touloukian, W. R. Judd and R.F. Roy (ed.), Hemisphere Publishing Corporation, New York, p. 123–176.

Halbertsma, H.L. (1959): Nomenclature of Upper Carboniferous and Permian strata in the subsurface of the Peace River area; Journal of the Alberta Society Petroleum Geologists., v. 7, p. 109–118.

Harris, R.G. and Bustin, R. (2000): Diagenesis, reservoir quality, and production trends of Doig Formation sand bodies in the Peace River area of Western Canada; Bulletin of Canadian Petroleum Geology, v. 48, p. 339–359.

Hearn, M.R. and Rostron, B.J. (1997): Hydrogeologic, stratigraphic, and diagenetic controls on petroleum entrapment in Devonian reefs, Bashaw area, Alberta; *in* CSPG–SEPM Joint Convention, June, Calgary, Alberta, Core Conference Proceedings, p. 89–101.

Hedberg, H.D. (1974): Relation of methane generation to undercompacted shales, shale diapirs, and mud volcanoes; AAPG Bulletin, v. 58, p. 661–673.

Henderson, C.M., Richards, B.C. and Barclay, J.E. (1994): Permian Strata of the Western Canada Sedimentary Basin; *in* Geological Atlas of the Western Canada Sedimentary Basin, G.D. Mossop and I. Shetsen (comp.), Canadian Society of Petroleum Geologists and Alberta Research Council, Special Report 4, p. 251–258.

Hess, E.B. (1968): Charlie Lake study: correlation and nomenclature; Pacific Petroleums Limited Report to British Columbia Department of Mines, 57 pp..

Hitchon, B. (1969a): Fluid flow in the Western Canada Sedimentary Basin, 1. effect of topography, Water Resources Research, v. 5, p. 186–195.

Hitchon, B. (1969b): Fluid flow in the Western Canada Sedimentary Basin, 2. effect of geology; Water Resources Research, v. 5, p. 460–469.

Hitchon, B. (1996): Rapid evaluation of the hydrochemistry of a sedimentary basin using only "standard" formation water analyses: example from the Canadian portion of the Williston Basin; Applied Geochemistry, v. 11, p. 789–795.

Hitchon, B. and Brulotte, M. (1994): Culling criteria for "standard" formation water analyses; Applied Geochemistry, v. 9, p. 637–645.

Hitchon, B., Bachu, S. and Underschultz, J.R. (1990): Regional subsurface hydrogeology, Peace River arch area, Alberta and British Columbia; Bulletin of Canadian Petroleum Geology, v. 38A, p. 196–217.

Hitchon, B., Perkins, E.H. and Gunter, W.D. (2001): Recovery of trace metals in formation waters using acid gases from natural gas; Applied Geochemistry, v. 16, p. 1481–1497.

Holtz, M.H. (2003): Optimization of CO_2 sequestered as a separate phase in brine-saturated formations; *in* Second Annual Conference on Carbon Sequestration, Alexandria, Virginia, May 5–8, 2003, Abstracts.

Jackson, P.C. (1984): Paleogeography of the Lower Cretaceous Mannville Group of Western Canada; *in* Elmworth – Case Study of a Deep Basin Gas Field, J.A. Masters (ed.), American Association of Petroleum Geologists, Memoir 38, p. 49–78.

Jumikis, A.R. (1983): Rock Mechanics (2nd Edition); Trans Tech Publications, Rockport, MA., 613 p.

Keushnig, H. (1995): Hydrogen sulphide – if you don't like it, put it back; Journal of Canadian Petroleum Technology, v. 34:6, p. 18–20.

Lambe, T.W. and Whitman, R.V. (1979): Soil Mechanics, SI version; John Wiley and Sons Inc., New York, 553 p.

Law, J. (1981): Mississippian correlations, northeastern British Columbia, and implications for oil and gas exploration; Bulletin of Canadian Petroleum Geology, v. 29, p. 378–398.

Lindeberg, E. and Wessel-Berg, D. (1997): Vertical convection in an aquifer column under a gas cap of CO_2; Energy Conversion and Management, v. 38S, p. 229–234.

Longworth, H.L., Dunn, G.C. and Semchuk, M. (1996): Underground disposal of acid gas in Alberta, Canada: regulatory concerns and case histories; *in* Proceedings of the Gas Technology Symposium, Calgary, Alberta, April 28–May 1, 1996, SPE Paper 35584, p. 181–192.

Machel, H.G., Cavell, P.A. and Patey, K.S. (1996): Isotopic evidence for carbonate cementation and recrystallization, and for tectonic expulsion of fluids into the Western Canada Sedimentary Basin; Geological Society of America Bulletin, v. 108, p. 1108–1119.

Masters, J.A. (ed.) (1984): Elmworth: case study of a deep basin gas field; American Association of Petroleum Geologists, Memoir 38, 316 p.

McLellan, P.J. and Cormier, K. (1996): Borehole stability in dipping fissile shales, northeastern British Columbia; *in* Proceedings of the Gas Technology Symposium, Calgary, Alberta, April 28–May 1, 1996, SPE paper 35634, Abstract.

McLennan, J.D., Elbel, J., Mattheis, E. and Lindstrom, L. (1982): A critical evaluation of the mechanical properties log (MPL) on a basal quartz well in the Caroline area, *in* Annual Technical Meeting of the Petroleum Society of CIM, Paper 82, p. 33–45.

McPherson, B.J.O.L. and Cole, B.S. (2000): Multiphase CO_2 flow, transport and sequestration in the Powder River Basin, Wyoming, USA; Journal of Geochemical Exploration, v.69, p. 65–69.

Michael, K. and Bachu, S. (2001): Fluids and pressure distributions in the foreland-basin succession in the west-central part of the Alberta basin, Canada: evidence for permeability barriers and hydrocarbon generation and migration; American Association of Petroleum Geologists Bulletin, v. 85, p. 1231–1252.

Michael, K. and Bachu, S. (2002): Origin, chemistry and flow of formation waters in the Mississippian–Jurassic sedimentary succession in the west-central part of the Alberta Basin, Canada; Marine and Petroleum Geology, v. 19, p. 289–306.

Michael, K., Machel, H.G. and Bachu, S. (2003): New insights into the origin and migration of brines in deep Devonian aquifers, Alberta, Canada; Journal of Geochemical Exploration, v. 80:2–3, p. 193–219.

Miller, S.L.M. and Stewart, R.R. (1990): Effects of lithology, porosity, and shaliness on P- and S-wave velocities from sonic logs; Canadian Journal of Exploration Geophysics, v. 26, p. 94–103.

Mossop, G.D. and Shetsen, I. (comp.) (1994): Geological Atlas of the Western Canada Sedimentary Basin; Canadian Society of Petroleum Geologists and Alberta Research Council, Special Report 4, 510 p.

Naqvi, I.H. (1972): The Belloy Formation (Permian), Peace River area, northern Alberta and northeastern British Columbia; Bulletin of Canadian Petroleum Geology, v. 20, p. 58–88.

Nesbitt, B.E. and Muechlenbachs, K. (1993): Synorogenic fluids of the Rockies and their impact on paleohydrogeology and resources of the Western Canada Sedimentary Basin; *in* Alberta Basement Transect Workshop, G.M. Ross (ed.), Lithoprobe Secretariat, University of British Columbia, Lithoprobe Report 31, p. 60–62.

Ng, H-J., Carroll J.J. and Maddocks, J.R. (1999): Impact of thermophysical properties research on acid-gas injection process design; *in* Proceedings of the 78th Gas Processors Association Annual Convention, Nashville, TN, March 1–3, 1999, p. 114–120.

Nordbotten, J.M, Celia, M.A. and Bachu, S. (2004): Analytical solutions for leakage through abandoned wells; Water Resources Research, v. 40, W04204, doi:10.1029/2003WR002997, 2004, 10 p.

Nordbotten, J., Celia M.A. and Bachu S. (2005): Injection and storage of CO2 in deep saline aquifers: analytical solution for CO2 plume evolution during injection; Transport in Porous Media, v. 58(3), p. 339–360.

Norgard, G. (1997): Structural inversion of the Middle Triassic Halfway Formation, Monias Field, northeast British Columbia; Bulletin of Canadian Petroleum Geology, v. 45, p. 614–623.

Nurkowski, J.R. (1984): Coal quality, coal rank variation and its relation to reconstructed overburden, Upper Cretaceous and Tertiary plains coals, Alberta, Canada; American Association of Petroleum Geologists Bulletin, v. 68, p. 285–295.

Osborne, M.J. and Swarbrick, E. (1997): Mechanisms for generating overpressures in sedimentary basins: a reevaluation; AAPG Bulletin, v. 81(6), p. 1023–1041.

Parks, K.P. and Tóth, J. (1993): Field evidence for erosion-induced underpressuring in Upper Cretaceous and Tertiary strata, west central Alberta, Canada; Bulletin of Canadian Petroleum Geology, v. 43, p. 81–292.

Packard, J.J., Al-Aasm, I. and Devon Exploration Team (2004): Reflux dolomitization of Mississippian-age sabkha and restricted subtidal sediments resulting in a 1.6 Tcf giant gas field: the upper Debolt Formation of west-central Alberta; CSPG Seminar and core conference, Calgary, Alberta, Abstracts, CD-ROM.

Porter, I.W., Price, R.A. and McCrossan, R.G. (1982): The Western Canada Sedimentary Basin; Philosophical Transactions of Royal Society of London, Series A, v. 305, p. 169–182.

Poulton, T.P., Tittemore, J. and Dolby, G. (1990): Jurassic strata of northwestern (and west-central) Alberta and northeastern British-Columbia; Bulletin of Canadian Petroleum Geology, v. 38A, p. 159–175.

Richards, B.C., Barclay, J.E, Bryan, D., Hartling, A. and Hinds, R.C. (1994): Carboniferous Strata of the Western Canada Sedimentary Basin; *in* Geological Atlas of the Western Canada Sedimentary Basin, G.D. Mossop and I. Shetsen (comp.), Canadian Society of Petroleum Geologists and Alberta Research Council, Special Report 4, p. 221–250.

Ricketts, B.D. (ed.) (1989): Western Canada Sedimentary Basin – a case history; Canadian Society of Petroleum Geologists, 320 p.

Rostron, B.J. and Tóth, J. (1996): Ascending fluid plumes above Devonian pinnacle reefs: numerical modeling and field example from west-central Alberta, Canada; *in* Hydrocarbon Migration and its Near-Surface Expression, D. Schumacher and M.A. Abrams (ed.), American Association of Petroleum Geologists, Memoir 66, p. 185–201.

Rostron, B.J. and Tóth, J. (1997): Cross-formational fluid flow and the generation of a saline plume of formation waters in the Mannville Group, west-central Alberta; *in* Petroleum Geology of the Cretaceous Mannville Group, S.G. Pemberton and D.P. James (ed.), Canadian Society of Petroleum Geologists, Memoir 18, p. 169–190.

Rowe, A.M. and Chou, J.C.S. (1970): Pressure-volume-temperature-concentration relation of aqueous NaCl solutions; Journal of Chemical and Engineering Data, v. 15(1), p. 61–66.

Scherer, G.W., Celia, M.A., Prévost, J-H., Bachu, S., Bruant, R., Duguid, A., Fuller, R., Gasda, S.E., Radonjic, M. and Vichit-Vadakan, W. (2004): Leakage of CO_2 through abandoned wells: role of corrosion of cement; *in* The CO2 Capture and Storage Project, D.C. Thomas and S.M. Benson (ed.), CCP, v. II, p. 823–844.

Smith, D.G. (1994): Paleogeographic evolution of the Western Canada Foreland Basin; *in* Geological Atlas of the Western Canada Sedimentary Basin; G.D. Mossop and I. Shetsen (comp.), Canadian Society of Petroleum Geologists and Alberta Research Council, Special Report 4, p. 277–296.

Spencer, R.J. (1987): Origin of Ca-Cl brines in Devonian formations, Western Canada Sedimentary Basin; Applied Geochemistry, v. 2, p. 373–384.

Sturrock, D.L. and Dawson, S.W. (1991): The Ring/Border field: a significant gas discovery in the Triassic Montney Formation; *in* CSPG Reservoir, Canadian Society of Petroleum Geologists, Abstract, v. 18, p. 1–2.

Thompson, M.J. (1989): Gas fields, formation-fluid flow and hydrochemistry in Early Cretaceous formations, Peace River region, N.W. Alberta, Canada; M.Sc. thesis, University of Alberta, 160 p.

Tóth, J. (1963): A theoretical analysis of groundwater flow in small drainage basins; Journal of Geophysical Research, v. 68 (16), p. 4795–4811.

Tóth, J. (1978): Gravity-induced cross-formational flow of formation fluids, Red Earth region, Alberta, Canada: analysis, patterns, and evolution; Water Resources Research, v. 14, p. 805–843.

Tóth, J. and Corbet, T. (1986): Post-Paleocene evolution of regional groundwater flow-systems and their relation to petroleum accumulations, Taber area, southern Alberta, Canada; Bulletin of Canadian Petroleum Geology, v. 34, p. 339–363.

Wang, Z., Hirsche, W.K. and Sedgwick, G. (1991): Electrical and petrophysical properties of carbonate rocks; SPE paper 22661.

Whatley, L. (2000): Acid gas injection proves economic for west-Texas plant; Oil and Gas Journal, v. 98:21, p. 58–61.

Wichert, E. and Royan, T. (1996): Sulfur disposal by acid gas injection; *in* Proceedings of the Gas Technology Symposium, Calgary, Alberta, April 28–May1, 1996, SPE Paper 35585, p. 193–200.

Wichert, E. and Royan, T. (1997): Acid gas injection eliminates sulfur recovery expense; Oil and Gas Journal, v. 95:17, p. 67–72.

Wilkinson, P.K. (1995): Is fluid flow in Paleozoic formations of west-central Alberta affected by the Rocky Mountain thrust belt?; M.Sc. thesis, University of Alberta, 102 p.

Wright, G.N., McMechan, M.E. and Potter, D.E.G. (1994): Structure and architecture of the Western Canada Sedimentary Basin; *in* Geological Atlas of the Western Canada Sedimentary Basin, G.D. Mossop and I. Shetsen (comp.), Canadian Society of Petroleum Geologists and Alberta Research Council, p. 25–40.

Young, F.G. (1997): Iconoclastic view of mid-Triassic stratigraphy, Umbach-Wargen area, British Columbia; Bulletin of Canadian Petroleum Geology, v. 45, p. 577–594.

Appendix 1

Down-Hole Stratigraphic Model West-Stoddart

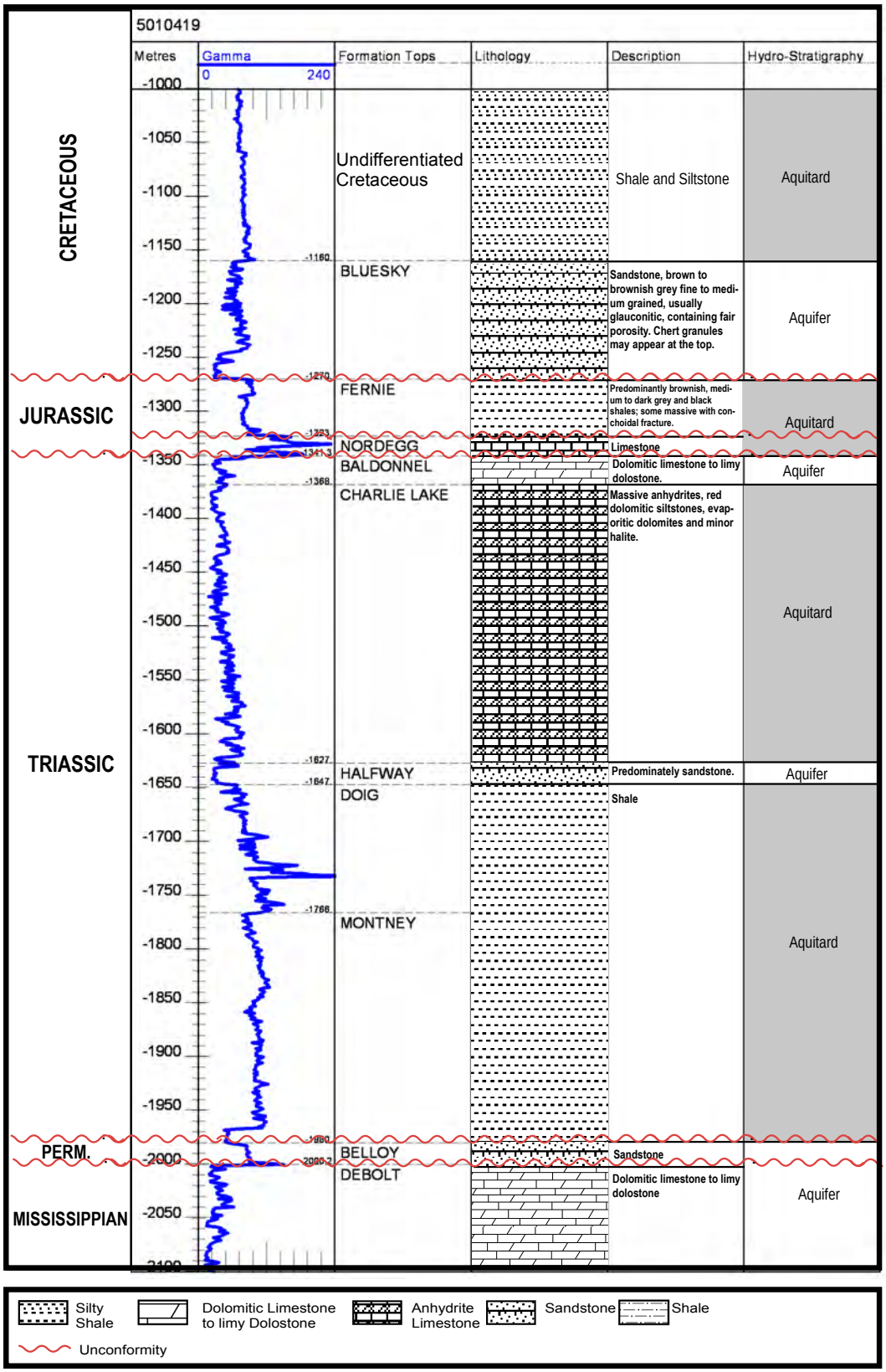

Down-Hole Stratigraphic Model Ring

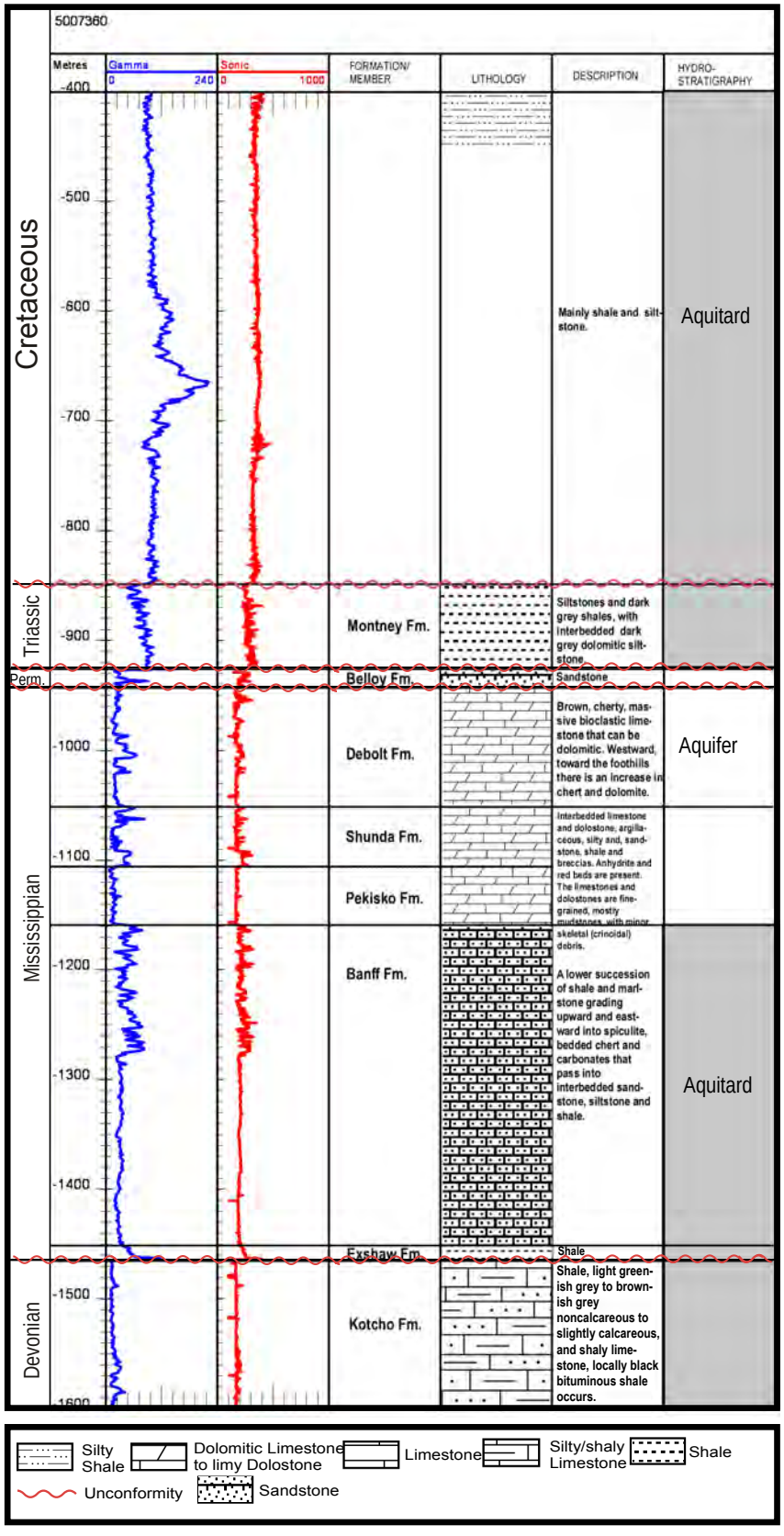

Down-Hole Stratigraphic Model Boundary Lake-South

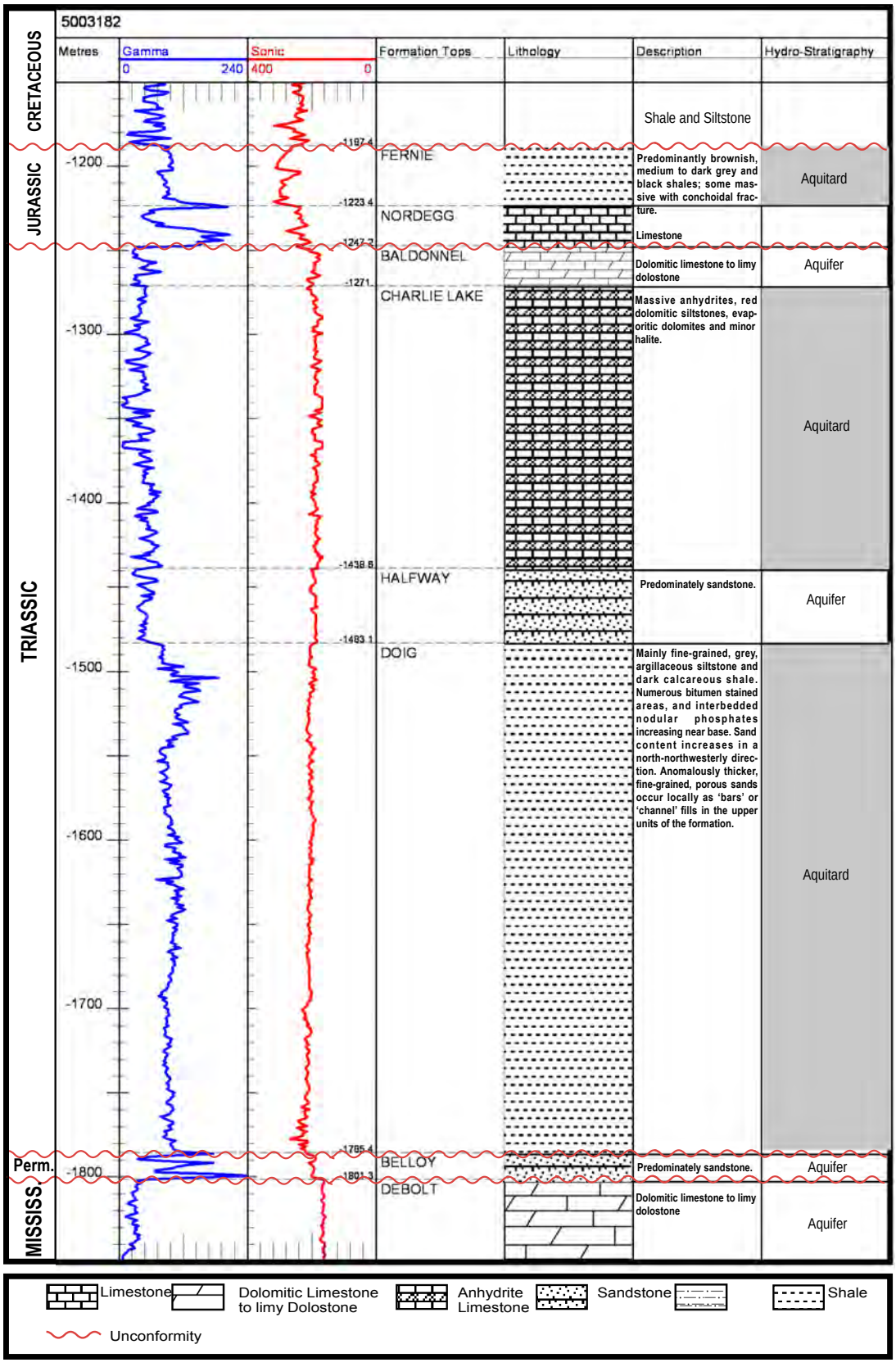

Down-Hole Stratigraphic Model Bubbles-Jedney

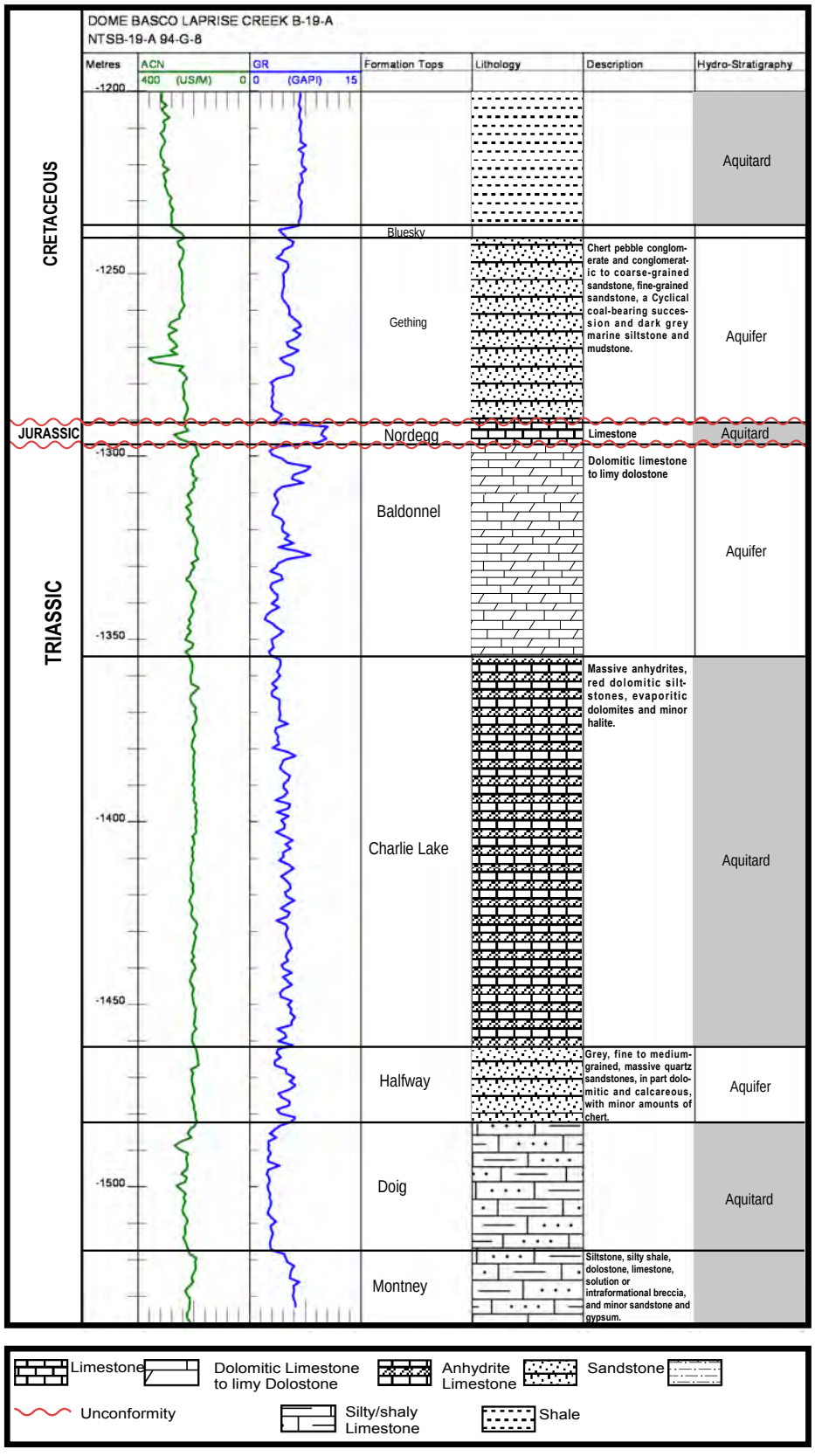

Down-Hole Stratigraphic Model Caribou